The effects of combinations of a green tea extract and an active ingredient thereof, with standard antiretroviral drugs on SC-1 cells infected with the LP-BM5 virus

Andreia Dias

UNIVERSITEIT VAN PRETORIA
UNIVERSITY OF PRETORIA
YUNIBESITHI YA PRETORIA

The effects of combinations of a green tea extract and an active ingredient thereof, with standard antiretroviral drugs on SC-1 cells infected with the LP-BM5 virus

By

Andreia Dias

Thesis submitted in partial fulfillment of the requirement for the degree

MASTER of SCIENCE

in the

FACULTY OF HEALTH SCIENCES

Department of Anatomy
University of Pretoria

2008

The effects of combinations of a green tea extract and an active ingredient thereof, with standard antiretroviral drugs on SC-1 cells infected with the LP-BM5 virus.

By

ANDREIA DIAS

SUPERVISOR: Dr MJ Bester
COSUPERVISOR: Prof. Z Apostolides
DEPARTMENT: Anatomy
DEGREE: MSc (Anatomy with specialization in Cell Biology)

Abstract

The introduction of highly active antiretroviral therapy (HAART) has resulted in a significant decrease in the mortality and morbidity associated with the acquired immunodeficiency syndrome (AIDS). Several problems are associated with HAART and include high costs of treatments, poor availability of drugs in low-income countries, poor compliance, severe adverse effects and drug resistance. Therefore, the focus of current research is the development of new antiretroviral drugs, improved treatment strategies and the discovery of new drugs derived from plants.

Green tea (GT) and its active constituent epigallocatechin gallate (EGCg) have been found to be protective against cancer, cardiovascular and neurodegenerative diseases and were found also to have antimicrobial, antimalarial and more importantly antiviral activity. EGCg, *in vitro* has been shown to inhibit the human immunodeficiency virus (HIV) viral enzymes reverse transcriptase and protease, destroy viral particles and interfere with the attachment of gp120 to cellular receptor CD4.

The aims of this study were firstly to investigate the *in vitro* antiretroviral activity of GT and EGCg on the LP-BM5 defective murine leukemia virus (MuLV) that induces a disease in C57BL/6 mice similar to AIDS in humans and secondly to investigate the effects of GT and EGCg on the *in vitro* cytotoxicity and antiretroviral activity of current antiretroviral drugs zidovudine (AZT), indinavir (IDV), hydroxyurea (HU) and chloroquine (CQ).

To achieve the above aims an *in vitro* model that represents cell-to-cell spreading of the LP-BM5 MuLV was developed. Firstly the presence of the LP-BM5-defective virus in the BM5 cell line was confirmed using transmission electron microscopy (TEM) to identify viral particles, PCR and RT-PCR were used to determine the presence of viral DNA and RNA respectively and viral infectivity was confirmed in C57BL/10 mice. The cytotoxicity of each drug and combination was evaluated with the MTT assay in the SC-1 cell line, the predominant cell type in the *in vitro* cell culture model. GT was the least cytotoxic, followed by AZT, IDV, EGCg, HU and CQ. Co-cultures (BM5:SC-1, 1:10000) that represented cell-to-cell transmission of the virus were established. Real time PCR for proviral DNA revealed that IDV, AZT and HU completely suppressed, CQ dose dependently reduced while GT and EGCg had no effect on viral transmission. Findings using AZT and IDV thus validated the use of this *in vitro* co-culture model for first line screening of new drugs and plant extracts.

The effect of GT or EGCg in combination with AZT, IDV, HU or CQ was also evaluated as GT or EGCg could enhance the antiretroviral effects or decrease cellular toxicity of these drugs. For GT with AZT a mix of synergism and antagonism on cell toxicity was observed with little to no effect on the antiretroviral activity of AZT. Antagonism on cell toxicity was observed for GT with IDV, with no effect on the antiretroviral activity of IDV. In contrast EGCg significantly reduced the antiretroviral activity of IDV. A strong antagonistic effect was observed for GT with HU, with GT reducing the antiretroviral effect of HU. For combinations of AZT with EGCg and HU with EGCg a similar effect was observed as for AZT and HU respectively combined with GT. Synergism in cytotoxicity was observed between GT and CQ associated with a significant decrease in viral loads while EGCg combined with CQ had an opposite effect at higher concentrations.

In conclusion, the *in vitro* co-culture model of BM5 and SC-1 cells was successfully used to evaluate combinations of GT and EGCg with AZT, IDV, HU and CQ. Interesting and often contradicting effects were observed, such as seen for IDV in combination with GT and EGCg as well as CQ in combination with GT and EGCg. These effects may be of clinical relevance and further investigation is warranted.

UNIVERSITEIT VAN PRETORIA
UNIVERSITY OF PRETORIA
YUNIBESITHI YA PRETORIA

Declaration

I, Andreia Dias hereby declare that this research dissertation is my own work and has not been presented for any degree of another University;

Signed……

Date……

Department of Anatomy, School of Medicine, Faculty of Health Sciences,
University of Pretoria

South Africa

Acknowledgements

I acknowledge with gratitude the following people and institutions:

My two amazing promoters Dr Megan Bester, Department of Anatomy and Prof. Zeno Apostolides, Department of Biochemistry on this long and sometimes very frustrating journey! Words cannot express how much all your input, knowledge, guidance, support, motivation and time have meant to me. Thank you.

The Departments of Anatomy, Biochemistry, Genetics, Chemical Pathology and the Laboratory for Microscopy and Microanalysis for allowing me to use your facilities to conduct my research.

Sandra van Wyngaardt for teaching me everything I know about cell culture. Thank you for all your time, knowledge and support.

My wonderful husband and parents for all your support, motivation, understanding and financial assistance. Without you none of this would be possible!

Lastly, I would like to dedicate this to my late brother Rui. You always believed that I could do it!

Table of Contents

List of Tables

List of Figures

List of Abbreviations, symbols and chemical formulae

3TC	Lamivudine
%	Percentage
℃	Degree Celsius
A	Alpha
B	Beta
Ml	Microliter
Mm	Micrometer

A

A	Adenine
Agm	African green monkey
AIDS	Acquired immunodeficiency syndrome
AMDET	Absorption, metabolism, distribution, excretion and toxicity
APC	Antigen presenting cell
ATCC	American Type Culture Collection
AZT	Azidothymidine
AZTTP	Azidothymidine triphosphate

B

BFU-E	Erythroid bust-forming units
BHAP	Bis(heteroaryl)piperazines
BIV	Bovine immunodeficiency virus
Bp	Base pair

C

C	Cytosine
CAEV	Caprine arthritis-encephalitis virus
CD	Cluster of differentiation
cDNA	Complimentary deoxyribonucleic acid
CFU-c	Colony forming units in culture
CFU-GM	Granulocyte/macrophage colony forming units
CI	Combination Index
CINF	Consensus interferon
Cm	Centimeter
CNS	Central nervous system
ConA	Concavalin A
CPE	Cytopathic effect
Cpz	Chimpanzee
CQ	Chloroquine
CSF	Cerebrospinal fluid

CTL	Cytotoxic T-lymphocytes
CV	Crystal Violet

D

D	Dose
dATP	Deoxyadenosine triphosphate
dCTP	Deoxycytidine triphosphate
ddH_2O	Double distilled and deionized water
ddI	Didanosine
def	Defective
DEPC	Diethyl pyrocarbonate
dGTP	Deoxyguanosine triphosphate
DHEA	Dehydroepiandrosterone
DIC	Differential interference contrast
D_m	Median-effect dose
DMEM	Dulbecco's minimum essential medium
DMSO	Dimethylsulfoxide
DNA	Deoxyribonucleic acid
DRI	Dose-reduction index
ds cDNA	Double-stranded complimentary deoxyribonucleic acid
dTTP	Deoxythimidine triphosphate
dUTP	Deoxyuridine triphosphate
DX	Didox

E

ED_{50}	Effective dose that kills 50% of the virus
EDTA	Ethylenediamine tetraacetic acid
EGCg	Epigallocatechin gallate
EIAV	Equine infectious anemia virus
ELISA	Enzyme linked immunosorbant assay

F

f_a	Fraction affected by dose
FAIDS	Feline acquired immunodeficiency syndrome
FBS	Fetal bovine serum
FDA	Food and Drug Administration
fddA	2'-β-fluoro-2',3'-dideoxyadenosine
FIV	Feline immunodeficiency virus
f_u	Fraction unaffected by dose

G

g	Gram

G	Guanine
G6PDH	Glucose-6-phosphate dehydrogenase
GALT	Gut-associated lymphoid tissue
GIT	Gastrointestinal tract
GSH	Glutathione
GT	Green tea

H

h	Hour
H_2O	Water
HAART	Highly active antiretroviral therapy
HEPA	High Efficiency Particulate Air
HIV	Human immunodeficiency virus
HPLC	High performance liquid chromatography
H_2O	Water
H_2O_2	Hydrogen peroxide
HU	Hydroxyurea

I

IDV	Indinavir
IFN	Interferon
Ig	Immunoglobulin
IL	Interleukin
IN	Integrase
ISH	*In situ* hybridization

K

KH_2PO_4	Potassium dihydrogen phosphate

L

L	Liter
LASEC	Laboratory and Scientific Equipment Company
log	Logarithm
LTR	Long terminal repeats

M

m	Signifies the sigmoidicity (shape) of the dose-effect curve
M	Molarity
Mac	Macaque
MAIDS	Murine acquired immunodeficiency syndrome
MCP	Macrophage chemotactic protein
MDM	Monocyte-derived macrophages

mg	Milligram
$MgCl_2$	Magnesium chloride
Min	Minute
ml	Milliliter
mM	Millimolar
Mnd	Mandrill
mt	Mitochondrial
MTT	3-(4,5-dimethylthiazol-2-yl)-2,5-diphenyltetrazolium bromide
MuLV	Murine leukemia virus
MVV	Maedi-visna virus
MW	Molecular weight

N

N_3	Azide
NA	Numerical aperture
NaCl	Sodium chloride
$NaHCO_3$	Sodium hydrogen carbonate
$NaH_2PO_4.H_2O$	Sodium dihydrogen phosphate-1hydrate
$Na_2HPO_4.2H_2O$	Disodium hydrogen phosphate
NK	Natural killer
Nm	Nanometer
nM	Nanomolar
NNRTI	Nonnucleoside reverse transcriptase inhibitor
NRTI	Nucleoside reverse transcriptase inhibitors

O

OsO_4	Osmium tetroxide

P

PBMC	Peripheral blood mononuclear cells
PBS	Phosphate buffered saline
PCR	Polymerase chain reaction
PEG	Polyethylene glycol
pH	Logarithmic scale used to measure the acidity and alkalinity of an aqueous solution
PI	Protease inhibitor
PMEA	9-phosphonylmethoxyethyl adenine
pmol	Picomolar
PMPA	9-phosphonylmethoxypropyl adenine (Tenofovir)
PSF	Penicillin/Streptomycin/Fungizone
p-value	Statistical significance, probability that observed relationship or difference in a sample occurred by pure chance

R

R	Linear correlation
RBC	Red blood cell
RNA	Ribonucleic acid
Rpm	Revolutions per minute
ROS	Reactive oxygen species
RT	Reverse transcriptase
RT-PCR	Reverse transcriptase polymerase chain reaction

S

SA	South Africa
SAIDS	Simian acquired immunodeficiency syndrome
SCID	Severe combined immunodeficient
Sec	Seconds
SEM	Scanning electron microscopy
SEM	Standard error of the mean
SHIV	Chimeric virus of SIV and HIV
SI	Selectivity index
SIV	Simian immunodeficiency virus
Sm	Sooty mangabeys
SPF	Specific pathogen free
SYBR	Syber
Syk	Sykes'

T

T	Thymine
Taq	Thermus Aquaticus
TBE	Tris/boric acid/EDTA
TD_{50}	Toxic dose that kills 50% of the cells
TEM	Transmission electron microscopy
Thy/liv	Thymus/liver
TNF	Tumor necrosis factor
Tris	Tris[hydroxymethyl]aminomethane
TX	Trimidox

U

U	Units
UK	United Kingdom
UPBRC	University of Pretoria Biomedical Research Centre
USA	United States of America
UV	Ultraviolet

W

WBC	White blood cell

Chapter 1: Introduction

In the development of new drugs and therapeutic strategies for the treatment of HIV/AIDS several different animal models such as the simian AIDS (SAIDS), feline AIDS (FAIDS) and murine AIDS (MAIDS) models are used (Koch and Ruprecht, 1992). MAIDS is induced by inoculating C57BL/6 mice with a complex of retroviruses termed the LP-BM5 murine leukemia virus (MuLV). LP-BM5 consists of a replication-defective virus and two helper viruses, the β-tropic replication-competent virus and a mink cell focus-inducing virus. The replication-defective virus has been identified as the disease-causing agent while the two helper viruses assist in the cell-to-cell spreading of the defective virus and thereby accelerate the progression of the disease (Chattopadhyay *et al.,* 1991; Jolicoeur, 1991; Liang *et al.,* 1996). An advantage to this model is that these viruses are non-pathogenic to humans and only replicate in the species of origin (Liang *et al.,* 1996).

MAIDS, induced in C57BL/6 mice has several similarities to HIV/AIDS in humans and is characterized by lymphadenopathy, splenomegaly, susceptibility to opportunistic infections, abnormal T and B cell functions and late onset B cell aggressive lymphomas (Chattopadhyay *et al.,* 1991; Jolicoeur, 1991; Liang *et al.,* 1996). However, there are a few differences between AIDS and MAIDS in that the major cellular targets in MAIDS are the B-cells and not the $CD4^+$ T cells as in AIDS. In spite of this, this *in vivo* model has been used to evaluate the effectiveness of known antiretroviral drugs like azidothymidine (AZT) (Eiseman *et al.,* 1991), hydroxyurea (HU) (Mayhew *et al.,* 2002, Sumpter *et al.,* 2004) and tenofovir (PMPA) (Suruga *et al.,* 1998), as well as potential antiretrovirals like tyrphostin AG-1387 (Sklan *et al.,* 2000), trimidox and didox (Mayhew *et al.,* 2002, Sumpter *et al.,* 2004).

The initial evaluation of drugs with potential antiretroviral activity usually involves the use of an *in vitro* cell culture system. Advantages of such systems are that several drugs can be rapidly and cost effectively evaluated. However, in an *in vitro* cell culture system, the absorption, metabolism, distribution, excretion and toxicity (AMDET) of the drug compound cannot be fully investigated and for these reasons, an *in vivo* animal model is used following initial drug evaluation in an *in vitro* cell culture system. Infection of SC-1 (feral mouse embryo fibroblast) cell line that is permissive to murine retroviruses (Hartley and Rowe, 1975), with the same virus as used in the *in vivo* MAIDS model holds great promise for initial drug evaluation in either acutely or chronically infected cells. This *in*

vitro cell culture system has been used by Suruga *et al.,* 1998 and Sklan *et al.,* 2000 to first assess the effect of drugs i.e. PMPA and tyrphostin AG-1387 respectively, on viral load before evaluating their efficacy in the *in vivo* MAIDS model. These drugs reduced viral load in both the *in vitro* and *in vivo* models (Suruga *et al.,* 1998, Sklan *et al.,* 2000).

The United States (US) Food and Drug Administration (FDA) has approved several drugs for the treatment of HIV/AIDS and includes nucleoside reverse transcriptase inhibitors (NRTIs) zidovudine (AZT), lamivudine (3TC) and abacavir, nonnucleoside NRTIs (NNRTIs) nevirapine, efavirenz and delaviridine, protease inhibitors (PIs) indinavir (IDV), ritonavir and nelfinavir, fusion inhibitor fuzeon (enfuvirtide,T-20), CCR5 co-receptor antagonist selzentry and integrase strand transfer inhibitor isentress and can be viewed at http://www.fda.gov/oashi/aids/virals.htlm. These drugs worked only modestly well alone and thus combination therapy was introduced. Highly active antiretroviral therapy (HAART) consists of a double or triple combination of any NRTIs, NNRTIs and PIs (Sension, 2004; Dieterich *et al.,* 2006). The use of HAART resulted in a notable decline in the morbidity and mortality of patients infected with HIV/AIDS (Correll *et al.,* 1998; Palella *et al.,* 1998; Detels *et al.,* 1999; Louwagie *et al.,* 2007). HAART, however, is also associated with several problems and these include high cost of treatment and poor availability of drugs in low-income countries (Yazdanpanah, 2004), severe adverse effects (Ter Hofstede *et al.,* 2003; Montessori *et al.,* 2004) and poor compliance (Maggiolo *et al*., 2003). Therefore the search for new, more affordable and more effective drug combination therapies is the focus of many research endeavors.

Two cheaper drugs that have been identified as having antiretroviral activity are chloroquine (CQ) and hydroxyurea (HU) (Paton *et al.,* 2002). When combined with didanosine both drugs significantly reduced the viral load and were well tolerated by patients with only mild side-effects. Furthermore several medicinal plants have been identified as having antiretroviral activity and include extracts from *Rhizophora apiculata, Hypericum polyanthemum*, *Hypericum cannatum, Urtica dioica* L., *Parietaria diffusa* M. et K. and *Sambucus nigra* L. which have been evaluated in the SAIDS and FAIDS models (Premanathan *et al.,* 1999; Schmitt *et al.,* 2001; Manganelli *et al.,* 2005). Therefore active ingredients of such medicinal plants should be isolated and studied further. Two compounds that hold great promise are Chinese green tea (*Camellia sinensis*) and its active ingredient epigallocatechin gallate (EGCg). Both have been found to have beneficial effects such as anti-carcinogenic, antibacterial, antifungal, anti-diabetic, antioxidant, antimalarial and anti-HIV activity (Nakane and Ono, 1990; Yamaguchi *et al.,* 2002; Kawai *et al.,* 2003; Zaveri, 2006; Sannella *et al*., 2007). To date,

no studies have been undertaken that specifically investigates the combined effect of drug and plant derived products such as green tea and EGCg. The possibility of a synergistic, additive or antagonistic effect should be investigated.

To be able to study the effects of drugs on the viral load *in vitro,* several different techniques can be used and these include electron microscopy, the polymerase chain reaction (PCR), reverse transcription PCR (RT-PCR), the plaque assay and enzyme linked immunosorbant assay (ELISA). Quantification of the effect of different drugs on the viral load is essential and the methods of choice are the plaque assay, quantitative and semi-quantitative PCR and ELISA. Semi-quantitative PCR has been used by Mayhew *et al*., 2002 and Sumpter *et al.,* 2004 to test the effect of HU, trimidox and didox and combinations of these drugs with abacavir on the viral load in the spleens of C57BL/6 mice infected with LP-BM5 MuLV. These drugs decreased the viral load and thus correlated with a reduction in MAIDS symptoms observed. Quantitative, real-time RT-PCR has been used by Cook *et al*., 2003 to quantitatively compare the relative amounts of the replication-defective and the ecotropic helper viruses in LP-BM5 viral stocks and murine tissues infected with LP-BM5 MuLV. It was found that the defective virus was more abundant in LP-BM5 viral stocks and LP-BM5 infected tissues of MAIDS susceptible mice. Therefore the focus of this study was to establish an *in vitro* cell culture model and to use this model to study the effect of drugs and plant derived compounds alone and in combination on the LP-BM5-defective viral load.

Chapter 2: Literature review

2.1 Introduction

Several animal models for HIV/AIDS have been established and include chimpanzees infected with HIV, simian immunodeficiency virus (SIV) model, feline immunodeficiency virus (FIV) model, ungulate lentivirus models, HIV infection of rabbits, transgenic mice, severe combined immunodeficient (SCID) mice as well as several murine oncornavirus models such as the LP-BM5 MuLV model (Koch and Ruprecht, 1992). These models have been extensively studied and have provided valuable information on the pathogenesis of HIV/AIDS as well as the efficacy of antiretroviral drugs, drug combinations and medicinal plants.

In this review the animal models that are the most widely used will be reviewed, specifically the SIV model due to similarities in the pathogenesis of disease to humans, the FIV and the LP-BM5 model due to wide availability and the SCID murine model that combines components of both systems. The pathogenesis of disease, the use of each model in the evaluation of drugs, drug combinations and plant extracts for antiretroviral activity either in the animal model or in the *in vitro* cell culture equivalent will be discussed in addition to the inherent advantages and disadvantages of using each model.

2.2 Animals models for HIV/AIDS

Twenty different animal models have been used to study HIV/AIDS (Kindt *et al*., 1992; Koch and Ruprecht, 1992; Lewis and Johnston, 1995) and are listed in Table 2.1.

Table 2.1 Animal models for the study of HIV/AIDS

Animal	Virus	Disease	Reference
Primate			
African Green Monkey	SIV_{agm}	Virus actively replicates but animals do not develop immunodeficiency	Norley ,1996
Sooty Mangabeys	SIV_{sm}	Chronically viremic but do not develop any disease	Ansari , 2004
Mandrill monkey	SIV_{mnd}	High levels of viremia but its non-pathogenic to the host	Onanga *et al*., 2002
Sykes' monkey	SIV_{syk}	Persistently infected but remain clinically healthy	Hirsch *et al*., 1993
Rhesus monkeys	$SIV_{mac/sm}$	AIDS-like disease with immunodeficiency and opportunistic infections	Hirsch *et al*., 1994
Cynomolgus monkeys	SIV_{mac}	AIDS-like disease with immunodeficiency	Giavedoni *et al.,* 2000
Pigtail monkeys	$SIV_{sm/agm}$	AIDS-like disease with immunodeficiency	Hirsch *et al.,* 1994
Chimpanzees[#]	HIV	Long-term persistent infection but no signs of clinical disease	Fultz *et al.,* 1989
Rhesus, pig-tailed, cynomolgus and bonnet monkeys	SHIV chimeric virus of SIV and HIV	AIDS-like disease with organ-specific diseases	Joag *et al.,* 1997
Ungulates			
Cows	BIV	Persistent lymphocytosis and lymphadenopathy	Carpenter *et al.,* 1992
Goats	CAEV	Arthritis, encephalomyelitis, wasting, pneumonia	Straub *et al.,* 1989
Sheep	MVV	Progressive pneumonia, encephalomyelitis	Petursson *et al.,* 1989
Horses	EIAV	Fever, weight loss, anemia, edema	Coggins *et al.,* 1986
Feline			
Cats	FIV	AIDS-like disease in naturally infected cats. Experimental cats do not develop fatal immunodeficiency	Willet *et al.,* 1997
Murine			
SCID Mice	HIV	Severe $CD4^+$ T-cell depletion can remain persistently infected for 16 weeks	Pincus *et al.,* 2004
Transgenic Mice	Complete HIV-1 proviral sequences, subgenomic fragments or reporter genes linked to HIV-1 LTR	Skin and renal lesions, cardiomyopathy, nephropathy, CNS damage, immunoabnormalities	Pincus *et al.,* 2004
Mice	LP-BM5 MuLV	Lymphadenopathy, splenomegaly and hypergammaglobulemia. Mice die of respiratory failure	Jolicoeur *et al.,* 1991
Mice	Moloney MuLV	Chronic T-cell lymphopoiesis and leukemia	Fan *et al.,* 1991
Mice	Friend MuLV	Hepatosplenomegaly, anemia and leukemia	Koch *et al.,* 1992
Mice	Rauscher MuLV	Lymphoid leukemia, erythrocytopoiesis, splenomegaly	Rauscher *et al.,* 1962

Research with chimpanzees infected with HIV/SIV is now banned in several countries.

Four different classes of animal models shown in Table 2.1, namely primate, ungulate, feline and murine models are available for the study of HIV/AIDS. The rabbit and the rat models were excluded from Table 2.1. Rabbits can be experimentally infected with HIV however these animals fail to develop any AIDS-like symptoms despite p24 detection and isolation of HIV from peripheral blood mononuclear cells (PBMC) (Kulaga *et al*., 1998). Recently it was discovered that cotton rats could be infected with HIV and proviral HIV DNA could be isolated from the spleen and brain (Rytik *et al.,* 2004). The rats developed fever, weight loss, pulmonary disorders and inflammatory reactions in the brain and spleen. This rat model appears to hold great promise but it has not been widely used.

The purpose of this study was to identify a model from each class of animal that is most frequently used for the evaluation of drugs and plant extracts. In the primate and feline class, macaques infected with African SIV strains and specific pathogen-free cats infected with FIV respectively were identified as models most frequently used for drug and plant extract evaluation. From the ungulate class, no animal model was selected as these are very large experimental animals and these animals are rarely used for the evaluation of drugs or plant extracts. The murine class could be further subdivided into murine models infected with HIV, the SCID murine model and murine models infected with murine leukemia virus, the LP-BM5 model.

The pathogenesis of disease in each model, application in the evaluation of drugs, drug combinations and plant extracts as well as the inherent advantages and disadvantages of each model are discussed. A comparison of the genetic organization of the virus in HIV, SIV, FIV and MuLV is shown in Figure 2.1.

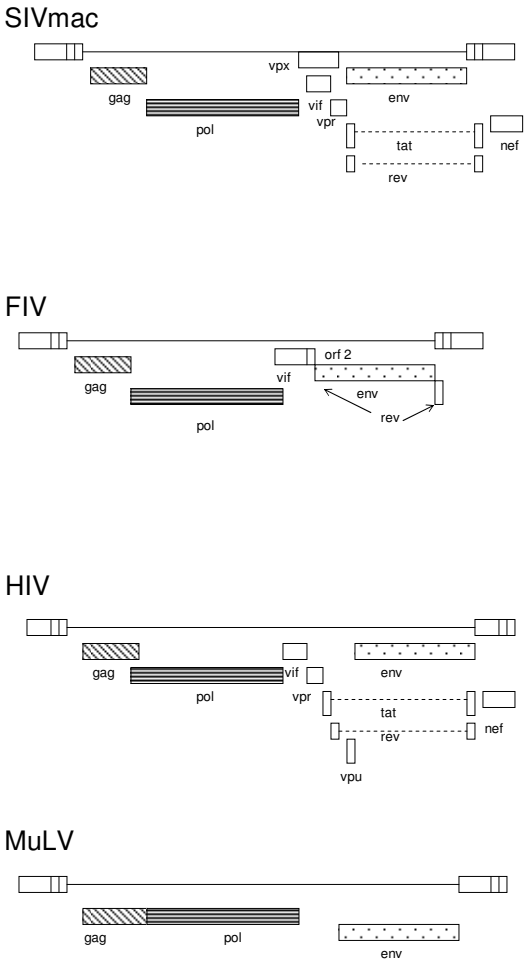

Figure 2.1. Comparison of the genetic organization of SIV, FIV, HIV and LP-BM5 MuLV.

2.3 The Simian immunodeficiency virus model

The Simian immunodeficiency viruses (SIVs) are perhaps the closest known relatives of HIV-1 and HIV-2 with very similar genomic organization. Several SIV isolates have been identified: SIV_{mac}/SIV_{sm} isolated from sooty mangabeys, SIV_{agm} from healthy African Green monkey, SIV_{mnd} from mandrills, SIV_{syk} from Sykes' monkey and SIV_{cpz} isolated from healthy chimpanzees (Hirsch *et al.,* 1995). It is speculated that HIV-1 originally arose from SIV_{cpz} and HIV-2 from SIV_{sm}. African Green monkeys and sooty mangabeys naturally infected with SIV_{agm} and SIV_{sm} respectively remain asymptomatic throughout their life and do not develop any disease despite being persistently infected (Norley, 1996; Ansari, 2004). In contrast macaque monkeys such as *Macaca mulatta* (rhesus monkeys)*, M. nemenstria* (pigtail monkeys) and *M. fascicularis* (cynomolgus monkeys) infected with SIV_{mac} or SIV_{sm} develop fatal disease characterized by severe immunodeficiency, susceptibility to opportunistic infections and finally death and have

been reviewed by Hirsch and Johnson, 1994. Due to the pathogenesis of disease being similar to HIV in humans, these experimentally infected monkeys have been used extensively to study the pathogenesis of HIV/AIDS, test antiviral efficacy of several compounds as well as develop and test vaccines.

Following inoculation of monkeys like *M. mulatta* or *M. fascicularis* with SIV_{mac} 251, the virus spreads rapidly and can be detected 4 days post-infection (Otani *et al.*, 1998). Plasma viremia normally peaks at 8-14 days post-infection and then gradually decreases to a steady-state level by 2 months (Schmitz *et al.,* 1999; Staprans *et al.,* 1999; Monceaux *et al.,* 2003; Mattapallil *et al.,* 2004). Clearance of plasma viremia is associated with the appearance of SIV-specific $CD8^+$ cytotoxic T-lymphocytes (CTL) and neutralizing antibodies. These two immune responses are responsible for controlling primary SIV infection (Schmitz *et al.,* 1999 and 2003). If these two immune responses are unable to reduce plasma viremia the animals rapidly progress to AIDS.

Lymphopenia with a loss of B-cells occurs in the peripheral blood during the first week of infection while T-cell counts stay steady for several weeks before decreasing to below control levels (Mattapallil *et al.,* 2004). This initial steady state is due to a decrease in CD4 T-cells that is compensated by an initial increase in CD8 T-cells. As the viral load decreases, the CD8 T-cells also decrease resulting in a decrease in total T-cell counts. There is also a loss in naïve CD4 and naïve CD8 cells early in infection and this may represent changes in homeostatic control mechanisms i.e. homing of CD4 memory T-cell subsets from the periphery to secondary lymphoid organs. There are also changes in the CD8 memory T-cell subset. Early after infection there is an expansion of fully differentiated CD8 memory T-cells followed by a decrease and replacement of differentiated CD8 memory T-cells by undifferentiated cells.

In the lymph nodes, productively infected cells can be detected 5-8 days post infection and the viral RNA levels in the T-cells parallels p27 antigenemia in the blood (Reimann *et al.,* 1994). The proportion of B cells in the lymph nodes is initially increased but then returns to normal levels (Giavedoni *et al.,* 2000). There is also a decrease in $CD4^+$ T-cells nodes and increase in $CD8^+$ T-cells that correlates with clearance of plasma antigenemia (Reimann *et al.,* 1994).

SIV infection also induces cytokine dysregulation. High viral loads are associated with high levels of IFN-α/β and if the plasma IFN-α/β persists, the animals will progress rapidly to disease (Giavedoni *et al.,* 2000). Other cytokines that are also found to

increase during infection are IL-12, IL-18, IL-1β, IL-6, TNF- α and IL-10 (Benveniste *et al.*, 1996; Giavedoni *et al.,* 2000).

If the animals are able to control primary infection, an asymptomatic phase occurs that is characterized by low or undetectable levels of plasma viremia and the animals appear to be healthy. A strong SIV-specific antibody response controls viral replication and maintains low levels of viremia. During this phase that can vary from a few months to years there is a continued depletion of CD4 lymphocytes and a progression in lymph node pathology (Monceaux *et al.,* 2003).

The terminal phase of disease is characterized by immunodeficiency, disseminated opportunistic infections and SIV invasion of most tissues. A decline in $CD4^+$ lymphocytes occurs, disruption of macrophage functions, increased viral burden in the lymph nodes, spleen and plasma and a widespread dissemination of SIV in almost all the tissues and organ systems especially the gastrointestinal tract (GIT) with many animals dying from gastrointestinal dysfunction (Hirsch *et al.,* 1991). Infected monkeys are also more susceptible to opportunistic infections such as cytomegalovirus (Sequar *et al.,* 2002), microsproridia infections (Green *et al.,* 2004) and *Mycobacterium bovis* infections (Shen *et al.,* 2001).

2.3.1 SIV induced central nervous system (CNS) disease

Infection of *M. nemenstria* with a macrophage tropic and neurovirulent recombinant virus SIV/17E-Fr and an immunosuppressive virus SIV/DeltaB670 serves as a good model for the study of SIV invasion of the CNS. SIV enters and replicates in the CNS during the acute phase of infection, then becomes undetectable and re-appears 2 months post-infection (Mankowski *et al.,* 2002). Viral RNA is down-regulated after acute infection while viral DNA persists in all parts of the brain at steady-state levels throughout infection (Clements *et al.,* 2002). $CD4^+$ cells are the predominant cell type in the brain parenchyma of uninfected and acutely infected monkeys. There is an increase in the $CD8^+$ lymphocyte population in animals with moderate to severe encephalitis (Mankowski *et al.,* 2002). Severity of encephalitis can also be correlated with increased viral load, elevated levels of IL-6 and macrophage chemotactic protein-1 (MCP-1) in the cerebrospinal fluid (CSF) (Mankowski *et al.,* 2004).

In *M. nemenstria* inoculated with SIV_{smmFGb}, infection results in lesions of the brain parenchyma and includes perivascular accumulation of macrophages, multinucleated

giant cells and lymphocytes, parenchymal giant cells, microglial nodules, parenchymal granulomas and vacuolation of white matter tracts of the cerebrum and cerebellum often associated with choriomeningitis (O' Neil *et al.,* 2004). Physiological abnormalities can be detected within the first month in *M. mulatto* infected with SIV_{mac251} and include increase in temperature, decrease in motor activity and changes in auditory-evoked potentials (Horn *et al.,* 1998).

2.3.2 Evaluation of antiviral therapy

The SIV *in vivo* and *in vitro* cell culture models have extensively been used to assess the efficacy of several antiretroviral drugs and plant extracts. The animals that have been used are Rhesus monkeys infected with SIV_{mac239}, SIV/deltaB670, SIV_{smE66} and SIV_{mac251} and Cynomolgus monkeys infected with SIV_{mac251}, $SIV_{mac251/32H}$. *In vitro* cell culture models include human PBMC infected with SIV/deltaB670*,* co-cultures of human $CD4^+$ Molt-4 cells and persistently infected Jurkat/SIV_{agm} cell, MT4 and 174 x CEM cells with SIV_{mac251}, CEM-SS T-cells with SIV (Delta), MT4 cells with SIV_{mac}, Molt-4 cells with SIV_{agm3} or SIV_{mndGB1}. Several drugs including N-aminoimidazoles, methionine enkephalin and NNRTIs: tivirapine, loviride, delavirdine, nevirapine, pyridinone, MCK-442, drug combinations such as AZT, IDV and lamivudine as well as HU and *Rhizophora apiculata* (mangrove plant) extracts have been evaluated and the findings are summarized in Table 2.2.

2.3.3 Advantages and disadvantages

The advantages in using the SIV model are that the viral genome has great homology with HIV (Figure 2.1), and the disease and disease progression are very similar to HIV/AIDS. The use of an equivalent *in vitro* cell culture model allows rapid evaluation of drug toxicity and efficiency in reducing proviral DNA incorporation and viral replication in the host cell. Drugs with beneficial effects are subsequently used in the *in vivo* animal model to confirm antiretroviral activity and to determine the AMDET of the drug or drug combination. This model has several disadvantages and these include the high cost of the animals (macaques cost between $5 000-$12 000 per animal) and housing. Also, availability of animals is limited and there is a risk to investigators of SIV infection and therefore specialized laboratory facilities are required (Sotir *et al.,* 1997).

Table 2.2 Drugs, drug combinations and plants extracts evaluated in the SIV animal model

Compound	*In vitro/ in vivo*	Results	Reference
6-Chloro2',3'dideoxy guanosine	*In vivo* Rhesus monkeys with SIV_{mac239}	↓ viral burden and suppressed hyperactivation of B-cell proliferation	Otani *et al.,* 1997
Cyclosporin A	*In vitro* human PBMC with SIV/deltaB670	Did not suppress SIV replication by measurement of p27 levels.	Martin *et al.,* 1997
	In vivo Rhesus monkeys with SIV/deltaB670	↓ duration of antigenemia, transient ↓ in virus burden, slower loss of $CD4^+$ cells	
Synthetic ajoene (active principle of garlic)	*In vitro* Co-cultures of human $CD4^+$ Molt-4 cells with persistently infected Jurkat/SIV_{agm} cells	Inhibited SIV-mediated cell fusion	Walder *et al.,* 1998
Interferon	*In vitro* MT4 and 174 x CEM cells with SIV_{mac251}	Blocked early stage of SIV replication, step between attachment and reverse transcription	Taylor *et al.,* 1998
Didanosine/ddI	*In vivo* Cynomolgus monkeys with SIV_{mac251}	↓ in viral load during acute infection, transient ↑ in IL6, IL1β, TNFα, IL10	Gigout *et al.*, 1998
12-oxocalonolide A (non-nucleoside reverse transcriptase inhibitor NNRTi)	*In vitro* CEM-SS T-cells with SIV (Delta)	Inhibited SIV replication	Xu *et al.*, 1999
Extract from *Rhizophora apiculata* (mangrove plant)	*In vitro* MT4 cells with SIV_{mac}	Inhibited virus-induced cytopathogenicity	Premanathan *et al.,* 1999
NNRTIs: tivirapine, loviride, delavirdine, nevirapine, pyridinone, MCK-442	*In vitro* MT4 cells with SIV_{mac} and Molt-4 cells with SIV_{agm3} or SIV_{mndGB1}	All NNRTIs inhibited SIV_{agm3}, nevirapine, delavirdine and pyridinone not effective against SIV_{mac251} and SIV_{mndGB1}. The concentrations required to inhibit the SIV strains were 50-fold the concentrations required to inhibit HIV-1.	Witvrouw *et al.,* 1999
Tenofovir/PMPA	*In vivo* Rhesus monkeys with SIV_{smE660}	Did not block infection but prevented establishment of persistent productive infection	Lifson *et al.,* 2000
Thalidomide	*In vivo* Cynomolgus monkeys with $SIV_{mac251/32H}$	Inhibited TNFα production, restored proliferative responses to SIV peptides, no reduction in viral burden	Di Fabio *et al.*, 2000
Protease inhibitors: IDV, saquinavir, ritonavir	*In vitro* HeLa H1-JC.37 cell line, 174 x CEM cells and PBMC with SIV_{mac239}, SIV_{mac251} and 3' half clone of SIV_{mac239}	Susceptibility to the protease inhibitors was similar to HIV	Giuffre *et al.*, 2003
AZT, IDV and lamivudine combination	*In vivo* Cynomolgus monkeys with SIV_{mac251}	Did not prevent infection but one treatment regimen allowed better control of viral replication	Benlhassan-Chahour *et al.,* 2003
N-aminoimidazoles	*In vitro* MT4 cells with SIV_{mac251}	18 derivatives were capable of inhibiting SIV replication, 7 were equally potent inhibitors of HIV-1, HIV-2 and SIV	Lagoja *et al.*, 2003

Table 2.2 Cont'd

Methionine enkephalin	*In vitro* 174 x CEM cells with SIV_{mac239}	Enhanced viability of SIV-infected cells and ↓ number of apoptotic cells	Li *et al*., 2004
Hydroxyurea, PMPA and didanosine combination	*In vivo* Rhesus monkeys with SIV_{mac251}	↑ peripheral CD4 T cells without affecting expression of activation markers	Lova *et al*., 2005
Tenofovir/PMPA	*In vivo* Rhesus monkeys with SIV_{mac251}	↓ mucosal viral loads, restoration of $CD4^+$ T cells in GALT and peripheral blood	George *et al*., 2005

↑: increase, ↓: decrease

2.4 Feline immunodeficiency virus

The feline immunodeficiency virus (FIV) is a T-lymphotropic lentivirus that shares some homology with HIV and other lentiviruses (Talbott *et al.,* 1989). FIV was first isolated from a group of immunodeficient cats in Petaluma, California and has subsequently been found to infect cats in all parts of the world (Pedersen *et al.,* 1987; Carpenter *et al.,* 1998). This immunodeficiency is not limited to feral and domesticated cats but can also be induced experimentally in specific pathogen free (SPF) cats (Kohmoto *et al.,* 1998). These cats, however, can take several years (more than eight years) to develop the fatal immunodeficiency as they are kept in a pathogen-free environment and thus their exposure to other pathogens is limited. The FIV model for HIV has been reviewed by Willet *et al.,* 1997.

Following infection, plasma virus and PBMC-associated virus can be detected 2 weeks post-infection (Beebe *et al.,* 1994). FIV proviral DNA can be detected as early as 1 week post-infection in the peripheral and mesenteric lymph nodes and peaks at 8 weeks in all lymph nodes (Flynn *et al.,* 2002). Serum antibodies become detectable from 2 weeks post-infection (Beebe *et al.,* 1994). Cats develop a flu-like illness characterized by fever, diarrhea, dehydration and depression by 4-5 weeks following infection. Leucopenia with lymphopenia and neutropenia are also present and a decrease in the percentage and absolute number of $CD4^+$ cells after inoculation occurs that remains low throughout infection (Ackley *et al.,* 1990; Torten *et al.,* 1991; Hoffmann-Fezer *et al.,* 1992; English *et al.,* 1993; Dean *et al.,* 1996). $CD8^+$ cells, however, are found to increase following infection with a subsequent decrease in the $CD4^+/CD8^+$ cell ratio followed by an inversion of the ratio (Ackley *et al.,* 1990; Torten *et al.,* 1991; Hoffmann-Fezer *et al.,* 1992; English *et al.,* 1993; Beebe *et al.,* 1994). B-cell percentage and absolute number in the peripheral blood are not significantly altered nor are there significant changes in serum IgM and IgA. There is however, a significant elevation in IgG levels 2 years after infection (Ackley *et al.,* 1990).

Unlike HIV and SIV, FIV has a broader cell tropism by infecting Ig+/B cells in addition to $CD4^+$, $CD8^+$, monocytes/macrophages (English *et al.,* 1993; Beebe *et al.,* 1994; Magnani *et al.,* 1995; Dean *et al.,* 1996). During acute and chronic infection, FIV provirus can be detected in $CD4^+$, $CD8^+$ and B-cells with the highest viral burden occurring in $CD4^+$ cells during the acute infection and B cells during chronic infection. A decrease in the $CD4^+$

cell population is caused by the elimination of cells, immune responses targeting infected cells or changes in $CD4^+$ cell turnover kinetics (Dean *et al.,* 1996).

The non-cytolytic T-cells (non-CTL) elicit the first antiviral immune response to FIV and activity can be detected in the peripheral and mesenteric lymph nodes, spleen and blood 1 week after inoculation (Flynn *et al.,* 2002). Virus-specific CTL responses are only detected in the blood 4 weeks post-infection and much later in the spleen and lymph nodes. The cell-mediated suppression of FIV-replication can be detected at 4 weeks post-infection and corresponds with the appearance of virus-specific CTL. Suppressor activity declines at week 8 post-infection, peaks again at 47 weeks and is absent in blood at 113 weeks. Long-term infection with FIV results in a progressive immune dysfunction characterized by an absence of primary and secondary antibody responses to T-dependent immunogens but these animals retain the ability to elicit primary antibody responses to T-independent antigens (Siebelink *et al.,* 1990; Torten *et al.,* 1991).

Lymphadenopathy is associated with FIV infection and the virus can be detected in the lymph nodes, spleen, gut-associated lymphoid tissue (GALT), bone marrow, thymus and tonsils (Beebe *et al.,* 1994). Lesions are observed in the peripheral and central lymphoid organs as well as non-lymphoid organs and are characterized by a progressive hyperplasia and infiltration of lymphocytes, lymphoblasts, macrophages and apoptotic cells (Callanan *et al.,* 1993; Beebe *et al.,* 1994).

2.4.1 FIV CNS disease

FIV infection of the CNS is associated with several neurological abnormalities. These include development of a persistent anisocoria (inability of iris to constrict completely in response to light) by 3 months post-infection, intermittent delayed righting reflex and papillary responses, delays in auditory and visual evoked responses and dramatic changes in sleep patterns. Virus can be isolated from cerebral cortex, midbrain and cerebellum while FIV-specific antibodies can be detected in the CSF (Phillips *et al.,* 1994). Neuronal loss and glial activation is accompanied with increased levels of glutamate. Widespread gliosis, perivascular cuffing and activation of astrocytes and microglia are observed while neuronal dropout is confined to the frontal cortices and basal ganglia (Power *et al.,* 1997).

2.4.2 Antiviral drug testing in FIV model

The FIV *in vivo* model used for antiviral testing includes SPF cats infected with FIV-Petaluma or FIVUK8 and female cats infected with FIV-CABCpady00C. The *in vitro* cell culture model makes use of different cell types or cell lines and includes MYA-1 cells infected with the FIV strain T91 or N91, the fetal glial cell line G355-5 infected with FIV-34TF10 or PPR-34TF10env chimeric virus, Crandell feline kidney cells infected with FIV-Petulama *or* FIV-34TF10 or PBMC infected with FIV-Petaluma. Drugs like AZT, cyclosporin, dehydroepiandrosterone (DHEA) and dideoxycytidine 5'-triphosphate, drug combinations like AZT/3TC and plant extracts of *Hypericum caprifoliatum, H. polyanthemum* and *H. cannatum* and *Urtica dioica L.*, *Parietaria diffusa M. et K.* and *Sambucus nigra L.* have been evaluated in the FIV model and the findings of these studies are presented in Table 2.3.

2.4.3 Advantages and disadvantages

The advantages of this model are that FIV is a lentivirus like HIV and has some homology to the HIV virus (Figure 2.1). The disease and disease progression also shares several similarities with HIV/AIDS. The virus is non-pathogenic to humans and is available in the *in vitro* cell culture and *in vivo* animal format. Another advantage is that cats are widely available and one can use SPF or domestic cats. The disadvantages are that SPF cats are fairly expensive ($500-$800) and the fatal immunodeficiency takes a long time to develop. All cats including control animals are at risk of becoming infected, as FIV is a natural host-virus system.

Table 2.3 Drugs, drug combinations and plant extracts evaluated in the FIV animal model

Compound	*In vitro/ in vivo*	Results	Reference
AZT and cyclosporine separately	*In vitro* MYA-1 cells with FIV strain T91 or N91	Only AZT tested *in vitro*. Dose-dependent protection against FIV-induced cell death as well as dose-dependent decrease in RT activity.	Meers *et al*., 1993
	In vivo Conventional adult cats with FIV	Drugs did not prevent infection but lowered plasma virus titers at two weeks p.i. but levels then increased. No effect on PBMC virus titers.	
Dehydroepiandrosterone (DHEA)	*In vitro* Feline T cell FL4 with FIV-Petaluma	Inhibited RT activity as measured in culture supernatants	Bradley *et al.,* 1995
Dideoxycytidine 5'-triphosphate	*In vitro* Monocyte-derived macrophage and peritoneal macrophage cell cultures with FIV	Reduced FIV production by macrophages	Magnani *et al.,* 1995
	In vivo SPF cats with FIV isolate Pisa-M2	Protected most peritoneal macrophages	
9-[2R,5R-2,5-dihydro-5-phosphonomethoxy)-2-furanyl]adenine (D4API)	*In vitro* PBMC with FIV-Petaluma	Higher efficacy than AZT and PMEA but with more toxicity.	Hartmann *et al.,* 1997
	In vivo SPF cats with FIV-Petaluma	Abolished viremia and antibody responses but was severely toxic causing death of animals.	
Hypericum caprifoliatum, H. polyanthemum and *H. cannatum*	*In vitro* Crandell feline kidney cells with FIV-34TF10	Methanol extracts of *H. polyanthemum* and *H. cannatum* ↓ FIV in culture supernatant	Schmitt *et al*., 2001
AZT/3TC combination	*In vitro* Feline T-cell lines chronically infected with FIVPet(FL-4 cells), FIVBang (FIVBang/FeT-J cells), FIVShi (FIVShi/FeT-J cells) or T-cell enriched PBMC with FIVUK8	Inhibition of FIV replication in T-cell enriched cultures. Combination had an additive to synergistic effect on this culture. No significant effects on RT activity as measured in cell culture supernatant of the chronically infected T-cell lines	Arai *et al.,* 2002
	In vivo SPF cats with FIVUK8	Majority of cats were completely protected from FIV infection. Others showed delay in infection and antibody seroconversion. Toxicity seen at high doses	
1,8-Diaminooctane	*In vitro* Crandell feline kidney cells with FIV-34TF10	↓ viral replication in dose-dependent manner, ↓ Rev-dependent CAT system expression, ↓ unspliced and singly spliced viral mRNAs	Hart *et al.,* 2002
DNA binding polyamides	*In vitro* Fetal glial cell line G355-5 with FIV-34TF10 or PPR-34TF10env chimeric virus	↓ replication of FIV	Sharma *et al.,* 2002

Table 2.3 Cont'd

Protease inhibitor TL-3	*In vivo* Female cats with FIV-CABCpady00C	Did not prevent viremia but ↓ viral loads and ↑ survival rate of symptomatic cats	De Rozieres *et al.,* 2004
Extracts from plants *Urtica dioica L., Parietaria diffusa M. et K.* and *Sambucus nigra L.*	*In vitro* Crandell feline kidney cells with FIV-Petulama	All extracts showed antiviral activity against FIV by inhibiting syncytia formation	Manganelli *et al.,* 2005

↑, ↓ as in Table 2.2

2.5 Severe combined immunodeficient (SCID) murine model

Severe combined immunodeficient (SCID) mice carry an autosomal, recessive mutation that prevents them from producing functional B and T lymphocytes (Bosma *et al.,* 1983). The mice are unable to repair double-stranded DNA breaks or recombine their VDJ regions (Hendrickson *et al.,* 1991). However, these mice continue to have a normal innate immunity with functional macrophages and natural killer activity (Davis and Stanley, 2003). Due to this SCID mutation, mice can be reconstituted with human tissues such as human thymus, liver, lung, lymph nodes, PBMC, U937 cells, HIV-infected monocytes, intestinal tissue and vaginal tissue (Namikawa *et al.,* 1990; Kaneshima *et al.,* 1991; Hasselton *et al.,* 1993; Grandadam *et al.,* 1995; Persidsky *et al.,* 1996; Gibbons *et al.,* 1997; Lapenta *et al.,* 1997; Kish *et al*., 2001). The SCID mouse model for studying HIV has been reviewed by Goldstein *et al.,* 1996.

2.5.1 The thy/liv model

Human fetal thymus and liver of about 14-23 gestational weeks are implanted in SCID mice under the left or right or both kidney capsules (Namikawa *et al.,* 1990; Kollmann *et al.,* 1994; Jamieson *et al.,* 1996). The two tissues fuse and form a co-joint organ called the thy/liv implant (Jamieson 1996). This co-joint organ can sustain continued human T lymphopoiesis for a year and T cells can be detected in the peripheral circulation at 6 months (Namikawa *et al.,* 1990). The grafts have the appearance of normal human thymus with normal architecture and active T cell lymphopoiesis can be seen in the cortical and medullary areas (Namikawa *et al.,* 1990; Jamieson *et al.,* 1996). Thymocytes, hematopoietic blast cells, immature and mature forms of myelomonocytic cells and megakaryocytes are present and these implants have human progenitor cell activity for CFU-c, colonies of CFU-GM and BFU-E (Namikawa *et al.,* 1990).

Mice can be infected with HIV either by direct injection of the implant with HIV or by intraperitoneal injection (Kollmann *et al.,* 1994). HIV can be isolated from thymocytes, splenocytes and PMBC 1 month after infection. HIV *gag* DNA and RNA as well as *tat/rev* mRNA can be detected in the implant, PMBC, spleen and lymph nodes. This indicates that productive infection has been established and active viral replication is occurring. After HIV infection there is an increased expression of TNF-α, TNF-β and IL-2 mRNA in the peripheral lymphoid compartment. HIV can also be detected in $CD4^+$ cells and this is associated with a rapid depletion of these cells at about 3 weeks post-infection with the

majority of cells being depleted within a 6-day period (Jamieson *et al*., 1997). The viral burden peaks when the $CD4^+$ cell depletion occurs and then begins to decrease, as the $CD4^+$ cells are almost all lost. It is suggested that this depletion is caused by direct viral killing of the cells rather than by apoptosis.

This model has also been engrafted with syngeneic human fetal large intestine tissue to create a model that may serve useful to study the mucosal transmission of HIV (Gibbons *et al.,* 1997). Closure of the ends of the implant occurs 4 months after implantation and a lumen is formed that contains histologically normal GIT mucosa. $CD4^+$ cells are scattered throughout the lamina propria and appear to have migrated from the thy/liv implant since these cells are not seen in mice that only receive an intestinal implant. The mice are infected with HIV by injecting HIV into the intestinal implant or into the thy/liv implant. Scattered HIV-infected cells are seen in the intestinal crypts and the lamina propria when either infection route is used. This shows that HIV can spread from the intestine and infect the thy/liv implant or it could spread from the thy/liv implant and infect the intestinal implant.

2.5.2 The hu-PBL-SCID model

This model was developed in attempt to overcome the difficulties of obtaining human fetal thymus and liver tissue for the thy/liv model. SCID mice are injected intraperitoneally with human PBMC (Mosier, 1996). There is survival and expansion of human $CD3^+$ T cells as well as small number of B cells, monocytes and NK cells. $CD3^+$ T cells show signs of activation and the memory T cells in $CD4^+$ and $CD8^+$ subsets are selectively expanded. A low number of T-cells are found in the peripheral blood and other lymphoid organs. Human B cells survive as differentiated plasma cells and are found in the lymph nodes and as cell adhesions to the peritoneal cavity. Immunoglobulin production can occur for up to a year. A small number of monocytes/macrophages can also be observed in lymphoid tissue. No human cells are detected in the thymus but are found in the perithymic lymph nodes adjacent to the thymic capsule.

HIV can be introduced by either intraperitoneal injection of the virus or by injecting the mice with HIV-infected PBMC (Mosier *et al.,* 1991; Koup *et al.,* 1994; Boyle *et al.,* 1995). Mice that are infected intraperitoneally become infected after 3-4 weeks but then the percentage of infected mice decreases between 6-8 weeks. Some animals can remain persistently infected for 16 weeks (Mosier *et al.,* 1991). HIV can be detected in plasma,

spleen, peritoneal lavage, peripheral blood lymphocytes, thymus, bone marrow and lymph nodes but can be more frequently isolated from the peritoneal lavage (Mosier *et al.,* 1991; Koup *et al.,* 1994). HIV p24 antigen can be detected in plasma, spleen and peritoneal lavage, but no antibodies to HIV can be detected. In mice that are infected by reconstitution with HIV-infected PBMC virion, RNA can first detected after 7 days, peaks on day 11 and persists through day 17 (Boyle *et al.,* 1995). Severe $CD4^+$ lymphocyte depletion is observed 18-25 days after engraftment in the infected mice and the human immunoglobulin produced has a broad reactivity against HIV. HIV can be detected in the spleen, blood and peritoneal wash cells. This latter method of infection may be more valuable as the viral strains are obtained from the donor and directly transferred to the mice without manipulations in cell culture. Also, key elements of the host immune response may be transferred.

2.5.3 HIV encephalitis SCID model

HIV-infected monocyte-derived macrophages (MDM) can be injected into the caudate, putamen, internal capsule and cortex of SCID mice (Persidsky *et al.,* 1996; Limoges *et al.,* 2000). These mice develop a disease pathologically similar to HIV encephalitis characterized by astrogliosis, neuronal injury and inflammatory response. MDM are immune activated and express HLA-DR, IL-1β, IL-6 and TNF-α (Persidsky *et al.,* 1996). HIV p24 positive cells can be detected (Limoges *et al.,* 2000). MDM can migrate and their migration results in the initiation of pathological changes in brain tissue distant from the site of initial injury (Persidsky *et al.,* 1996). The spread of infection is accompanied by cytopathic effects and includes multinucleated giant cell formation (Limoges *et al.,* 2000). Neural-inflammatory cell responses start soon after inoculation and neural damage is observed 3 days after inoculation and is prominent around the HIV-infected cells (Persidsky *et al.,* 1996). Pronounced astrogliosis, formation of migroglial nodules and signs of widespread migroglial activation is seen around the MDM (Limoges *et al.,* 2000). There is a direct correlation between the number of virus-infected cells, astrogliosis and neuronal damage. A disadvantage of this model is that it does not allow for the study of regional differences and since there is no intact CNS, the anatomical and neuropathological events cannot be correlated (Persidsky *et al.,* 1996).

2.5.4 Antiviral therapy testing

The SCID models, with SCID mice reconstituted with human fetal lymph node, lymphocytes, peripheral blood leukocytes, fetal thymus and liver, U937 cells, HIV-infected monocyte-derived macrophages have been used during the last decade to assess the short-term efficacy of several antiviral compounds. These drugs include bis(heteroaryl)piperazines (BHAPs), 2'-β-fluoro-2',3'-dideoxyadenosine (fddA), MDL 74,968 (acyclonucleotide derivative of guanine), nucleoside reverse transcriptase inhibitors (NRTIs): Abacavir, AZT, lamivudine, didanosine, stavudine and the findings of these studies are summarized in Table 2.4.

2.5.5 Advantages and disadvantages

The advantages identified with this model are that it is a small animal model; the mice are widely available and are excellent models for rapid drug evaluation. Another advantage is that this model makes use of HIV and many aspects of disease and disease progression is similar to that described for SIV and HIV/AIDS. Inbred mice are used in this model and this may been seen as both an advantage and disadvantage. The advantage is that because the mice are genetically identical, there should be less experimental variation that is better for statistical purposes. The disadvantage to using inbred mice is that one cannot assess whether the drug would work differently amongst different individuals. The other disadvantages are that this model is fairly difficult to establish and reconstitution success is not one hundred percent. The availability and the ethical issues surrounding the acquisition of fetal tissue are further factors that need to be considered.

Table 2.4 Drugs and drug combinations evaluated in the SCID murine model

Drug	Model	Results	Reference
Bis(heteroaryl)piperazines (BHAPs)	SCID mice reconstituted with human fetal lymph node	Could block HIV replication but not as effective as AZT	Romero *et al*., 1991
AZT	SCID mice reconstituted with human lymphocytes	Dose-response reduction in p24 antigen levels	Alder *et al.,* 1995
2'-β-fluoro-2',3'-dideoxyadenosine (fddA)	SCID mice reconstituted with human peripheral blood leukocytes	↓ frequency of viral recovery from peritoneal and splenic tissues, ↓ $CD4^+$ T cell depletion	Boyle *et al.,* 1995
Sulfated pentagalloyl glucose (Y-ART-3)	SCID mice reconstituted with human peripheral blood leukocytes	↓ frequency of mice infected with HIV but not statistically significant. But semi-quantitative measure of HIV detection showed significant effect of drug.	Nakashima *et al.,* 1996
MDL 74,968 (acyclonucleotide derivative of guanine)	SCID.beige mice reconstituted with human peripheral blood leukocytes	↓ in virus burden and severity of infection	Bridges *et al*., 1996
SID 791 (a bicyclam)	SCID mice reconstituted with human fetal thymus and liver	Inhibition of p24 antigen formation, dose-dependent ↓ in viremia	Datema *et al.,* 1996
Saquinavir	SCID mice reconstituted with human fetal thymus and liver	HIV infection was not prevented but viral loads were significantly ↓	Pettoello-Mantovani *et al*., 1997
Type 1 consensus interferon (CINF)	SCID mice reconstituted with human U937 cells	Suppression of HIV infection and ↓ CD4 T cell depletion	Lapenta *et al.,* 1999
Nucleoside reverse transcriptase inhibitors (NRTIs): Abacavir, AZT, lamivudine, didanosine, stavudine	SCID mice inoculated with HIV-infected human monocyte-derived macrophages	Abacavir and lamivudine were the most successful in reducing both HIV-1 p24 antigen and viral load	Limoges *et al*., 2000
2'-deoxy-3'-oxa-4'-thiocytidine (BCH-10652)	SCID mice reconstituted with human fetal thymus and liver	Dose-dependent inhibition of HIV replication	Stoddart *et al.,* 2000
SCH-C (SCH 351125)	SCID mice reconstituted with human fetal thymus and liver	Dose-dependent inhibition of HIV replication	Strizki *et al.,* 2001
Stampidine	SCID mice reconstituted with human peripheral blood lymphocytes	Dose-dependent inhibition of a NRTI-resistant HIV-strain	Uckin *et al.,* 2002

↑, ↓ as in Table 2.2

2.6 LP-BM5/murine acquired immunodeficiency syndrome (MAIDS) model

The LP-BM5 murine leukemia virus (MuLV) was originally described by Laterjet and Duplan and was derived from C57BL/6 mice that had received fractionated, low-dose irradiation (Mosier *et al.,* 1985). This model has been reviewed in detail by Jolicoeur, 1991. The LP-BM5 MuLV is a complex of retroviruses and consists of a replication-defective virus and two helper viruses (Chattopadhyay *et al.,* 1991). The replication-defective virus has been identified as the disease-causing agent while the two-helper viruses are a B-tropic replication-competent virus and a mink cell focus-inducing virus. The helper viruses assist in the cell-to-cell spreading of the defective virus thereby accelerating the progression of disease. Not all mouse strains are susceptible to LP-BM5 and susceptible strains include C57BL/6, C57BL/10, B10.F, B10.F (13R), B10.P (10R) and I/St while resistant strains include CBA/J, LG/J, C57L/J and A/J mice (Hartley *et al.,* 1989; Huang *et al.,* 1992).

Following intraperitoneal inoculation of C57BL/6 mice with LP-BM5, the virus spreads rapidly and can be detected in the mediastinal lymph nodes 2 days post inoculation. The virus then spreads to the spleen and other lymph nodes (lumbar, cervical and inguinal) and can be detected in these organs after one week (Simard *et al.,* 1994). Virus can also be detected in thymus, liver, lungs, kidneys, bone marrow and brain at later stages (Hartley *et al.,* 1989; Simard *et al.,* 1994). Like FIV infection, the defective virus is expressed in B-cells, macrophages and T-cells with the highest levels being expressed in the B-cells (Kim *et al.,* 1994). Splenic and peritoneal Mac-1^+ cells are also targets. $CD4^+$ T-cells and $CD8^+$ T cells start decreasing after 4 weeks, while B-cells, macrophages and MAC-1^+ cells are increased (Yetter *et al.,* 1988). There is a rapid loss of T lymphocyte blastogenic responses to mitogens and alloantigens, loss of helper T-cell function and B-cell function. There is an increase in the extracellular Ig levels particularly in IgM which increases by five-fold (Pattengale *et al.,* 1982; Yetter *et al.,* 1988).

MAIDS also causes cytokine dysregulation and during the first week of infection, there is a transient expression of IFN-γ, IL-2, IL-5 and at lower levels IL-4 and IL-10 in the absence of restimulation or mitogens (Gazzinelli *et al.,* 1992). At 3-12 weeks, high levels of cytokines of Th2 clones including IL-4 and IL-10 are detected as well as the expression of IL-6, IL-1 and TNF. Th-1 related cytokines like Il-2 and IFN-γ production

are, however, reduced. Th-2 cytokines are expressed variably but usually at high levels during the later stages of disease.

Splenomegaly and lymphadenopathy develop at 4 weeks post infection (Yetter *et al.,* 1988). Splenomegaly is characterized by an increase in follicle size and progressive replacement of normal population of small lymphocytes with immunoblasts, plasmacytoid cells and plasma cells (Hartley *et al.,* 1989). The spleen increases in size and weight and the normal architecture is destroyed. During the advanced stages of diseases, the spleen is filled with nodular masses of lymphoid cells. In the lymph nodes there is infiltration of deep cortex, medulla and thymic medullae by immunoblasts, plasmacytoid cells and plasma cells. Normal architecture is destroyed and almost all the nodes are enlarged and congested. During the advanced stages of disease the lungs, kidneys and liver are also infiltrated and there is extensive replacement of normal parenchyma (Pattengale *et al.,* 1982). The mice eventually die at approximately 24 weeks due to respiratory failure caused by enlargement of the mediastinal lymph nodes (Mosier *et al.,* 1985).

2.6.1 LP-BM5-induced CNS disease

Neurological signs can be seen at 12 weeks and include hind limb weakness progressing to paralysis, hind limb clasping, ataxia and a generalized tremor (Klinken *et al.,* 1988). The brain undergoes extensive infiltration by lymphoid cells. There is infiltration of small areas of the choroid plexus and meninges with extensions into perivascular space by immunoblasts and plasmacytoid cells. This causes extensive destruction of choroid plexus and meninges. No lesions, however, can be seen in the spinal cord or brain.

2.6.2 Antiviral drug testing

Besides the *in vivo* animal model, an *in vitro* cell culture model has been established and this consists of LP-BM5-infected bone-marrow cell cultures and SC-1 mouse fibroblast cells with LP-BM5 virus. Both models have been used to evaluate a wide range of drugs such as AZT and lithium, IL-3 in combination with AZT and ddI and plant extracts of *Glycyrrhizin* and *Chlorella vulgaris.* The results of these studies are summarized in Table 2.5.

Table 2.5 Drugs, drug combinations and plant extracts evaluated in the LP-BM5/MAIDS model

Compound	*In vitro/in vivo*	Results	Reference
AZT	*In vivo*	↓ splenomegaly, restored APC activity and mitogenic responses, prevented immunosuppression when given immediately after inoculation, ↓ RT activity in serum.	Ohnota *et al.,* 1990
AZT	*In vivo*	Protected mice when given orally or by subcutaneous infusion. Delayed but did not prevent infection.	Eiseman *et al.,* 1991
IL-3 in combination with AZT and ddI	*In vitro* LP-BM5-infected bone-marrow cell cultures	IL-3 ↓ bone-marrow toxicity of AZT and ddI when used in combination with either drug. It was less effective when used in triple combination.	Gallicchio *et al*., 1994
Lithium	*In vivo*	↑ hematocrit, white blood cell count and platelets. ↑ bone marrow and spleen CFU-CM, BFU-E and CFU-Meg.	Gallicchio *et al.,* 1995
Vitamin E	*In vivo*	Improved immune dysfunction caused by virus. Suppressed ↑ lipid peroxides, splenomegaly and lymphadenopathy. ↑ NK activity, proliferation of T-cells and improved cytokine dysregulation.	Okishima *et al.,* 1996
Glycyrrhizin (plant extract)	*In vivo*	Extended survival, suppressed splenomegaly and lymphadenopathy	Watanbe *et al.,* 1996
Chlorella vulgaris (hot water extract)	*In vivo*	↑ IL-12 expression in macrophages and spleen, ↑ IFN-γ in spleen, enhance resistance to *Listeria monocytogenes*, ↓ IL-10.	Hasegawa *et al.,* 1997
PMPA and PMEA	*In vitro* SC-1 mouse fibroblast cells with LP-BM5	Less effective than AZT in inhibiting BM5eco. PMPA was the least toxic.	Suruga *et al.,* 1998
	In vivo	Prevented splenomegaly and lymphadenopathy, conserved mitogenic responses and ↓ activated B cells and viral replication.	
AZT and fludarabine monophosphate combination	*In vivo*	Fludarabine given alone ↓ disease progression and viral load. In combination with AZT: ↓ proviral DNA in spleen, bone marrow and lymph nodes and restored mitogenic responses	Fraternale *et al.,* 2000
Vitamin E and AZT	*In vivo*	Both inhibited splenomegaly but AZT was more effective. Both drugs normalized changes in INF-γ and TNF-α. Only Vitamin E suppressed NF-κβ	Hamada *et al.,* 2000
Tyrphostin AG-1387	*In vitro* SC-1 mouse fibroblast cells with LP-BM5	Dose-dependent inhibition of RT activity in culture supernatant. ↓ in viral protein amount.	Sklan *et al*., 2000
	In vivo	↓ splenomegaly and lymphadenopathy. Restored responses to ConA. No viral RNA could be detected in treated mice.	
AZT, ddI and glutathione (GSH)-loaded erythrocyte triple combination	*In vivo*	Greater ↓ in bone marrow and brain proviral DNA content of macrophages than in mice treated with AZT and ddI combination. Restored proliferative responses to mitogens.	Fraternale *et al*., 2002
Heteronucleotide of AZT and PMPA (AZTpPMPA)	*In vivo*	↓ in IgG level and proviral DNA in lymph nodes but greater ↓ was observed with AZT and PMPA combination or PMPA alone. ↓ in splenomegaly and lymphadenopathy.	Rossi *et al.,* 2002

Table 2.5 Cont'd

Ribonucleotide reductase inhibitors: trimidox (TX), didox (DX) and hydroxyurea (HU)	*In vivo*	All drugs inhibited splemomegaly, ↓ IgG and proviral DNA content of spleen. HU was however more toxic and ↓ WBC, hematocrit femur cellularity, CFU-GM and BFU-E.	Mayhew *et al.,* 2002
Combinations of abacavir with either HU, TX or DX	*In vivo*	All combinations ↓ splenomegaly, IgG level, proviral DNA content of spleen. HU combination caused gross toxicity, ↓RBC count and CFU-GM	Sumpter *et al.,* 2004
Combinations of ddI with either HU, TX or DX	*In vivo*	↓ in splenomegaly, IgG level, B-cell activation and proviral DNA content of spleens by all combinations with DX and ddI combination being the most effective. Toxicity: combinations ↓ WBC count, HU combination ↓ hematocrit , HU and TX combinations ↓ femur cellularity, HU combination ↓ CFU-GM and BFU-E.	Mayhew *et al.,* 2005

↑, ↓ as inTable 2.2

2.6.3 Advantages and disadvantages

The advantages of this model are that it is small, inexpensive ($10-$20), widely available and an *in vitro* cell culture equivalent that is suitable for rapid drug evaluation is available. Further advantages are that the risk for infection is low, as the virus is non-pathogenic to humans and the immunodeficiency induced in these mice has several similarities with HIV/AIDS. The disadvantages identified with this model are that the virus is not a lentivirus and lacks accessory genes of HIV (Figure 2.1) and the major cellular targets are the B cells and the $CD4^+$ T-cell populations.

2.7 Summary

The advantages and disadvantages of each model are summarized and compared in Table 2.6.

2.8 Conclusion

Several *in vivo* animal models and *in vitro* cell culture models are available for the evaluation of the antiretroviral activity of drugs, drug combinations and plant extracts. The animal models reviewed here, have extended present knowledge regarding the biochemical mechanisms, toxicity and the efficacy of many antiretroviral drugs. In conclusion, the SIV model is most similar to HIV/AIDS in humans particularly in disease progression. Disease progression is slow, cost of housing is high and availability of these animals is limited. A small animal model may therefore be more convenient for rapid screening. Two murine models are available that allows for rapid drug screening and these are SCID mice and the LP-BM5/MAIDS model. In both models, disease progression is rapid and drugs can be rapidly evaluated. However the distinct differences between these two models are that the SCID model utilizes HIV the MAIDS model utilizes the LP-BM5 virus that differs from HIV in the structure and pathogenesis. The availability, low cost of murine animal models and the rapid progression of disease in these models are ideal for drug evaluation especially when evaluating double or triple drug combinations.

Advantages and disadvantages of the SIV, FIV, SCID and LP-BM5/MAIDS models in the evaluation of the antiretroviral activity of drugs and plants.

Model:	SIV model	FIV model	SCID mouse	LP-BM5/MAIDS
Virus type	Lentivirus	Lentivirus	Lentivirus	Type C oncornavirus
Natural virus-host system	No	Yes	No	No
Risk of investigator infection	Yes	No	Yes	No
Availability	Rhesus monkeys becoming scarce	Widely	Widely	Widely
Cost per animal ($)	5 000 – 12 000	500 – 800	40 – 60	10 – 20
Per diem costs ($)	10 – 20	4 – 6	Less than 1	Less than 1
Experimental duration	Variable depending on SIV strain. Very rapid strains like $SIV_{smm}PBj$ cause death in 7-14 days, $SIV_{mac}239$ causes death in 3-6 months, SIV_{mne} 1 year, $SIV_{mac}BK28$ 2-5 years	Experimentally infected cats take several years (more than eight) to develop AIDS	HIV infection usually stable for a month but some can stay persistently infected for up to 16 weeks	Mice die after approximately 4 – 6 months
Similarities with HIV/AIDS:				
Major cell targets	CD4 T cells, macrophages	CD4 T cells, macrophages	CD4 T cells, monocyte-derived macrophages	B-cells are major targets but CD4 T cells are needed to spread disease
Receptor	CD4, CCR5, few use CXCR4	CXCR4, may use feline homologue of CD9, maybe CCR5	Same as HIV	Unknown
Disease progression of acute phase, asymptomatic phase, terminal phase	Yes	Terminal phase only in naturally infected cats	Acute phase	No latency period
CD4 depletion	Yes	Yes	Yes	Yes
Virus-specific responses	CTL and antibodies	CTL and antibodies	Can engraft T lymphocytes that then develop CTL responses	No
Variable disease progression	Months-years	Months-years	Infection can be stable up to 16 weeks	No
Opportunistic infections	Yes	Yes	Yes	Yes
CNS disease	Yes	Yes	Yes	Yes
Destruction of lymph node architecture	Yes	Yes	No	Yes
Lymphomas	Yes	Yes	Yes	Yes
Used for drug evaluation	Yes	Yes	Yes	Yes

Table 2.6 Cont'd

Used for medicinal plant evaluation	Yes	Yes	No	Yes
***In vivo* and *in vitro* models**	Yes	Yes	Yes *In vitro* model of humans cells infected with HIV	Yes
Used for vaccine evaluation	Yes	Yes	Yes	No

2.9 Aims of the study

Rapid and cost effective screening of drugs that inhibit specific pathways essential for retroviral survival and replication will lead to the identification of drugs that can be used in animal studies and subsequent phase 1 drug trials for the treatment of HIV/AIDS. The establishment of an *in vitro* cell culture model infected with the LP-BM5 MuLV will assist in achieving this goal without compromising safety and ethic considerations associated with other *in vitro* models such as HIV infected human cells. Furthermore, the existence of a similar *in vivo* MAIDS model will assist in extrapolating the *in vitro* findings. Although this model does not completely mimic HIV it has been used to study many aspects of the pathogenesis of HIV/AIDS and to successfully determine the efficacy of known anti-HIV drugs like AZT, HU and PMPA as well as potential antiretrovirals like tyrphostin AG-1387, trimidox and didox. Therapeutic strategies often involve combination drug therapies as it increases therapeutic efficacy, lowers the toxicity towards the host and target tissues, increases the selectively of the therapeutic index and delays the development of drug resistance. The *in vitro* cell culture model infected with the LP-BM5 MuLV is ideal to evaluate possible drug interactions such as synergism, antagonism and additive effects.

The main aim of this study is to establish an *in vitro* cell culture model infected with the LP-BM5 MuLV as well as the methodologies for the quantification of viral DNA and viral RNA. The established *in vitro* cell culture model will be evaluated using drugs known to have antiretroviral activity such as AZT, HU, IDV and CQ before the antiretroviral activity of plant derived products like GT and EGCg is evaluated. Thereafter, GT and EGCg will be evaluated in combination with AZT, HU, IDV or CQ. The possibility of a synergistic or additive effect will be investigated as this could lead to the identification of new therapeutic strategies that are more effective, affordable and safer.

The aims of this study were therefore to;

(i) Establish SC-1 and BM5 cell lines to create a model that can be used for rapid screening of the antiretroviral properties of drugs.

(ii) To confirm the presence and absence of the LP-BM5-defective virus in the BM5 and SC-1 cell lines respectively using TEM (viral particles), semi-quantitative PCR and RT-PCR (viral DNA and RNA), animal studies (infectivity) and real-time PCR (quantification of viral DNA levels).

(iii) To develop a co-culture model that represents cell to cell transmission of the LP-BM5 virus.

(iv) Validate the use of this *in vitro* co-culture model by evaluating the effects of AZT, IDV, HU and CQ on the viral load at sub-toxic concentrations.

(v) Evaluate the antiretroviral properties of experimental compounds GT and EGCg in the *in vitro* co-culture model at sub-toxic concentrations.

(vi) Evaluate the effect of GT and EGCg on the antiretroviral activity as well as the cytotoxicity of the antiretroviral drugs AZT, IDV, HU and CQ when the antiretroviral drugs are combined with either GT or EGCg.

(vii) Identify drug combinations that can be further investigated in the *in vivo* MAIDS model.

2.10 Hypotheses

Hypothesis I: An *in vitro* co-culture model of SC-1 and BM5 cells can be used for screening the antiretroviral properties of drugs.

Hypothesis II: GT and EGCg will show significant antiretroviral activity in the *in vitro* co-culture model of SC-1 and BM5 cells.

Hypothesis III: GT or EGCg will strongly enhance the antiretroviral activity of at least one antiretroviral drug AZT, IDV, HU or CQ

Chapter 3: Establishment of an *in vitro* co-culture model of SC-1 and BM5 cells and techniques for the demonstration of viral infectivity

3.1 Introduction

Murine AIDS (MAIDS) is induced by inoculating C57BL/6 mice with the LP-BM5 MuLV complex (Chattopadhyay *et al.,* 1991). MuLVs are classified as retroviruses that contain the enzyme reverse transcriptase (RT) that converts the retroviral RNA genome into double stranded complimentary DNA (ds cDNA) (Murphy *et al.,* 1995). The LP-BM5 MuLV complex consists of two-helper viruses, the β-tropic replication-competent ecotropic virus and a mink cell focus-inducing virus (Chattopadhyay *et al.,* 1991). The disease-causing virus is a replication defective retrovirus. Defective retroviruses lack all or part of the structural genes needed for replication and thus require a replication-competent helper (Levy *et al.,* 1994). The exact mechanism of how defective retroviruses replicate is largely unknown. One mechanism may be by incorporation of the defective genome into the envelope of the replication-competent retrovirus thus creating psuedotypes. In other cases, the defective genome carried in the helper envelope is brought into a cell without an accompanying replicating helper. Integration and transformation may occur if RT enzyme is present but infection with a competent retrovirus is needed to rescue the genome from the cell and cause the production of new virus progeny.

The genome of the LP-BM5 defective virus is only 4.8 kb in size with large open reading frame in the *gag* gene and major deletions and alterations in the *env* and *pol* genes (Figure 3.1) (Chattopadhyay *et al.,* 1991). The *gag* gene encodes a polyprotein precursor Pr60 that is smaller than the typical MuLV precursor. The polyprotein is made up of proteins p15, p30, p10 and p12 that have been modified. The precursor protein is myristylated, phosphorylated and associated with the cell membrane. It is not cleaved in non-producer fibroblasts and only partially cleaved in presence of a helper MuLV. There is also a second open reading frame near the remnants of the *pol* and *env* genes but it is not known to synthesize any other proteins (Huang and Jolicoeur, 1990).

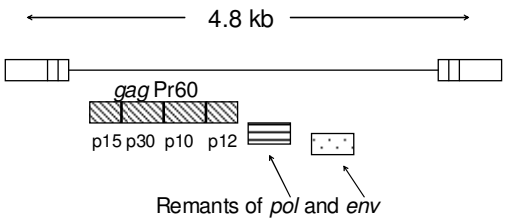

Figure 3.1. LP-BM5 defective retrovirus genome.

Typically as shown in Figure 3.2, retroviral replication involves [1] receptor recognition and binding, followed by [2] fusion of viral membrane with the host cell membrane and entry into host cell. In the cytoplasm [3] the release and uncoating of viral core shell occurs and subsequent [4] reverse transcription of viral RNA into ds cDNA. The proviral DNA is [5] imported into the nucleus and becomes [6] integrated into the host cell genome. The proviral DNA is [7] transcribed into viral RNA with [8 and 9] translation into viral proteins followed by the [10] assembly of virus particles, [11] budding of virus from host cell membrane and [12] maturation of viral core.

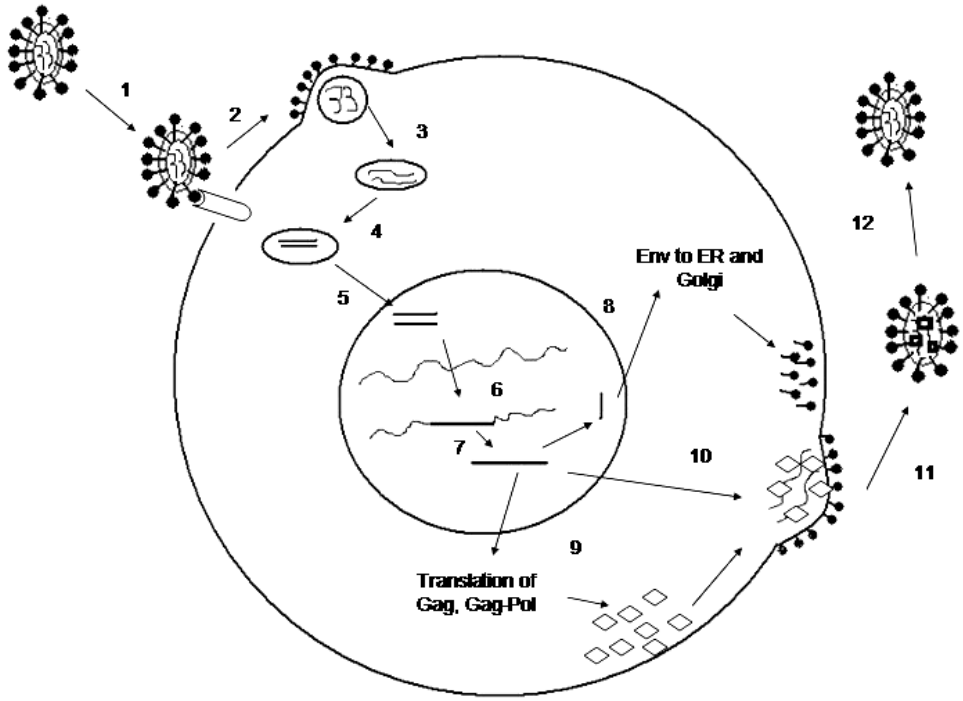

Figure 3.2. The retroviral replication cycle.

Four different types of virus-cell interactions have been identified. The interactions can be cytocidal (lytic), persistent (productive or non-productive), transforming or abortive (Dimmock and Primrose, 1987; White and Fenner, 1994). In a cytocidal or lytic interaction, the infectious virions that are produced, can inhibit DNA, RNA and protein synthesis causing death of the host cell. The cell damage caused by the virions, known as the cytopathic effect (CPE), can be visibly seen as inclusion bodies and syncytia in cell monolayers. Inclusion bodies are accumulations of viral structural components found in either the nucleus or cytoplasm. The syncytia that can be seen are caused by fusion of the infected cell with another infected cell or uninfected cell.

In persistent infection, the viruses do not kill the host cell and in these cells the virus replicates and causes few or no changes to protein, RNA and DNA synthesis. The cells continue to divide and may or may not produce infectious virions (latent infection). In the latter case, the virus inserts a copy of its genome into the host cell DNA thus ensuring that it is transmitted to daughter cells when the host cell replicates. In latent infection, cells can be induced to produce infectious virions by co-cultivation with uninfected cells, irradiation or by chemical mutagens. Transformation infections often occur with oncogenic retroviruses and may lead to cancer. Copies of the viral DNA genome are incorporated into the host cell and the cells become permanently altered causing them to replicate much faster than the uninfected cells. The viral infected cells may cause tumours in experimental animals when transplanted. In some virus-cell interactions, there is an incompatibility between the virus and the host cell and the replication cycle of the virus is obstructed. The resulting effect is a decrease in the production of virus. This type of infection is known as an abortive or non-permissive infection.

Three different *in vitro* models can be established to investigate the effects of different drugs on viral infection. The models can be cells acutely infected with virus, co-cultures of uninfected cells with cells chronically infected with virus and thirdly cells chronically infected with virus (Lambert *et al.,* 1993). The acutely infected model represents the acute phase of viral infection that occurs immediately following exposure to the virus *in vivo*. From this model, it can be determined whether the drug being tested either inhibits the virus from entering the cell or blocks its replication in the host cell. The co-culture model represents cell-to-cell transmission of the virus and can be used to determine whether a drug can prevent a viral infection from becoming a chronic infection. Chronically infected cells represent the *in vivo* viral reservoir found in viral diseases and can be used to determine if a drug can eradicate or rescue a cell from viral infection.

Infectivity can be determined by using techniques that can detect the presence of viral particles (scanning electron microscopy (SEM), transmission electron microscopy (TEM) and the plaque assay), viral RNA (RT-PCR, *in situ* hybridisation (ISH)), viral DNA (PCR and ISH) and viral proteins (ELISA and immunohistochemistry) (Cann, 1997).

TEM has been used to study the life cycle of HIV-1 (Goto *et al.,* 1998), HIV-host cell interactions (Pudney and Song, 1994) and HIV virion structure (Ohagen *et al.,* 1997). In the plaque assay for the LP-BM5 virus complex, the cells infected with the virus are UV irradiated and then overlaid with the XC cell line. The XC cells are derived from a rat tumour cell that was induced by the Prague strain of the Rous sarcoma virus. Syncytia are formed when the LP-BM5 MuLV comes in contact with the XC cells. These syncytia are the so called plaques that can be seen and counted under a microscope.

Molecular methods like PCR have been used for the detection and quantification of several retroviruses including HIV, LP-BM5 and FIV. Various types of PCR assays have been developed for the detection and quantification of the LP-BM5-defective virus and include semi-quantitative PCR, competitive PCR, real-time PCR and RT-PCR as well as PCR with anion exchange HPLC. Semi-quantitative PCR has been used to quantifying the effects of drugs trimidox, didox, HU, abacavir and didanosine on the LP-BM5-defective retrovirus (Mayhew *et al.,* 2002, 2004 and 2005). Competitive PCR assay has been used by several authors to test the effects of azidothymidine homodinucleotide, AZT, alternate administration of AZT and fludarabine monophosphate, fludarabine + AZT + DDI, addition of GSH-loaded erythrocytes to AZT and DDI, and a heterodinucleotide of AZT and PMPA (Fraternale *et al.,* 1996; 2000; 2002; 2002; Casabianca *et al.,* 1998; Rossi *et al*., 2002). A competitive quantitative RT-PCR method has been used by Hasegawa *et al.,* 1997 to determine the viral load in mice treated with a hot water extract of *Chlorella vulgaris*. Hulier *et al.,* 1996 have developed a PCR method whereby the PCR products are quantified with anion-exchange HPLC.

In drug studies the quantification of the effect of a drug on viral DNA and RNA is essential and with the recent development of real-time PCR, various researchers have developed real-time PCR and RT-PCR assays for quantification of the LP-BM5-defective and ecotropic replication-competent retroviruses (Cook *et al.,* 2003; Casabianca *et al.,* 2004; Paun *et al.,* 2005). The major advantages of real-time PCR are that it is faster than conventional PCR and the gene product is measured in real

time rather than at the end of amplification. Besides PCR methods, RT assays as well as ELISA assays can be used for the detection of MuLVs (Ohnota *et al.,* 1990; Hollingshead *et al.,* 1992).

The aims of this study were to:

(viii) Determine the differences in cellular morphology and growth properties between the SC-1 and BM5 cell lines.

(ix) To confirm the presence of the LP-BM5 virus in the BM5 cell line as well as the absence of LP-BM5 virus in the SC-1 cell line by using TEM, conventional PCR, RT-PCR and real-time PCR.

(x) To conclusively determine whether a viral extract of the BM5 cell line induces MAIDS in female C57BL/10 mice.

(xi) Lastly, to develop an *in vitro* co-culture model for the evaluation of antiretroviral drugs.

3.2 Materials

3.2.1 Cell lines

The uninfected mouse feral embryo fibroblast cell line (CRL-1404, designated SC-1) was obtained from the American Type Culture Collection (ATCC), Virginia, United States of America (USA). SC-1 cells chronically infected with the LP-BM5 MuLV (designated BM5 cell line) were kindly donated by Professor V. Gallicchio from the University of Kentucky, USA.

3.2.2 Media, supplements and reagents

Dulbecco's Minimum Essential Medium (DMEM) powder, Penicillin/ Streptomycin/ Fungizone (PSF, 100x solution), Fetal Bovine Serum (FBS) and Sodium Pyruvate were obtained from Highveld Biological, Lyndhurst, South Africa (SA). Trypsin-EDTA (1x solution) was obtained from Gibco BRL Products supplied by Laboratory and Scientific Equipment Company (LASEC), Cape Town, SA. Sodium hydrogen carbonate ($NaHCO_3$), sodium chloride (NaCl), potassium dihydrogen phosphate (KH_2PO_4) and sodium hydrogen phosphate-1-hydrate ($NaH_2PO_4.H_2O$) were obtained from Merck, Wadeville, SA. Trypan Blue, dimethylsulfoxide (DMSO), polyethylene glycol (PEG), Tris[hydroxymethyl]aminomethane (Tris), boric acid, ethylenediamine tetraacetic acid (EDTA), 2-mercaptoethanol, diethyl pyrocarbonate (DEPC) were obtained from the Sigma-Aldrich Company, Atlasville, SA. Glycerol was from Bio-zone Chemicals, Van Riebeeck Park, SA. Ethidium bromide was from Bio-Rad

Laboratories Ltd, Johannesburg SA. Absolute ethanol was obtained from Chemical Suppliers (PTY) LTD, Booysens, SA.

The primers used in this study were synthesized by Integrated DNA Technologies supplied by WhiteHead Scientific, Brackenfell, SA. All PCR reagents, the Improm-II reverse transcription system were from the Promega Corporation supplied by Whitehead Scientific, Brackenfell, SA. The GFX genomic blood DNA purification kit was from Amersham Biosciences supplied by Separation Scientific, Honeydew, SA. The RNeasy Protect Mini kit was from Qiagen supplied by Southern Cross Biotechnology, Cape Town, SA. LightCycler® 480 SYBR Green I Master was supplied by Roche Diagnostics (South Africa) Pty. Ltd., Randburg, SA.

Disodium hydrogen phosphate ($Na_2HPO_4.2H_2O$), glutaraldehyde, sodium dihydrogenphosphate-2-hydrate ($NaH_2PO_4.H_2O$), Crystal Violet (CV), acetic acid and uranyl acetate were obtained from Merck, Johannesburg, SA. Osmium tetroxide (OsO_4) was supplied by Spi Suppliers, West Chester, USA and the resin (Quetol 651) and glutaraldehyde was obtained from TAAB Laboratories, Reading AGAR Scientific Ltd, Essex, United Kingdom (UK). Reynold's lead citrate was supplied Polaron Equipment Ltd, Watford, UK.

Water was double distilled and deionized (ddH_2O) with Milipore Q system and sterilized at 121°C for 30min. Glassware was also sterilized at 121°C for 30min in an autoclave.

3.2.3 Disposable plasticware

The 25cm^2 cell culture flasks, 24- and 96-well plates and 50 ml tubes were from Greiner Bio-one supplied by LASEC, Cape Town, SA. One milliliter 29-gauge insulin syringes were from EDNA Medical Distributors, Pretoria, SA. Cryotubes were from Nunc Brand Products supplied by AEC Amersham (PTY) LTD, Kelvin, SA. The 0.2µm Sartorius ministart-plus CA-membrane and GF-prefilter filters and the 0.2µm Sartorius ministart non-pyrogenic hydrophilic filters were from Vivascience supplied by National Separations, Halfway House, SA. The 0.22µm Sartorius Cellulose acetate filters were from Goettingen, Germany supplied by National Separations LTD, Halfway House, SA. The 10ml tubes were from Sterilab and were supplied by Adcock Ingram Critical Care Pty Ltd, Johannesburg, SA. The 20ml and 1ml syringes were from the New Promex Corporation, Bergvlei, SA. The 0.6ml PCR and 1.5ml reaction tubes and the 10µl and 20µl tips were supplied by Whitehead Scientific,

Brackenfell, SA. The 200µl and 1000µl tips were from Corning Life Sciences and were supplied by Adcock Ingram Critical Care Pty Ltd, Johannesburg, SA. LightCycler® 480 Multiwell Plates 384 was supplied by Roche Diagnostics (South Africa) Pty. Ltd., Randburg, SA.

3.2.4 Laboratory facilities

All research was conducted in the research facilities of the Department of Anatomy and Chemical Pathology of the Faculty of Health Sciences, the Department of Biochemistry and the Department of Genetics, Faculty of Natural and Agricultural Sciences, University of Pretoria. TEM was performed at the Laboratory for Microscopy and Microanalysis, NW2 Building, University of Pretoria.

3.3 Methods

3.3.1 Cultivation and maintenance of the SC-1 and BM5 cell lines

For all studies, the SC-1 and BM5 cell lines were maintained in DMEM supplemented with PSF, sodium pyruvate and 10% FBS. The PSF and sodium pyruvate were purchased as working solutions that were aliquoted in 11ml volumes, frozen at -20°C and thawed at 37°C when needed. The FBS was heat-inactivated at 56°C for 30 min before use then kept at -20°C and thawed at 37°C when needed. DMEM powder was dissolved in 1L ddH_2O and 3.7g $NaHCO_3$ was added. The pH was adjusted to 7.1-7.2 with hydrochloric acid using a Mettler Toledo MP220 pH meter. Aliquots of 11ml of PSF and sodium pyruvate were then added to the medium. The medium was filtered through a 0.22µm Sartorius Cellulose acetate filter under aseptic conditions in a laminar flow hood. Aliquots of 200ml medium were stored at 4°C and warmed to 37°C before use. Before the FBS was added to the medium, it was filtered through a 0.2µm Sartorius ministart-plus filter containing a cellulose acetate membrane and GF-prefilter.

Cells were grown in 25cm^2 flasks and sub-cultured once confluent with Trypsin-EDTA. The Trypsin-EDTA was purchased as a working solution that was aliquoted in 10ml volumes, stored at -20°C and thawed at 37°C when needed. The medium was removed and placed in a 10ml tube. A volume of 1ml Trypsin-EDTA was added and left for about 5 min until the cells detached. The Trypsin-EDTA was inactivated with 3ml medium and the medium containing cells in the flask was placed in the 10ml tube. A volume of 5ml of fresh medium was added to the sub-cultured flask. The tube

was centrifuged at 1100 rpm (125xg) for 10 min in a BHO Hermle Z320 bench top centrifuge. The supernatant was removed, the pellet re-suspended in 3ml medium and transferred to a 24-well plate. The cell suspension was resuspended through a 29' gauge needle coupled to a 1ml syringe 5 times and an aliquot of 40µl was mixed with an equal volume of trypan blue solution in phosphate buffered saline (PBS) and counted with a hematocytometer. A 0.2% trypan blue solution was made in 1xPBS.

If the cells were not used for any experiments, they were frozen at -70°C or in liquid nitrogen. The cells were suspended in freezing medium for storage. The freezing medium was prepared with 80% FBS, 10% DMSO and 10% DMEM (not supplemented with FBS). One ml of the cell suspension was transferred to a 1.5ml cryotube, wrapped in gauze and placed at -70°C. Cells were stored immediately with minimum loss of viability. Cells that were meant for liquid nitrogen storage were removed the following day from the -70°C freezer and placed in the liquid nitrogen storage tank.

The vials containing SC-1 and BM5 cells were thawed rapidly in a water bath at 37°C. The thawed suspension was added to a 10ml tube containing 8ml medium and centrifuged at 1100rpm (125xg) for 10min. The supernatant was removed and the cell pellet was resuspended in 1ml fresh medium and placed in a 25cm^2 culture flask containing 5ml medium.

3.3.2 Growth rate study of the SC-1 and BM5 cell lines

The SC-1 and BM5 cells were plated in 25cm^2 cell culture flasks at a concentration of 2.5 x 10^5 cells in 6ml of DMEM supplemented with 10% FBS. Five cell culture flasks were plated for each cell line and the cells were fixed in the medium with 2.5% glutaraldehyde for 20 min at the following times: 3, 24, 48, 72 and 96 hours after plating. The medium containing glutaraldehyde was removed and the flasks dried. A 0.1% Crystal violet (CV) dye solution was prepared in ddH_2O. The cells were stained with CV for 10 min and the plates were then washed thoroughly under tap water and dried. The CV dye was solubilized with 2.5ml of 10% acetic acid and 200µl from each cell culture flask was transferred to a 96-well plate. The absorbency was read at 595nm with a Multiscan Ascent plate reader from AEC Amersham, Kelvin, SA.

3.3.3 Microscopic analysis of SC-1 and BM5 cell lines

3.3.3.1 Crystal Violet staining of SC-1 and BM5 cell lines

The SC-1 and BM5 cell culture flasks that were used in growth rate studies were restained with CV for 10 min, washed thoroughly under tap water, dried and photographed with Zeiss Inverted Fluorescence microscope with high-NA brightfield and DIC optics microscope.

3.3.3.2 Transmission electron microscopic analysis of SC-1 and BM5 cells

To confirm the presence of LP-BM5 virus in the BM5 cell line and the absence of the virus in the SC-1 cell line TEM was used. TEM was also used to study the process of viral budding in the BM5 cell line. The BM5 and SC-1 cells were plated in 25cm^2 cell culture flasks at a cell concentration of 5 x 10^5 cells in 4.3 ml of DMEM supplemented with 10% FBS. The cells were left overnight at 37^{o}C, 5% CO_2. The cells were then harvested using trypsin-EDTA, collected by centrifugation at 1100rpm (125xg) for 10 min, washed with DMEM supplemented with 10% FBS before the cells were collected in 1xPBS at 1100rpm (125xg) for 10min. The supernatant was removed and the pellet fixed in 2.5% glutaraldehyde in 0.075M phosphate buffer, pH 7.4 and placed at 4^{o}C overnight.

The fixative was removed and the cells washed three times, 10 min each in 0.075M phosphate buffer, pH 7.4. The cells were post-fixed in 0.5% aqueous osmium tetroxide for 1.5 hours and then washed three times with ddH_2O. A dehydration procedure compromising of a series of steps of different percentages of ethanol 30%, 50%, 70%, 90% and 3 x 100% (10 min each), was then followed. The cells were left overnight at room temperature in 100% ethanol.

The ethanol was removed and 50% Quetol epoxy resin in 100% ethanol was added to each reaction tube. The Quetol epoxy resin was prepared by mixing Quetol, MNA, DDSA, RD2 and S1 (39: 44.6: 16.6: 0.02: 0.01). After 1 hour, the resin was removed and 500µl of pure resin (100%) was added. This was replaced by another 500µl of pure resin (100%) after 4 hours and the specimen was polymerized at 60^{o}C for 36-48 hours. Ultrathin sections were then cut and placed on grids. The grids were stained with aqueous uranyl acetate in the dark for 30 min, washed thoroughly in distilled water and then stained with Reynold's lead citrate for 3 min in the dark. The grids were washed thoroughly with distilled water, dried and viewed under the Philips 301 TEM.

3.3.4 *In vivo* MAIDS animal studies

An *in vivo* animal study was undertaken to demonstrate that a crude viral isolate derived from the BM5 cell line could induce MAIDS in female C57BL/10 mice. The viral isolate was prepared as follows; the supernatant from two confluent 75cm^2 flasks of BM5 cells was removed and the monolayer of cells was subjected to three freeze and thaw cycles in liquid nitrogen. After the final thaw phase the supernatant was returned to the flask, the cellular components and the supernatant were mixed together, collected by centrifugation at 1100rpm (125xg) for 10 minutes. The supernatant was filtered through a Millex 0.45µm filter. The supernatant was used undiluted (high), diluted 1:10 (medium) and 1:100 (low). Female C57BL/10 mice (5 per group) aged 7-8 weeks were used. Ethics clearance was obtained form the Animal Use and Care Committee, University of Pretoria (Study of CE Medlen). The mice were housed individually in a sterile cage rack system with HEPA filtered air circulation at 22℃ with a 12:00 h light: 12:00 h dark cycle, 60% humidity, and 12 air changes/h according to standard procedures used at the UPBRC. The mice were fed autoclaved lab chow and sterile water *ad libitum*. Mice were acclimatized for 1 week before the experimental procedure was initiated. MAIDS was induced by intraperitoneal (i.p.) injection of the above described preparation of LP-BM5 virus. All of the mice were weighed on the first day of the experiment and once weekly thereafter, the mice were terminated after 7 weeks. The mice were evaluated for lymphadenopathy and splenomegaly and the spleen of each animal was removed and weighed.

3.3.5 Semi-quantitative PCR methodology for the detection and quantification of LP-BM5-defective viral DNA and murine glucose-6-phosphate dehydrogenase (G6PDH) gene

3.3.5.1 DNA isolation and quantification

DNA was isolated using the GFX genomic blood DNA purification kit. The medium of confluent SC-1 and BM5 25cm^3 cell culture flasks was removed and cells were washed once with 1xPBS. Cells were lysed directly in the cell culture flask by adding of 600µl of extraction solution for 5 min. The extraction solution was removed and transferred to a GFX column. Thereafter the manufacturer's recommendations were followed with two exceptions i.e. the centrifugation times were doubled and DNA was isolated in 130µl of ddH_20.

A 20µl aliquot of the isolated DNA was diluted 1:5 with 1xTBE buffer and measured against 1xTBE buffer. The absorbency at 260 and 280nm was measured using Gene

Quant Spectrophotometer. The concentration of the sample was determined from the 260 nm absorbance reading and the purity from the 260/280 nm ratios.

3.3.5.2 PCR amplification of the LP-BM5-defective viral DNA regions and the G6PDH housekeeping gene

The PCR parameters namely annealing temperature, $MgCl_2$ concentration and number of cycles were optimized for detection of the amplification of the LP-BM5 DNA viral regions and the G6PDH housekeeping gene. LP-BM5 viral regions were amplified using primer sequences published by Mayhew *et al.,* 2002 for the p12 gag region of the LP-BM5 defective virus (BM5-def) genome while a region of the G6PDH gene was used as an endogenous control (Table 3.1). Several parameters for each PCR needed to be optimized and included the annealing temperature, $MgCl_2$ concentration and cycle number. For optimization, DNA was isolated from SC-1 (negative control) and BM5 (positive control) cells.

Table 3.1 Primer sequences for BM5-def and G6PDH genes

BM5-def forward primer	5'-CCT TTT CCT TTA TCG ACA CT-3'
BM5-def reverse primer	5'-ACC AGG GGG GGA ATA CCT CG-3'
G6PDH forward primer	5'-TGA TTG GGG GCT CCA AGA A-3'
G6PDH reverse primer	5'-AGG GGT TCA TGA ATG GAT GCT-3'

PCR amplification was carried out in total volume of 25µl consisting of a 3µl volume of genomic DNA and 22µl PCR reaction mix. All PCR reactions were carried out using a Thermal Cycling System from Hybaid Limited, Teddington, Middlesex, UK, supplied by Scientific Group, Cape Town, SA.

The 10mM dNTP working solution of each nucleotide was prepared by mixing together 10µl of each of the 100mM dGTP, dCTP, dATP and dTTP and 60µl ddH_2O. Aliquots of 20µl were prepared and stored at –20ºC. All other reagents were also stored at –20ºC and thawed at room temperature.

A stock PCR primer solution of 1nmol/µl was prepared by adding sterile ddH_2O to the purchased freeze-dried primers. Volumes of 10µl were aliquoted into micro-centrifuge tubes and stored at –20 ºC. A working primer solution of 100pmol/µl was prepared by making a further 10 times dilution of the primer stock solution. A primer concentration of 50pmol in a reaction volume of 25µl was used (2pmol/µl).

For BM5-def and G6PDH PCR amplification of 10 tubes, the following mixture of all PCR reagents was prepared and added in the following order into a 1.5 ml centrifuge tube: 128.75µl ddH_2O, 50µl of 5x Green GoTaq Flexi PCR buffer, 20µl of 25mM $MgCl_2$, 10µl of 10mM dNTP, 5µl of each of the two 100pmol/µl primers and 1.25µl of 5U/µl GoTaq Flexi DNA polymerase. A volume of 22µl of the PCR mixture was transferred into each of the 600µl thin walled PCR tubes and a 3µl volume of genomic DNA, which had been mixed by gentle vortexing, was added to each of the tubes. The caps of the tubes were closed, the contents were mixed by vortex and the samples were centrifuged for 30 seconds at 8000rpm (1000xg). The BM5-def and G6PDH PCR amplifications were performed in a separate reaction tubes. The final optimized PCR reaction consisted of Green GoTaq Flexi PCR buffer, 400µM each of the nucleotides dATP, dGTP, dCTP, and dTTP, 2mM $MgCl_2$, 2pmol of each primer and 0.625U Taq polymerase.

3.3.5.2.1 Optimisation of annealing temperature and number of cycles

A Hybaid Touchdown Thermocycler was used and the cycling conditions for the BM5-def viral DNA PCR were the method from Selematsela, 2001. The cycling conditions were as follows an initial denaturation step (94^0C for 10 min), followed by three cycles of denaturation (94^0C for 45 sec), primer annealing (50^0C for 1min 15sec) and extension (72^0C for 1min 45 sec). This was followed by 15, 20, 25, 30 or 35 cycles of denaturation (94^0C for 35 sec), primer annealing (50^0C for 45 sec) and extension (72^0C for 1min 15 sec). The cycling conditions for the G6PDH gene were similar to those for the BM5-def PCR except that the annealing temperature was evaluated at 55, 60 or 65^0C.

3.3.5.2.2 Optimisation of $MgCl_2$ concentration

Different concentrations of $MgCl_2$ prepared from a 25mM $MgCl_2$ stock solution were evaluated at an annealing temperature of 50^0C for the BM5-def and 60^0C for the G6PDH. Volumes of 1, 2 and 4µl representing a concentration of 1, 2 and 4mM were evaluated in a final reaction volume of 25µl using the cycling conditions describe above.

3.3.5.2.3 Electrophoresis of the BM5-def and the G6PDH gene regions

A 2% agarose gel was prepared in 1xTBE buffer (0.089M Tris, 0.079M Boric acid, 0.002M EDTA at pH 8.3). Electrophoresis was carried out using a Hoefer Submarine

Gel Electrophoresis System coupled to a Pharmacia PS 3000 DC power supply. The gel was then visualized by ultraviolet illumination and photographed using UVIdoc Gel Documentation System manufactured by UVItec Limited, St John's Innovation Centre, Cambridge, UK and supplied by Whitehead Scientific, Cape Town SA. A volume of 10µl of each PCR product was loaded directly onto the gel. The Green GoTaq Flexi buffer supplied with the Taq DNA polymerase already contains a tracing dye so it was not necessary to add bromophenol blue. The amplification products of 246 base pairs for BM5-def and the 363 base pairs for G6PDH gene product were separated at 120V for 90 minutes. Thereafter, the gel was stained in a 0.01% Ethidium Bromide solution made up in 1 x TBE buffer for 30min. For quantification purposes, the intensity of the BM5-def band was normalized to its corresponding G6PDH band and quantified by Quantity One software supplied by Bio-Rad Laboratories Ltd, Johannesburg SA.

3.3.6 RNA isolation and quantification

Total RNA was isolated from SC-1 (negative control) and BM5 (positive control) cells using the RNeasy Protect Mini kit. Cells were harvested using Trypsin-EDTA and centrifuged as in Section 3.3.1. The cell pellet was resuspended in 1xPBS, transferred to a 1.5ml centrifuge tube and centrifuged at 1100rpm (125xg) for 5 minutes. The PBS was removed and the cells were resuspended in 1ml of RNA stabilizing reagent and stored at -20 ^{0}C. The cells were then thawed at 37 ^{0}C and pelleted at 8000rpm (1000xg) for 3min. The stabilizing reagent was removed and the cells were processed for RNA isolation according to the manufacturer's recommendations.

RNA was quantified as described in Section 3.3.5.2.

3.3.7 Detection of BM5-def viral RNA and G6PDH by two step RT-PCR

3.3.7.1 Reverse transcription of isolated RNA into cDNA

Reverse transcription of the isolated RNA into cDNA was performed with the ImProm-II Reverse Transcription System. A 1.2kb Kanamycin RNA supplied with the kit served as a positive control for RNA. Reverse transcription reaction mixture was prepared by first combining 2µl of isolated RNA, 1µl of Oligo$(dT)_{15}$ primer, 0.5µg/µl (0.5µg/reaction) or random hexamer primer, 0.5µg/µl (0.5µg/reaction) and 2µl of nuclease-free water in a 0.6ml reaction tube. The Oligo$(dT)_{15}$ and random hexamer

primers (supplied with the ImProm-II Reverse Transcription System) allows the amplification of cDNA from RNA without prior knowledge of the RNA/cDNA sequence of the experimental RNA sample. The Oligo$(dT)_{15}$ primer initiates the synthesis of the first-strand by annealing with the 3' end of any polyadenylated RNA molecule while the random hexamers produce cDNA products that have been primed internally along the entire RNA sequence. The tube was placed on a preheated 70^0C heat block for 5 minutes and then on ice. The following reagents were then added to the reaction tube, 3.7µl nuclease-free water, 4µl ImProm-II 5xReaction buffer, 4.8µl $MgCl_2$ (final concentration 6mM), 1µl dNTP mix 10mM each dNTP (final concentration 0.5mM), 0.5µl Recombinant RNasin Ribonuclease Inhibitor and 1µl ImProm-II Reverse Transcriptase. The final volume of the reaction tube was 20µl. The manufacturer's cycling recommendations for annealing (25℃ for 5 min), extension (42℃ for 60 min) and RT inactivation (72℃ for 15 min) were followed.

3.3.7.2 PCR amplification of cDNA

PCR amplification of the cDNA was performed using the primer sequences in Table 3.1. A volume of 6µl cDNA was added to a PCR reaction mixture consisting of 9.9µl water, 5µl of 5x Green GoTaq Flexi PCR buffer, 2µl of 25 mM $MgCl_2$, 1µl of 10 mM dNTP, 0.5µl of the two 100pmol/µl primers and 0.125µl of 5U/µl GoTaq Flexi DNA polymerase. The final concentration of the reagents was as in Section 3.3.6.

The cycling conditions used were the same as in Section 3.3.6.1.1. Thirty five cycles of amplification were performed and an annealing temperature of 60^0C was used for the G6PDH gene. Electrophoresis of the products was carried out as in Section 3.3.6.1.3.

3.3.8 Real-time PCR for the detection and quantification of the BM5-def viral DNA and murine G6PDH gene

Real-time PCR was performed using the LightCycler® 480 Instrument available from Roche Diagnostics (SA) Pty. Ltd., Randburg, SA at the Department of Genetics, Faculty of Science, University of Pretoria. The SYBR Green dye format was used for detection and quantification of BM5-def viral DNA and murine G6PDH gene. The LightCycler® 480 SYBR Green I Master is supplied as a ready-to-use hot-start PCR mix already containing the FastStart Taq DNA Polymerase, reaction buffer, dNTP mix (using dUTP instead of dTTP), SYBR Green I dye and $MgCl_2$. Only the water, primer pairs and DNA had to be added to the PCR mix. Each reaction was performed in a total volume of 5µl consisting of 2.5µl of SYBR Green I master mix, 0.0375µl of

the forward primer, 0.0375µl of the reverse primer, 1.175µl water and 1.25µl DNA. The final concentration of each primer was 0.75pmol.

The DNA was isolated as in Section 3.3.5.1. Real-time PCR amplification of the BM5-def and G6PDH DNA was performed on separate LightCycler® 480 Multiwell Plates consisting of 384 wells. The BM5 cell DNA served as the positive control for BM5-def viral DNA while SC-1 cell DNA served as a negative control for BM5-def viral DNA and a positive control for G6PDH. Water served as a negative control for both BM5-def viral DNA and G6PDH gene. A standard curve for the BM5-def and the G6PDH gene was created by diluting the BM5 DNA with SC-1 DNA (Table 3.2) and diluting SC-1 DNA with ddH_2O (Table 3.3) respectively. Both standard curves were analysed with the LightCycler® 480 Absolute Quantification Software.

Table 3.2 Volumes used for the standard curve for the BM5-def viral DNA

%**BM5-def**	**100**	**50**	**10**	**1**	**0.1**	**0.01**	**0.001**	**0.0001**
%**SC-1**	**0**	**50**	**90**	**99**	**99.9**	**99.99**	**99.999**	**99.9999**
Volume BM5 DNA	10µl	5µl	1µl →	1µl →	1µl →	1µl →	1µl →	1µl
Volume SC-1 DNA	0µl	5µl	9µl	9µl	9µl	9µl	9µl	9µl
Total volume	10µl	10µl	10µl	10µl	10µl	10µl	10µl	10µl

→ Indicates dilution series1:10

Table 3.3 Volumes used for the standard curve for the G6PDH gene

%**G6PDH**	**100**	**50**	**10**	**1**	**0.10**	**0.01**	**0.001**	**0.0001**
Volume SC-1 DNA	10µl	5µl	1µl →	1µl →	1µl →	1µl →	1µl →	1µl
ddH_2O	0µl	5µl	9µl	9µl	9µl	9µl	9µl	9µl
Total volume	10µl	10µl	10µl	10µl	10µl	10µl	10µl	10µl

→ Indicates dilution series, 1:10

3.3.8.1 Protocol for the amplification of BM5-def viral DNA and G6PDH gene

The protocols for amplification of BM5-def viral DNA and the G6PDH gene were the same except that the annealing temperature for the BM5-def primers was 50^0C while the temperature for the G6PDH primers was 60^0C (Table 3.4).

Table 3.4 Protocol for amplification of BM5-def viral DNA and G6PDH gene using real-time PCR

Program	**Cycles**	**Analysis Mode**		
Activation	1	None		
Temp (°C)	**Time (s)**	**Ramp Rate (°C/s)**	**Acquisition (per °C)**	**Acquisition Mode**
95	300	4.8		None
Program	**Cycles**	**Analysis Mode**		
Stepup	3	Quantification		
Temp (°C)	**Time (s)**	**Ramp Rate (°C/s)**	**Acquisition (per °C)**	**Acquisition Mode**
95	10	4.8		None
50 or 60*	30	2.5		None
72	12	4.8		Single
Program	**Cycles**	**Analysis Mode**		
PCR	47	Quantification		
Temp (°C)	**Time (s)**	**Ramp Rate (°C/s)**	**Acquisition (per °C)**	**Acquisition Mode**
95	10	4.8		None
50 or 60*	10	2.5		None
72	12	4.8		Single
Program	**Cycles**	**Analysis Mode**		
Melting curve	1	Melting curve		
Temp (°C)	**Time (s)**	**Ramp Rate (°C/s)**	**Acquisition (per °C)**	**Acquisition Mode**
95	2	4.8		None
65	15	2.5		None
72			10	Continuous
Program	**Cycles**	**Analysis Mode**		
Cool	1	None		
Temp (°C)	**Time (s)**	**Ramp Rate (°C/s)**	**Acquisition (per °C)**	**Acquisition Mode**
40	1	2.5		None

* 50^0C for BM5-def; 60^0C for G6PDH

3.3.9 Establishment of an *in vitro* co-culture model of SC-1 and BM5 cells

BM5 and SC-1 cells were used to create a co-culture model that would be used to study the effects of different drugs and drug combinations on cell-to-cell transmission of the virus. For this, the cell–cell ratio for minimum successful infection had to be determined.

Co-culture models were created by combining SC-1 and BM5 cells at 6 different ratios from 1:1 to 1:100,000 in 25cm^2 cell culture flasks (Table 3.5) and growing them for 72 hours. The DNA was isolated as in Section 3.3.4 and the amount of BM5-def viral DNA was then quantified relative to G6PDH gene using conventional PCR and real-time PCR as in Sections 3.3.5 and 3.3.8, respectively. A 25cm^2 cell culture flask containing BM5 cells only served as a positive control for BM5-def viral DNA while a

25cm^2 cell culture flask containing SC-1 cells served as a negative control for BM5-def viral DNA. Three independent experiments were conducted.

Table 3.5 Co-culture models created with BM5 and SC-1 cells

BM5:SC-1 ratio	1:1	1:10	1:100	1:1,000	1:10,000	1:100,000
BM5 cell number	125 000	25 000	2 500	250	25	2.5
SC-1 cell number	125 000	225 000	247 500	249 750	249 975	249 997.5
Total cell number	250 000	250 000	250 000	250 000	250 000	250 000

3.4 Results and discussion

3.4.1 Morphology and growth characteristics of the SC-1 and BM5 cell lines

The SC-1 and BM5 cell lines were grown in DMEM supplemented with 10% FBS, sodium pyruvate and PSF in cell culture flasks and maintained in an incubator at 37℃, 5%CO_2. The SC-1 cells were observed to be more regularly-shaped cells with a long spindle-like fibroblast shape while the BM5 cells were more pleomorphic in shape and some looked spindle-like while others had a tendency to be large and distended (Figure 3.3). Besides the overall shape of the cells, no other differences could be seen between the two cell lines with light microscopy.

Uninfected cells like the SC-1 cells typically grow in a very ordered fashion as a monolayer attached to the plastic surface of the cell culture flask and their cell division is density dependent (Fraenkel and Kimball, 1982). Once all the available space of the cell culture flask has been occupied by the monolayer, cell division is inhibited and if the SC-1 cells are not trypsinised and subdivided the cells will detach and die. In Figure 3.4(A), it can be seen that the long spindle-shaped SC-1 cells grew in a parallel fashion tightly packed next to its neighbour, typical of fibroblasts. In transformed cells like the BM5 cells, the cells show a more disorganized growth pattern. In Figure 3.4(B), it can be seen that the BM5 cells are randomly distributed and growing into clusters. Transformed cells tend to lose their density-dependent inhibition (topoinhibition) and continue to divide forming a multilayered culture (Dulbecco and Ginsberg, 1990). This was true of the BM5 cells as higher cell counts were always obtained with a confluent BM5 cell culture flask than with a confluent SC-1 cell culture flask suggesting that the BM5 cells were growing in layers. Also, once the BM5 cells had reached confluency, these cells tended to bunch up and start forming small cell clusters due to anchorage independent growth (Figure 3.5). These

cell clusters eventually detached from the surrounding cells and the surface of the cell culture flask and float in the medium.

The BM5 cells were observed to adapt better to culture conditions and the cells attached faster to the surface of the cell culture flask. The BM5 cells also grew at a faster rate than the SC-1 cells. This is typical of cells transformed with an oncogenic retrovirus (Dimmock and Primrose, 1987). Figure 3.6 represents a growth curve for the SC-1 and BM5 cells.

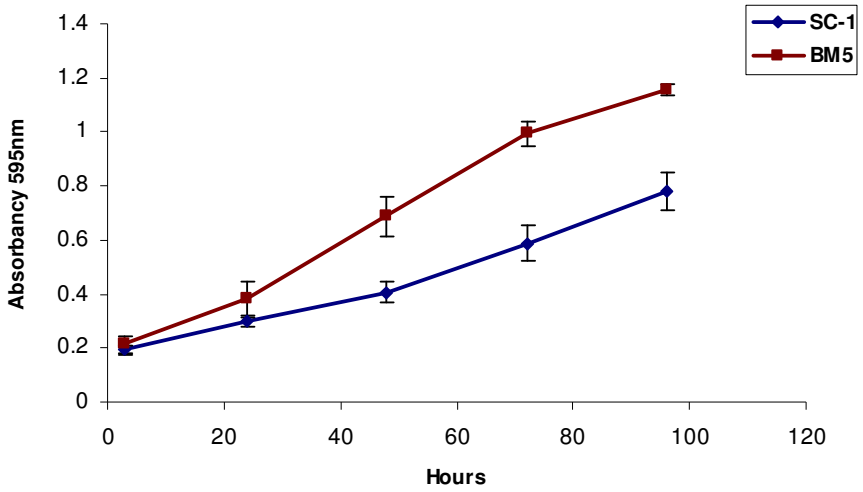

Figure 3.6. Growth curve of SC-1 and BM5 cells. BM5 cells (■) were observed to attach and grow faster than the SC-1 cells (♦). Cells were stained with Crystal Violet and the absorbency was determined at 595nm. Error bars represent the standard error of the mean for three independent experiments.

It can clearly be seen that the BM5 cells divided at a faster rate than the SC-1 cells. The cells were plated at the same concentration, allowed to grow and divide for a few hours and then stained with CV. CV stains proteins within the cells and the amount of proteins stained gives an indication of the number of cells present (Gillies *et al.,* 1986) Therefore, the more intense purple colour and higher absorbency reading obtained, the higher the cell number.

When trypsinizing confluent cell culture flasks of SC-1 and BM5 cells, the BM5 cell attachments were broken more easily than the SC-1 cells indicating that the SC-1 cells grew more tightly packed together with stronger intracellular connections. Both cell types had to be passaged through a 29' gauge needle coupled to a 1ml syringe when being counted to break up cell clumps and obtain an even distribution of cells in the cell suspension. The medium of the BM5 cells turned orange to yellow when confluent while the SC-1 cell medium was pink to slightly orange in colour upon confluency.

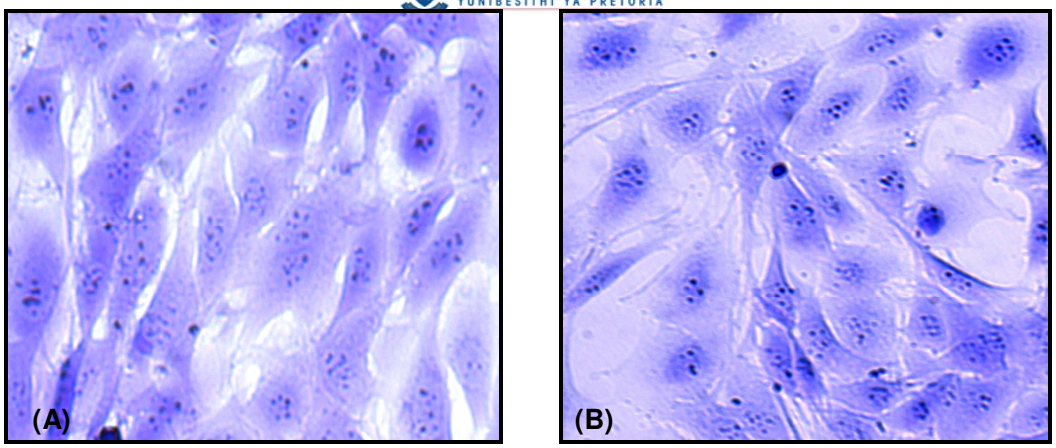

Figure 3.3. General morphology of confluent layers of SC-1 (A) and BM5 (B) cells. (A) SC-1 cells have typical fibroblast shape, long and spindle-like, (B) BM5 cells are large, distended and pleomorphic in shape. Crystal Violet staining. Magnification 20x.

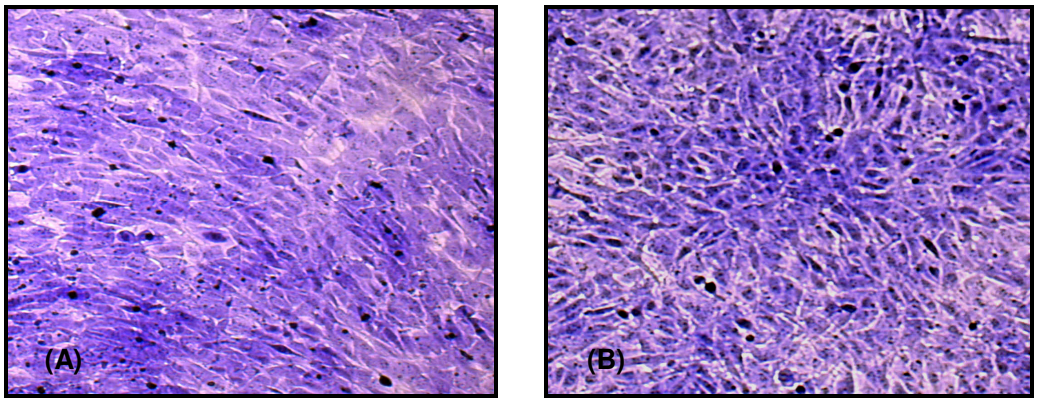

Figure 3.4. Growth pattern of confluent SC-1 (A) and BM5 (B) cells. (A) SC-1 cells are growing in an orderly parallel fashion while (B) BM5 cells are randomly distributed growing in a cluster. Crystal Violet staining. Magnification 5x.

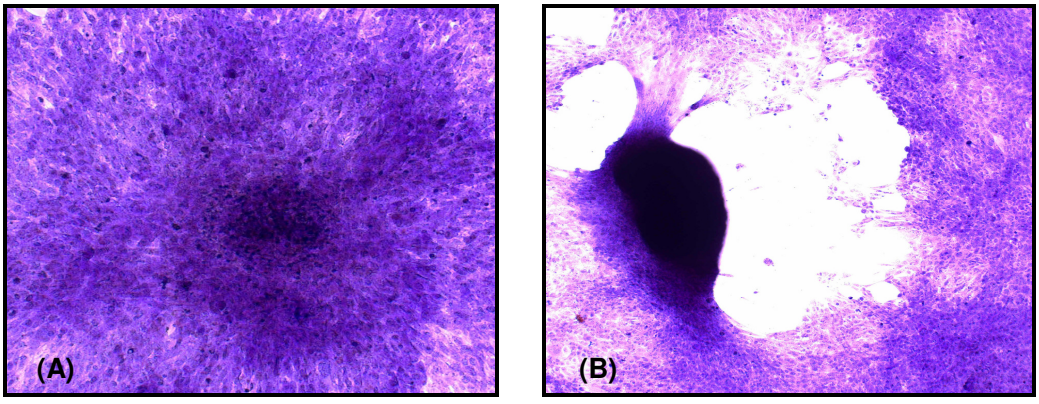

Figure 3.5. Formation of BM5 cell clusters 'cell tumour'. (A) BM5 cells growing in a densely packed, multilayered cell cluster that (B) starts detaching from the surrounding cells and eventually floats in the medium. Crystal Violet staining. Magnification 5x.

3.4.2 Ultrastructure of the SC-1 and BM5 cell lines

Transmission electron microscopy is a powerful tool used by scientists to study the structure of cells and viruses. Here it was used not only to study the LP-BM5 virus structure but also to show that the BM5 cells were indeed infected with the virus and that these cells were producing virions. The SC-1 cells were used as a negative control to show that they were not infected with virus as well as to determine if any structural differences between the two cell types could be seen.

In general appearance, the BM5 cells appeared to be larger, more distended cells with a smaller nucleus eccentrically located. The BM5 cells had fewer mitochondria and darkly stained cytoplasmic vesicles indicating that some changes had occurred in the cell structure due to viral infection (Figure 3.7(A) and Figure 3.7(B)). The viral particles in Figure 3.7 (C) and (D) appeared to have a double membrane surrounding a condensed darkly stained icosahedral-shaped central inner core typical of MuLVs (Levy *et al.,* 1994).

The first step in retroviral infection is gaining entry into the host cell. Retroviruses can gain entry to a cell by binding to receptors on the cell surface and fusing with the cell membrane (pH-independent) or they can be taken in by the process of endocytosis (pH-dependent) (Nisole and Saib, 2004). HIV is known to use CD4 as its cell-surface receptor while ecotropic MuLVs use the CAT-1 amino-acid transporter. In the BM5 cells, viral particles were observed to be closely associated with the cell membrane of the BM5 cells and the cells developed several invaginations around the viral particles (Figure 3.7(C)). These invaginations of the cell membrane indicated that the viral particles were taken up through phagocytosis. Coated pits were also observed on the cell membrane in the vicinity of viral particles indicating that some viral particles could also have been taken up by receptor-mediated endocytosis (Figure 3.7(E)).

The viral particles, once taken up into the BM5 cell, were packaged into cytoplasmic vesicles perhaps endosomes before undergoing uncoating and reverse transcription (Figure 3.7(D)). The endosome in Figure 3.7(D) was located in the vicinity of the nucleus. Notice the absence of such particles in the SC-1 cytoplasmic vesicles in Figure 3.7(F).

A

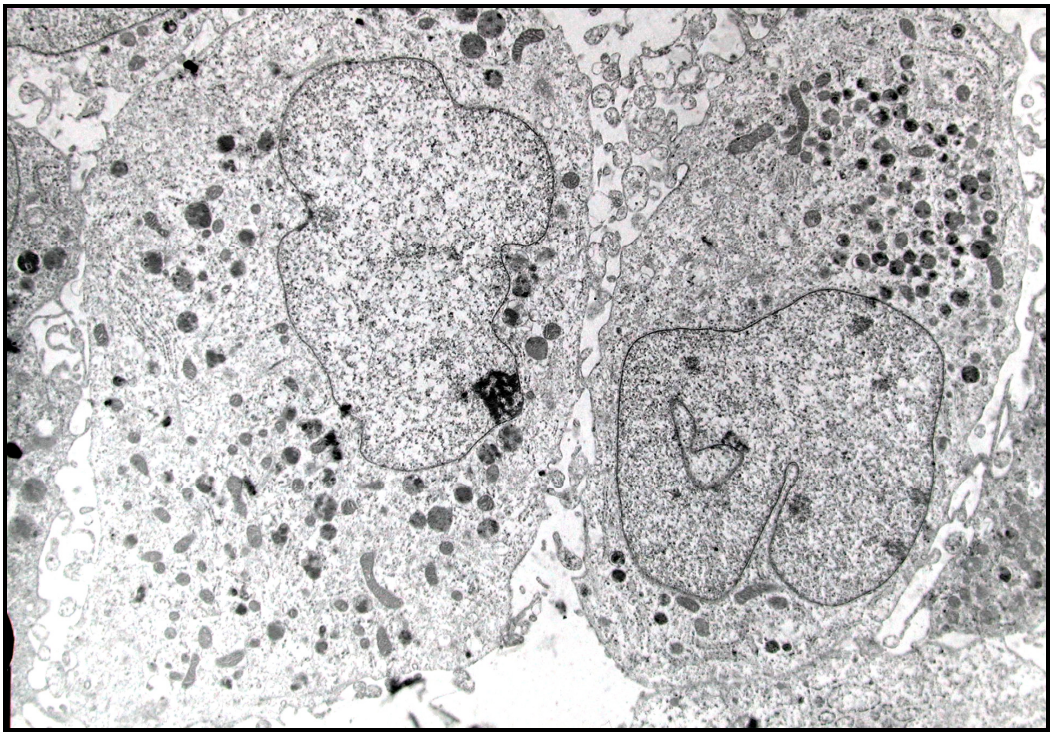

B

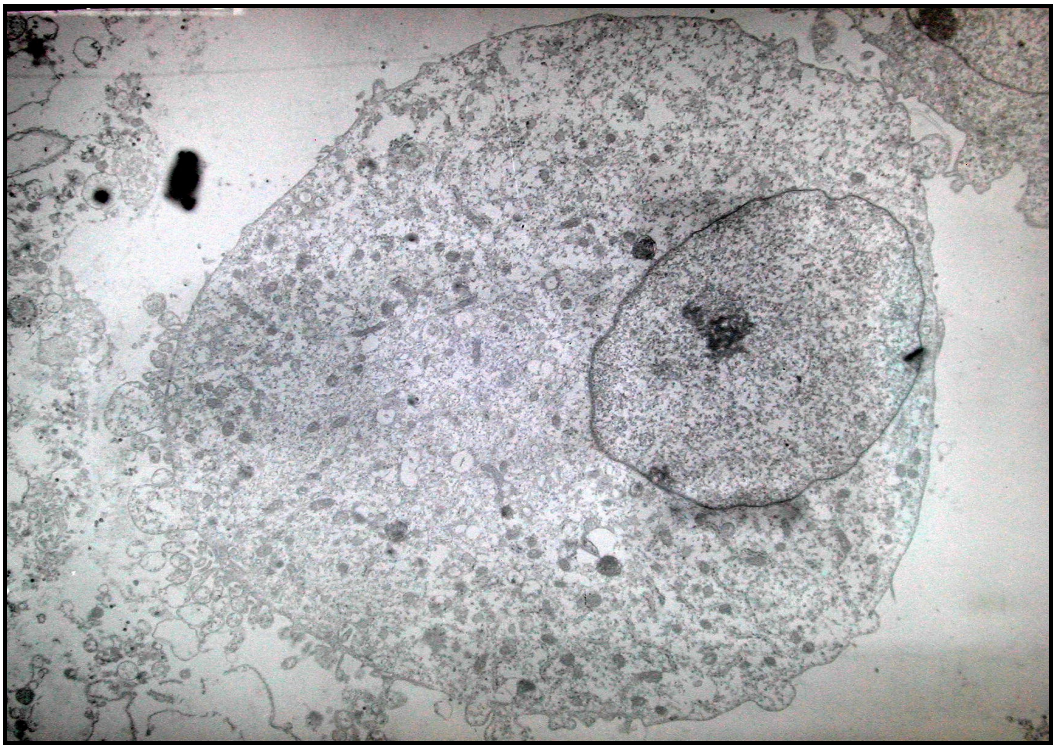

Figure 3.7 A and B. TEM micrographs of SC-1 and BM5 cells. (A) SC-1 whole cells magnification 3000x. (B) BM5 whole cell magnification 3600x.

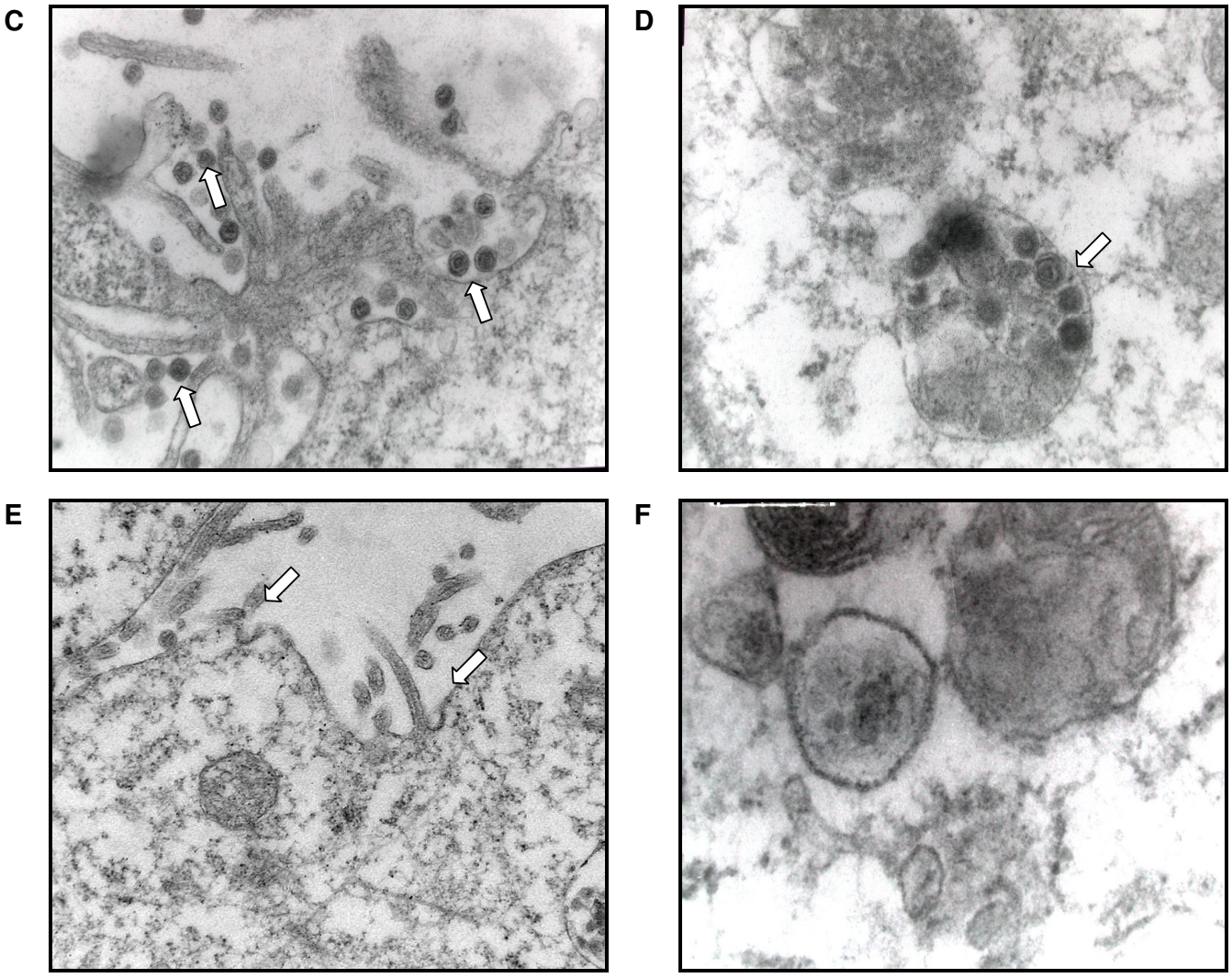

Figure 3.7 C-F TEM micrographs of SC-1 and BM5 cells. (C) Putative LP-BM5 virus particles (arrows) taken up by phagocytosis on the cellular membrane of BM5 cells 36 000x. (D) Putative LP-BM5 viral particles inside vesicles (arrow) in the BM5 cell cytoplasm 59 000x. (E) Viral particles in the vicinity of coated pits (arrows) on the BM5 cell membrane 13 000x. (F) Absence of viral particles inside cytoplasmic vesicles of SC-1 cells 43 000x.

Although the next steps in retroviral replication could not be followed as the cell preparations were not treated with immunogold labelled antibodies, it is well known that following uncoating and reverse transcription, MuLVs enter the nucleus during mitosis when there are breaks in the nuclear membrane (Katz *et al.,* 2005). If immunogold labelled antibodies had been used, it would have been possible to determine how the disease causing defective genome gained access to the cell, if it was indeed carried in following incorporation of itself into the envelope of the replication-competent retroviruses. Following entry into the nucleus, the viral genome is then integrated into the host cell genome and viral RNA is transcribed and translated into viral proteins that will form part of the new virions (Figure 3.2).

The MuLVs are classified as type-C retroviruses as assembly of the viral progeny occurs at the inner surface of the cell membrane and during budding (Murphy *et al.,* 1995). Although the distinctive darkly stained crescent that forms on the cell membrane during typical retroviral budding could not be seen, a newly formed viral particle was observed in the process of budding from the cell in Figure 3.7(G). The viral membrane is continuous with the host cell membrane. The newly released viral particle also stained very lightly at the inner core indicating that this viral particle may still be immature and that the core would only be processed once the viral particles had been released from the cell membrane as in Figure 3.7(H). Besides budding from the cell surface, the viral particles also appeared to bud from the tips of villi (Figure 3.7(I)).

G

H

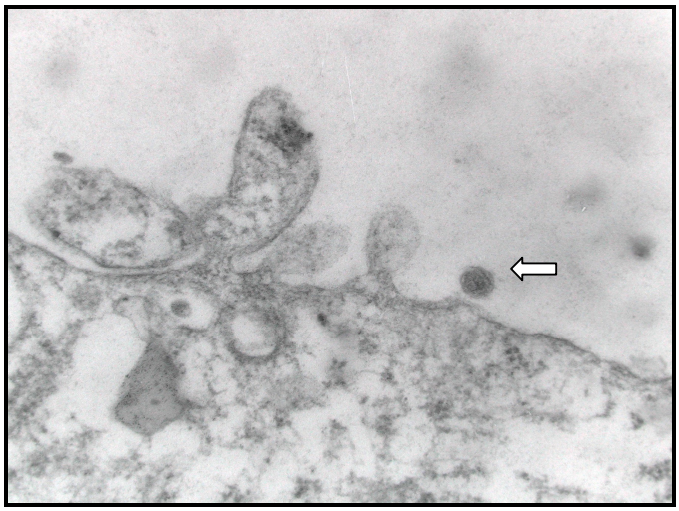

I

Figure 3.7 G-I. TEM micrographs of BM5 cells. (G) Newly formed viral particle (arrow) being released at the BM5 cell membrane 59 000x. (H) Newly released LP-BM5 viral particle (arrow) through a break in the BM5 cellular membrane 43 000x. (I) Newly formed viral particle (arrow) being released from villus tip (arrow) magnification 22 000x.

3.4.3 Semiquantitative PCR and RT-PCR for detection of viral DNA and viral RNA

Traditionally virus particles are quantified with the plaque assay. This assay shows the amount of infectious virions present (Rowe *et al.,* 1970). This technique was attempted in our laboratories but was found to be difficult, time-consuming and tedious. It was thus concluded that the plaque assay was not a suitable method for the rapid evaluation of the antiviral effect of drugs. Therefore a more rapid and sensitive method that allows the evaluation of a large number of samples namely PCR and RT-PCR was used.

The methodology for conventional PCR was developed to detect the LP-BM5-defective viral DNA and to semi-quantify the viral DNA in cells treated with drugs. The G6PDH gene was used as an internal control to compensate for differences in the DNA amount used. All LP-BM5-defective products would be normalized to the G6PDH gene during quantification. Various parameters such as $MgCl_2$, annealing temperature and number of cycles had to be optimized. Three longer cycles in the initial phase of amplification were added as this improved primer annealing. The annealing temperature for the primers needed to be optimized as a too low annealing temperature would result in non-specific amplification while a too high annealing temperature would cause a reduction in product yield and purity (Rychlik *et al.,* 1990). The annealing temperature used in Selematsela, 2001 was used in this study for the LP-BM5-defective DNA namely 50°C (Figure 3.8(A)). For the G6PDH gene the annealing temperature had to be optimized and three different annealing temperatures were evaluated namely 55, 60 or 65^0C. In Figure 3.8(B), it can be seen that an annealing temperature of 55^0C produced no PCR products while at 60^0C and 65^0C products were formed. An annealing temperature of 60^0C was selected as it produced the sharpest bands with no or little non-specific product.

Similarly, the $MgCl_2$ concentration for the LP-BM5-defective and G6PDH genes had to be optimized. The $MgCl_2$ concentration can affect the specificity and yield of the PCR reaction (Kidd and Ruano, 1995). If the $MgCl_2$ concentration was too low then the DNA Taq polymerase could not function properly as it was a co-factor for the enzyme whereas if the $MgCl_2$ concentration was too high, it could inhibit DNA denaturation and also promote incorrect primer annealing thus increasing the amount of non-specific products. Three $MgCl_2$ concentrations namely 1, 2 and 4mM were evaluated for the LP-BM5-defective and G6PDH genes. It was found that the optimal $MgCl_2$ concentration was 2mM for both the LP-BM5 defective and G6PDH genes at

annealing temperatures of 50℃ and 60℃ respectively (Figure 3.9). This $MgCl_2$ concentration of 2mM was then used for all further experiments.

The last parameter that was optimized was the number of cycles. The PCR reaction resembles a typical enzyme reaction where there is a lag phase followed by a log phase and finally a plateau phase. The lag and plateau phases are unsuitable for quantification purposes as in the lag phase the product yield will be below detection levels while in the plateau phase non-specific products may be present (Kidd and Ruano, 1995). The log phase thus appears to be the best phase for quantifying any differences in viral load as this is where the amplicon products start appearing from the background. In Figure 3.10 the LP-BM5-defective gene (A) and G6PDH gene (B) were amplified for 20, 25, 30 or 35 cycles. At 20 cycles practically no product was detected, at 25 cycles some product formed while at 30 and 35 cycles it appeared that the reaction has reached the plateau phase. A cycle number of 25 was thus selected for quantification purposes as this appeared to be when the PCR reaction was in the log phase.

The methodology for RT-PCR was developed for the detection of viral RNA. A two-step RT-PCR method was used where firstly the isolated RNA was reverse transcribed into cDNA and then the cDNA underwent PCR amplification in a separate reaction tube. No optimization was needed for either step as the reverse transcription phase worked well with the ImProm-II manufacturer's recommendations and the PCR conditions had already been optimized as described above. Three controls were included in the process namely a kanamycin RNA positive control to test the reverse transcriptase activity of the ImProm-II RT enzyme. A no RT enzyme control was included to show that the isolated RNA was not contaminated with DNA as if the RNA was contaminated then some product would be visible on the gel. And lastly, a no cDNA control was included to show that there was no contamination of the PCR reagents. Figure 3.11 shows that the G6PDH RNA was successfully amplified in both the SC-1 and BM5 cells. As expected, no viral RNA band was present for the uninfected SC-1 cells while BM5 cells containing the LP-BM5-defective genome were positive for the viral RNA band. The positive kanamycin control did work indicating that the RT enzyme was indeed active and that the bands visible for G6PDH and LP-BM5-defective RNA were not false positives.

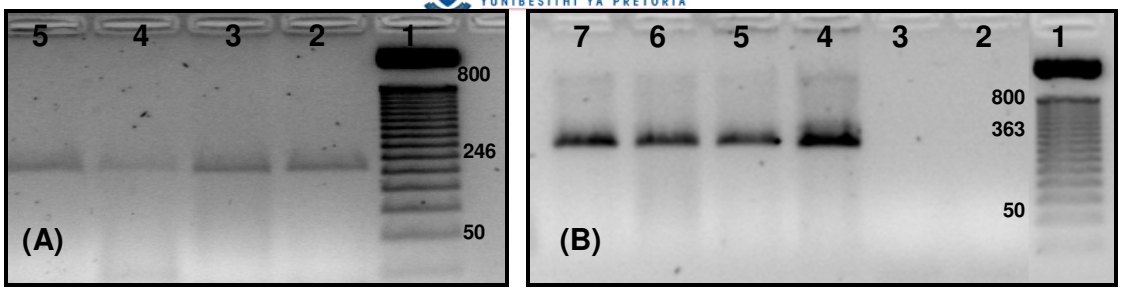

Figure 3.8. (A) BM5-def viral 246bp gene products produced at an annealing temperature of 50℃. Lane 1: 50bp DNA step ladder; Lanes 2, 3, 4 and 5: BM5-def gene products at 50℃. (B) G6PDH 363bp gene products produced at various annealing temperatures. Lane 1: 50bp DNA step ladder; Lanes 2 and 3: annealing temperature of 55^0C; Lanes 4 and 5: annealing temperature of 60^0C. Lanes 6 and 7 annealing temperature of 65^0C.

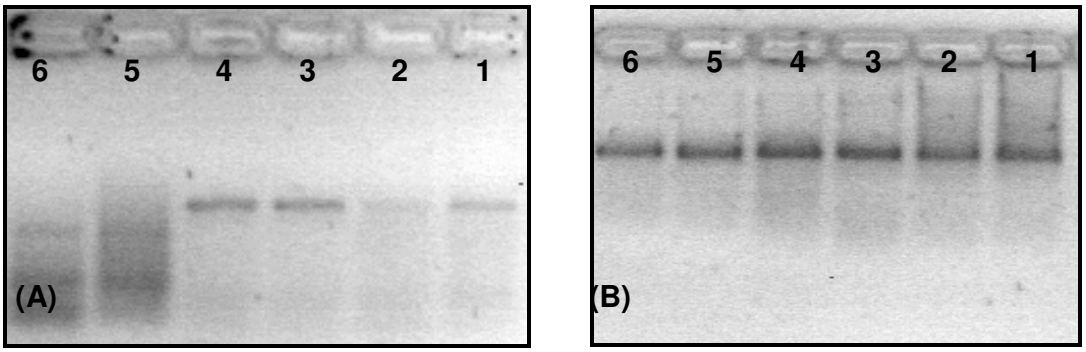

Figure 3.9. Effect of different $MgCl_2$ concentrations on the formation of BM5-def gene products at 50℃ annealing temperature (A) and G6PDH gene products at 60℃ annealing temperature (B). (A) The BM5-def gene product has an optimal $MgCl_2$ concentration at 2mM (Lanes 3 and 4) as this concentration produced the sharpest bands. Lanes 1 and 2: 1mM produce only faint bands while Lanes 5 and 6: 4mM produce non-specific products. (B) The G6PDH gene products also have an optimal $MgCl_2$ concentration at 2mM (Lanes 3 and 4) with 1mM (Lanes 1 and 2) and 4mM (Lanes 5 and 6) producing fainter bands.

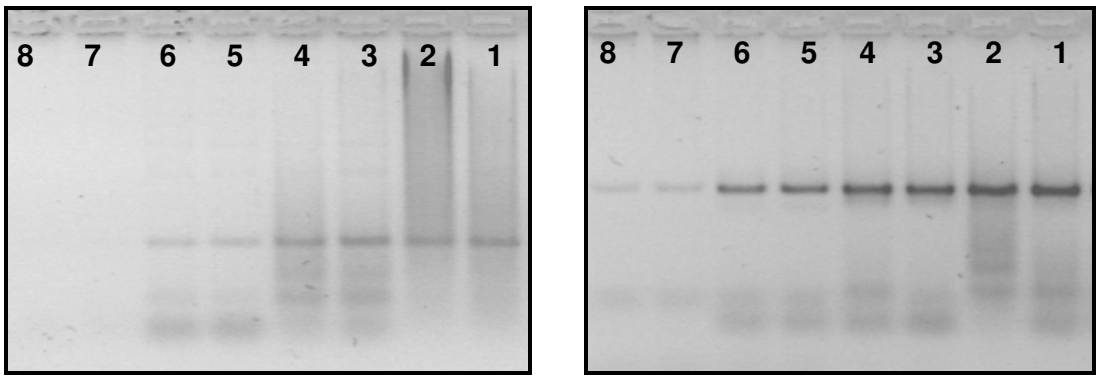

Figure 3.10. Determination of optimal cycle number for quantification of the BM5-def gene at 50℃ annealing temperature and 2mM $MgCl_2$ (A) and G6PDH gene at 60℃ annealing temperature 2mM $MgCl_2$ (B). (A) The BM5-def viral gene was amplified for 20 (Lanes 7 and 8), 25 (Lanes 5 and 6), 30 (Lanes 3 and 4) and 35 cycles (Lanes 1 and 2). Optimal cycle number is 25 cycles, with only specific product forming with little or no non-specific product. (B) The G6PDH gene was also amplified for 20 (Lanes 7 and 8), 25 (Lanes 5 and 6), 30 (Lanes 3 and 4) and 35 cycles (Lanes 1 and 2). Similarly, the optimal cycle number was 25 cycles.

The no RT enzyme and no cDNA control lanes were empty indicating that there was no DNA contamination of the isolated RNA or of any of the reagents used. In conclusion the optimized DNA and RNA PCR confirmed the presence of viral cDNA and viral RNA. However difficulties especially with reproducibility were experienced when these methods were used for quantification and therefore the real-time PCR methodologies were developed based on the above optimised parameters.

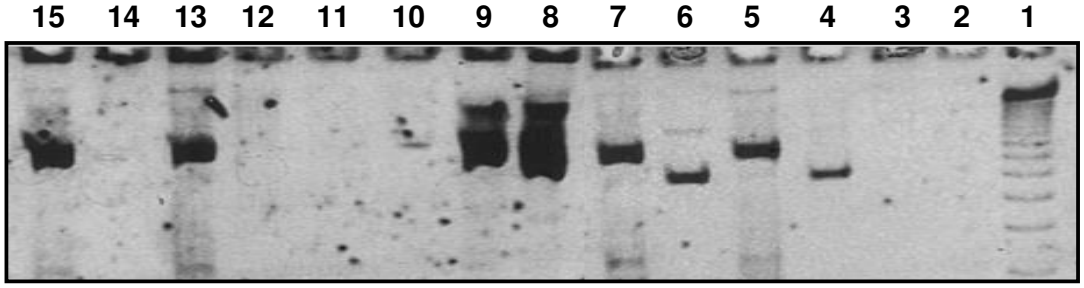

Figure 3.11. Gel representing RT-PCR amplification of the BM5-def and G6PDH genes from BM5 and SC-1 cell DNA. Lane 1: 50bp DNA step ladder; Lane 2: No RT control; Lane 3: No cDNA control; Lane 4: BM5-def gene from BM5 cell DNA using Oligo$(dT)_{15}$ primers ; Lane 5: G6PDH gene from BM5 cell DNA using Oligo$(dT)_{15}$ primers; Lane 6: BM5-def gene from BM5 cell DNA using random hexamer primers; Lane 7: G6PDH gene from BM5 cell DNA using random hexamer primers; Lanes 8 and 9: Kanamycin positive control; Lane 10: No RT control; Lane 11: No cDNA control; Lane 12: BM5-def gene from SC-1 DNA using Oligo$(dT)_{15}$ primers; Lane 13: G6PDH gene from SC-1 cell DNA using Oligo$(dT)_{15}$ primers; Lane 14: BM5-def gene from SC-1 cell DNA using random hexamer primers; Lane 15: G6PDH gene from SC-1 cell DNA using random hexamer primers.

3.4.4 Real-time PCR for the detection of proviral DNA

In this study real-time PCR methods were developed for the detection of proviral DNA and not for RNA as the former will later be used (Chapter 4 and 5) for the first level of evaluation of the effects of drugs and drug combinations in the *in vitro* co-culture model (Section 3.4.6). In this chapter real-time PCR was used to determine the presence and absence of the LP-BM5-defective virus in the BM5 and SC-1 cell lines respectively and during the development of the *in vitro* co-culture model to quantify the amount of proviral DNA.

Real-time PCR and RT-PCR are rapidly becoming the new gold standards for the detection and quantification of viruses. Real-time PCR allows the investigator to monitor the product as it amplifies in real-time and uses the point at which the product emerges from the background fluorescence for quantification purposes rather than at the end of the amplification process as in conventional PCR (Watzinger *et al.,* 2006). Two different detection formats can be used namely DNA-binding dyes such as SYBR Green or fluorescent probes. The SYBR Green format was used in

this study for detection and quantification purposes as this appeared to be the more economical and easier option.

The cycling conditions used for real-time PCR were essentially the same as that for conventional PCR except that the cycling times for each phase were considerably shorter meaning that the real-time PCR assay took only 1 hour to complete compared to the 3 hours for conventional PCR amplification. Also, no electrophoresis of the amplicon products was necessary as the fluorescence that is related to the amount of product formed was continuously monitored by the optical detection system in real-time PCR.

The isolated BM5 cell and SC-1 cell DNA together with ddH_2O were amplified for viral and G6PDH (housekeeping) genes using the programme in Table 3.4. The BM5 cell DNA served as a positive control for both the virus and G6PDH gene while the SC-1 DNA served as a negative control for the virus as these cells were expected to be uninfected and as a positive control for the G6PDH gene. The ddH_2O was included as a no template control so one could visualize the cycle number at which the primer dimers started emerging from the background. The LP-BM5-defective gene was amplified on a separate plate in a separate run from the G6PDH gene as their primers had different annealing temperatures, 50℃ for the viral and 60℃ for the G6PDH primers.

In Figure 3.12 amplification curves measuring the fluorescence against cycle number for the viral (A) and G6PDH (B) genes can be seen. For viral amplification, the products from the BM5 cell DNA emerged around cycle number 18 while products from the SC-1 DNA and ddH_2O sample only emerged around cycle 30. This indicated that specific product (LP-BM5-defective gene) was amplified from the BM5 cell DNA while the SC-1 DNA and ddH_2O samples contained primer dimers and perhaps non-specific products. For G6PDH gene amplification, the products amplified from the BM5 cell and SC-1 cell DNA emerged at approximately the same cycle number, cycle number 25, indicating that the two have similar DNA concentrations. The primer dimers from the ddH_2O sample only emerged at cycle number 30 the same as for the viral PCR. Comparison of the cycle numbers obtained for the viral and G6PDH genes from the BM5 cell DNA indicated that the BM5 cell DNA contained more copies of the viral gene than of the housekeeping gene meaning that the LP-BM5 defective virus did not insert just one copy into the host cell DNA but several copies.

A melting curve analysis was then performed on each of the products to determine the specificity of the amplified PCR products (Figures 3.12 (C) and (D). This analysis

discriminated between specific product and primer dimers. In Figure 3.12(C) a melting curve analysis was performed for the LP-BM5–defective genome amplified from SC-1 and BM5 cell DNA. The LP-BM5-defective gene products melted at a temperature of 86.23℃ ± 0.167℃ while the primer dimers in the ddH_2O sample melted at a temperature of approximately 81℃. The two peaks for primer dimer and specific product are relatively close to each other probably due to the high GC content of the primers (Table 3.1). The products from viral amplification of the SC-1 DNA melted at a temperature of 82.72℃ ± 0.176℃. This temperature falls close to that for the primer dimers of the ddH_2O sample indicating that the majority of the SC-1 DNA PCR products are primer dimers and that the cells are not infected with virus. There is however a slight shift in melting temperature of the products from the SC-1 DNA from the peak of the primer dimers and this may indicate that some non-specific primer annealing occurred.

A melting curve analysis was also performed for the G6PDH gene. SC-1 and BM5 cell DNA were used as positive controls for the house-keeping gene while the ddH_2O served as a negative control. From Figure 3.12(D) it can be seen that the G6PDH gene products from the SC-1 and BM5 cells melted at approximately the same temperature namely 85.71℃ ± 0.057℃ for SC-1 G6PDH gene and 86.46℃ ± 0.027℃ for BM5 G6PDH gene. The primer dimers in the water sample melted at approximately 81℃. Once again the temperatures are near each other due to the high GC content of the primers (Table 3.1).

A standard curve for the LP-BM5-defective and G6PDH genes was constructed to determine the efficiency of the PCR reaction. From Figure 3.13 (A and B) it can also be seen that the higher the concentration of the gene the faster (after fewer cycles) the product emerges from the background. The dilutions of 0.01, 0.001 and 0.0001% formed primer dimers as they contained very small amounts of either gene and thus had to be excluded from the standard curve (Figure 3.13(C)). In Figure 3.13 (E and F) linearity was found for both the viral and house-keeping genes between 0.1 and 100%. The efficiency of the viral PCR was 1.944 with an error of 0.170 while the efficiency of the G6PDH PCR was 2.005 with an error of 0.136. The efficiencies of both reactions were thus close to 2.0 meaning that during relative quantification an efficiency of 2.0 could be correctly assumed and that it would not be necessary to employ standard curves for relative quantification.

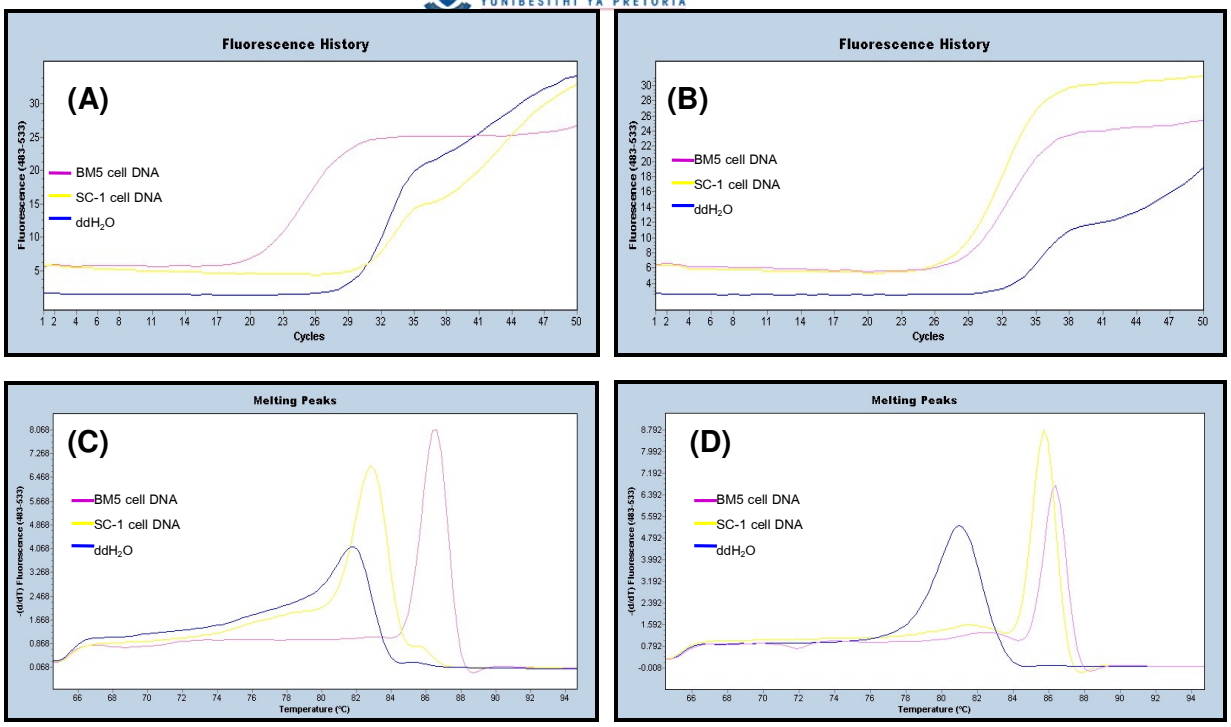

Figure 3.12. Real-time PCR amplification and melting curve analysis of the BM5 and G6PDH genes from BM5 and SC-1 cell DNA. (A) Amplification curve for the BM5-def gene amplified from BM5 and SC-1 cell DNA. (B) Amplification curve for the G6PDH gene amplified from BM5 and SC-1 cell DNA. (C) Melting curve analysis for the BM5-def gene amplified from BM5 and SC-1 cell DNA. (D) Melting curve analysis for the G6PDH gene amplified from BM5 and SC-1 cell DNA.

3.4.5 The *in vivo* MAIDS model

The presence of viral particles, proviral DNA and RNA and cDNA has been confirmed in the BM5 cell line. The final and conclusive indication that this cell line was indeed infected with LP-BM5 MuLV was to infect C57Bl/10 mice to induce MAIDS. To test this, a crude viral isolate was prepared from the supernatant of lysed BM5 cells. This preparation was injected intraperitoneally at three different concentrations (low, medium and high). These mice were terminated after 7 weeks and were evaluated for two common symptoms of infection with the LP-BM5 MuLV complex namely lymphadenopathy and splenomegaly (Yetter *et al.,* 1988). Figure 3.14 shows the lymph nodes of an uninfected (Labelled C) and infected mice (No 2-6). The infected mice had enlarged submandibular lymph nodes compared to the example of the control mouse indicating that the mice were developing lymphadenopathy a classical symptom of infection with LP-BM5 virus complex. The spleen of each mouse was weighed and the average was calculated.

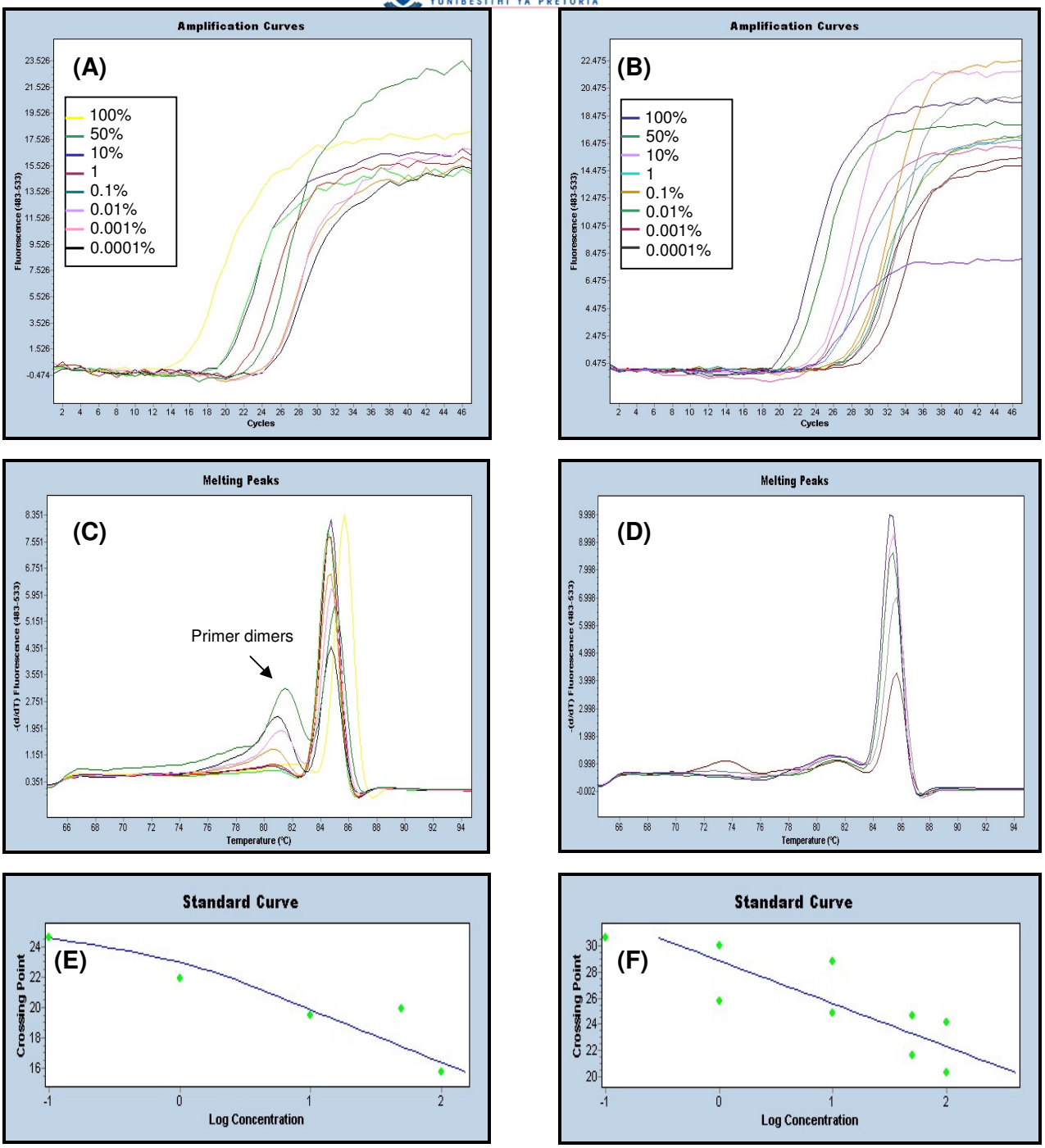

Figure 3.13. Standard curve construction for the BM5-def and G6PDH genes for determination of the PCR efficiency. (A) Amplification curve for the serial dilutions (Table 3.2) of the BM5-def gene. (B) Amplification curve for the serial dilutions (Table 3.3) of the G6PDH gene. (C) Melting curve analysis of the products amplified from serial dilutions of the BM5-def gene. (D) Melting curve analysis of the products amplified from serial dilutions of the G6PDH gene. (E) Standard curve determined with the absolute quantification software for the BM5-def gene using dilutions 0.1% to 100%. (F) Standard curve determined with the absolute quantification software for the G6PDH gene using dilutions 0.1% to 100%.

The average mass of the spleen of the control mice was 0.06g; the mice receiving a low dosage had an average mass of 0.24g, medium dosage 0.39g and the high dosage 0.43g. Mice that were exposed to the LP-BM5 virus showed a significant increase in the spleen mass indicating splenomegaly.

(A)

(B)

Figure 3.14. Comparison of the sizes of the lymph nodes (A) and spleens (B) of mice inoculated with viral extract from BM5 cells (2-6) and control mice not innoculated (C).

Table 3.6. Comparison of the spleen weights from control mice (n=5) and mice receiving different volumes (5 mice per group) of BM5 viral extract.

Virus dose	Average spleen mass (g)	Standard deviation (g)	p-value
Control	0.06	0.006	ns
Low	0.24	0.167	ns
Medium	0.39	0.089*	0.0046
High	0.43	0.041*	4.43×10^{-5}

** significantly different from control, students t test*

3.4.6 The *in vitro* co-culture model of SC-1 and BM5 cells

Three different *in vitro* models can be developed for antiviral screening of drugs. These are acute infection, co-culture model and chronic infection (Lambert *et al.,* 1993). The BM5 and SC-1 cells were used to create a co-culture model to study the effects of different drugs and drug combinations on cell-to-cell transmission of the virus. The BM5 and SC-1 cells were combined at different ratios to identify the minimum infection possible for a reproducible model. The cells were mixed and grown for 3 days where after, the DNA was isolated and amplified with semi-quantitative PCR and real-time PCR. BM5 DNA was used as a positive control for the LP-BM5-defective genome while SC-1 DNA was used as a negative control.

In Figure 3.15(A), it can be seen that both controls worked namely the BM5 cells produced a viral band while the SC-1 cells did not. It was observed that as the number of BM5 cells increased in the co-cultures, so did the intensity of the viral band. From the density ratios (Figure 3.15(B)) the 1:1, 1:10 and 1:100 co-cultures had the same amount virus as the BM5 cell line whereas for cell ratios 1:1,000, 1:10,000 and 100,000 the amount of viral DNA was lower. The effect of the 1:1, 1:10 and 1:100 ratios not being significant was possibly due to the fact that the BM5 cells were observed to grow faster than the SC-1 cells (Figure 3.6). The standard error of the mean and the coefficient of variation of the 1:100,000 co-culture was so high because one of the experiments failed to produce a detectable viral band. This may have been due to the fact that the amount of the viral DNA was below the detection limit of the method or that to plate a 1:100,000 ratio is difficult if 250,000 cells were plated per experiment (only 2.5 BM5 cells) (Table 3.5). Therefore a co-culture of 1:10,000 was thus selected as the best model for antiviral screening of drugs as it was within a linear region of detection and the results obtained were reproducible (low standard error of the mean and low coefficient of variation).

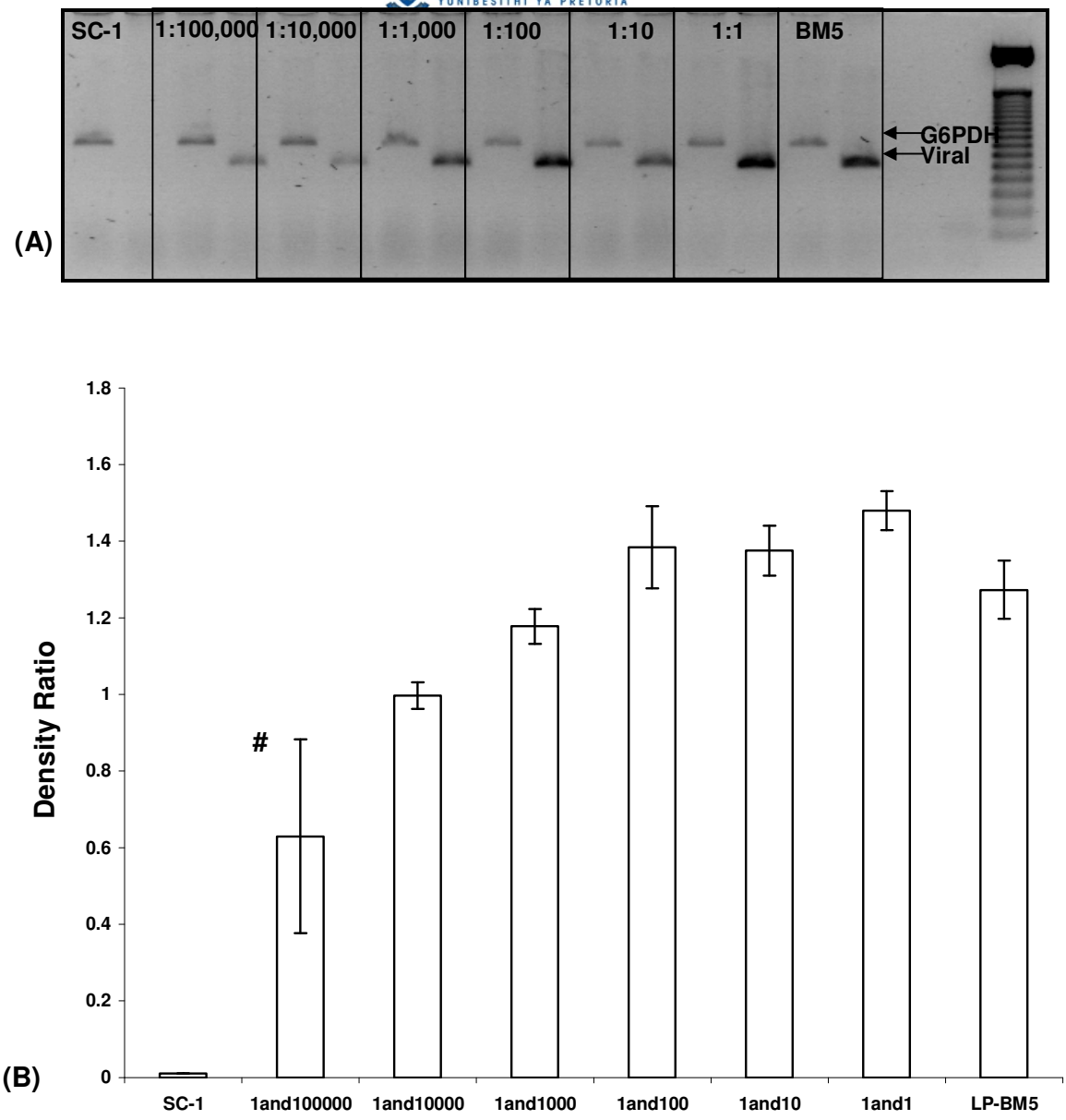

Figure 3.15. Semi-quantitative PCR analysis of the co-cultures at different ratios of BM5:SC-1 cells. (A) Agarose gel representing one of the three independent co-culture experiments. (B) Average of the density ratios (BM5-def band intensity corrected to G6PDH band intensity) of three independent co-culture experiments. Error bars represent the standard error of the mean for three independent experiments. **#** Error bar for the 1:100 000 co-culture is so high because one experiment failed to produce a detectable viral band. The coefficient of variation for each of the co-cultures was as follows: BM5 = 10.4%; 1:1 = 5.9%; 1:10 = 8.3%; 1:100 = 13.4%; 1:1,000 = 6.8%; 1:10,000 = 6.1%; 1:100,000 = 69.6%.

Real-time PCR analysis on the co-culture DNA was also performed. The highest viral infection was found in the 1:1, 1:10 and 1:100 as the products from these samples were some of the first to appear from the background fluorescence (Figure 3.16(A)). The lowest viral infection was found in the 1:10,000 and 1:100,000 co-cultures with the products from the 1:100,000 co-culture emerging close to those from the SC-1 DNA (negative control). A melting curve analysis was performed on the products and from Figure 3.16(C) it was clearly visible that the 1:100,000 co-culture did contain some viral DNA but that primer dimers were also present thus causing this sample to be unsuitable for quantification purposes. Therefore, the assumption from the conventional PCR analysis that the 1:100,000 co-culture was an unsuitable model, was confirmed by real-time PCR and for all further studies a 1:10,000 cell ratio was used. Figures 3.16 (B) and (D) show that G6PDH gene products were amplified from all the co-culture DNA samples and that no sample produced any primer dimers.

Relative quantification analysis was performed on each of the co-cultures except for the 1:100,000 co-culture as it produced primer dimers. The analysis quantified the expression level of the viral gene relative to the G6PDH gene (housekeeping gene) to correct for differences in the amount and quality of the various DNA samples. This ratio (viral/G6PDH) was then normalized by the calibrator (BM5 cell DNA) so that the three independent experiments could be compared. Figure 3.16 (E) compares the relative viral infection of the different co-culture DNA samples to the calibrator. It showed that the 1:1 and 1:10 co-cultures had similar viral infection levels as that of the calibrator, the 1:1,000 co-culture had slightly less while the 1:10,000 co-culture had the lowest viral infection with the infection being about half of that of the calibrator.

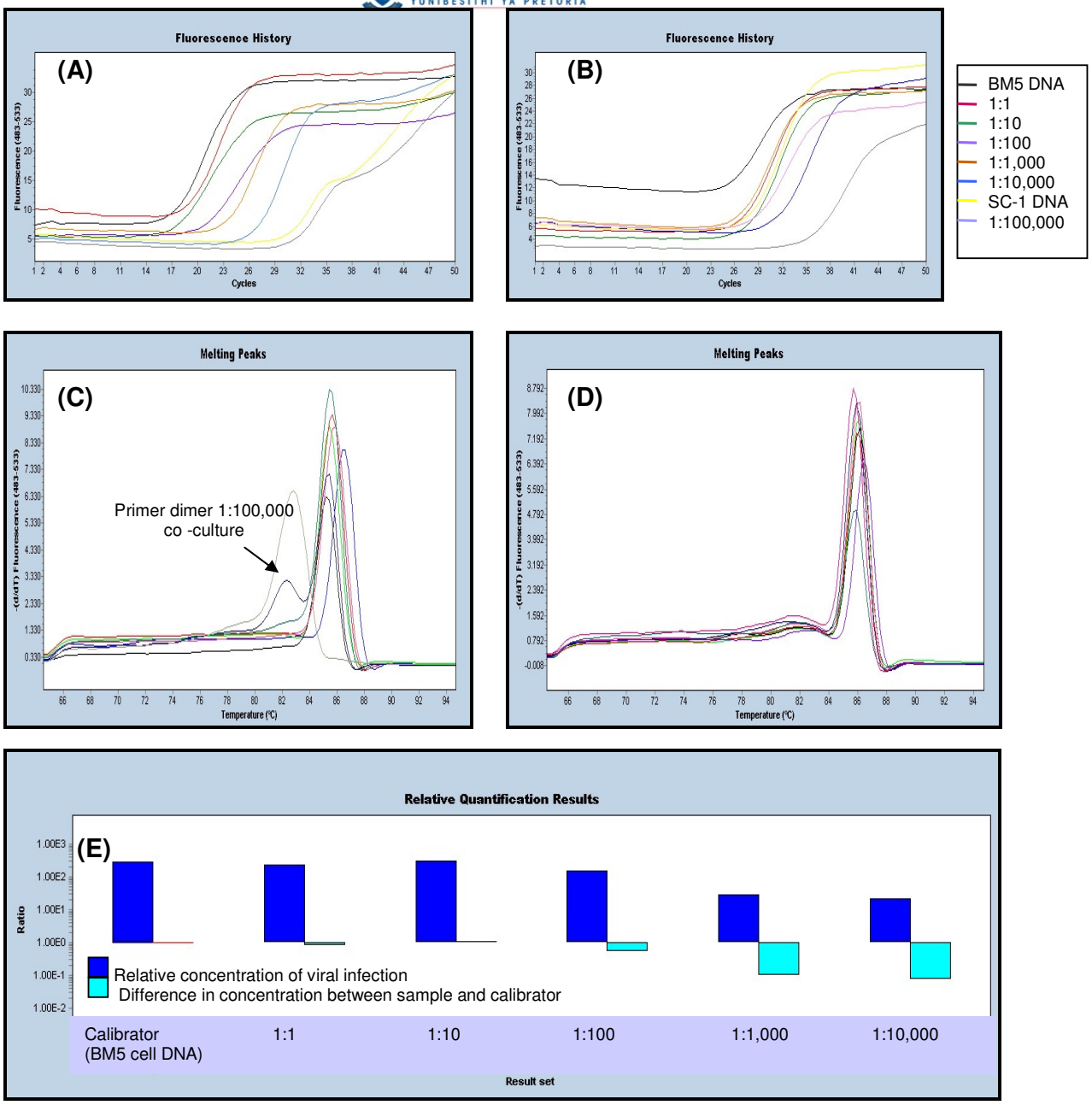

Figure 3.16. Real-time PCR analysis of one of the co-culture experiments. (A) Amplification curve for the BM5-def gene from the various co-culture DNA. (B) Amplification curve for the G6PDH gene from the various co-culture DNA. (C) Melting curve analysis of the BM5-def gene products amplified from the various co-culture DNA. (D) Melting curve analysis of the G6PDH gene products amplified from the various co-culture DNA. (E) Relative quantification plot for the three co-culture experiments. Relative quantification analysis of the 1:100,000 co-culture was not included as it produced primer dimers.

3.5 Conclusion

The SC-1 and BM5 cell lines as well as the co-culture model were successfully established. Firstly the morphology and growth characteristics of each cell line were determined. The SC-1 cells had the typical morphology of uninfected fibroblasts. These cells had a long spindle-like shape and were closely packed parallel to each other. The BM5 cells on the other hand were shown to be a transformed cell line in which the cells were pleimorphic in shape, grew more rapidly, formed multilayers as well as cell clusters 'cell tumours' when confluent.

The techniques for detection of viral infection were also successfully established and included transmission electron microscopy, PCR and RT-PCR. Electron micrographs taken of the BM5 cells clearly show that viral particles were entering and being produced by BM5 cells. PCR and RT-PCR showed the presence and the absence of proviral DNA and viral RNA in the BM5 and the SC-1 cell lines respectively. The virus isolated from the BM5 cell line was infectious as mice infected with this virus showed classical symptoms of LP-BM5 virus infection, namely lymphadenopathy and splenomegaly.

A co-culture model of 1:10,000 BM5:SC-1 cells was established to later investigate the effects of different drugs on the cell-to-cell transmission of the virus (Chapter 4 and 5). The semi-quantitative and real-time PCR methodologies were used to quantify the relative amounts of virus infection in the different co-culture models created. The real-time PCR method was found to be the method of choice for quantifying proviral DNA levels due to its greater speed, sensitivity and reproducibility when compared to conventional semi-quantitative PCR.

Chapter 4: Evaluation of the toxicity and antiretroviral activity of experimental compounds green tea and EGCg relative to the antiretroviral drugs AZT, HU, IDV and CQ.

4.1 Introduction

Since HIV was identified as the etiological agent of the acquired immunodeficiency syndrome (AIDS), the US FDA has approved over 20 different antiretroviral drugs. These drugs have been divided into six classes namely the NRTIs, NNRTIs, PIs, fusion inhibitors, entry inhibitors and HIV integrase strand transfer inhibitor (viewed at http://www.fda.gov/oashi/aids/virals.htlm).

Zidovudine (Retrovir), 3'-azido-3'-deoxythymidine (AZT), was the first antiretroviral drug approved by the FDA for the treatment of HIV/AIDS and can be viewed at http://www.fda.gov/oashi/aids/virals.htlm. This NRTI was originally synthesized in 1964 by Dr. Jerome Horwitz and associates as a potential anticancer drug, but due to lack of activity against animal cancers it was discarded (Pattishall, 1993). Early in 1981, Wellcome Research Laboratories in the US and UK synthesized two 3'-azido-3'-deoxythymidines and both underwent several bioactivity assessments. One of these drugs, AZT was found to be active against several gram-negative enteric bacteria such as *Escherichia coli* B, *Salmonella typhimurium, Shigella flexineri, Klebsiella pneumoniae* and *Enterobacter aerogenes.* AZT was however, inactive against gram-positive bacteria, anaerobic bacteria, mycobacteria, several fungi and various DNA and RNA viruses. In 1984, AZT was screened in the plaque reduction assay that used the Friend leukemia virus and Harvey sarcoma virus in FG-10 murine cells and was found to be active against both and this led to the further evaluation of this drug. AZT was found to completely inhibit p24 *gag* production and protect against the cytopathic effect of HIV *in vitro* at concentrations of 5 and 10μM. It was also found to completely inhibit reverse transcriptase production at concentrations of 0.5μM or more (Mitsuya *et al.,* 1985). AZT has been extensively evaluated both *in vitro and in vivo* against several other retroviruses such as Rauscher MuLV (Ruprecht *et al.,* 1986) avian myeloblastosis virus (Eriksson *et al.,* 1987), feline leukemia virus (Hartmann *et al*., 1992), FIV (Hartmann *et al.,* 1992; North *et al.,* 1989; Meers *et al.,* 1993; Arai *et al.,* 2002), SIV (Le Grand *et al.,* 1994; van Rompay *et al.,* 1995), LP-BM5 (Ohnota *et al.,* 1990; Basham *et al.,* 1990; Eiseman *et al.,* 1991) and HIV in SCID mice (Alder *et al.,* 1995; Limoges *et al.,* 2000). However widespread resistance to AZT by HIV-1 and HIV-2 has developed and has thus

prompted scientists to search for new antiretroviral drugs (Arts *et al.,* 1998; Reid *et al.,* 2005) or drug combinations.

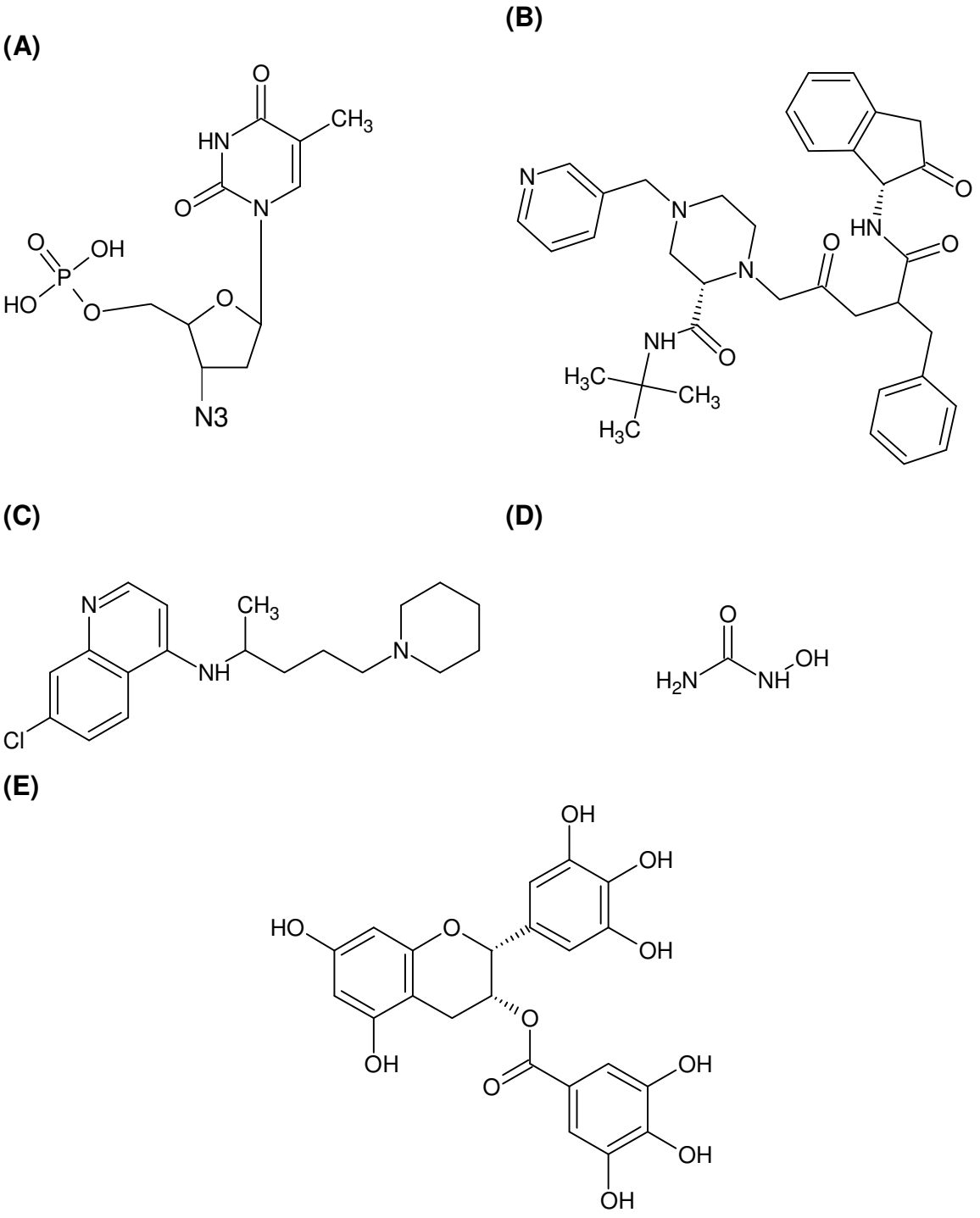

Figure 4.1: The chemical structure of (A) AZT, (B) IDV, (C) CQ, (D) HU and (E) EGCg.

The PI group of drugs was specifically designed to inhibit the HIV enzyme protease. One of these drugs Indinavir (IDV), Crixivan, was approved for the treatment of HIV/AIDS in March of 1996 (http://www.fda.gov/oashi/aids/virals.htlm). This protease inhibitor was developed by Merck Research Laboratories using structure-assisted drug design based

on crystallographic and NMR studies of the HIV protease (Lin, 1997; Wlodawer and Vondrasek, 1998). IDV was found to be effective against HIV-1 T-lymphoid cell adapted variants, primary virus isolates and monocytotropic variants *in vitro* (Vacca *et al.,* 1994). IDV has also been shown to have activity against SIV_{mac251} (Vacca *et al.,* 1994), SIV_{mac239} (Giuffre *et al.,* 2003), *Leishmania major* (Savoia *et al.,* 2005), *Cryptococcus neoformans* (Blasi *et al*., 2004), *Pneumocystis carinii* (Atzori *et al.,* 2000), human fungal pathogen *Fonsecaea pedrosoi* (Palmeira *et al.,* 2006) as well as *Candida albicans, Cryptosporidium parvum, Toxoplasma gondii and Pneumocystis carinii (*Pozio and Morales, 2005*).* However the use of IDV in HIV/AIDS treatment has resulted in several adverse effects and thus has limited its use in the treatment of HIV/AIDS. These adverse effects include hyperbilirubinaemia (Zucker *et al.,* 2001) insulin resistance and diabetes (Yarasheski *et al.,* 1999; Murata *et al.,* 2000), kidney dysfunction (Olyaei *et al.,* 2000) and changes in fat metabolism (Hermieu *et al.,* 1999).

Hydroxyurea (HU) and chloroquine (CQ) have been identified and evaluated as two possibly more economical options for the treatment of HIV/AIDS (Paton *et al.* 2002). Both drugs when combined with didanosine *in vitro* were shown to exhibit an additive anti-HIV effect. This combination was also found to significantly reduce viral load *in vivo* and was well tolerated by patients with only mild side-effects.

HU was traditionally used in the treatment of cancer and blood disorders such as sickle-cell anemia (Gwilt and Tracewell, 1998). It was first synthesized by Dressler and Stein in Germany and was later shown to be effective against several different cancers in 1963. More recently and more importantly, HU has been shown to have anti-HIV effects. These antiretroviral effects have been extensively reviewed by Lori, 1999; Lori and Lisziewicz, 2000; Zala *et al.,* 2000; Lisziewicz *et al*., 2003; Kelly *et al.,* 2004. HU in the treatment of HIV/AIDS not only has an effect on the virus but also on the immune cells responsible for spreading the virus by inhibiting the replication of CD4 T-lymphocytes. HU has also been found to be an inhibitor of the cellular enzyme ribonucleotide reductase that converts ribonucleosides into deoxyribonucleosides. Reduced levels of dNTPs halt the important conversion of viral RNA into viral DNA. In combination with NRTIs, HU assists in the conversion of NRTIs pro-drugs into active drugs by promoting the kinase activity responsible for this conversion. HU has also been shown to have activity against the LP-BM5 MuLV in the *in vivo* MAIDS model (Mayhew *et al.,* 2002; Sumpter *et al*., 2004).

The synthesis of CQ was originally based on the structure of quinine, the active ingredient from the bark of the cinchona tree first used to treat malaria (O'Neill *et al.,* 1998). CQ was found to be one of the most effective and affordable treatments for malaria until drug resistance developed (Jiang *et al.,* 2006). Recently, it was discovered that CQ is effective against HIV *in vitro* and *in vivo* (Tsai *et al*., 1990; Savarino *et al.,* 2001 and 2004; Sperber *et al.,* 1995 and 1997) and against the SARS virus *in vitro* (Keyaerts *et al.,* 2004, Vincent *et al.,* 2005). Several different mechanisms of CQ action has been proposed, these include interfering with the glycosylation of the viral proteins (Tsai *et al.,* 1990, Savarino *et al.,* 2001 and 2004), inhibiting the viral enzyme integrase (Fesen *et al.,* 1993) and inhibiting Tat-induced cytokine secretion by monocytes and T-cells (Rayne *et al.,* 2004).

The development of drug resistance to the available antiretroviral drugs has been a major obstacle in the treatment of HIV/AIDS. The selection of drug-resistant strains is often caused by suboptimal intracellular antiretroviral drug concentrations, selective pressure under long-term therapy, misincorporation of nucleotides and the lack of proofreading activity by the HIV RT enzyme (Frenkel and Tobi, 2004, Imamichi, 2004). Suboptimal intracellular antiretroviral drug concentrations can arise from poor patient compliance (major cause), poor drug absorption, drug-drug interactions, rapid excretion, and high protein binding (Frenkel and Tobi, 2004). Another problem is that people can be infected with viral strains that are already drug-resistant. Drug resistance development can lead to cross resistance (multiple drug resistance) that then limits the treatment options (Imamichi, 2004). For this reason, there is a constant endeavor by scientists to design and identify new drugs that target other viral pathways or improve the efficacy of existing drugs. One such compound is EGCg, the active ingredient of GT.

Tea is one of the most consumed beverages in the world and it was first mentioned in literature in 350BC in China and then later moved to the Japan in the 6th century (Weisburger, 1997). Tea is derived from the leaves of the evergreen plant *Camellia sinensis* that contains the enzyme polyphenol oxidase that is responsible for oxidizing the polyphenols found in the leaves. Different tea types are produced depending on the different degrees of oxidation; GT is produced from fresh tea leaves in which no oxidation has occurred, black tea is produced after 45-90min oxidation while Oolong tea is produced from partially oxidized tea leaves (Graham, 1992).

Compounds found in GT include catechins, flavonols, theogallin, ascorbic acid, gallic acid, quinic acid, theaninie, methylxanthines, caffeine, carbohydrates and minerals (Graham, 1992). The main component of GT is the catechins and these include catechin, epicatechin, epicatechin gallate, epigallocatechin, gallocatechin and epigallocatechin-3-gallate (Peterson *et al.,* 2005). EGCg (Figure 4.1), most abundant catechin in GT, is believed to be the catechin responsible for the beneficial effects of drinking GT and has been extensively reviewed by Dufresne and Farnworth, 2001 and Zaveri, 2006. GT and EGCg have been shown to have protective effects against several different types of cancers, cardiovascular and neurodegenerative diseases. GT and EGCg have also been shown to have antimicrobial activity against *Staphylococcus aureus* and *Escherichia coli* (Shimamura *et al.,* 2007) and antimalarial activity (Sannella *et al.,* 2007). GT and EGCg have been shown to have antiviral effects against HIV, the Epstein-Barr virus (Chang *et al.,* 2003), adenovirus (Weber *et al.,* 2003), rota- and enteroviruses (Mukoyama *et al.,* 1991), human T-cell lymphotropic virus (Sonoda *et al.,* 2004) and the influenza virus (Nakayama *et al.,* 1993). EGCg has been shown to inhibit the HIV enzyme reverse transcriptase in enzyme based assays with the same strength as AZT (Nakane and Ono, 1990; Tao, 1992; Chang *et al.,* 1994), to inhibit the viral enzyme protease and destroy viral particles *in vitro* (Yamaguchi *et al*., 2002) as well as to interfere with the binding of gp120 to the cellular receptor CD4 *in vitro* (Kawai *et al*., 2003). These multiple effects of GT and EGCg on HIV replication make it a worthy candidate for further investigation and may prove beneficial (synergistic or additive) when used in combination with other known antiretrovirals. To date, GT and EGCg have not yet been evaluated in any of the animal models for HIV/AIDS.

The aims of this study were therefore to;

(xii) Determine the cytotoxicity (TD_{50}) of the AZT, IDV, HU, CQ, GT and EGCg in the uninfected SC-1 cell line using the MTT assay.

(xiii) Use sub-toxic concentrations of AZT, IDV, HU and CQ to evaluate their effects on the viral load in co-cultures of BM5 and SC-1 cells. This will validate this *in vitro* co-culture model for use in antiretroviral screening of compounds.

(xiv) And lastly to evaluate the effects of GT and EGCg on the viral load at sub-toxic concentrations in this *in vitro* co-culture model.

4.2 Materials

4.2.1 Cell lines

Same as Section 3.2.1.

4.2.2 Media, supplements, reagents and disposables

Same as Section 3.2.2 and 3.2.3 and 3-(4,5-dimethylthiazol-2-yl)-2,5-diphenyltetrazolium bromide (MTT), AZT, CQ and HU were obtained from Sigma-Aldrich Company, Atlasville, SA. IDV was obtained from a local pharmacy, Hatfield, SA. Freshpak green tea was obtained from Pick 'n Pay, Hillcrest, SA. Teavigo (EGCg) was obtained from Roche Chemicals, Japan.

4.3 Methods

4.3.1 Preparation of drug stock solutions

AZT, IDV and EGCg were prepared as 2mM stock solutions while CQ was prepared as a 500µM stock solution and HU as a 1.5mM stock solution in autoclaved ddH_2O. GT was prepared by soaking 2 tea bags in 250ml of boiling water for 10 min. The tea bags were removed and the tea was then cooled at room temperature for 30 min followed by a further 30 min at 4°C. All compounds were filtered through 0.2µm Sartorius ministart non-pyrogenic hydrophilic filters. AZT, IDV, CQ, EGCg and HU were aliquoted and stored at -20°C while GT was freshly prepared for each experiment.

4.3.2 Determination of the cytotoxicity of AZT, CQ, IDV, HU, GT and EGCg

SC-1 cells were plated in 25cm^2 cell culture flasks at a concentration of 2.5 x 10^5, 4ml of DMEM supplemented with 10% FBS was added and the cells were left to settle overnight (17 hours) in the incubator at 37°C, 5% CO_2. The SC-1 cells were then exposed to various concentrations of AZT, IDV, HU, CQ, GT or EGCg (Table 4.1). Seven flasks of SC-1 cells were plated for each drug. One flask served as a control and the other six were exposed to various concentrations of the drug. The volume of each flask was adjusted to 6ml with medium after the addition of the drug. The flasks were then placed in the incubator at 37°C, 5% CO_2 for 72 hours.

A volume of 300µl of a 1mg/ml MTT solution prepared in 20xPBS was added to each flask. The flasks were incubated for 1 hour at 37°C, 5% CO_2. The medium was removed

and the purple formazan product was solubilized in 2.5ml of DMSO. Six volumes of 100µl of the solubilized formazan from each flask were transferred to a 96-well plate. The absorbency was read at 550nm with a Multiscan Ascent plate reader from AEC Amersham, Kelvin, South Africa. The cellular toxicity of each drug was evaluated in three independent experiments.

Table 4.1 Concentrations used to determine the cytotoxicity (TD_{50}) of each drug

AZT mg/ml (µM)	IDV mg/ml (µM)	HU mg/ml (µM)	CQ mg/ml (µM)	GT mg/ml	EGCg mg/ml (µM)
0	0	0	0	0	0
0.008 (31.3)	0.011 (15.6)	0.0003 (3.75)	0.0032 (6.25)	0.125	0.005 (11.3)
0.017 (62.5)	0.022 (31.3)	0.0006 (7.5)	0.0065 (12.5)	0.250	0.010 (22.5)
0.033 (125)	0.045 (62.5)	0.0011 (15)	0.013 (25)	0.500	0.021 (45)
0.067 (250)	0.089 (125)	0.0023 (30)	0.026 (50)	1	0.041 (90)
0.134 (500)	0.178 (250)	0.0046 (60)	0.052 (100)	2	0.083 (180)
0.267 (1000)	0.356 (500)	0.0091 (120)	0.103 (200)	4	0.165 (360)

4.3.2.1 Data management and statistics

The mean of the absorbency values of each drug concentration was calculated and expressed as a percentage of the control with the control being 100% (no drug added). A fraction affected was also calculated with the following formula: (control mean – drug concentration x mean)/control mean as this is the format used by the median effect equation of T-C Chou (Chou, 1991). The fraction affected for the control was thus 0. Data analysis was done using the Calcusyn Programme for Windows software (Version 2.0, 2004) that is based on the median effect equation of T-C Chou (Chou, 1991) and a TD_{50} value for each drug experiment was calculated. The mean, standard error of the mean (SEM) and coefficient of variation was calculated from three independent experiments.

4.3.3 Determination of the antiretroviral activity of AZT, CQ, IDV, HU, GT and EGCg.

The antiretroviral activity of the different compounds was evaluated in 1:10,000 co-cultures of BM5:SC-1 cells. The total number of cells plated for each co-culture was 2.5 x 10^5 cells in 25cm^2 cell-culture flasks. A dilution series of the BM5 cells was created in 24-well plates starting with 2.5 x 10^5 cells in 1ml of DMEM supplemented with 10% FBS up to 25 BM5 cells in 1ml of DMEM supplemented with 10% FBS. The number of SC-1

cells then added to the 25 BM5 cells was 249 975 making a 1:10,000 co-culture of BM5:SC-1 cells. The two cell types were mixed together and added to the 25cm^2 cell-culture flasks already containing 4 ml of DMEM supplemented with 10% FBS. The flasks were then left to settle overnight (17 hours) in the incubator at 37℃, 5% CO_2. AZT, CQ, IDV, HU, GT or EGCg was added at concentrations of 0, 1/8 TD_{50}, 1/4 TD_{50}, 1/2 TD_{50} of compound (determined by the MTT assay) and the final volume of each flask was adjusted to 6 ml with DMEM supplemented with 10% FBS. Five flasks of co-cultures were plated for each of the two independent experiments. The co-cultures were incubated for 72 hours at 37℃, 5% CO_2 where after the DNA was extracted.

4.3.3.1 Extraction of genomic DNA

Same as Section 3.3.4.

4.3.3.2 Real-time PCR for quantification of the BM5-def viral DNA and murine G6PDH gene

Real-time PCR of the BM5-def viral DNA and G6PDH gene was performed as in Section 3.3.8. The LightCycler® 480 Relative Quantification software was used to quantify the BM5-def viral DNA relative to G6PDH gene. BM5 cell DNA served as the target calibrator (BM5-def) and reference calibrator (G6PDH) to normalize samples between runs. A melting curve analysis was also performed on all products to detect primer dimers. A sample with high primer dimer content was rejected and not included in the relative quantification analysis. An efficiency of 2.0 for the PCR reactions was used as the standard curves generated in Chapter 3 showed that the viral and G6PDH PCR efficiency was close to 2.0. There was thus no need to use standard curves for relative quantification.

The mean of the concentrations obtained from the relative quantification software analysis of each drug concentration was calculated and expressed as a percentage of the control with the control representing a 100% as no drug was added to the control so it was assumed that viral infection was allowed to proceed uninhibited.

4.4 Results and discussion

4.4.1 Cytotoxicity of AZT, IDV, HU, CQ, GT and EGCg on SC-1 cells

Uninfected SC-1 cells were used to determine the toxic dose (TD_{50}) of each drug as these cells were the predominant cell type present in the co-culture model. The cells were exposed to various concentrations of each drug (Table 4.1) for 72 hours and the toxicity was measured using the MTT assay. The MTT is a yellow-coloured substrate that is converted to an insoluble blue formazan product by the mitochondrial dehydrogenase of metabolically active cells (Mosmann, 1983). The assay thus measures the number of metabolically active living cells. A mean of the spectrophotometric readings for each drug concentration was obtained and expressed as a percentage of the control with the control being 100% (no drug added) and complete cell death 0%.

Figure 4.2 represents the cell viability relative to the control for the various concentrations of (A) AZT, (B) IDV, (C) HU, (D) CQ, (E) GT and (F) EGCg. AZT (A) and EGCg (F) appeared to stimulate cell growth at low concentrations i.e. 0.008mg/ml (31.25µM) for AZT and 0.0052mg/ml (11.25µM) and 0.0103mg/ml (22.5µM) for EGCg. But then, as the drug concentrations for AZT and EGCg increased, so did the toxicity. For CQ, HU, IDV and GT a typical dose-response effect for toxicity was observed.

A series of fractions affected for the different drugs was then calculated as in Section 4.3.2 and submitted to the Calcusyn Programme for Windows software (version 2.0, 2004). This Programme is based on median-effect principle derived by T-C Chou from the mass-action law (Chou, 1991). The median-effect equation relates the dose to the effect and is used to calculate the median-effect dose (TD_{50} or ED_{50}).

Median-effect equation:

$$f_a/f_u = (D/D_m)^m$$

f_a = fraction affected by dose; f_u = fraction unaffected by dose; D = dose of drug; D_m = median-effect dose i.e. TD_{50} or ED_{50}; m = signifies the sigmoidicity (shape) of the dose-effect curve.

The series of fractions affected for the various concentrations of each drug was used by the Programme to create the median-effect plot that plotted x = log (D) vs y = log (f_a/f_u). The m value was determined from the slope of the straight line while the D_m was determined from the x-intercept of the straight line. Figure 4.3 represents the median-effect plot for AZT, IDV, HU, CQ, GT and EGCg drawn by the Calcusyn Programme for Windows software (Version 2.0, 2004).

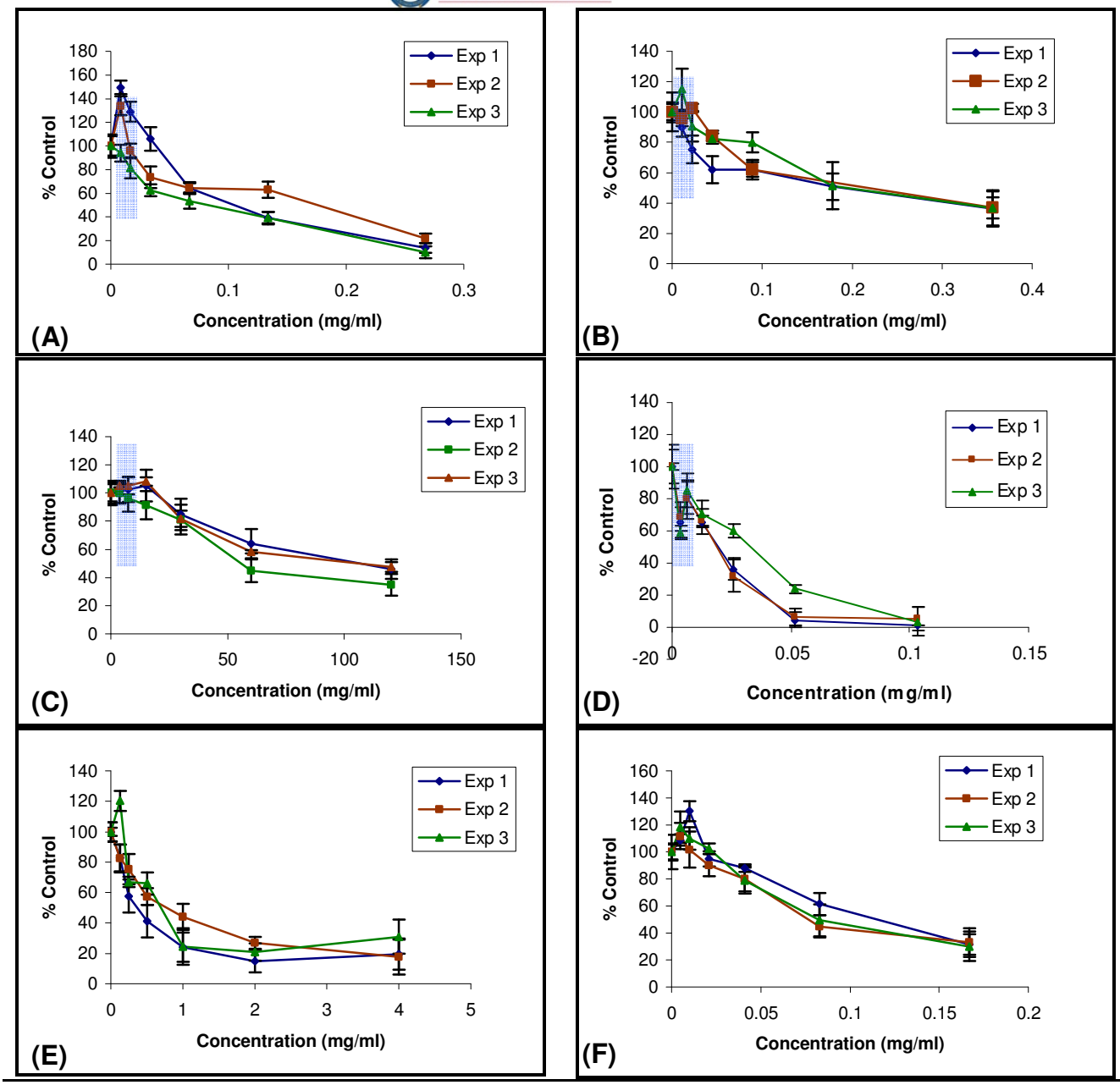

Figure 4.2. Dose-response curves for SC-1 cells exposed to various concentrations of (A) AZT, (B) IDV, (C) HU, (D) CQ, (E) GT and (F) EGCg. Exp = experiment. Cells were exposed to various concentrations of each compound as shown in Table 4.1 for 72 hours where after the cell viability was measured with the MTT assay. The shaded region represents the cell viability for the concentration range used to determine the antiretroviral effects of each drug in the *in vitro* co-culture model of SC-1 and BM5 cells.

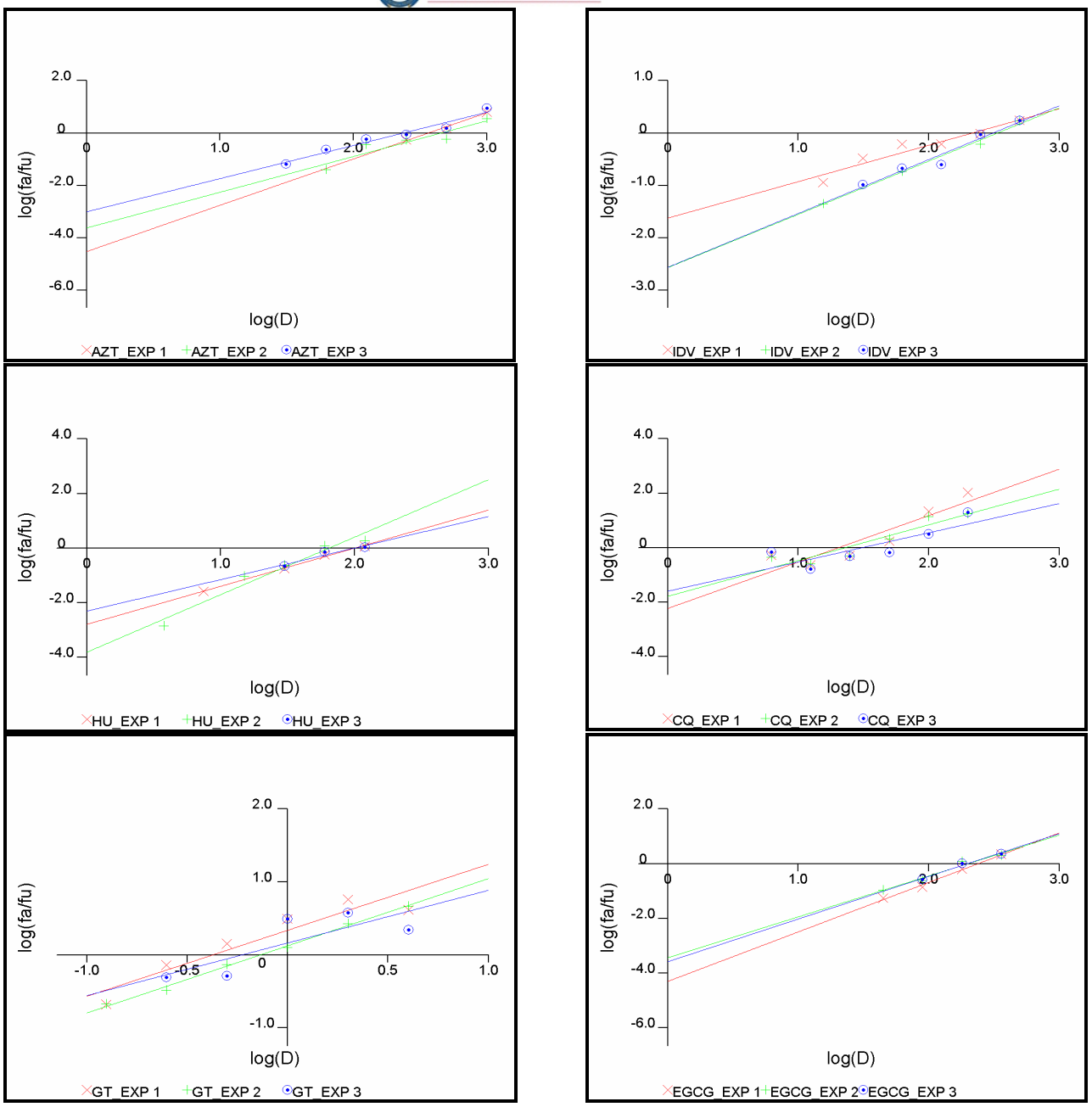

Figure 4.3. Median-effect plots produced with the median-effect equation of T-C Chou by the Calcusyn Programme for (A) AZT, (B) IDV, (C) HU, (D) CQ, (E) GT and (F) EGCg for three independent experiments.

The Programme then yields a summary report containing the D_m (TD_{50}) for each of the drug's three independent experiments (Table 4.2).

Table 4.2. Summary report for AZT experiments (Exp) 1-3 obtained with the median effect equation and plot of T.-C Chou. Similar reports were obtained for IDV, HU, CQ, GT and EGCg.

Drug	Combination Index Values at					
	ED_{50}	ED_{75}	ED_{90}	D_m	m	r
AZT Exp 1	N/A	N/A	N/A	0.098mg/ml (365.0µM)	1.763	0.996
AZT Exp 2	N/A	N/A	N/A	0.122mg/ml (455.2µM)	1.361	0.934
AZT Exp 3	N/A	N/A	N/A	0.063mg/ml (236.9µM)	1.264	0.979

ED = effective dose; D_m = median-effect dose; m = slope of median-effect plot; r = linear correlation.

The three D_m (TD_{50}) values were used to calculate a mean TD_{50} and SEM that would then be used for further experiments namely antiretroviral effect of each drug alone as well as the toxicity and antiretroviral effect of the different drug combinations (Table 4.3).

Table 4.3. The mean TD_{50} for all the drugs tested singularly on SC-1 cells.

Drug/Compound	TD_{50}	
	mg/ml (SEM)	µM (SEM)
AZT	0.094 ± 0.014	352.4 ± 51.70
CQ	0.013 ± 0.001	24.63 ± 2.560
HU	0.007 ± 0.001	88.07±9.590
IDV	0.206 ± 0.022	288.7 ± 30.22
EGCg	0.098 ± 0.005	212.7 ± 11.03
GT	0.582 ± 0.073	1270 ± 158.9#

For comparison purposes the molecular mass of EGCg was used to calculate a micromolar concentration for GT as it is the main component of GT.

From Table 4.3, it can be seen that when comparing drugs in mg/ml GT was the least toxic while HU was the most toxic and the order of toxicity went as follows: GT < IDV < EGCg < AZT < CQ < HU. However, when comparing the drugs in micromolar concentrations and using the molecular mass of EGCg for GT, a better indication of toxicity is obtained. CQ was the most toxic while GT was still the least and the toxicity order was GT < AZT < IDV < EGCg < HU < CQ.

AZT cytotoxicity has been evaluated with several different assays in various cell line types (Table 4.4). The differences in AZT cytotoxic effects shown in Table 4.4 between various cell types or lines may be due to different cell types used, the ability of the various cell lines to convert AZT into AZTTP, sensitivity of the bioassays used as well as experimental design. Differences are observed in studies where cells from the same lineage are used, for example H9 immortalized human T cells versus T-Ly T-

lymphocytes. Lymphocytes, such as MT-4 human T cells showed greater sensitivity to the toxic effects of AZT than SC-1 fibroblasts (29.4 µM compared to 508 µM and 352 µM) Different assays are used to determine cytotoxicity and include the trypan blue exclusion and the MTT assay which differ in the parameter measured and sensitivity. Trypan blue exclusion assay measures the integrity of the plasma membrane whereas the MTT assay measures mitochondrial dehydrogenase activity. Furthermore there is also a difference in the TD_{50} for AZT in SC-1 cells used in this thesis and in the experiment of Suruga *et al* 1998. This may be due to differences in the cell densities used. In this thesis, 2.5 x 10^5 cells were plated in 25cm^2 cell culture flask (cell density 1X10^4 cells/cm^2) while in that of Suruga *et al.,* 1998, 1 x 10^4 cells were plated in flat-bottomed microtiter plate well, surface area 0.6cm^2 (cell density 1.7 X10^4 cells/cm^2). Due to the higher cell density of cell cultures of Suruga *et al.,* 1998, the cells were plated closer to each other and therefore less susceptible to the cytotoxic effects of AZT.

Table 4.4 Comparison of the various TD_{50}s for AZT in the literature

Cell line	Assay	TD_{50} (µM)	Reference
H9 immortalized human T cells	Erythrosin B exclusion	>1000	Furman *et al.,* 1986
PBLs Human peripheral blood	Erythrosin B exclusion	500	Furman *et al.,* 1986
H9 immortalized human T cells	Trypan Blue dye exclusion	20	Perno *et al.,* 1992
T-Ly T-lymphocytes	Trypan Blue dye-exclusion	20	Perno *et al.,* 1992
U937 monocytoid	Trypan Blue dye-exclusion	20	Perno *et al.,* 1992
M/M monocyte/macrophage	Trypan Blue dye-exclusion	>50	Perno *et al.,* 1992
MT-2 CD4 positive T-cell lymphoma	Finter's Neutral Red dye	349	Essey *et al.,* 2001
MT-4 human T cells	MTT assay	29.4	Ohrui, 2006
Crandell feline kindney (CrFK) cells	MTT assay	216.79	Bisset *et al.,* 2002
SC-1 cells	MTT assay	508	Suruga *et al.,* 1998
Con A activated spleen cells	MTT assay	161	Suruga *et al.,* 1998
SC-1 cells	MTT assay	352	Present study

The cytotoxicity of AZT has been attributed to its direct effects on the mitochondria and has been reviewed by Barile *et al.,* 1998. Long-term treatment with AZT has been shown to cause several abnormalities in the mitochondrial structure and include enlarged size, abnormal cristae, abnormal organelle proliferation, electron-dense deposits in the mitochondrial matrix and a decrease in mtDNA, mtRNA and mitochondrial polypeptide synthesis. These effects of AZT on the mitochondria have been ascribed to the ability of AZT to enter the mitochondria and inhibit the mitochondrial adenylate kinase and ADP/ATP translocator thus decreasing the availability of cellular ATP for other biological

activities. AZT has also been shown to be a competitive-mixed type inhibitor of DNA polymerase γ which is responsible for the synthesis of mitochondrial DNA. Inhibition of the production of mitochondria would therefore inhibit the amount of energy available for the cell to replicate and perform its biological functions and thus inhibit cellular replication. Therefore the MTT assay that measures the activity of the mitochondrial enzyme succinate dehydrogenase is a better assay for the detection of the cytotoxic effects of AZT than the Trypan Blue and the Erythrosin B exclusion assays.

IDV showed a dose-response effect on cellular toxicity namely, the higher the drug concentration, the higher the cytotoxicity observed. IDV is known to induce several adverse effects and these adverse effects are believed to be caused by IDV inhibiting enzyme function and other processes required for normal cell function. IDV has been described to have a pro-apoptotic effects at concentrations above 10-25μM (Badley, 2005; Jiang *et al.,* 2007) and can affect mitochondrial function (Jiang *et al.,* 2007; Mukhopadhyay *et al.,* 2002). In the study by Jiang *et al.,* 2007, IDV was shown to increase the production of reactive oxygen species (ROS) and also decrease the mitochondrial transmembrane potential. The production of ROS can have several effects on the cell and cause cytotoxicity and damage the DNA. Changes in the mitochondrial transmembrane potential affects the mitochondrial electron transport system and energy metabolism as well as initiating the caspase cascade resulting in apoptosis. In the study of Mukhopadhyay *et al.,* 2002, IDV was found to inhibit the mitochondrial processing protease of yeast. This enzyme is responsible for removing the leader peptide sequence of mitochondrial proteins and thus producing mature forms of these proteins. By inhibiting this enzyme, proteins that are essential for mitochondrial functions are not available and this may lead to mitochondrial dysfunction.

HU and CQ were found to be the most toxic of all the drugs/compounds evaluated. The cytotoxicity of HU can be explained using the mechanism of action whereby HU inhibits HIV and LP-BM5-defective retrovirus activity namely inhibition of the cellular enzyme ribonucleotide reductase. This mechanism will be fully discussed in Section 4.4.2. Another mechanism whereby HU may induce cytotoxicity is via the production of free radicals. HU has also been shown to induce the production of free radicals which in turn has cytotoxic effects on the cell (Przybyszewski and Kasperczyk, 2006). The exact mechanism for the cell death induced by HU via free radical production is largely unknown but it is proposed that the radicals attack the cellular membrane resulting in the leakage of hydrolytic enzymes. These hydrolytic enzymes leaked from the cell membrane then cause lytic death of the cell.

The cytotoxicity observed for CQ may be explained by the multiple effects of CQ on the cell. CQ as stated above interferes with the glycosylation of proteins (Savarino *et al.,* 2001). At low concentrations, CQ will affect the glycosylation of the viral proteins due to the higher rate of replication of the virus as compared with the cell but then as the concentration increases, CQ may also start inhibiting the glycosylation of essential cellular proteins and thus induce cytotoxicity. The second cytotoxic effect of CQ may be caused through the permeabilization of the lysosomal membrane. Hydroxychloroquine, a derivative of CQ, has been shown to induce permeabilization of the lysosomal membrane by accumulating within the lysosomes and decreasing the lysosomal pH gradient (Boya *et al.,* 2003). This resulted in caspase activation, exposure of phosphatidylserine, chromatin condensation and ultimately apoptotic cell death. CQ has also been shown to have several devastating effects on the mitochondria and for this reason the MTT assay was suitable for quantifying the cytotoxic effects of CQ. CQ, in rat liver mitochondria, has been shown to inhibit NADH dehydrogenase, succinate dehydrogenase, and cytochrome c oxidase (Deepalakshmi *et al.,* 1994). CQ was also shown to act as an uncoupler on the phosphorylation sites II and III resulting in decreased rates of ADP phosphorylation (Katewa and Katyare, 2004). These effects cause a decrease in ATP synthesis and thus reduced levels of available energy for the cell to perform its functions.

For the effects of the experimental compounds on cell viability, GT showed a more dose-response effect while EGCg showed a slight stimulation at very low concentrations but then as the drug concentrations increased so did the toxicity to the SC-1 cell line. The cytotoxicity observed with GT and EGCg may be attributed to the fact that phenolic compounds have been shown to undergo auto-oxidation in different cell culture medium particularly DMEM which was used in this study (Long *et al.,* 2000 and 2007; Chai *et al.,* 2003). EGCg undergoes auto-oxidation into two dimers at a pH of 7.2-7.4 and this is accompanied by a significant increase in hydrogen peroxide (H_2O_2) production. A concentration dependent effect was observed which caused cell membrane and DNA damage leading to cell death. The presence of cells growing in cell culture medium was shown to some degree to stabilize the EGCg molecule (Hang *et al.,* 2002). Therefore some of the EGCg should be entering the cell and cytotoxicity may also be due to direct effects of EGCg on cellular components. In a study conducted by Galati *et al.,* 2006, it was shown that EGCg and other catechins were able to decrease the mitochondrial membrane potential and induce the production of reactive oxygen species (ROS) in rat hepatocytes. A change in the mitochondrial membrane potential may cause changes in the electron transport system and induce apoptosis. EGCg was also shown to inhibit the

activity of RNA Polymerase III by inhibiting the protein expression of TFIIIB subunits Brf1 and Brf2 which is responsible for initiating transcription by RNA polymerase III (Jacob *et al.,* 2007). RNA polymerase III is responsible for transcribing the genes encoding for tRNA, 55 rRNA and small, stable RNAs (Lodish *et al.,* 2002). So EGCg by inhibiting this enzyme could inhibit protein synthesis as tRNA and rRNA are involved in this process.

4.4.2 Antiretroviral activity of AZT, IDV, HU, CQ, GT and EGCg in the *in vitro* co-culture model

A co-culture of 1:10,000 of BM5:SC-1 cells was used to evaluate the antiretroviral properties of each of the drug compounds. In a co-culture model of uninfected and chronically infected cells as used in this study the rate of viral infection can increase either by the replication of the chronically infected BM5 cells, direct cell-to-cell transmission of the virus or by the release of virions into the medium that can infected the uninfected SC-1 cells. However, the latter method has been reported by Sato *et al.,* 1992 not to play a significant role in spreading of the virus and that the most efficient way of spreading virus infection is through fusion of a chronically infected cell with an uninfected cell.

The co-culture was exposed to three different concentrations below the TD_{50} of each drug namely 1/8 TD_{50}, 1/4 TD_{50} and 1/2 TD_{50} for 72 hours (Table 4.5). Thereafter, the DNA was isolated and the amount of BM5-def gene was amplified and quantified with real-time PCR relative to the G6PDH gene. A total of two independent experiments were conducted for each drug. If when using AZT, IDV, HU or CQ the viral load in this co-culture model is significantly decreased, then the use of the *in vitro* co-culture model of BM5 and SC-1 cells for first line screening of compounds with antiretroviral activity is validated. In this study GT and EGCg served as experimental compounds. Figure 4.4 shows the effect of AZT (A), IDV (B), HU (C), CQ (D), GT (E) and EGCg (F) on the viral DNA load. The control was assigned 100% as these co-cultures were not exposed to any drug so it was expected that the viral infection would be allowed to proceed freely. Complete suppression of the viral load was represented by 0%.

Table 4.5. Concentrations used to determine the antiretroviral activity of each drug

	AZT mg/ml (µM)	IDV mg/ml (µM)	HU mg/ml (µM)	CQ Mg/ml (µM)	GT mg/ml	EGCg mg/ml (µM)
1/8TD_{50}	0.012 (44)	0.026 (36)	0.001 (11)	0.002 (3)	0.073	0.012 (27)
1/4TD_{50}	0.024 (88)	0.052 (72)	0.002 (22)	0.004 (6)	0.146	0.025 (53)
1/2TD_{50}	0.047 (176)	0.103 (144)	0.004 (44)	0.007 (12)	0.291	0.049 (106)

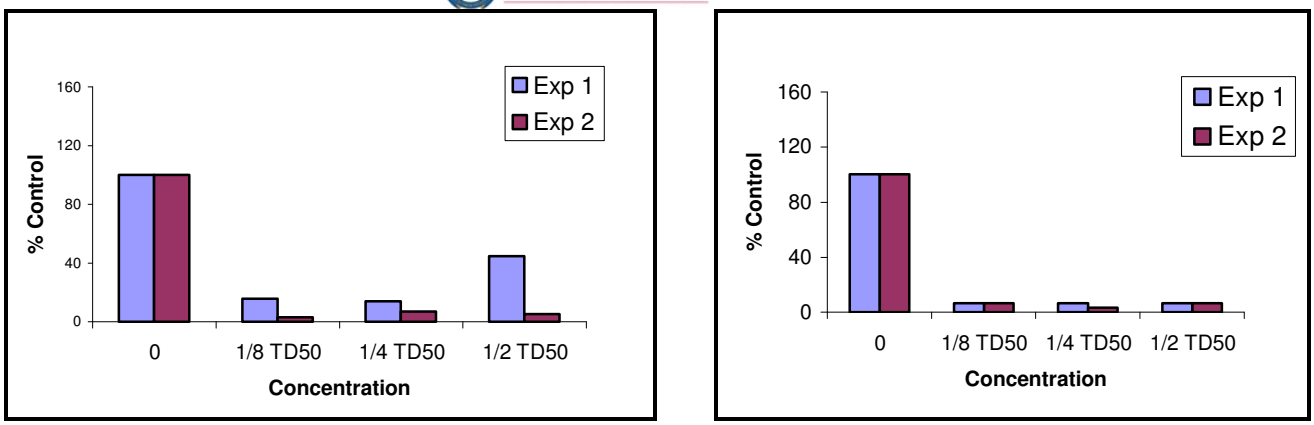

(A) AZT

(B) IDV

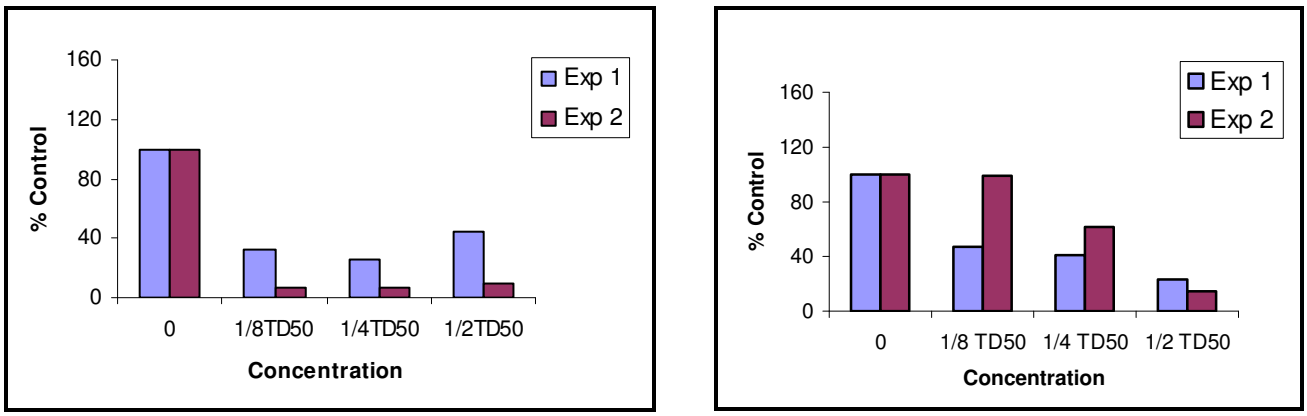

(C) HU

(D) CQ

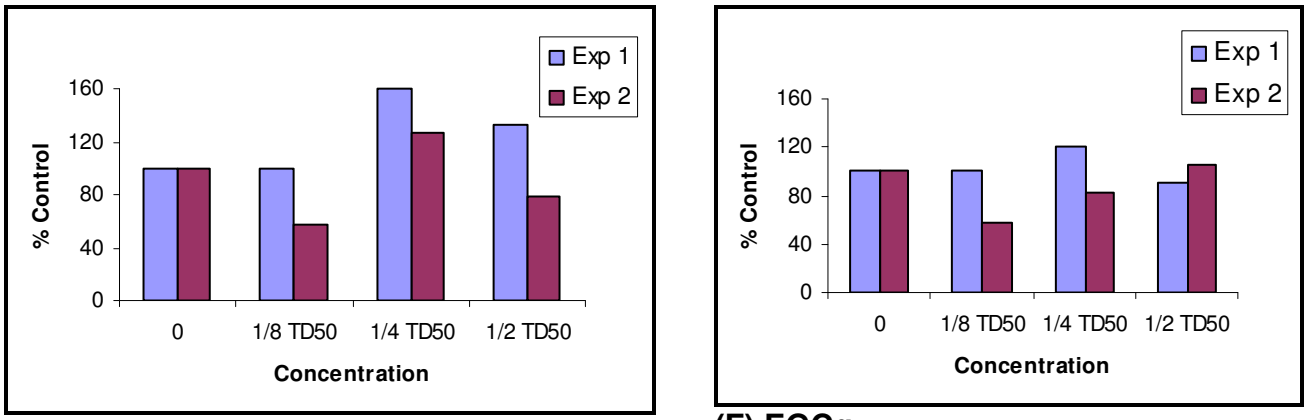

(E) GT

(F) EGCg

Figure 4.4. Plots representing the percentage inhibition of the viral load relative to the control at sub-toxic concentration of (A) AZT, (B) IDV, (C) HU, (D) CQ, (E) GT and (F) EGCg. Cells were exposed to sub-toxic concentrations of each of the drugs (Table 4.5) where after the DNA was isolated and the LP-BM5-def gene was quantified relative to the G6PDH gene with real-time PCR.

Treatment of the co-culture with AZT revealed that AZT suppressed the cell-to-cell transmission of the virus at concentrations below the TD_{50} of the drug that was $1/8TD_{50}$, $1/4TD_{50}$ and $1/2TD_{50}$ (Figure 4.4 (A)). The maximum amount of viral suppression was already obtained at the lowest AZT dose namely $1/8TD_{50}$. At this concentration, the cell viability was between 90-98% (shaded region in Figure 4.2 (A)) indicating that there was little or no toxic effect on the cells in the co-culture. IDV and HU also suppressed viral infection at concentrations below the TD_{50} of each drug and like AZT, the most effective concentration for either drug was the lowest drug dose used to the co-culture. For IDV the most effective concentration was $1/8TD_{50}$ where the cell viability is 80-90% (shaded region in Figure 4.2 (B)) but the viral infection is down to approximately 10% (shaded region in Figure 4.4 (B)).

For HU, the most effective concentration was also $1/8TD_{50}$ where the cell viability was at about 98% (shaded region in Figure 4.2 (C)) and the viral load had been reduced by 80% (Figure 4.4 (C)). Due the effectiveness of AZT, IDV and HU to reduce viral loads it will be necessary to repeat these experiments with drug concentrations below the $1/8TD_{50}$ of each drug so that the ED_{50} and selectivity index (SI) for each drug can be calculated.

CQ showed a more dose-response effect on viral DNA load (Figure 4.4 (D)). Its most effective concentration was the highest CQ dose given to the co-culture model namely $1/2TD_{50}$. At this concentration, viral DNA was reduced to approximately 20% (Figure 4.4 (D)) while cell viability was at about 70% (shaded region in Figure 4.2 (D)). As CQ shows a dose-response effect on inhibition of the virus, the data could be imported into the Calcusyn Programme for Windows software (Version 2.0, 2004) and the median effect equation derived by T-C Chou (Chou, 1991) could be used to calculate an ED_{50}. The calculated ED_{50} for CQ was 0.003mg/ml (5.95µM) ± 0.001mg/ml (2.95µM) and together with the TD_{50} of 0.013mg/ml (24.63µM) a selectivity index for CQ could also be calculated. The selectivity index of CQ was calculated to be 4.3. The effect of HU and CQ on the viral load was not as dramatic as was observed for AZT and IDV. This is possibly due to the greater target specificity of AZT and IDV for the LP-BM5 virus where as HU and CQ act on cellular factors essential for viral replication.

Antiretroviral drugs, AZT, IDV, HU and CQ have effectively reduced the presence of proviral DNA namely reduced infectivity in co-cultures infected with the LP-BM5 MuLV complex. These results thus validated this *in vitro* co-culture model as a model that could

be used to screen compounds for their antiretroviral properties. The next step in this study was to evaluate the experimental compounds GT and EGCg for antiretroviral properties using this model. EGCg was evaluated as this compound is suspected to be the active ingredient of GT that is responsible for all the beneficial effects of drinking tea. If, however, EGCg shows no effect but GT does then it will be necessary to screen other constituents of GT for antiretroviral properties. Both experimental compounds GT and EGCg showed little to no effect on the viral infection within the co-cultures as shown in Figures 4.4 (E) and (F), respectively, with the effects of the different drug concentrations staying at approximately the same level as the control namely 100%.

AZT was one of the first drugs approved for the treatment of HIV/AIDS. It has also been extensively evaluated in the *in vivo* MAIDS model and is a known inhibitor of the LP-BM5 MuLV complex. In this study AZT was shown to reduce the viral DNA load by 85-95% (Figure 4.4 (A)) with minimal loss to cell viability (shaded region Figure 4.3 (A)). However, as the drug concentration increased so did the toxicity without a further decrease in viral load. AZT is an analogue of the DNA base thymidine that substitutes the 3' hydroxyl group on the sugar ring with a 3' azide (N_3) group (Figure 4.1 (A)). It enters the cell via passive diffusion and is subsequently converted into a triphosphate. The three cellular enzymes responsible for converting AZT into a mono-, di- and triphosphate are thymidine kinase, thymidylate kinase and nucleoside diphosphate kinase, respectively (Furman *et al.,* 1986). The second phosphorylation is the rate-limiting step in the conversion of AZT to a triphosphate. AZT reduces dTTP, dCTP and dGTP levels but causes an increase in dATP levels. AZT shows preference for HIV RT over DNA polymerase α and β and competes with dTTP for the enzyme HIV RT resulting in premature chain termination of the newly synthesized DNA molecule (Furman *et al.,* 1986; St. Clair *et al.,* 1987). It is believed that the monophosphate form of AZT is responsible for the cytotoxic effects while the triphosphate form is responsible for its antiviral effects (Tornevik *et al.,* 1995). The rate-limiting step is the conversion from monophosphate to triphosphate. The high antiviral effect associated with low cellular toxicity indicates that the efficient phosphorylation of AZT occurs in this model.

AZT's inhibitory effects on retroviral infection have been attributed to the fact that it competes with dTTP for the retroviral enzyme reverse transcriptase (St. Clair *et al.,* 1987). The reverse transcriptase enzyme is responsible for converting the viral RNA genome into cDNA so that it can be inserted into the host cell genome to produce new virions. Incorporation of AZT into the growing viral cDNA causes premature chain

termination due to the presence of an azide group on C2 group that prevents elongation. The consequence of this process is that AZT therefore prevents the retrovirus from continuing its replication cycle and producing viral progeny.

IDV is a peptidomimetic hydroxyaminopentane amide that competitively inhibits HIV-1 and HIV-2 proteases by binding to the active sites of these enzymes (Vacca *et al.,* 1994; Chen *et al.,* 1994). The HIV protease is an aspartyl protease which is responsible for cleavage of the *Gag-Pol* polyprotein precursor (Dunn *et al.,* 2002; Swanstrom and Erona, 2000). Cleavage of the *Gag* precursor gives rise to the matrix, caspid and nucleocaspid proteins while cleavage of the *Pol* precursor releases RT and IN enzymes. Inhibition of this process gives rise to immature, non-infectious viral particles. Treatment of the co-culture with IDV appeared to have the same effect as AZT that is almost complete suppression at the lowest drug concentration and then stabilization of that effect in viral infection despite the higher drug concentration used. As for AZT not all viral DNA is eliminated, the most likely explanation is that the remaining 10% of viral DNA reflects the integrated viral genome that cannot be eradicated. Once in the cell, IDV exerts its antiretroviral effect by binding to the active site of the retroviral protease enzyme thereby preventing the enzyme from cleaving *Gag-Pol* polyprotein precursor which results in immature viral particle formation. This means that IDV can inhibit the virus from replicating and spreading to uninfected cells but it has no effect on the percentage of viral genomes already integrated into the host cell genome. In the chronically infected BM5 cells it can only prevent the cells from producing new virions but it cannot prevent the cell from transmitting its already integrated viral copy into new daughter cells. As the data is expressed as viral DNA relative to the presence of the housekeeping gene G6PDH this increase in the number of daughter cells with integrated viral DNA is detected and therefore will remain constant.

HU and CQ have been evaluated for their antiretroviral effects as these two drugs are being proposed as more economical options for the treatment of HIV/AIDS (Paton *et al.,* 2002). Despite being shown as two of the most toxic of all the drugs/compounds, HU and CQ were found to be effective in reducing the LP-BM5-def viral load in the co-cultures. The cytotoxicity and antiretroviral activity observed for HU can be explained by the fact that HU is an inhibitor of the cellular enzyme ribonucleotide reductase (Lisziewicz *et al.,* 2003). This enzyme is responsible for the conversion of ribonucleoside diphosphates into deoxyribonucleoside diphosphates (Campbell, 1999). The dNDPs are in turn converted into dNTPs which are the building blocks of the DNA. HU therefore

inhibits ribonucleotide reductase activity and thus inhibits DNA synthesis. By preventing this conversion, HU reduces the deoxynucleotide pools and with insufficient dNTPs, the important conversion of viral RNA into viral DNA is inhibited and viral replication is halted. Nevertheless the decreased deoxynucleotide pools will also have an adverse effect on cellular DNA synthesis. However, due to the higher rate of viral replication compared to cellular replication at low HU concentrations, HU will affect viral replication with little or no loss in cellular viability.

Several different mechanisms of action have been proposed for how CQ exerts its anti-HIV effects and these include interfering with the glycosylation of the viral proteins (Tsai *et al.,* 1990; Savarino *et al.,* 2001 and 2004), inhibiting the viral enzyme integrase (Fesen *et al.,* 1993) and inhibiting Tat-induced cytokine secretion by monocytes and T-cells (Rayne *et al.,* 2004). CQ inhibits the glycosylation of viral envelope proteins by entering the acidic vesicles in the cell responsible for glycosylation and raising the pH within these vesicles (Savarino *et al.,* 2001). This increase in pH disrupts the enzymes and thus inhibits glycosylation. By interfering with viral protein glycosylation, CQ inhibits the amount and infectivity of HIV produced by chronically infected cells (Tsai *et al.,* 1991).

CQ was found to also inhibit both the cleavage and strand-transfer (integration) processes of the HIV enzyme integrase at concentrations of 13.1µM for cleavage and 5.14µM for integration (Fesen *et al.,* 1993). The integrase enzyme is an important enzyme for viral replication as it is responsible for inserting a copy of the viral DNA into the host cell DNA (Asante-Appiah and Skalka, 1997). Without this step, the virus cannot produce the necessary proteins to form new virions. The ED_{50} for CQ was 5.95µM ± 2.95µM which is in the same order for CQ inhibiting the integration but not the cleavage step of the HIV enzyme integrase (Fesen *et al.,* 1993).

The effects of CQ on the accessory protein Tat may also play an important in the *in vivo* environment. The accessory protein Tat is needed during the transcription and replication of HIV (Brigati *et al.,* 2003). It acts by binding to the viral promoter TAR and recruits transcriptional complexes that modify the chromatin conformation at the proviral integration site. It is also responsible for phosphorylating RNA polymerase II to promote elongation of the transcript. Tat has also been shown to be released from the cells and to activate different signal transduction pathways. CQ exerts its affects on Tat by inhibiting the translocation of protein from the endosomes to the cytosol and thus prevents the Tat from inducing cytokine secretion (Rayne *et al.,* 2004). LP-BM5 MuLV

complex does not have accessory genes like the Tat protein of HIV and this mechanism of action of CQ would not have an effect on the model used in this study. Only the first two antiretroviral mechanism of CQ may thus be responsible for the observed decline in the LP-BM5-def viral load.

EGCg and GT exhibited little to no antiviral effects on the LP-BM5-def virus as seen in Figures 4.4 (E) and 4.4 (F), respectively. EGCg has been reported to inhibit the reverse transcriptase enzyme of HIV (Nakane and Ono, 1990; Tao, 1992; Chang *et al.,* 1994), inhibit the HIV protease enzyme and destroy viral particles *in vitro* (Yamaguchi *et al*., 2002) and inhibit the binding of gp120 to cell surface receptor CD4 thereby inhibiting the entrance of HIV (Kawai *et al.,* 2003). There are four possible explanations for the observed lack of antiviral effects of GT and EGCg on the LP-BM5-def viral load.

The first possible explanation is that due to the auto-oxidation of EGCg in medium, very little EGCg is actually entering the cell and thus maybe EGCg and GT's antiviral effects should be investigated in a different type of medium. The second possibility is that EGCg and possibly the other catechins in GT have little to no effect on the LP-BM5 MuLV complex and thus have no ability to inhibit the reverse transcriptase and protease enzyme of these MuLV unlike HIV. This is very surprising as EGCg has been shown to inhibit the HIV reverse transcriptase enzyme at the same low concentrations as AZT and AZT was shown here to specifically inhibit the cell-to-cell transmission of the LP-BM5-def virus. It is therefore possible that EGCg and the other catechins inhibit the HIV-RT and HIV-protease enzymes using a different mechanism to AZT and IDV. Thirdly, the ability of EGCg to directly destroy viral particles as in the study of Yamaguchi *et al.,* 2002 is not applicable to our co-culture model. In a co-culture model such as the system used in this study, it is proposed that the virus spreads efficiently from cell-to-cell by fusion of a chronically infected cell with an uninfected cell rather than by infection through the release of virions into the medium (Sato *et al.,* 1992). So although EGCg could be destroying some of the viral particles released into the medium in our model, it is not inhibiting the fusion of the chronically infected BM5 cell with the uninfected SC-1 cell and thus the transmission of the virus from cell-to-cell is not inhibited.

The last possible explanation as to why no antiviral effects were seen is due to the effects of EGCg on the proteasome and the importance of the proteasome to virus replication. It has been shown that an active proteasome is necessary for the assembly, release and maturation of HIV particles and that treatment with proteasome inhibitors

inhibits these steps in the virus' replication cycle (Schubert *et al.,* 2000). The use of proteasome inhibitors, however, has also resulted in an increased infection rate of cells with HIV and a subsequent increase in proviral DNA (Schwartz *et al.,* 1998; Dueck and Guatelli, 2007). A possible explanation is that the proteasome is involved in the degradation of the viral proteins as the virus first enters the cell and inhibition of the proteasome results in increased permissiveness of the cell to the virus due to changes in or activation of a unidentified cellular factor or changes in the cell cycle status that aids in increasing the permissiveness of the cell. EGCg has been shown to inhibit the chymotrypsin-like activity of proteasome (Nam *et al.,* 2001). This means that EGCg can therefore be having contradictory effects on viral replication. It promotes the uptake of the virus into the cell and possibly prevents viral proteins from being degraded but then prevents new virions from being formed and released. Thus the effects of EGCg may be canceling each other out and that the viral infection is being allowed to proceed as if no drug was added.

4.5 Conclusion

Several different drugs have been approved for the treatment of HIV/AIDS and many more are currently being investigated for their antiretroviral properties. The initial evaluation of drugs with potential antiretroviral activity usually involves the use of an *in vitro* cell culture system as several drugs can be evaluated rapidly and cost effectively. An *in vitro* co-culture model of SC-1 and BM5 cells was developed and used in this study to evaluate the antiretroviral properties of GT and EGCg. The use of this model was validated by evaluating known antiretroviral drugs AZT, IDV, HU and CQ. All four drugs significantly inhibited the cell-to-cell transmission of the virus from chronically infected cells to uninfected cells at sub-toxic concentrations. The exact mechanism by which this particular virus spreads from cell-to-cell is unknown and should be investigated.

The experimental compounds GT and EGCg showed little to no effect on the viral load. This however, does not mean that the compounds will not be beneficial when combined with the other known antiretrovirals but rather that the drugs have no effect on the virus itself. The compounds may still enhance the antiretroviral effects of AZT, IDV, HU and CQ when used in combination by perhaps increasing the cellular uptake of the drug. This will be investigated in the following chapter. Although GT showed little inhibition of the viral load, it does not mean that other compounds present in very low concentrations in GT do not possess antiretroviral properties. It therefore may still be worthwhile to investigate these other compounds, particularly caffeine as caffeine has been shown to

inhibit the integration step of HIV (Nunnari *et al.,* 2005). This effect was not seen here, possibly because the concentration of caffeine present within the GT was too low.

Chapter 5: Evaluation of the toxicity and antiretroviral activity of experimental compounds green tea and EGCg in combination with the antiretroviral drugs AZT, HU, IDV and CQ.

5.1 Introduction

The concept of combination drug therapy or highly active antiretroviral therapy (HAART) for the treatment of HIV/AIDS was introduced in the mid nineties after it was observed that the use of a single antiretroviral drug resulted in the rapid development of drug resistance (Dieterich *et al.,* 2006). The use of HAART in HIV/AIDS infected persons was associated with a significant reduction in the morbidity and mortality of HIV/AIDS (Correll *et al.,* 1998; Palella *et al.,* 1998; Detels *et al.,* 1999; Louwagie *et al.,* 2007). HAART however does not cure HIV/AIDS, instead it prolongs the life of the HIV-infected person by reducing the HIV viral load to below detection levels and restores immune function (Chen *et al.,* 2007). Drug combination therapy can be one of the following combinations: 2 NRTIs with 1 PI, 2 NRTIs with 1 NNRTI or 3 NRTI (Sension, 2004; Dieterich *et al*., 2006). In the US Department of Health and Human Services (DHHS) guidelines there are 91 possible antiretroviral drug combinations that may be used (Dieterich *et al*., 2006).

Despite having a significant impact on morbidity and mortality of HIV/AIDS, treatment with combination drug therapy has resulted in several problems. These include high cost of treatment and poor availability of drugs in low-income countries (Yazdanpanah, 2004), severe adverse effects (Ter Hofstede *et al*., 2003; Montessori *et al*., 2004) and poor compliance (Maggiolo *et al*., 2003). The adverse effects associated with HAART have been reviewed by Hofstede *et al.,* 2003 and Montessori *et al.,* 2004. These include mitochondrial toxicity, the lipodystrophy syndrome, skin rash, osteoporosis and osteonecrosis. Mitochondrial toxicity is often associated with the NRTIs and results in lactic acidosis, hepatic steatosis, pancreatitis, neuropathy and (cardio) myopathy. The lipodystrophy syndrome is caused by both the NRTIs and the PIs. This syndrome consists of hyperlipidaemia, hyperglycaemia, insulin resistance with diabetes mellitus, lipoatrophy and central adiposity. The NNRIs are suspected to be the culprits for the skin rash. Another major concern for effective treatment of HIV/AIDS is poor patient compliance which is often caused by the large number of pills consumed per day, the complexity of the regimens as well as the toxicities associated with antiretroviral drugs

(Maggiolo *et al.,* 2003). The consequence of poor compliance is drug resistance development that then limits the treatment options.

Due to the problems associated with toxicity, cost, patient compliance and drug resistance, the focus of recent research is the identification of new drugs and the development of new treatment strategies that are as effective as the current approved antiretroviral drugs. Ethopharmacology is the scientific multi-disciplinary study of materials from animal, vegetal and mineral origins and related knowledge and practices that different cultures use for therapeutic and diagnostic purposes. The study of traditional medicinal plants and the isolation and characterization of active constituents has led to several to the identification new drugs such as quinine and artemisinin that are used in the treatment of malaria (O' Neill *et al.,* 1998, Krishna *et al.,* 2004).

Many of these plants, however, have not been subjected to scientific evaluation and this has caused much concern as very little is known about the effects of these medicinal plants and herbs on the progression of HIV/AIDS. Also, many HIV/AIDS patients on combination antiretroviral drug therapy also take these medicinal herbs and plant derived preparations that are readily available over the counter as supplements to boost immunity or are provided to patients by herbalists. Little is known regarding the interactions of these preparations with the antiretroviral drugs and they may have contradicting effects by either directly lowering a patients viral load, improving a patients immune response or may be toxic by interfering with the therapeutic effects of existing antiretroviral drugs.

In a study conducted by Van den bout-van den Beukel *et al.,* 2006, several plants and herbs were identified as having possible negative interactions with antiretroviral drugs. These plants were Asian, American and Siberian ginseng, *Catharantus roseus*, cranberry, devil's claw, Echinacea, eucalyptus oil, evening primrose, garlic, ginger, ginkgo biloba, *Hypoxia hemerocallidea*, milk thistle, soy, St. John's wort, *Sutherlandia frutescens* and valerian. These plants were found to interfere with antiretroviral drug metabolism by interfering with or altering cytochrome P450, UDP-glucuronosyltransferases or P-glycoprotein activity. Green tea was also investigated by these authors and their findings were that there was no significant adverse interaction between green tea and the metabolism of the antiretroviral drugs. Consequently green tea and its constituents such as EGCg should be further evaluated especially as in other studies EGCg has been shown to have antiretroviral activity (Nakane and Ono, 1990; Tao, 1992; Chang *et al.,* 1994; Yamaguchi *et al*., 2002; Kawai *et al*., 2003).

The effect of GT and its active constituent EGCg in combination with antiretroviral drugs was determined in this study. The co-culture model used in Chapter 4 to study the effects of single drugs AZT, IDV, HU, CQ, GT and EGCg on antiretroviral activity was used here to study the effects of GT and EGCg in combination with the antiretroviral drugs AZT, IDV, HU and CQ. Although GT and EGCg showed insignificant effects on the cell-to-cell transmission of the BM5-def virus determined by real-time PCR in the previous chapter, these compounds could still be beneficial in combination with an antiretroviral drug by improving the uptake of the drug into the cell, inhibiting a cellular metabolite that competes with the drug, decreasing the efflux of the drug from the cell and enhancing the metabolic activation of the drug into its active form. Another important factor is that GT and EGCg when used in combination with the antiretrovirals may reduce the cytotoxicity of the antiretroviral drugs without having a negative effect on the antiretroviral activity of the drug.

The aims of this study were therefore to;

(xv) Determine whether combinations of the antiretroviral drugs AZT, IDV, HU or CQ with either GT or EGCg at a constant ratio resulted in a synergistic, additive or antagonistic effect on cell toxicity.

(xvi) Determine whether GT and EGCg when in combination with the antiretroviral drugs AZT, IDV, HU or CQ enhanced, suppressed or had no effect on the antiretroviral activity of AZT, IDV, HU and CQ.

(xvii) Determine whether any combinations warrant further investigation in the *in vivo* MAIDS model.

5.2 Materials

5.2.1 Cell lines, media, supplements, reagents and plasticware

Same as used in Sections 3.2.1, 4.2.2. and 3.2.3

5.3 Methods

5.3.1 Preparation of drug stock solutions

Same as Section 4.3.1.

5.3.2 Determination of the toxicity of drug combinations

The SC-1 cells were plated in 25cm^2 cell culture flasks at a concentration of 2.5 x 10^5 cells in 4ml of supplemented DMEM and left to settle overnight (17 hours) in the incubator at 37℃, 5% CO_2. The SC-1 cells were then exposed to various concentrations of the drug combinations. The drug combinations are shown in Table 5.1. Six flasks of SC-1 cells were plated for each drug combination. One flask served as a control and the other five were exposed to the various concentrations of the drug combinations mentioned above. The volume of each flask was adjusted to 6ml with medium after the addition of the drug. The flasks were then placed in the incubator at 37℃, 5% CO_2 for 72 hours.

A volume of 300µl of a 1mg/ml MTT solution prepared in 20xPBS was added to each flask. The flasks were incubated for 1 hour at 37℃, 5% CO_2. The medium was removed and the purple formazan product was solubilized in 2.5ml of DMSO. Six volumes of 100µl of the solubilized formazan from each flask were transferred to a 96-well plate. The absorbency was read at 550nm with a Multiscan Ascent plate reader from AEC Amersham, Kelvin, SA. The cellular toxicity of each drug combination was determined in three independent experiments.

Table 5.1 Concentration of each antiretroviral drug used in the different combinations with GT or EGCg

	Drug Combinations			
Concentration µM + mg/ml	**AZT+GT**	**IDV+GT**	**HU+GT**	**CQ+GT**
1/16TD$_{50}$ + 1/16TD$_{50}$	22.0 + 0.036	18.0 + 0.036	5.5 + 0.036	1.5 + 0.036
1/8TD$_{50}$ + 1/8TD$_{50}$	44.1 + 0.073	36.1 + 0.073	11.0 + 0.073	3.1 + 0.073
1/4TD$_{50}$ + 1/4TD$_{50}$	88.1 + 0.146	72.2 + 0.146	22.0 + 0.146	6.2 + 0.146
1/2TD$_{50}$ + 1/2 TD$_{50}$	176.2 + 0.291	144.1+ 0.291	44.0 + 0.291	12.3 + 0.291
TD$_{50}$ + TD$_{50}$	352.4 + 0.582	288.7 + 0.582	88.1 + 0.582	24.6 + 0.582
Concentration µM + µM	**AZT + EGCg**	**IDV + EGCg**	**HU+EGCg**	**CQ+EGCg**
1/16TD$_{50}$ + 1/16TD$_{50}$	22.0 + 13.3	18.0 + 13.3	5.5 + 13.3	1.5 + 13.3
1/8TD$_{50}$ + 1/8TD$_{50}$	44.1 + 26.6	36.1 + 26.6	11.0 + 26.6	3.1 + 26.6
1/4TD$_{50}$ + 1/4TD$_{50}$	88.1 + 53.2	72.2 + 53.2	22.0 + 53.2	6.2 + 53.2
1/2TD$_{50}$ + 1/2 TD$_{50}$	176.2 + 106.4	144.1+ 106.4	44.0 + 106.4	12.3 + 106.4
TD$_{50}$ + TD$_{50}$	352.4 + 212.7	288.7 + 212.7	88.1 + 212.7	24.6 + 212.7

5.3.3 Determination of the antiretroviral activity of the various drug combinations.

The antiretroviral activity of the different drug combinations as in Section 5.3.2 was evaluated in 1:10,000 co-cultures of BM5:SC-1 cells. The total number of cells plated for each co-culture was 2.5 x 10^5 cells in 25cm^2 cell-culture flasks. A dilution series of the BM5 cells was created in 24-well plates starting with 2.5 x 10^5 cells in 1ml of complete medium up to 25 BM5 cells in 1ml of complete medium. The number of SC-1 cells then added to the 25 BM5 cells was 249,975 making a 1:10,000 co-culture of BM5:SC-1 cells. The two cell types were mixed together and added to the 25cm^2 cell-culture flasks already containing 4ml of complete medium. The flasks were then left to settle overnight (17 hours) in the incubator at 37°C, 5% CO_2. The drug combinations were then added and the final volume of each flask was adjusted to 6ml with complete medium. Five flasks of co-cultures were plated for each drug combination at the same concentrations as in Table 5.1 (combination of TD_{50} + TD_{50} was not included) and a control (no drug added). The co-cultures were incubated for 72 hours at 37°C, 5% CO_2 where after the DNA was extracted. The antiretroviral activity of each drug combination was determined from two independent experiments.

5.3.3.1 Extraction of genomic DNA

Same as Section 3.3.4.

5.3.3.2 Real-time PCR for quantification of the BM5-def viral DNA and murine G6PDH gene in the drug combinations

Real-time PCR of the BM5-def viral DNA and G6PDH gene was performed as in Section 3.3.8. The LightCycler® 480 Relative Quantification software was used to quantify the BM5-def viral DNA and G6PDH gene. LP-BM5 DNA served as the target calibrator (BM5-def) and reference calibrator (G6PDH) to normalize samples between runs. A melting curve analysis was also performed on all products to detect primer dimers. A sample with high primer dimer content was rejected and not included in the relative quantification analysis.

The mean of the concentrations obtained from the relative quantification software analysis of each drug concentration was calculated and expressed as a percentage of

the control with the control representing a 100% as no drug was added to the control so it was assumed that viral infection was allowed to proceed uninhibited.

5.3.4 Data management and statistics

For the toxicity studies the mean absorbency values of each drug concentration was calculated and expressed as a percentage of the control with the control being 100% as no drug was added. These results gave rise to the dose-effect plots. The fraction affected was also calculated with the following formula: (control mean – drug concentration x mean)/ control mean as this is the format used by the median effect equation of T-C Chou (Chou, 1991). The fraction affected for the control was thus 0. The combination index (CI) equation and plot of Chou-Talalay derived from enzyme kinetics models (Chou, 1991) were used to calculate CI values that determine whether a combination is additive, synergistic or antagonistic.

For the real-time PCR quantification of the BM5-def viral DNA, the relative quantification software was used. The relative quantification analysis quantified the expression level of the viral gene relative to the G6PDH gene (housekeeping gene) for each drug concentration. This corrected for differences in the amount and quality of the various DNA samples. This ratio (viral/G6PDH) for each drug concentration was then normalized by the calibrator (BM5 cell DNA) and expressed as a concentration value. The mean of the concentration values obtained from the relative quantification analysis of each drug concentration was calculated and expressed as a percentage of the control by dividing the concentration value of each drug concentration by the concentration value of the control and multiplying by 100%. The control represented a 100% as no drug was added to the control so it was assumed that viral infection was allowed to proceed uninhibited.

5.4 Results and discussion

5.4.1 Cytotoxicity of GT or EGCg in combination with AZT, IDV, HU or CQ

The cytotoxicity of each drug combination was determined in the SC-1 cell line and quantified with the MTT assay that measures mitochondrial dehydrogenase activity. The concentrations used were the 1/16, 1/8, 1/4 and ½ of the TD_{50} of each individual drug as determined in Chapter 4, Table 4.2. The SC-1 cells were exposed to the different drug combinations at different concentrations (Table 5.1) for 72 hours. Each experiment was

done in triplicate and a mean and the standard error of the mean (SEM) was determined.

For all drug combinations the CI equation and plot of Chou-Talalay were used to determine if a drug combination had a synergistic, additive or antagonistic effect on cell toxicity. Figure 5.1 and 5.2 show the dose-response curves of the different combinations in relation to the single drugs on cell viability as determined with the MTT assay for the drugs combined with GT and EGCg respectively.

In the previous chapter, it was found that GT and EGCg alone had little to no effect on the BM5-def viral load. A beneficial effect such as the enhancement of the antiretroviral activity or reduction of toxicity of known antiretroviral drugs such as AZT, IDV, HU and CQ when used in combination with GT and EGCg should be considered.

Synergistic and antagonistic effects could be determined from the cytotoxicity data as for each of the drugs a TD_{50} was determined. The effects of the single drugs alone on cell viability at drug concentrations of 1/16 TD_{50}, 1/8 TD_{50}, 1/4 TD_{50}, 1/2 TD_{50} and TD_{50} were not determined experimentally. Instead, the fraction affected for the particular dose of each drug was determined using the median effect equation and plot of T-C Chou (Chou, 1991). From the three dose-response curves obtained for the cellular toxicity for each of the drugs alone in Chapter 4, the median-effect plot was constructed and from these plots, the D_m and m for each of the three curves of each drug was determined. By knowing, the D_m and m, an alternative form of the median effect equation shown in Chapter 4 to determine the fraction affected for a particular dose could be used. The three fractions affected obtained for each of the drugs at a particular dose were added together and a mean was obtained as well as a standard error of the mean.

Alternative form of the median-effect equation: $f_a = 1/[1 + (D_m/D)^m]$
(Definitions for fa, D_m, D and m are given in Chapter 4 Section 4.4).

In Figure 5.1 and 5.2, it can be seen that the combination of AZT and GT (Figure 5.1 (A)) results in only a slight increase in cell toxicity at concentrations above $1/2TD_{50}$ + 1/2 TD_{50}. For AZT in combination with EGCg a toxic effect was observed at the lowest concentrations $1/16TD_{50}$ + $1/16TD_{50}$ when compared to AZT and EGCg (Figure 5.2 (A)) alone. For IDV combined with GT (Figure 5.1 (B)) a similar increase in toxicity was observed as for AZT and GT with increased toxicity being observed at concentrations

above $1/2TD_{50}$ + 1/2 TD_{50}. Likewise, IDV in combination with EGCg (Figure 5.2 (B)), a significant increase in toxicity was seen already at $1/16TD_{50}$ + $1/16TD_{50}$.

The combination of HU and GT (Figure 5.1 (C)) showed no effect on toxicity at all concentrations. For the combination of HU and EGCg at concentrations above the $1/4TD_{50}$ + $1/4TD_{50}$ an increase in toxicity is observed (Figure 5.2 (C)). Of all the drug combinations evaluated the combination of CQ and GT (Figure 5.1 (D)) had the largest effect with significant increases in toxicity above the $1/16TD_{50}$ + $1/16TD_{50}$. Although for CQ in combination with EGCg (Figure 5.2 (D)) a lesser effect is observed indicating that other constituents besides EGCg in GT may be contributing to this cytotoxic effect.

To determine whether these effects were antagonistic, additive or synergistic, the percentages of the control obtained for each concentration were then converted into a fraction affected using the formula as in Section 5.3.2. The median effect equation of T-C Chou as well as the CI equation and plot of Chou-Talalay (Chou, 1991) were then used to determine the CI values and fa-CI plots. Table 5.2 lists the descriptions given by the Calcusyn manual for the various possible CI values. Three types of effects (i) synergism, (ii) additive and (iii) antagonism of varying degrees (very strong, strong, moderate and slight) are determined according to the range of the CI values.

Table 5.2. Descriptions recommended for describing the various possible combination index (CI) values

Description	Range Of CI
Very strong synergism	< 0.1
Strong synergism	0.1 - 0.3
Synergism	0.3 - 0.7
Moderate synergism	0.7 - 0.85
Slight synergism	0.85 - 0.90
Nearly additive	0.90 - 1.10
Slight antagonism	1.10 - 1.20
Moderate antagonism	1.20 - 1.45
Antagonism	1.45 - 3.3
Strong antagonism	3.3 – 10
Very strong antagonism	> 10

Table 5.3 (for GT) and Table 5.4 (for EGCg) show the CI values and description of these CI values of each combination at a particular concentration.

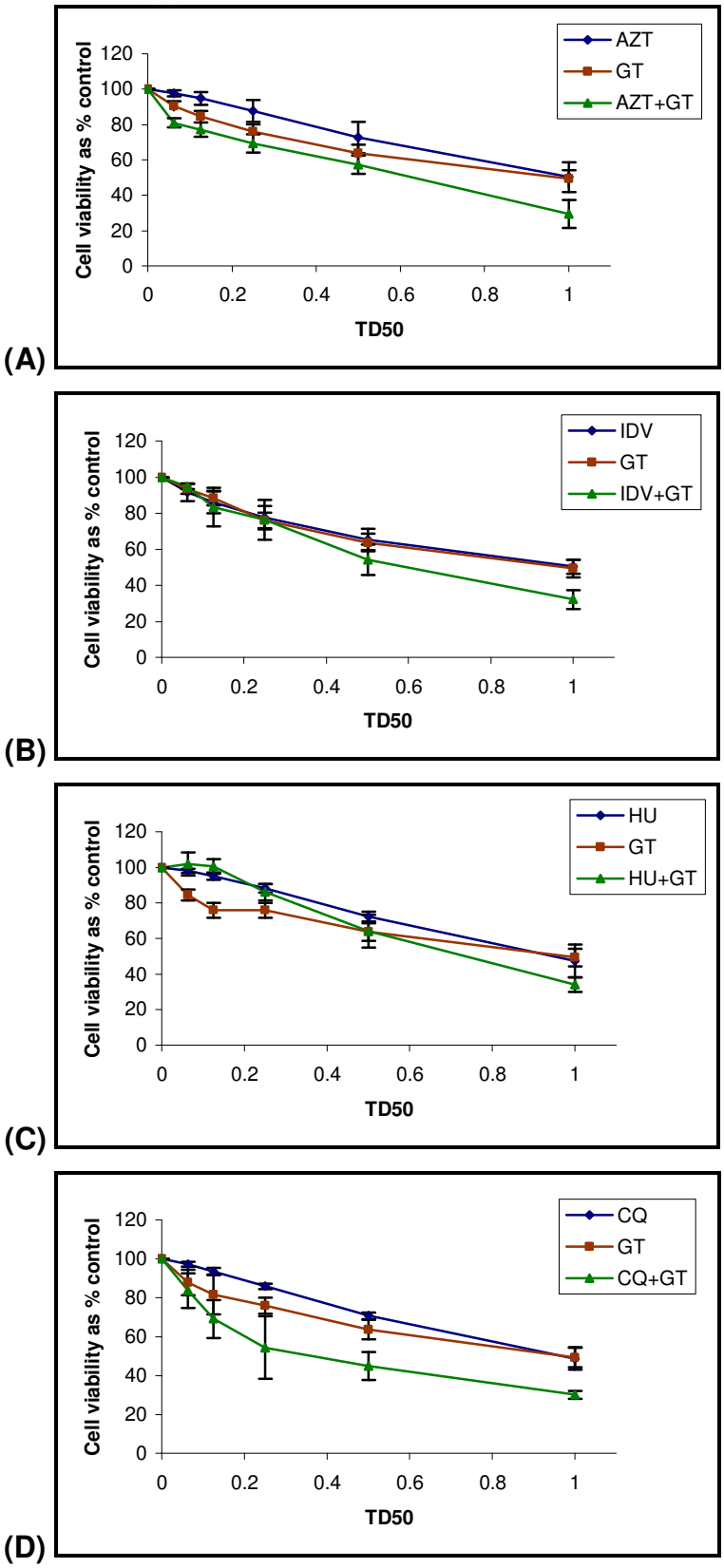

Figure 5.1. Dose-response curves for toxicity of the different known antiretroviral drugs combined with GT (A) AZT + GT (B) IDV + GT (C) HU + GT (D) CQ + GT as determined with the MTT assay. The concentrations used are presented in Table 5.1.

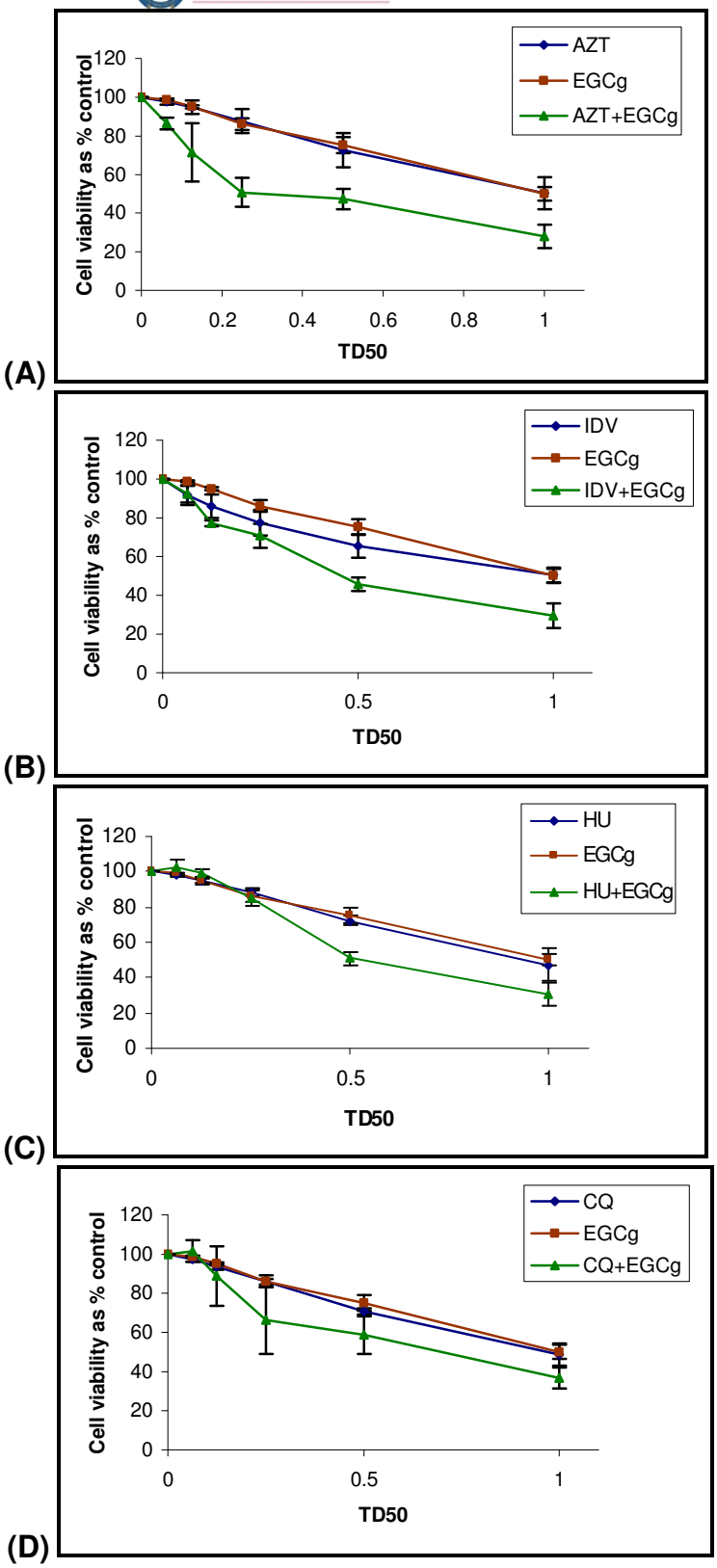

Figure 5.2. Dose-response curves for toxicity of the different known antiretroviral drugs combined with EGCg (A) AZT + EGCg (B) IDV + EGCg (C) HU + EGCg (D) CQ + EGCg as determined with the MTT assay. The concentrations used for each of the drugs in the combinations with EGCg are shown in Table 5.1.

Table 5.3 Combination index (CI) values obtained for the toxicity of the different concentrations of the drug combination with GT

Combination	Drug Concentration	Fraction Affected	CI	Description
AZT + GT	$1/16TD_{50}$ + $1/16TD_{50}$	0.189235	0.547	Synergism
	$1/8TD_{50}$ + $1/8TD_{50}$	0.227818	0.856	Slight Synergism
	$1/4TD_{50}$ + $1/4TD_{50}$	0.308142	1.115	Slight Antagonism
	$1/2TD_{50}$ + $1/2TD_{50}$	0.428101	1.324	Moderate Antagonism
	TD_{50} + TD_{50}	0.705404	0.87	Slight Synergism
IDV +GT	$1/16TD_{50}$ + $1/16TD_{50}$	0.05119	3.946	Strong Antagonism
	$1/8TD_{50}$ + $1/8TD_{50}$	0.167002	1.657	Antagonism
	$1/4TD_{50}$ + $1/4TD_{50}$	0.237073	1.973	Antagonism
	$1/2TD_{50}$ + $1/2TD_{50}$	0.457834	1.202	Moderate Antagonism
	TD_{50} + TD_{50}	0.678176	0.812	Moderate Synergism
HU +GT	$1/16TD_{50}$ + $1/16TD_{50}$	1.00E-06	6.17E+06	Very Strong Antagonism
	$1/8TD_{50}$ + $1/8TD_{50}$	1.00E-06	1.23E+07	Very Strong Antagonism
	$1/4TD_{50}$ + $1/4TD_{50}$	0.138763	14.733	Very Strong Antagonism
	$1/2TD_{50}$ + $1/2TD_{50}$	0.359323	6.914	Strong Antagonism
	TD_{50} + TD_{50}	0.65771	3.388	Strong Antagonism
CQ + GT	$1/16TD_{50}$ + $1/16TD_{50}$	0.162155	0.923	Nearly Additive
	$1/8TD_{50}$ + $1/8TD_{50}$	0.309341	0.675	Synergism
	$1/4TD_{50}$ + $1/4TD_{50}$	0.456591	0.635	Synergism
	$1/2TD_{50}$ + $1/2TD_{50}$	0.549979	0.811	Moderate Synergism
	TD_{50} + TD_{50}	0.698136	0.749	Moderate Synergism

Table 5.4. Combination index (CI) values obtained for the toxicity of the different concentrations of the drug combination with EGCg

Combination	Drug Concentration	Fraction Affected	CI	Description
AZT + EGCg	$1/16TD_{50}$ + $1/16TD_{50}$	0.135723	0.349	Synergism
	$1/8TD_{50}$ + $1/8TD_{50}$	0.286541	0.278	Strong Synergism
	$1/4TD_{50}$ + $1/4TD_{50}$	0.492918	0.264	Strong Synergism
	$1/2TD_{50}$ + $1/2TD_{50}$	0.526448	0.475	Synergism
	TD_{50} + TD_{50}	0.720333	0.499	Synergism
IDV + EGCg	$1/16TD_{50}$ + $1/16TD_{50}$	0.075442	1.495	Antagonism
	$1/8TD_{50}$ + $1/8TD_{50}$	0.229701	0.796	Moderate Synergism
	$1/4TD_{50}$ + $1/4TD_{50}$	0.343875	0.92	Nearly Additive
	$1/2TD_{50}$ + $1/2TD_{50}$	0.54302	0.854	Slight Synergism
	TD_{50} + TD_{50}	0.705536	0.911	Nearly Additive

Table 5.4 Cont'd

EGCg + HU	$1/16TD_{50} + 1/16TD_{50}$	0.005003	4.943	Strong Antagonism
	$1/8TD_{50} + 1/8TD_{50}$	0.017828	4.029	Strong Antagonism
	$1/4TD_{50} + 1/4TD_{50}$	0.144042	1.805	Antagonism
	$1/2TD_{50} + 1/2TD_{50}$	0.490021	1.068	Nearly Additive
	$TD_{50} + TD_{50}$	0.694871	1.151	Slight Antagonism
EGCg + CQ	$1/16TD_{50} + 1/16TD_{50}$	0.0318057	4.473	Strong Antagonism
	$1/8TD_{50} + 1/8TD_{50}$	0.0162791	19.365	Very Strong Antagonism
	$1/4TD_{50} + 1/4TD_{50}$	0.06156	8.331	Strong Antagonism
	$1/2TD_{50} + 1/2TD_{50}$	0.302326	2.296	Antagonism
	$TD_{50} + TD_{50}$	0.404241	2.925	Antagonism

The fa-CI plots (Figure 5.3 and 5.4) are a graphic representation of the overall effect of a particular combination.

Figures 5.3 and 5.4 show the overall synergism, addition or antagonism of each combination over the entire range of fractions affected (% inhibition). All the points (the x's) above 1 represent antagonism; points at 1 represent addition and point below 1 represent synergism. The combinations of CQ and GT (Figure 5.3 (D)) and AZT and EGCg (Figure 5.4 (A)) show an overall effect of synergism while combinations of HU and GT (Figure 5.3 (C)), HU and EGCg (Figure 5.4 (C)) and CQ and EGCg (Figure 5.4 (D)) show an overall effect of antagonism throughout the range of fractions affected. The combination of AZT and GT (Figure 5.3 (A)) showed synergism at low effects but antagonism at higher effects while the combination of IDV and GT (Figure 5.3 (B)) showed an opposite effect of antagonism at low effects but synergism at high effects. Only the combination of IDV and EGCg (Figure 5.4 (B)) showed an almost overall effect of addition of cytotoxicity. A summary of the effect of AZT, IDV, HU and CQ in combination with GT and EGCg is given in Table 5.5.

In Table 5.5, it is shown that the combination of AZT and GT showed synergy at the low concentrations but antagonism at higher concentrations while the combination of AZT and EGCg showed a synergistic effect throughout the concentration range examined on cell toxicity. The combination of IDV and GT showed antagonism at low concentrations but synergism at the higher concentrations while the combination of IDV and EGCg showed slight synergism at all concentrations examined. Antagonism on cell toxicity was seen in the combinations of HU and GT and HU and EGCg over the entire concentration range evaluated. The combinations of CQ and GT and CQ and EGCg

showed opposite effects on cell toxicity over the concentration namely synergism for the combination of CQ and GT but strong antagonism for the combination of CQ and EGCg.

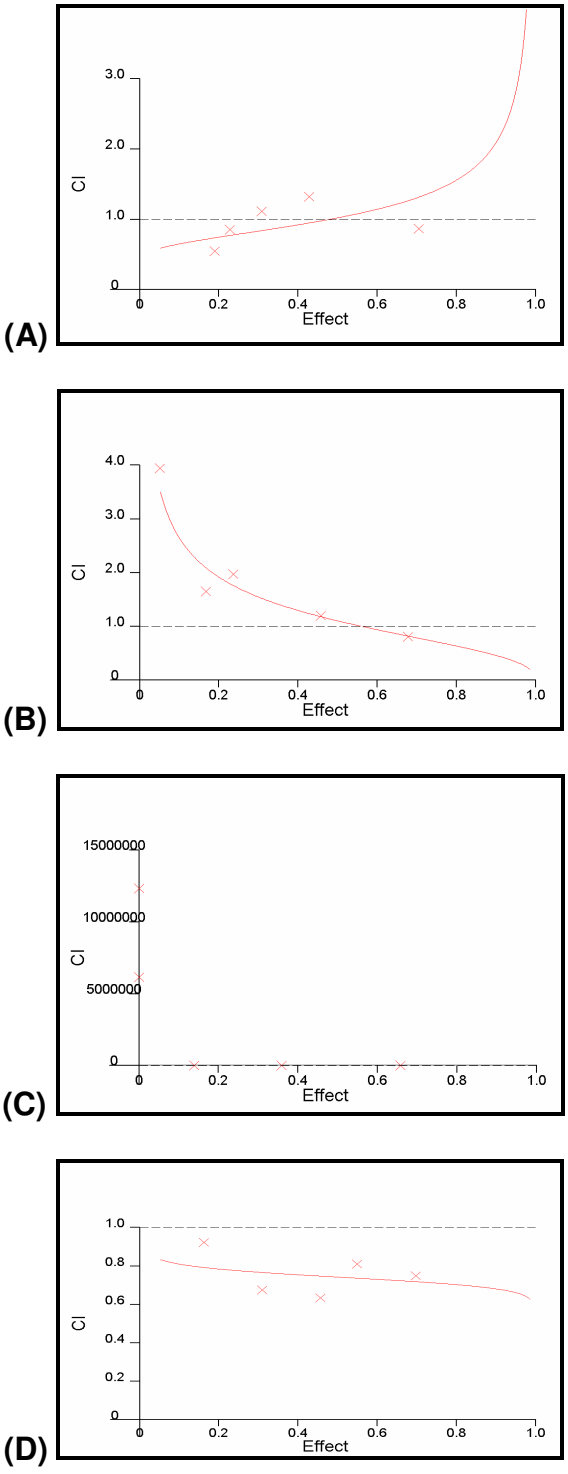

Figure 5.3. Fa-CI plots showing the overall effect of the combinations of the known antiretroviral drugs with GT on cell toxicity as determined with the CI equation and plot of Chou-Talalay (Chou, 1991). (A) AZT + GT, (B) IDV + GT, (C) HU + GT, (D) CQ + GT.

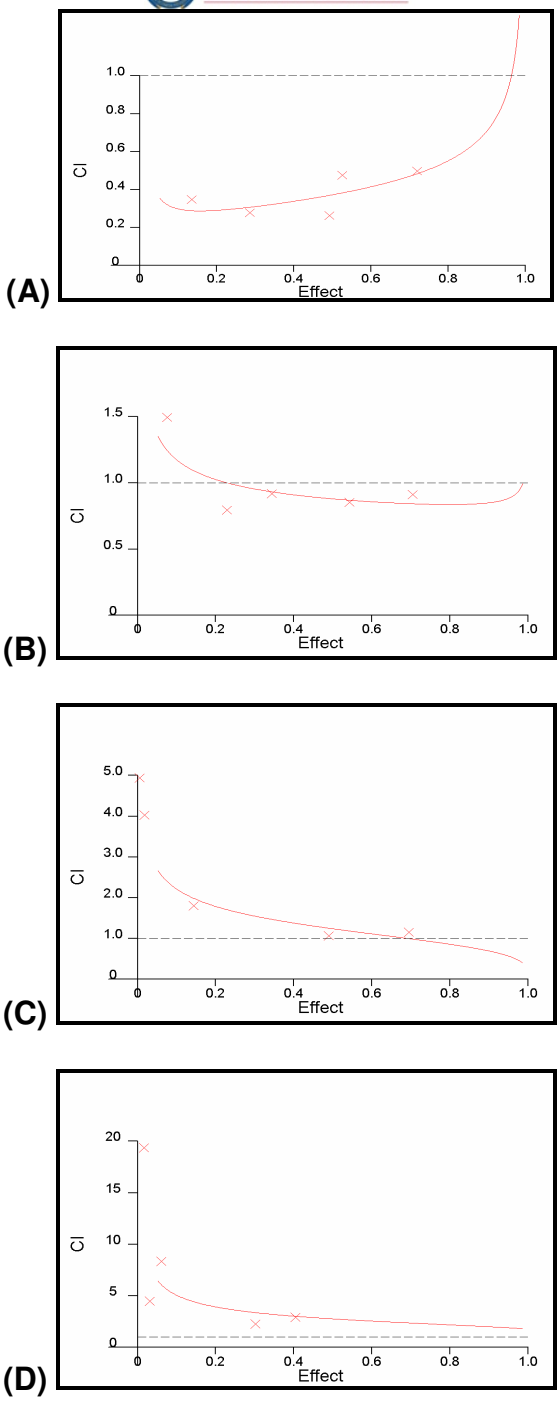

Figure 5.4. Fa-CI plots showing the overall effect of the combinations of the known antiretroviral drugs with EGCg on cell toxicity as determined with the CI equation and plot of Chou-Talalay (Chou, 1991). (A) AZT + EGCg, (B) IDV + EGCg, (C) HU + EGCg, (D) CQ + EGCg.

Table 5.5 Summary of the toxicity of drugs in combination with GT and EGCg.

AZT +GT		**AZT + EGCg**	
$1/16TD_{50} + 1/16TD_{50}$	Synergism	$1/16TD_{50} + 1/16TD_{50}$	Synergism
$1/8TD_{50} + 1/8TD_{50}$	Slight Synergism	$1/8TD_{50} + 1/8TD_{50}$	Strong Synergism
$1/4TD_{50} + 1/4TD_{50}$	Slight Antagonism	$1/4TD_{50} + 1/4TD_{50}$	Strong Synergism
$1/2TD_{50} + 1/2TD_{50}$	Moderate Antagonism	$1/2TD_{50} + 1/2TD_{50}$	Synergism
$TD_{50} + TD_{50}$	Slight Synergism	$TD_{50} + TD_{50}$	Synergism
IDV +GT		**IDV + EGCg**	
$1/16TD_{50} + 1/16TD_{50}$	Strong Antagonism	$1/16TD_{50} + 1/16TD_{50}$	Antagonism
$1/8TD_{50} + 1/8TD_{50}$	Antagonism	$1/8TD_{50} + 1/8TD_{50}$	Moderate Synergism
$1/4TD_{50} + 1/4TD_{50}$	Antagonism	$1/4TD_{50} + 1/4TD_{50}$	Nearly Additive
$1/2TD_{50} + 1/2TD_{50}$	Moderate Antagonism	$1/2TD_{50} + 1/2TD_{50}$	Slight Synergism
$TD_{50} + TD_{50}$	Moderate Synergism	$TD_{50} + TD_{50}$	Nearly Additive
HU +GT		**HU + EGCg**	
$1/16TD_{50} + 1/16TD_{50}$	Very Strong Antagonism	$1/16TD_{50} + 1/16TD_{50}$	Strong Antagonism
$1/8TD_{50} + 1/8TD_{50}$	Very Strong Antagonism	$1/8TD_{50} + 1/8TD_{50}$	Strong Antagonism
$1/4TD_{50} + 1/4TD_{50}$	Very Strong Antagonism	$1/4TD_{50} + 1/4TD_{50}$	Antagonism
$1/2TD_{50} + 1/2TD_{50}$	Strong Antagonism	$1/2TD_{50} + 1/2TD_{50}$	Nearly Additive
$TD_{50} + TD_{50}$	Strong Antagonism	$TD_{50} + TD_{50}$	Slight Antagonism
CQ +GT		**CQ + EGCg**	
$1/16TD_{50} + 1/16TD_{50}$	Nearly Additive	$1/16TD_{50} + 1/16TD_{50}$	Strong Antagonism
$1/8TD_{50} + 1/8TD_{50}$	Synergism	$1/8TD_{50} + 1/8TD_{50}$	Very Strong Antagonism
$1/4TD_{50} + 1/4TD_{50}$	Synergism	$1/4TD_{50} + 1/4TD_{50}$	Strong Antagonism
$1/2TD_{50} + 1/2TD_{50}$	Moderate Synergism	$1/2TD_{50} + 1/2TD_{50}$	Antagonism
$TD_{50} + TD_{50}$	Moderate Synergism	$TD_{50} + TD_{50}$	Antagonism

5.4.2 The relationship between the toxicity and the antiretroviral effects of GT or EGCg in combination with AZT, IDV, HU or CQ.

Synergism and antagonism could not be determined for the different combinations on the virus as GT and EGCg showed little to no effect on the virus when tested alone (Figure 4.4). To determine whether GT and EGCg augmented or inhibited the effects of the antiretroviral drugs AZT, IDV, HU and CQ when combined with these compounds at a constant molar ratio on the cell-to-cell transmission of the BM5-def virus, the *in vitro* MAIDS co-culture model developed in Chapter 4 was used. The co-culture was exposed to the different concentrations of the drugs as in Table 5.1 for 72 hours and there after the DNA was isolated and amplified and quantified with real-time PCR. The concentration of TD_{50}+TD_{50} was not evaluated since one wants to see

augmentation/inhibition of antiretroviral activity at sub-toxic doses where cellular viability is high. The relative concentration of each drug concentration in a given combination was then expressed as a percentage of the control with the control being 100% as this co-culture was not exposed to any drug.

Figures 5.5 and 5.6 graphically show the effects of the combinations on the cell-to-cell transmission of the virus as compared to when the co-culture was exposed to a single drug. As with the toxicity studies, the mean and SEM of two experiments was determined.

The combinations of AZT and GT (Figure 5.5 (A)) and AZT and EGCg (Figure 5.6 (A)) showed little change in the percentage inhibition as compared with AZT alone. It could therefore be conclude that GT and EGCg have no effect on the antiretroviral effect of AZT on the viral load except at high concentrations ($1/2TD_{50}$). Similarly, the combination of IDV and GT (Figure 5.5 (B)) showed little change in the percentage inhibition achieved as compared with IDV alone. However, in the combination of IDV and EGCg (Figure 5.6 (B)), EGCg clearly inhibited the anti-viral effects of IDV on the cell-to-cell transmission of the BM5-def virus.

In the combinations of HU and GT (Figure 5.5 (C)) and HU and EGCg (Figure 5.6 (C)), it can clearly be seen that GT and EGCg inhibited the antiviral effects of HU. Similarly, in the combination of CQ and EGCg (Figure 5.6 (D)), it can be seen that EGCg inhibited the antiviral effects of CQ at high concentrations. The only combination that showed potentiation was the combination of CQ and GT (Figure 5.5 (D)) where the BM5-def viral load was significantly reduced to below 10% over the concentration range tested. A summary of the effects of GT and EGCg on the cytotoxicity and antiretroviral activity of the antiretroviral drugs can be seen in Table 5.6.

AZT was one of the first antiretroviral drugs approved for the treatment of HIV/AIDS and is commonly used in HAART therapy. AZT in Chapter 4 showed very strong antiretroviral activity against the cell-to-cell transmission of the BM5-def virus. In the combinations of AZT and GT and AZT and EGCg, GT and EGCg appeared to have little to no effects on the antiretroviral activity of AZT. Possible explanations for this are that neither GT nor EGCg interfere with the antiretroviral activity of AZT or that the concentration range of AZT used was too high thus masking any possible potentiation of antiretroviral activity by GT or EGCg. Although GT and EGCg did not enhance the antiretroviral activity it was encouraging to see that they also did not inhibit the antiretroviral activity of AZT. And

thus these combinations of AZT and GT and AZT and EGCg should be further investigated at lower concentrations of AZT and/or different combination molar ratio.

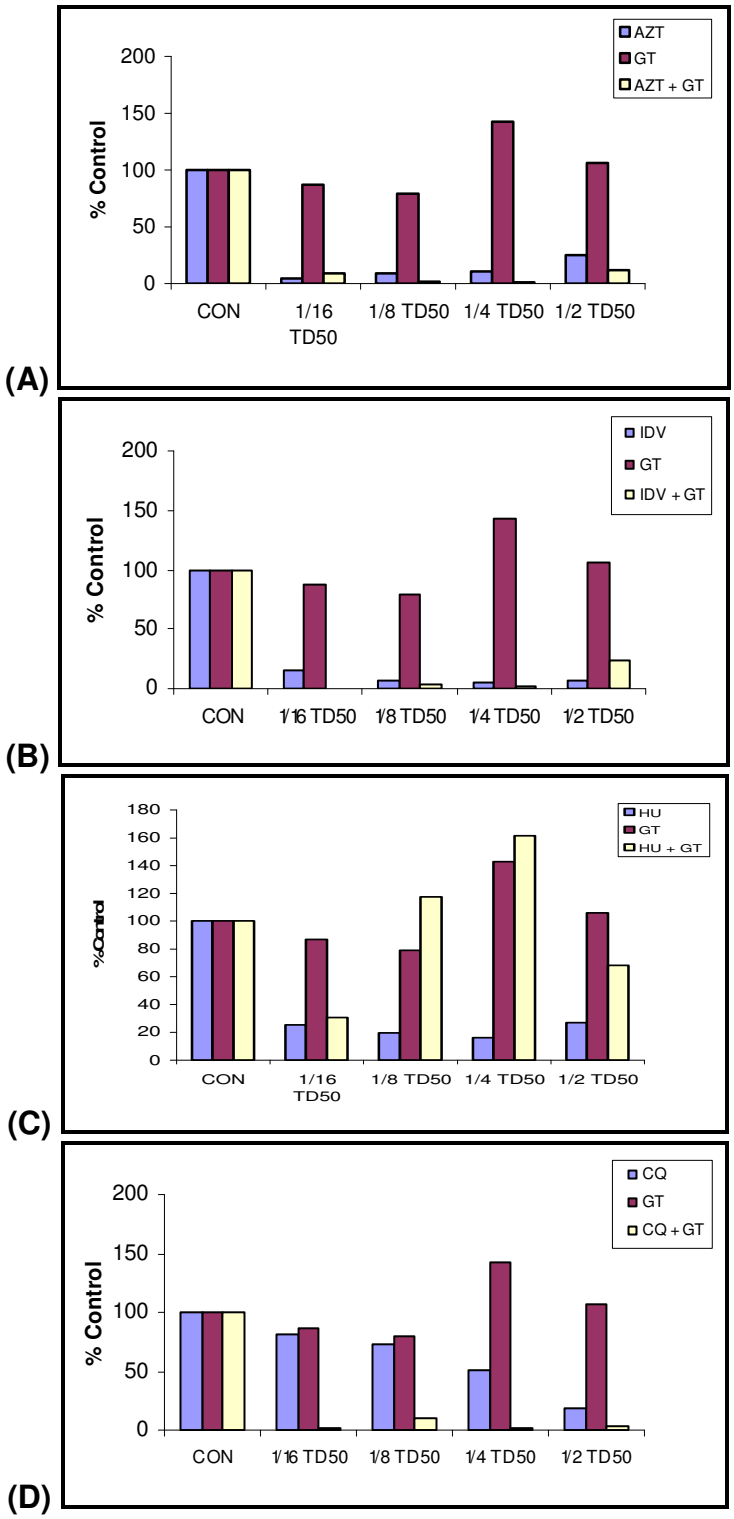

Figure 5.5. Dose-response plots showing the effect of GT on the antiretroviral activity of AZT (A), IDV (B), HU (C) and CQ (D) as determined by real-time PCR. The concentrations used for each of the drugs in the combinations with GT are shown in Table 5.1.

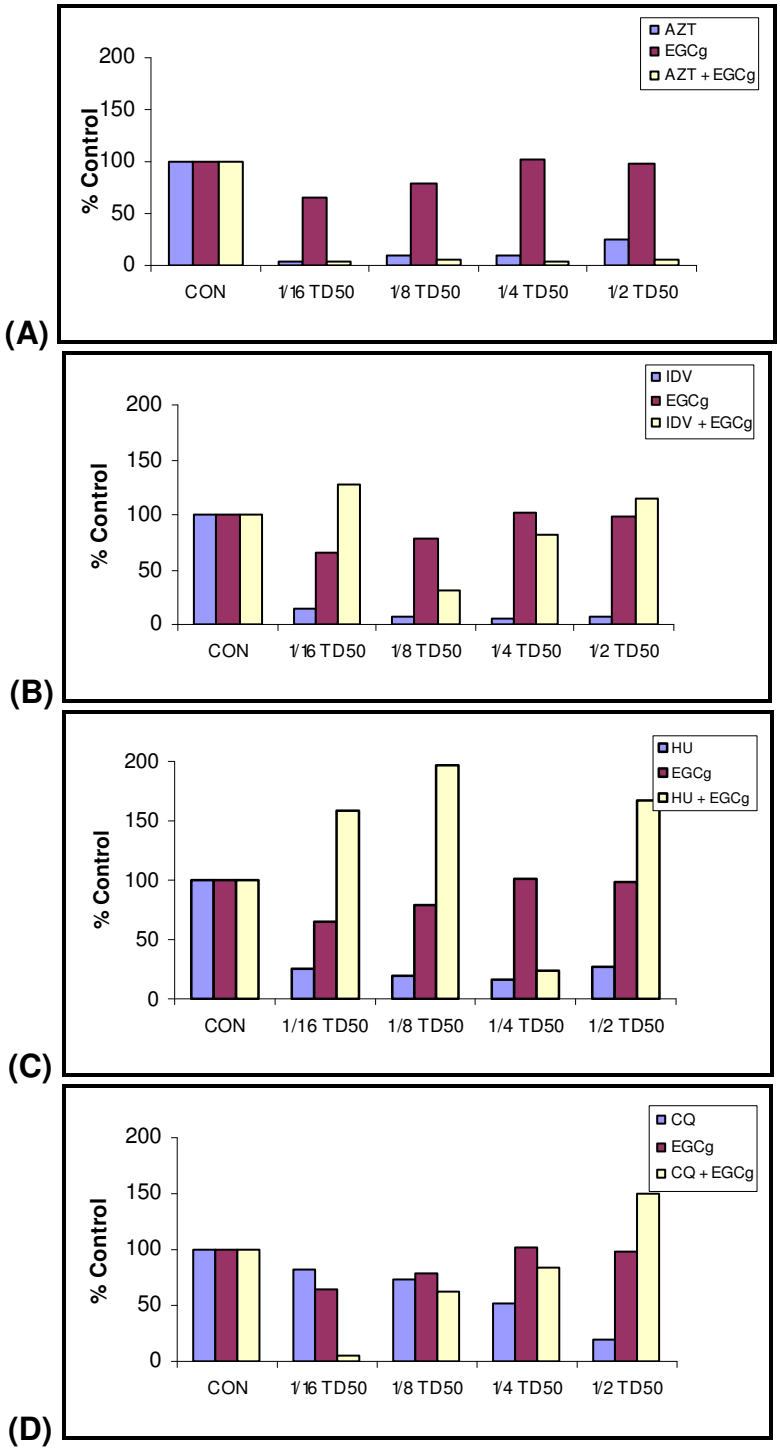

Figure 5.6. Dose-response plots showing the effect of EGCg on the antiretroviral activity of AZT (A), IDV (B), HU (C) and CQ (D) as determined by real-time PCR. The concentrations used for each of the drugs in the combinations with EGCg are shown in Table 5.1.

Table 5.6 Summary of drug combinations on cellular toxicity and viral loads in the co-culture model of SC-1 and BM5 cells.

Combinations	Cytotoxicity	Viral load	Cytotoxicity	Viral load
	AZT +GT		**AZT+EGCg**	
$1/16TD_{50}$ + $1/16TD_{50}$	Synergism	No effect	Synergism	No effect
$1/8TD_{50}$ + $1/8TD_{50}$	Slight Synergism	No effect	Strong Synergism	No effect
$1/4TD_{50}$ + $1/4TD_{50}$	Slight Antagonism	No effect	Strong Synergism	No effect
$1/2TD_{50}$ + $1/2TD_{50}$	Moderate Antagonism	Decrease	Synergism	Decrease
	IDV +GT		**IDV +EGCg**	
$1/16TD_{50}$ + $1/16TD_{50}$	Strong Antagonism	No effect	Antagonism	Increase
$1/8TD_{50}$ + $1/8TD_{50}$	Antagonism	No effect	Moderate Synergism	Increase
$1/4TD_{50}$ + $1/4TD_{50}$	Antagonism	No effect	Nearly Additive	Increase
$1/2TD_{50}$ + $1/2TD_{50}$	Moderate Antagonism	Increase	Slight Synergism	Increase
	HU +GT		**HU +EGCg**	
$1/16TD_{50}$ + $1/16TD_{50}$	Very Strong Antagonism	No effect	Very Strong Antagonism	Increase
$1/8TD_{50}$ + $1/8TD_{50}$	Very Strong Antagonism	Increase	Very Strong Antagonism	Increase
$1/4TD_{50}$ + $1/4TD_{50}$	Very Strong Antagonism	Increase	Very Strong Antagonism	No effect
$1/2TD_{50}$ + $1/2TD_{50}$	Strong Antagonism	Increase	Strong Antagonism	Increase
	CQ +GT		**CQ+ EGCg**	
$1/16TD_{50}$ + $1/16TD_{50}$	Nearly Additive	Decrease	Nearly Additive	Decrease
$1/8TD_{50}$ + $1/8TD_{50}$	Synergism	Decrease	Synergism	No effect
$1/4TD_{50}$ + $1/4TD_{50}$	Synergism	Decrease	Synergism	Increase
$1/2TD_{50}$ + $1/2TD_{50}$	Moderate Synergism	Decrease	Moderate Synergism	Increase

The combination of AZT and EGCg showed synergism on cell toxicity throughout the concentration range used as determined by the combination index values. The possible reason for this is that both compounds have been shown to exert cytotoxicity by affecting the mitochondria. AZT inhibits the mitochondria DNA polymerase γ while EGCg has been shown to interfere with the mitochondrial transmembrane potential, generate ROS and also inhibiting DNA polymerase γ and in combination a synergistic effect is observed (Barile *et al.,* 1998; Galati *et al.,* 2006; Jacob *et al.,* 2007). The combination of AZT and GT showed synergism at the low concentrations (1/16 TD_{50} + 1/16 TD_{50} and 1/8 TD_{50} + 1/8 TD_{50}) but antagonism at the higher concentrations (1/4 TD_{50} + 1/4 TD_{50} and 1/2 TD_{50} + 1/2 TD_{50}). EGCg is one of the most abundant compounds in GT so at the lower concentrations in the combination of AZT and GT, EGCg may be responsible for the synergism that is observed due to its mitochondrial effects. The amount of EGCg present increases with increasing concentrations of GT and so one expected to continue seeing synergism in cell toxicity. Antagonism, however, was seen with the higher

concentrations of GT. GT is a mixture of several compounds and perhaps at the higher concentrations of GT, one or more of the compounds other than EGCg present in GT are now at a concentration high enough to inhibit/ antagonize the cytotoxicity of AZT and EGCg.

The combination of IDV and GT, like AZT and GT, caused little to no change to the antiretroviral effect of IDV. The concentration range for IDV like that for AZT was possibly too high to determine whether GT could enhance the antiretroviral activity of IDV and like AZT, it was encouraging to observe that GT did not inhibit the antiretroviral effects of IDV. Another positive from this combination was that GT antagonizes the cytotoxicity of IDV as shown with the combination index values. For these two reasons, this combination of IDV and GT is maybe worth further investigation.

In the combination of IDV and EGCg, EGCg strongly inhibited the antiretroviral activity of IDV and had an additive to synergistic effect on cell toxicity. The additive/synergistic effect of this combination was expected as both compounds are suspected to exert their cytotoxicity by affecting the transmembrane potential of the mitochondria (Galati *et al.,* 2006; Jiang *et al.,* 2007). It was however, not expected that EGCg would inhibit the antiretroviral activity of IDV on the cell-to-cell transmission of the virus. No effect was observed with GT and this was probably due to the lower concentrations of EGCg in the more crude GT preparation. However, other compounds in GT could contribute to the effect of IDV and GT.

The combinations of HU and GT and HU and EGCg showed strong antagonism on cell toxicity indicating that GT and EGCg are having protective effects against the cytotoxicity induced by HU or vice verse. GT and EGCg, however, also strongly inhibited the antiretroviral activity of HU in these combinations. These results strongly suggested that EGCg and possibly the other compounds present in GT were interfering with the proper functioning of HU. EGCg and GT may have been interfering with the uptake of HU into the cell or increasing HU's efflux from the cell. They may also have been interfering with the binding of HU to its target ribonucleotide reductase. The possibilities are endless and the mechanism of interaction needs further investigation. These results indicate that the use of HU in combination with GT or EGCg should be avoided as the efficacy of HU could be compromised.

The possible reason for the adverse effect of EGCg on IDV and HU may be due to the direct binding of EGCg to these two drugs. EGCg has been found to have synergistic, indifferent and antagonistic effects when combined with different antibiotics (Hu *et al.,* 2002). The reason given for the antagonistic effects experienced with EGCg was that EGCg was actually binding to the peptide structure of the antibiotics teicoplanin, vancomycin and polymyxin B. IDV is known as a peptidomimetic drug meaning that it resembles a peptide and has a few peptide bonds while HU also has a peptide bond (Figure 4.1). This means that EGCg could possible be binding directly to IDV and HU through interaction of the OH groups of EGCg with the NH groups of IDV and HU. To prevent this from happening one could perhaps increase the molar ratio of IDV and HU to EGCg used in the combinations.

The only combination that showed a true positive combination for possible further investigation in an animal model was that of CQ and GT. GT was shown to strongly potentiation the antiretroviral activity of CQ. GT also showed synergy on cell toxicity with CQ when combined. Ideally for a drug combination, one wants strong enhancement of the antiretroviral activity but strong antagonism against the host (cytotoxicity). Nonetheless at the lowest concentration although an additive effect was observed on cell toxicity, almost complete inhibition of the cell-to-cell transmission of the virus was achieved. GT has recently been shown to potentiate the antimalarial effects of artemisinin *in vitro* through an unknown mechanism (Sannella *et al.,* 2007). CQ was once a popular antimalarial drug so perhaps GT is interacting with CQ in the same way as it interacted with artemisinin in the study of Sannella *et al.,* 2007.

The combination of CQ and EGCg showed opposite effects to that of CQ and GT. EGCg antagonized the cytotoxicity of CQ and inhibited the antiretroviral activity of CQ. What was interesting to see though was that at the lowest dose of EGCg (1/16 TD_{50}) used in the combination of CQ and EGCg produced the nearly the same potentiation of the antiretroviral activity of CQ as did GT in the combination of CQ and GT. But then as the concentration of EGCg increased, there was a decrease in the potentiation of EGCg on the antiretroviral activity of CQ and subsequently, the antiretroviral activity of CQ was inhibited. This indicated that low concentrations of EGCg in combination with CQ may have beneficial effects on the antiretroviral activity but that high concentrations inhibit this. Also, EGCg showed strong antagonism on the cytotoxic effects of CQ at this low concentration (1/16 TD_{50}) of EGCg. Thus it would perhaps be worth investigating a combination of CQ with low concentrations of EGCg.

5.5 Conclusion

Green tea and EGCg were investigated here for possible positive/negative interactions with the known antiretroviral drugs AZT, IDV, HU and CQ. In Chapter 4, GT and EGCg were shown to have little to no effects on the BM5-def viral load. Despite this, these compounds were still investigated in combination with the known antiretroviral drugs since GT, GT extracts and EGCg may be consumed by patients on antiretroviral medication and the interactions are unknown. The possibility of any inhibition or enhancement of GT and EGCg on the antiretroviral activity of these drugs needed to be investigated. Also, there may be a possibility that GT and EGCg can decrease the cytotoxicity of the antiretroviral drugs without interfering with the drug's antiretroviral activity.

The combination of CQ and GT was the only combination that showed an encouraging result for further investigation in the *in vivo* MAIDS model. In this combination, GT strongly potentiated the antiretroviral effects of CQ resulting in almost complete suppression of the BM5-def viral load at the lowest dose of the combination. The other combinations identified two problems one may experience when investigating a drug combination. The problems identified were finding the optimal drug concentration range and finding the optimal drug combination ratio.

The problem of the optimal drug concentration range was seen with the combinations of AZT and GT, AZT and EGCg and IDV and GT. GT and EGCg were observed to have little effect on the antiretroviral activity of AZT and IDV. Inhibition was not seen that was encouraging but neither was enhancement. This indicated that the concentrations of AZT and IDV used were perhaps too high and subsequently masked any possible enhancement by GT or EGCg. In the combination of CQ and EGCg, EGCg strongly potentiated the antiretroviral effect at the lowest concentration examined but at higher concentrations of EGCg the antiretroviral effect of CQ was inhibited. Also, in the combination of IDV and EGCg, EGCg strongly inhibited the antiretroviral activity of IDV but the concentration of EGCg present in the IDV and GT combination did not. This shows that perhaps the concentration of EGCg in the combination of IDV and EGCg was too high. All of these combinations warrant further investigation particularly the combination of CQ and EGCg as EGCg appeared to antagonize the cytotoxicity induced by CQ.

The second problem in drug combination investigation was finding the optimal drug concentration range. The combinations of HU and GT as well as HU and EGCg showed strong inhibition of the antiretroviral activity of HU. This was quite unfortunate since GT and EGCg showed antagonism on the cytotoxicity of HU. The amount of GT and EGCg in the drug combination molar ratios examined were perhaps too high (1:85.5 HU: GT and 1:15 HU: EGCg) and by changing the molar ratio, one may find that GT and EGCg are beneficial when combined with HU.

Chapter 6: Concluding discussion

The Food and Drug Administration of the United States has approved several drugs for the treatment of HIV/AIDS and includes nucleoside reverse transcriptase inhibitors (NRTIs), nonnucleoside NRTIs (NNRTIs), protease inhibitors (PIs) and fusion inhibitors. These drugs are used in combination with one another as it has been seen that monotherapy results in the rapid development of drug resistance. The introduction of combination drug therapy also known as highly active antiretroviral therapy (HAART) was associated with a notable decline in the morbidity and mortality of patients infected with HIV/AIDS. HAART, however, has also been associated with several problems like an inability to completely eradicate HIV as well as high costs of the treatments, poor availability of drugs in low-income countries, severe adverse effects and complex treatment strategies that all lead to poor adherence. To overcome these problems, the thrust of research is to (i) design new target specific drugs, (ii) to discover plants with active ingredients that have antiretroviral activity and (iii) develop new more effective treatment strategies. One such plant is green tea and its main catechin, EGCg that has been found to have anti-HIV activity. EGCg has been shown to inhibit the viral enzyme reverse transcriptase with the same low concentrations as AZT, to inhibit the viral enzyme protease and to interfere with the binding of gp120 to the cellular receptor CD4. These multiple effects of GT and EGCg on HIV replication make it a worthy candidate for further investigation and may prove beneficial (additive or synergistic) when used in combination with other known antiretrovirals.

Several animal models for the study of HIV/AIDS have been established. These models have not only provided valuable information on the disease progression of HIV/AIDS but have also been useful in determining the efficacy of antiretroviral drugs and drug combinations. One such model is the MAIDS model which is induced by the inoculation of C57BL/6 mice with a complex of retroviruses termed the LP-BM5 MuLV. The disease induced in the mice has several similarities to HIV/AIDS in humans and is characterized by lymphadenopathy, splenomegaly, susceptibility to opportunistic infections, abnormal B and T cell functions and late onset B cell aggressive lymphomas. Animal models, however, tend to be expensive, require ethical clearance and are time consuming for the initial drug screening. For these reasons, an *in vitro* cell culture system is often used for first line screening of drug. Although the AMDET of the experimental drug cannot be fully explored, an *in vitro* cell culture system allows the investigator to evaluate several drugs rapidly and cost effectively. The establishment of an *in vitro* co-culture model using BM5

cells chronically infected with the LP-BM5 MuLV complex and uninfected SC-1 cells that are permissive to murine retroviruses holds great promise as a system for initial drug evaluation. This model represents the cell-to-cell transmission of the virus as it occurs within HIV-infected persons following initial infection. The existence of the *in vivo* MAIDS model will then assist in extrapolating the *in vitro* findings.

The aim of this study was to develop an *in vitro* cell culture model that is based on the *in vivo* MAIDS model to investigate the effect of green tea and EGCg on the cytotoxicity and antiretroviral activity of the drugs AZT, IDV, HU and CQ. This will help to identify any possible beneficial (synergistic) combinations that can be further investigated in the *in vivo* MAIDS model. In order to achieve the aim of this study, the following objectives had to be achieved:

(i) Establish SC-1 and BM5 cell lines to create an *in vitro* co-culture model that can be used for rapid screening of the antiretroviral properties of drugs.

(ii) To confirm the presence and absence of the LP-BM5 virus in the SC-1 and BM5 cell lines respectively using TEM (viral particles), semi-quantitative PCR and RT-PCR (proviral DNA and RNA), animal studies (infectivity) and real-time PCR (quantification of proviral DNA levels).

(iii) To develop a co-culture model that represents cell-to-cell transmission of the LP-BM5 virus.

(iv) Validate the use of this *in vitro* co-culture model by evaluating the effects of AZT, IDV, HU and CQ on the viral load at sub-toxic concentrations

(v) Evaluate the antiretroviral properties of experimental compounds GT and EGCg in the *in vitro* MAIDS co-culture model at sub-toxic concentrations.

(vi) Evaluate the effect of GT and EGCg on the antiretroviral activity as well as the cytotoxicity of the antiretroviral drugs AZT, IDV, HU and CQ when the antiretroviral drugs are combined with either GT or EGCg.

(vii) Identify drug combinations that can be further investigated in the *in vivo* MAIDS model.

The uninfected SC-1 cell line that is permissive to murine retroviruses and the BM5 cell line that is chronically infected with the LP-BM5 MuLV complex were grown in DMEM supplemented with 10% FBS, sodium pyruvate and PSF in cell culture flasks and maintained in an incubator at 37°C, 5%CO_2. The SC-1 cells were observed to be typical fibroblasts that grew in a density-dependent orderly fashion. The BM5 cells, on the other hand, were more distended and pleimorphic in shape, grew in clusters that often gave

rise to small “cell tumours” and grew more rapidly than their uninfected counterparts, all characteristics of cells transformed with an oncogenic retrovirus.

The presence of virus within the BM5 cells was confirmed by several different techniques. TEM revealed that the viral particles had a double membrane surrounding a condensed darkly stained icosahedral-shaped central inner core typical of MuLVs. The viral particles were associated with the cell membrane and were shown to not only be taken up by the host cell but also produced by the host cell. No such viral particles as expected were seen in the SC-1 cells. Two-step RT-PCR revealed the presence of viral RNA in the BM5 cells and the absence of viral RNA within the SC-1 cells. The virus isolated from the BM5 cell line was also shown to be infectious as C57BL/10 mice infected with this virus show classical symptoms of LP-BM5 virus infection, namely lymphadenopathy and splenomegaly.

The methodologies of semi-quantitative PCR and real-time PCR were developed not only to detect the presence of virus but also to quantify the viral load. Semi-quantitative PCR methodology has been used for quantifying the effects of drugs trimidox, didox, HU, abacavir and didanosine on the LP-BM5-defective retrovirus *in vivo* while real-time PCR has been used for quantification of the LP-BM5-defective and ecotropic replication-competent retroviruses. Both methodologies revealed the presence of viral DNA within the BM5 cells and the absence of viral DNA within the SC-1 cells. The methodologies were used for quantification purposes when different co-culture models were developed to determine the minimum inoculum needed for reproducible infection. Viral DNA was used for quantification purposes as this represents the amount of viral particles that are undergoing reverse transcription and are being integrated into the host cell genome. The copy of viral DNA that is inserted into the host cell genome is responsible for the development of the viral reservoirs and chronic infection. Without integration no infection can occur.

Co-culture models were created at different ratios and allowed to grow for 72 hours. Thereafter, the DNA was isolated and the difference in viral load amongst the different co-cultures was quantified with semi-quantitative PCR and real-time PCR. Both methodologies revealed that the 1:10,000 co-culture represented the minimum inoculum needed for reproducible infection and this co-culture was then used for screening the antiretroviral drugs AZT, IDV, HU and CQ as well as experimental compounds GT and EGCg. Real-time PCR was found to be the method of choice for quantifying proviral DNA levels due to its greater speed, sensitivity and reproducibility when compared to

conventional semi-quantitative PCR. This method would be used to quantify the viral load following treatment of cells with AZT, IDV, HU, CQ, GT and EGCg.

The next step following the development of the *in vitro* co-culture model and real-time PCR methodology was to validate the use of this *in vitro* co-culture model with the antiretroviral drugs AZT, IDV, HU and CQ. The toxicity of these drugs was first determined in the SC-1 cells and quantified with the MTT assay. The MTT assay was used for quantification of the cytotoxicity as all compounds have been shown to have adverse effects directly or indirectly on the mitochondria. The SC-1 cells were used as this cell type represented the predominant cell type present in co-culture. From the MTT results the TD_{50} of each drug was determined with the median effect equation and plot of T-C Chou. The order of toxicity was GT< AZT< IDV< EGCg< HU<CQ.

Co-cultures at 1:10,000 ratio of BM5:SC-1 cells were then exposed to subtoxic concentrations ($1/8TD_{50}$, $1/4TD_{50}$, $1/2TD_{50}$) of each drug for 72 hours. The DNA was isolated and amplified with real-time PCR. Relative quantification was used to quantify the viral load. AZT, IDV and HU were observed to significantly reduce the viral load at the lowest concentration used (($1/8TD_{50}$). Thereafter, stabilization in the amount of inhibition was observed. The most likely explanation for this was that the remaining percentage of viral DNA reflected the integrated viral genome that could not be eradicated. Because of the effectiveness of AZT, IDV and HU to reduce the viral loads, it will be necessary to repeat these experiments with drug concentrations below the $1/8TD_{50}$ of each drug so that an ED_{50} and SI for each drug can be calculated. CQ showed a more dose-response effect on the viral load and because of this the data could be used in the median effect equation and plot of T-C Chou to calculate an ED_{50}. The ED_{50} for CQ was 0.003mg/ml (5.95µM) ± 0.001mg/ml (2.95µM) and the drug's selectivity index was 4.3. AZT and IDV were found to be more potent that HU and CQ in reducing the viral load possibly because AZT and IDV specifically targets processes that occur during viral replication while HU and CQ affect host cellular factors that are necessary for viral replication.

All the antiretroviral drugs, AZT, IDV, HU and CQ, effectively reduced the presence of proviral DNA namely reduced infectivity in co-cultures infected with the LP-BM5 MuLV complex. These results validated this *in vitro* co-culture model as a model that could be used to screen compounds for their antiretroviral properties. The next step in this study was thus to evaluate the experimental compounds GT and EGCg for antiretroviral properties using this model. The cytotoxicity of EGCg and GT were evaluated in the

same way as the antiretroviral drugs. Both compounds were found to also be toxic to the mitochondria. EGCg was observed to be more cytotoxic than GT possibly because a lower concentration of EGCg is present within the GT. A TD_{50} for both compounds was also calculated with the median effect equation and plot of T-C Chou. The *in vitro* co-culture model was then exposed to subtoxic concentrations of EGCg and GT for 72 hours. The effect of each compound on the viral load was quantified with real-time PCR. Both compounds were found to have little effect on the viral load.

Three possible explanations were given for the observed lack of antiretroviral activity observed with GT and EGCg. The first possible explanation was that because EGCg is known to undergo auto-oxidation in DMEM medium, very little EGCg is actually entering the cell and thus maybe EGCg and GT's antiviral effects should be investigated in a different type of medium. The second possibility was that EGCg and possibly the other catechins in GT have no ability to inhibit the reverse transcriptase and protease enzyme of these MuLV unlike with HIV. The last possible explanation given was due to the effects of EGCg on the proteasome and the importance of the proteasome to virus replication. An active proteasome has been found to be necessary for the assembly, release and maturation of HIV particles and that treatment with proteasome inhibitors inhibits these steps in the virus' replication cycle. The use of proteasome inhibitors has also resulted in an increased infection rate of cells with HIV and a subsequent increase in proviral DNA. EGCg has been shown to inhibit the chymotrypsin-like activity of proteasome. This meant that EGCg could therefore be having contradictory effects on viral replication. It promoted the uptake of the virus into the cell and possibly prevented viral proteins from being degraded by the proteasome but then prevented new virions from being formed and released. Thus the effects of EGCg may be canceling each other out and that the viral infection is being allowed to proceed as if no drug was added.

Although EGCg and GT showed little effect on the viral load of the *in vitro* co-culture model, it was decided that it would still be worthwhile to investigate these compounds in combination with the antiretroviral drugs as these two experimental compounds could improve the uptake of the drug into the cell, inhibit a cellular metabolite that competes with the drug, decrease the efflux of the drug from the cell or enhance the metabolic activation of the drug into its active form and so forth. Another important reason was that EGCg and GT could inhibit the cytotoxicity of the known antiretroviral drugs without having a negative effect on the antiretroviral activity of the drug.

The SC-1 cell line and the MTT assay were once again used to evaluate the cytotoxicity of the different combinations of EGCg and GT with the antiretroviral drugs AZT, IDV, HU and CQ. CI equation and plot of Chou-Talalay were used to determine whether the combinations were having a synergistic, additive or antagonistic effect on cell toxicity. The combinations of AZT and EGCg, IDV and EGCg and CQ and GT showed synergism on cell toxicity possibly due to the fact that these compounds have been shown to exert cytotoxicity by affecting the mitochondria. AZT has multiple adverse effects on the mitochondria including inhibition of DNA polymerase γ while EGCg has been shown to interfere with the mitochondrial transmembrane potential, generate ROS and also inhibit DNA polymerase γ. IDV, like EGCg, has been shown to also affect the transmembrane potential of the mitochondria. Combinations of IDV and GT, HU and GT, HU and EGCg and CQ and EGCg, however, showed antagonism on cell toxicity. GT and EGCg may be inhibiting the influx of the drugs into the cell or enhancing the efflux of these drugs out of the cell. The mechanisms need to be investigated as they may have important consequences *in vivo.* The combination of AZT and GT showed a mixture of synergism and antagonism. The combination showed synergism at low concentrations but antagonism at higher concentrations. It was suggested that one or more compounds present within GT at the higher concentrations may be protecting the cells from the adverse effects of AZT and EGCg on the mitochondria.

The *in vitro* co-culture model was then exposed to the different combinations for 3 days. The DNA was isolated, amplified with real-time PCR and the viral load was quantified by the relative quantification software. It was found that in the combinations of AZT and GT, AZT and EGCg and IDV and GT that GT and EGCg had little to no effect on the antiretroviral activity of AZT and IDV. The possible explanations were that neither GT nor EGCg interfered with the antiretroviral activity of AZT and IDV or that the concentration range of AZT and IDV used was too high and thus masked any possible potentiation of antiretroviral activity by GT or EGCg.

The combinations of IDV and EGCg, HU and GT, HU and EGCg and CQ and EGCg showed that GT and EGCg strongly inhibited the antiretroviral activity of these drugs. For IDV and EGCg, this was quite surprising as the combination showed synergism on cell cytotoxicity. A reaction may be occurring within the cell that prevents IDV from reaching its target the viral enzyme protease. The combinations of HU and GT and HU and EGCg showed strong antagonism in cytotoxicity as well as antiretroviral activity. This is important and should be further investigated as these effects would reduce drug efficiency and could lead to drug resistance.

For the combination of CQ and EGCg, it was interesting to see that at the lowest dose of EGCg (1/16 TD_{50}) used in the combination of CQ and EGCg produced strong enhancement of the antiretroviral activity of CQ but then as the concentration of EGCg increased, there was a decrease in the potentiation of EGCg on the antiretroviral activity of CQ and subsequently, the antiretroviral activity of CQ was inhibited. This possibly indicated that low concentrations of EGCg in combination with CQ may have beneficial effects on the antiretroviral activity but that high concentrations inhibit this.

The only combination that was shown to warrant further investigation in the *in vivo* MAIDS model was that of CQ and GT. GT was shown to strongly enhance the antiretroviral activity of CQ through an unknown mechanism. Although the combination showed synergism an adverse effect on host cell toxicity, the combination was still found worthy of further investigation since at the lowest dose of the combination given to the co-culture almost complete suppression of the viral load was experienced.

Hypothesis I: The *in vitro* co-culture model of SC-1 and BM5 cells can be used for screening the antiretroviral properties of drugs was supported by the observation that the known antiretroviral drugs AZT, IDV, HU and CQ that are currently being used for the treatment of HIV/AIDS significantly reduced the LP-BM5-defective viral load at sub-toxic concentrations.

Hypothesis II: GT and EGCg will show significant antiretroviral activity in the *in vitro* co-culture model had to be rejected since no significant inhibition on the cell-to-cell transmission of the virus was observed. The Null Hypothesis that EGCg and GT will have no antiretroviral activity against the LP-BM5 MuLV had to be accepted.

Hypothesis III: GT or EGCg will strongly enhance the antiretroviral activity of at least one antiretroviral drug AZT, IDV, HU or CQ was supported by the observation that GT significantly enhanced the inhibitory effects of CQ on the viral load when the two were used in a combination. This combination was shown to warrant further investigation within the *in vivo* MAIDS model.

The *in vitro* co-culture model of the SC-1 and BM5 cells was shown to be a model that could be used for screening the antiretroviral activity of drugs and plant extracts as well as drug combinations rapidly, cost-effectively and effortlessly. This model, however, also showed one of the greatest limitations of using an animal model based on HIV/AIDS

in that not all compounds that do or do not have an effect on the virus produce the same result on the human immunodeficiency virus. This was observed with GT and EGCg which have been previously shown to exhibit anti-HIV activity. Nevertheless these types of *in vitro* and *in vivo* models will always continue to be used and provide valuable information since the use of a model with HIV is still far too hazardous.

Future perspectives:

(i) Re-investigate the effects of AZT, IDV and HU on the cell-to-cell transmission of the LP-BM5-defective virus at concentrations below 1/8 TD_{50} in order to determine a selectivity index for these drugs within this *in vitro* co-culture model.

(ii) Re-investigate the combinations of AZT and GT, AZT and EGCg and IDV and GT at the new concentration range of AZT and IDV. Are there still no effects of GT and EGCg on the antiretroviral activity of AZT and IDV?

(iii) Re-investigate combinations of HU and GT and HU and EGCg at different combination ratios to determine whether strong inhibition still exists and if it does determine the mechanism of interaction as this can have serious implications *in vivo*.

(iv) Re-investigate the combination of CQ and EGCg at lower concentrations (lower than 1/16 TD_{50}) of EGCg as in this study, the lowest concentration of EGCg given showed strong enhancement of the antiretroviral activity of CQ but higher concentrations showed inhibition.

(v) Evaluate the combination of CQ and GT in the *in vivo* MAIDS model.

(vi) Confirm that known drug combinations (HAART) can be reproduced in this *in vitro* co-culture model.

Chapter 7: References

Ackley C.D., Yamamoto J.K., Levy N., Pedersen N.C. and Cooper M.D. (1990) Immunologic abnormalities in pathogen-free cats experimentally infected with feline immunodeficiency virus. *Journal of Virology* **64** (11): 5652-5655.

Alder J., Hui Y.H. and Clement J. (1995) Efficacy of AZT therapy in reducing p24 antigen burden in a modified SCID mouse model of HIV infection. *Antiviral Research* **27**: 85-97.

Anonymous. (2007) Drugs used in the treatment of HIV infection. *US Food and Drug Administration*, viewed 13 November 2007, <http://www.fda.gov/oashi/aids/virals.htlm.

Ansari A.A. (2004) Autoimmunity, anergy, lentiviral immunity and disease. *Autoimmunity Reviews* **3**: 530-540.

Arai M., Earl D.D. and Yamamoto J.K. (2002) Is AZT/3TC therapy effective against FIV infection or immunopathogenesis? *Veterinary Immunology and Immunopathology* **85**: 189-204.

Arts E.J., Quiñones-Mateu M.E. and Albright J.L. (1998) Mechanisms of clinical resistance by HIV-1 variants to zidovudine and the paradox of reverse transcriptase sensitivity. *Drug Resistance Updates* **1**: 21-28.

Asante-Appiah E. and Skalka A.M. (1997) Molecular mechanisms in retrovirus DNA integration. *Antiviral Research* **36**: 139-156.

Atzori C., Angeli E., Mainini A., Agostoni F., Micheli V. and Cargnel A. (2000) *In vitro* activity of human immunodeficiency virus protease inhibitors against *Pneumocystis carinii*. *Journal of Infectious Diseases* **181** (5): 1629-1634.

Badley A.D. (2005) *In vitro* and *in vivo* effects of HIV protease inhibitors on apoptosis. *Cell Death and Differentiation* **12**: 924-931.

Barile M., Valenti D., Quagliariello E. and Passarella S. (1998) Mitochondria as cell targets of AZT (Zidovudine). *General Pharmacology* **31** (4): 531-538.

Basham T., Rios C.D., Holdener T. and Merigan T.C. (1990) Zidovudine (AZT) reduces virus titer, retards immune dysfunction, and prolongs survival in the LP-BM5 murine induced immunodeficiency model. *Journal of Infectious Diseases* **161**: 1006-1009.

Beebe A.M., Dua N., Faith T.G., Moore P.F., Pedersen N.C. and Dandekar S. (1994) Primary stage of feline immunodeficiency virus infection: viral dissemination and cellular targets. *Journal of Virology* **68** (5): 3080-3091.

Benlhassen-Chahour K., Penit C., Dioszeghy V., Vasseur F., Janvier G., Rivière Y., Dereuddre-Bosquet N., Dormont D., Le Grand R. and Vaslin B. (2003) Kinetics of lymphocyte proliferation during primary immune response in macaques infected with pathogenic simian immunodeficiency virus SIVmac251: preliminary report of the effect of early antiviral therapy. *Journal of Virology* **77** (23): 12479-12493.

Benveniste O., Vaslin B., Le Grand R., Fouchet P., Omessa V., Theodoro F., Fretier P., Clayette P., Boussin F. and Dormont D. (1996) Interleukin 1β, interleukin 6, tumor necrosis factor α, and interleukin 10 responses in peripheral blood mononuclear cells of cynomolgus macaques during acute infection with SIVmac251. *AIDS Research and Human Retroviruses* **12** (3): 241-250.

Bisset L.R., Lutz H., Böni J., Homann-Lehmann R., Lüthy R and Schüpbach J. (2002) Combined effect of zidovudine (ZDV), lamivudine (3TC) and abacavir (ABC) antiretroviral therapy in suppressing *in vitro* FIV replication. *Antiviral Research* **53**: 35-45.

Blasi E., Colombari B., Orsi C.F., Pinti M., Troiano L., Cossarizza A., Esposito R., Peppoloni S., Mussini C. and Neglia R. (2004) The human immunodeficiency virus (HIV) protease inhibitor indinavir directly affects the opportunistic fungal pathogen *Cryptococcus neoformans*. *FEMS Immunology and Medical Microbiology* **42** (2): 187-95.

Bosma G.C., Custer R.P. and Bosma M.J. (1983) A severe combined immunodeficiency mutation in the mouse. *Nature* **301** (5900): 527-530.

Boya P., Gonzalez-Polo R.A., Poncet D., Andreau K., Vieira H.L., Roumier T., Perfettini J.L. and Kroemer G. (2003) Mitochondrial membrane permeabilization is a critical step of lysosome-initiated apoptosis induced by hydroxychloroquine. *Oncogene* **22** (25): 3927-3936.

Boyle M.J., Connors M., Flanigan M.E., Geiger S.P., Ford H.Jr., Baseler M., Adelsberger J., Davey R.T.Jr. and Lane H.C. (1995) The human HIV/peripheral blood lymphocyte (PBL)-SCID mouse. *The Journal of Immunology* **154**: 6612-6623.

Bradley W.G., Kraus L.A., Good R.A. and Day N.K. (1995) Dehydroepiandrosterone inhibits replication of feline immunodeficiency virus in chronically infected cells. *Veterinary Immunology and Immunopathology* **46**: 159-168.

Bridges C.G., Taylor D.L., Ahmed P.S., Brennan T.M., Hornsperger J.-M., Navé J.-F., Casara P. and Tyms A.S. (1996) MDL 74,968, a new acyclonucleotide analog: activity against human immunodeficiency virus *in vitro* and in hu-PBL-SCID.Beige mouse model of infection. *Antimicrobial Agents and Chemotherapy* **40** (5): 1072-1077.

Brigati C., Giacca M., Noonan D.M. and Albini A. (2003) HIV Tat, its TARgets and the control of viral gene expression. *FEMS Microbiology Letters* **220**: 57-65.

Callanan J.J. and Jarrett O. (1993) Pathogenesis of feline immunodeficiency virus infection. In: Racz P., Letvin N.L. and Gluckman J.C. (editors). *Animal models of HIV and other retroviral infections*. Basel, Karger: 108-114.

Campbell M.K. (1999) *Biochemistry 3rd edition*. Orlando, Harcourt Brace and Company: 669-670.

Cann A. (1997) *Principles of molecular virology 2nd edition*. San Diego, Academic Press, Inc.: 6-20.

Carpenter M.A., Brown E.W., MacDonald D.W. and O'Brien S.J. (1998) Phyloenic patterns of feline immunodeficiency virus genetic diversity in the domestic cat. *Virology* **251**: 234-243.

Carpenter S., Miller L.D., Alexandersen S., Whetstone C.A., Van Der Maaten M.J., Viuff B., Wannemuehler Y., Miller J.M. and Roth J.A. (1992) Characterization of early effects after experimental infection of calves with bovine immunodeficiency-like virus. *Journal of Virology* **66** (2): 1074-1083.

Casabianca A., Vallanti G. and Magnani M. (1998) Competitive PCR for quantification of BM5d proviral DNA in mice with AIDS. *Journal of Clinical Microbiology* **36** (8): 2371-2374.

Casabianca A., Orlandi C., Fraternale A. and Magnani M. (2004) Development of a real-time PCR assay using SYBR Green I for provirus load quantification in a murine model of AIDS. *Journal of Clinical Microbiology* **42** (9): 4361-4364.

Chai P.C., Long L.H. and Halliwell B. (2003) Contribution of hydrogen peroxide to the cytotoxicity of green tea and wines. *Biochemical and Biophysical Research Communications* **304**: 650-654.

Chang C.W., Hsu F.L. and Lin J.Y.(1994) Inhibitory effects of polyphenolic catechins from Chinese green tea on HIV reverse transcriptase activity. *Journal of Biomedical Science* **1** (3): 163-166.

Chang L.-K., Wei T.-T., Chiu Y.-F., Tung C.-P., Chuang J.-Y., Hung S.-K., Li C. and Liu S.-T. (2003) Inhibition of Epstein-Barr virus lytic cycle by (-)-epigallocatechin gallate. *Biochemical and Biophysical Research Communications* **301** (4): 1062-1068.

Chattopadhyay S.K., Sengupta D.N., Fredrickson T.N., Morse III H.C. and Hartley J.W. (1991) Characteristics and contributions of defective, ecotropic, and mink cell focus-inducing viruses involved in a retrovirus-induced immunodeficiency syndrome of mice. *Journal of Virology* **65** (8): 4232-4241.

Chen L.F., Hay J. and Lewin S.R. (2007) Ten years of highly active antiretroviral therapy for HIV infection. *Medical Journal of Australia* **186**: 146-151.

Chen Z., Li Y., Chen E., Hall D.L., Darke P.L., Culberson C., Shafer J.A. and Kuo L.C. (1994) Crystal structure at 1.9-Å resolution of human immunodeficiency virus (HIV) II protease complexed with L-735,524, an orally bioavailable inhibitor of the HIV proteases. *The Journal of Biological Chemistry* **269** (42): 26344-26348.

Chou T-C. (1991) The median-effect principle and the combination index for quantification of synergism and antagonism. In: Chou T-C. and Rideout D.C. (editors). *Synergism and Antagonism in Chemotherapy*. San Diego, Academic Press, Inc.: 61-101.

Clements J.E., Babas T., Mankowski J.L., Suryanarayana K., Piatak M.Jr., Tarwater P.M., Lifson J.D. and Zink M.C. (2002) The central nervous system as a reservoir for simian immunodeficiency virus (SIV): steady-state levels of SIV DNA in brain from acute through asymptomatic infection. *The Journal of Infectious Diseases* **186**: 905-913.

Coggins L. (1986). Equine retrovirus infection. In: Salzman LA (editor). *Animal models of retrovirus infection and their relationship to AIDS*. Florida, Academic Press, Inc.: 203-211.

Cook W.J., Green K.A., Obar J.J. and Green W.R. (2003) Quantitative analysis of LP-BM5 murine leukemia retrovirus RNA using real-time RT-PCR. *Journal of Virological Methods* **108**: 49-58.

Correll P.K., Law M.G., MacDonald A.M., Cooper D.A. and Kaldar J.M. (1998) HIV disease progression in Australia in the time of combination antiretroviral therapies. *Medical Journal of Australia* **169** (9): 469-472.

Datema R., Rabin L., Hincenbergs M., Moreno M.B., Warren S., Linquist V., Rosenwirth B., Seifert J. and McCune J.M. (1996) Antiviral efficacy *in vivo* of the anti-human immunodeficiency virus bicyclam SDZ SID 791 (JM 3100), an inhibitor of infectious cell entry. *Antimicrobial Agents and Chemotherapy* **40** (3): 750-754.

Davis P.H. and Stanley S.L.Jr. Breaking the species barrier: use of SCID mouse-human chimeras for the study of human infectious diseases. *Cellular Microbiology* **5** (12): 849-860.

Dean G.A., Reubel G.H., Moore P.F. and Pedersen N.C. (1996) Proviral burden and infection kinetics of feline immunodeficiency virus in lymphocyte subsets of blood and lymph node. *Journal of Virology* **70** (8): 5165-5169.

Deepalakshmi P.D., Parasakthy K., Shanthi S. and Devaraj N.S. (1994). Effect of chloroquine on rat liver mitochondria. *Indian Journal of Experimental Biology* **32** (11): 797-799.

De Rozières S., Swan C.H., Sheeter D.A., Clingerman K.J., Lin Y.-C., Huitron-Resendiz S., Hendriksen S., Torbett B.E. and Elder J.H. (2004) Assessment of FIV-C infection of cats as a function of treatment with the protease inhibitor, TL-3. *Retrovirology* **1**: 38.

Desrosiers R.C. and Ringler D.J. (1989) Use of simian immunodeficiency viruses for AIDS research. *Intervirology* **30**: 301-312.

Detels R., Muñoz A., McFarlane G., Kingsley L.A., Margolick J.B., Giorgi J., Schrager L.K. and Phair J.P. (1998) Effectiveness of potent antiretroviral therapy on time to AIDS and death in men with known HIV infection duration. Multicenter AIDS Cohort Study Investigators. *Journal of the American Medical Association* **280** (17): 1497-1503.

Dietrich D.T. (2006) Disease management-constructing optimal NRTI-based combinations: past, present, future. *Medscape General Medicine* **8** (1): 16.

Di Fabio S., Trabattoni D., Geraci A., Rizzante S., Panzini G., Fusi M.L., Chiarotti F., Corrias F., Belli R., Verani P., Dalgleish A., Clerici M. and Titti F. (2000) Study of immunological and virological parameters during thalidomide treatment of SIV-infected cynomolgus monkeys. *Journal of Medical Primatology* **29**: 1-10.

Dimmock N.J. and Primrose S.B. (1987) *Introduction to Modern Virology 3rd edition*. Oxford, Blackwell Scientific Publications: 206-212.

Dueck M. and Guatelli J. (2007) Evidence against a direct antiviral activity of the proteasome during early steps of hIV-1 replication. *Virology* **636**: 1-8.

Dufresne C.J. and Fanworth E.R. (2001) A review of latest research findings on the health promotion properties of tea. *Journal of Nutritional Biochemistry* **12**: 404-421.

Dulbecco R. and Ginsberg H.S. (1990) *Virology*. Cambridge, Harper and Row, Publishers: 942-1045.

Dunn B.M., Goodenow M.M., Gustchina A. and Wlodawer A. (2002) Retroviral proteases. *Genome Biology* **3** (4): reviews3006.1-3006.7.

Eiseman J.L., Yetter R.A., Fredrickson T.N., Shapiro S.G. MacAuley C. and Bilello J.A. (1991) Effect of 3' azidothymidine administered in drinking water or by continuous infusion on the development of MAIDS. *Antiviral Research* **16**: 307-326.

English R.V., Johnson C.M., Gebhard D.H. and Tompkins M.B. (1993) *In vivo* lymphocyte tropism of feline immunodeficiency virus. *Journal of Virology* **67** (9): 5175-5186.

Eriksson B., Vrang L., Bazin H., Chattopadhyaya J. and Oberg B. (1987) Different patterns of inhibition of avian myeloblastosis virus reverse transcriptase activity by 3'-azido-3'dexythymidine 5'-triphosphate an its threo isomer. *Antimicrobial Agents and Chemotherapy* **31** (4): 600-604.

Essey R.J., McDougall B.R. and Robinson W.E.Jr. (2001) Mismatched double-stranded RNA (polyI-polyC_{12}U) is synergistic with multiple anti-HIV drugs and is active against drug-sensitive and drug-resistant HIV-1 *in vitro*. *Antiviral Research* **51**: 189-202.

Fan H., Brightman B.K., Davis B.R. and Li Q.-X. (1991) Leukemogenesis by Moloney murine leukemia virus. In: Fan H.Y., Chen I.S.Y., Rosenberg N. and Sugden W. (editors). *Viruses That Affect the Immune System*. Washington, American Society for Microbiology: 155-174.

Fesen M.R., Kohn K.W., Leteurtre F. and Pommier Y. (1993) Inhibitors of human immunodeficiency virus integrase. *Proceedings of the National Academy of Sciences of the United States of America* **90**: 2399-2403.

Flynn J.N., Dunham S., Mueller A., Cannon C. and Jarrett O. (2002) Involvement of cytolytic and non-cytolytic T cells in the control of feline immunodeficiency virus infection. *Veterinary Immunology and Immunopathology* **85** (3-4): 159-170.

Fraenkel-Conrat H. and Kimball P.C. (1982) *Virology*. New Jersey, Prentice-Hall, Inc.: 315-341.

Fraternale A., Casabianca A., Rossi L., Chiarantini L., Laura B., Giorgio A., Gianfranca S., Giuditta F. and Magnani M. (1996) Inhibition of murine AIDS by combination of AZT and dideoxycytidine 5'-triphosphate. *Journal of Acquired Immune Deficiency Syndrome* **12** (2): 1654-173.

Fraternale A., Casabianca A., Tonelli A., Vallanti G., Chiarantini L., Brandi G., Celeste A.G. and Magnani M. (2000) Inhibition of murine AIDS by alternate administration of azidothymidine and fludarabine monophosphate. *Journal of Acquired Immune Deficiency Syndromes* **23**: 209-230.

Fraternale A., Casabianca A., Orlandi C., Cerasi A., Chiarantini L., Brandi G. and Magnani M. (2002) Macrophage protection by addition of glutathione (GSH)-loaded erythrocytes to AZT and DDI in a murine AIDS model. *Antiviral Research* **56**: 263-272.

Fraternale A., Casabianca A., Orlandi C., Chiarantini L., Brandi G., Silvestri G. and Magnani M. (2002) Repeated cycles of alternate administration of fludarabine and zidovudine plus didanosine inhibits murine AIDS and reduces proviral DNA content in lymph nodes to undetectable levels. *Virology* **302**: 354-362.

Frenkel L.M. and Tobin N.H. (2004) Understanding HIV-1 drug resistance. *The Drug Monitor* **26**: 116-121.

Fultz P.N., McClure H.M., Swenson R.B. and Anderson D.C. (1989) HIV infection of chimpanzees as a model for testing chemotherapeutics. *Intervirology* **30** (Suppl 1): 51-58.

Furman P.A., Fyfe J.A., St. Clair M.H., Weinhold K., Rideout J.L., Freeman G.A., Lehrman S.N., Bolognesi D.P., Broder S., Mitsuya H. and Barry D.W. (1986) Phosphorylation of 3'-azido-3'deoxythymidine and selective interaction of the 5'-triphosphate with human immunodeficiency virus reverse transcriptase. *Proceedings of the National Academy of Sciences of the United States of America* **83**: 8333-8337.

Galati G., Lin A., Sultan A.M. and O'Brien P.J. (2006) Cellular and *in vivo* hepatotoxicity caused by green tea phenolic acids and catechins. *Free Radical Biology and Medicine* **40**: 570-580.

Gallicchio V.S. and Hughes N.K. (1994) Influence of interleukin-3 (IL-3) on the hematopoietic toxicity associated with combination anti-viral drugs (zidovudine and DDI) *in vitro* using retrovirus-infected bone marrow cells. *International Journal of Immunopharmacology* **16** (4): 359-366.

Gallicchio V.S., Hughes N.K., Tse K.-F., Ling J. and Birch N.J. (1995) Effect of lithium in immunodeficiency: improved blood cell formation in mice with decreased hematopoiesis as result of LP-BM5 MuLV infection. *Antiviral Research* **26**: 189-202.

Gazzinelli R.T., Hartley J.W., Fredrickson T.N., Chattopadhyay S.K. Sher A. and Morse III H.C. (1992) Opportunistic infections and retrovirus-induced immunodeficiency: studies of acute and chronic infections with *Toxoplasma gondii* in mice infected with LP-BM5 murine leukemia viruses. *Infection and Immunity* **60** (10): 4394-4401.

Gazzinelli R.T., Makino M., Chattopadhyay S.K., Snapper C.M., Sher A., Hügin A.W. and Morse III H.C. (1992) $CD4^+$ subset regulation in viral infection. *Journal of Immunology* **148** (1): 182-188.

George M.D., Reay E., Sankaran S. and Dandekar S. (2005) Early antiretroviral therapy for simian immunodeficiency virus infection leads to mucosal $CD4^+$ T-cell restoration and enhanced gene expression regulating mucosal repair and regeneration. *Journal of Virology* **79** (5): 2709-2719.

Giavedoni L.D., Velasquillo M.C., Parodi L.M., Hubbard G.B. and Hodara V.L. (2000) Cytokine expression, natural killer cell activation, and phenotypic changes in lymphoid cells from rhesus macaques during acute infection with pathogenic simian immunodeficiency virus. *Journal of Virology* **74** (4): 1648-1657.

Gibbons C., Kollmann T.R., Pettoello-Mantovani M., Kim A. and Goldstein H. (1997) Thy/Liv-SCID-Hu mice implanted with human intestine: an *in vivo* model for investigation of mucosal transmission of HIV. *AIDS Research and Human Retroviruses* **13** (17):1453-1460.

Gigout L., Vaslin B., Matheux F., Caufour P., Neildez O., Chèret A., Lebel-Binay S., Théodoro F., Dilda P., Benveniste O., Clayette P., Le Grand R. and Dormont D. (1998) Consequences of ddI-induced reduction of acute SIVmac251 virus load on cytokine profiles in cynomolgus macaques. *Research in Virology* **149**: 341-354.

Gillies R.J., Didier N. and Denton M. (1986) Determination of cell number in monolayer cultures. *Analytical Biochemistry* **159** (1): 109-113.

Giuffre A.C., Higgins J., Buckheit Jr. R.W. and North T.W. (2003) Susceptibilities of simian immunodeficiency virus to protease inhibitors. *Antimicrobial Agents and Chemotherapy* **47** (5): 1756-1759.

Goldstein H., Pettoello-Mantovani M., Katopodis N.F., Kim A., Yurasov S. and Kollmann T.R. (1996) SCID-hu mice: a model for studying disseminated HIV infection. *Seminars in Immunology* **8**: 223-231.

Goto T., Nakai M. and Ikuta K. (1998) The life-cycle of human immunodeficiency virus type 1. *Micron* **29** (2/3): 123-138.

Graham H.N. (1992) Green tea composition, consumption, and polyphenol chemistry. *Preventative Medicine* **21**: 334-350.

Grandadam M., Cesbron J.-Y., Candotti D., Vinatier D., Pauchard M., Capron A., Debré P., Huraux J.-M., Autran B. and Agut H. (1995) Dose-dependent systemic human immunodeficiency virus infection of SCID-hu mice after intraperitoneal virus infection. *Research in Virology* **146**: 101-112.

Green L.C., Didier P.J., Bowers L.C. and Didier E.S. (2004) Natural and experimental infection of immunocompromised rhesus macaques (*Macaca Mulatta)* with the microsporidian *Enterocytozoon bieneusi* genotype D. *Microbes and Infection* **6**: 996-1002.

Gwilt P.R. and Tracewell W.G. (1998) Pharmacokinetics and pharmacodynamics of hydroxyurea. *Clinical Pharmacokinetics* **34** (5): 347-358.

Hamada M., Yamamoto S., Kishino Y. and Moriguchi S. (2000) Vitamin E suppresses the development of murine AIDS through the inhibition of nuclear factor-kappa B expression. *Nutrition Research* **20** (8): 1163-1171.

Hart R.A., Billaud J.-N., Choi S.J. and Philips T.R. (2002) Effects of 1,8-diaminooctane on FIV Rev regulatory system. *Virology* **304**: 97-104.

Hartley J.W. and Rowe W.P. (1975) Clonal cell lines from a feral mouse embryo which lack host-range restrictions or murine leukemia viruses. *Virology* **65**: 128-134.

Hartley J.W. Fredrickson T.N. Yetter R.A., Makino M. and Morse III H.C. (1989) Retrovirus-induced murine acquired immunodeficiency syndrome: natural history of infection and differing susceptibility of inbred mouse strains. *Journal of Virology* **63** (3): 1223-1231.

Hartmann K., Donath A., Beer B., Egberink H.F., Horzinek M.C., Hoffmann-Fezer G., Thum I. and Thefeld S. (1992) Use of two virustatica (AZT, PMEA) in the treatment of FIV and FeLV seropositive cats with clinical symptoms. *Veterinary Immunology and Immunopathology* **35** (1-2): 167-175.

Hartmann K., Ferk G., North T.W. and Pedersen N.C. (1997) Toxicity associated with high dosage 9-[(2R,5R-2,5-dihydro-5-phosphonomethoxy)-2-furanyl]adenine therapy and attempts to abort early FIV infection. *Antiviral Research* **36**: 11-25.

Hasegawa T., Kimura Y., Hiromatsu K., Kobayashi N., Yamada A., Makino M., Okuda M., Sano T., Nomoto K. and Yoshikai Y. (1997) Effect of hot water extract of *Chlorella vulgaris* on cytokine expression patterns in mice with murine acquired immunodeficiency syndrome after infection with *Listeria monocytogenes. Immunopharmacology* **35**: 273-282.

Hendrikson E.A., Qin X., Bump E.A., Schatz D.G., Oettinger M. and Weaver D.T. (1991) A link between double-strand break related repair and V(D)J recombination: the scid mutation. *Proceedings of the National Academy of Sciences of the United States of America* **88**: 4061-4065.

Hermieu J.F., Lepart C., Ravery V., Delmas V. and Boccon-Gibod L. (1999) Lipodystrophy: a complication of protease inhibitors in HIV seropositive patients. *Progrès en Urologie* **9** (3): 537-540.

Hesselton R.M., Koup R.A., Cromwell M.A., Graham B.S., Johns M. and Sullivan J.L. (1993) Human peripheral blood xenografts in the SCID mouse: characterization of immunologic reconstitution. *The Journal of Infectious Diseases* **168**: 630-640.

Hirsch V.M., Zack P.M., Vogel A.P. and Johnson P.R. (1991) Simian immunodeficiency virus infection of macaques: end-stage disease is characterized by widespread distribution of proviral DNA in tissues. *The Journal of Infectious Diseases* **163**: 976-988.

Hirsch V.M. and Johnson P.R. (1994) The pathogenic diversity of simian immunodeficiency viruses. *Virus Research* **32**: 183-203.

Hirsch V.M., Dapolito G., Goeken R. and Campbell B.J. (1995) Phylogeny and natural history of the primate lentiviruses, SIV and HIV. *Current Opinion in Genetics and Development* **5**: 798-806.

Hoffmann-Fezer G., Thum J., Ackley C., Herbold M., Mysliwietz J., Thefeld S., Hartmann K. and Kraft W. (1992) Decline in $CD4^+$ numbers in cats with naturally acquired feline immunodeficiency virus infection. *Journal of Virology* **66** (3): 1484-1488.

Hollingshead M.G., Westbrook L., Ross M.J., Bailey J., Qualls K.J. and Allen L.B. (1992) An ELISA system for evaluating antiretroviral activity against Rauscher murine leukemia virus. *Antiviral Research* **18**: 267-274.

Hong J., Lu H., Meng X., Ryu J.-H., Hara Y. and Yong C.S. (2002) Stability, cellular uptake, biotransformation, and efflux of tea polyphenol (-)-epigallocatechin-3-gallate in HT-29 human colon adenocarcinoma cells. *Cancer Research* **62**: 7241-7246.

Horn T.F.W., Huitron-Resendiz S., Weed M.R., Hendriksen S.J. and Fox H.S. (1998) Early physiological abnormalities after simian immunodeficiency virus infection. *Proceedings of the National Academy of Science of the United States of America* **95**: 15072-10577.

Hu Z.-Q., Zhao W.-H., Yoda Y., Asano N., Hara Y. and Shimamura T. (2002) Additive, indifferent and antagonistic effects in combinations of epigallocatechin gallate with 12 non-β-lactam antibiotics against methicillin-resistant *Staphyococcus aureus. Journal of Antimicrobial Chemotherapy* **50**: 1051-1054.

Huang M., Simard C. and Jolicoeur P. (1992) Susceptibility of inbred strains of mice to murine AIDS (MAIDS) correlates with target cell expansion and high expression of defective MAIDS virus. *Journal of Virology* **66** (4): 2398-2406.

Huang M. and Jolicoeur P. (1994) Myristylation of $Pr60^{gag}$ of the murine AIDS-defective virus is required to induce disease and notably for the expansion of its target cells. *Journal of Virology* **68** (9): 5648-5655.

Hulier E., Pétour P., Marussig M., Nivez M.-P., Mazier D. and Rénia L. (1996) Quantitative assessment of murine retrovirus LP-BM5 infection in MAIDS by PCR and anion exchange HPLC. *Journal of Virological Methods* **60**: 109-117.

Imamichi T. (2004) Action of anti-HIV drugs and resistance: reverse transcriptase inhibitors and protease inhibitors. *Current Pharmaceutical Designs* **10**: 4039-4053.

Jacob J., Cabarcas S., Veras I., Zaveri N. and Schramm L. (2007) The green tea component EGCG inhibits RNA polymerase III transcription. *Biochemical and Biophysical Research Communications* **360**: 778-783.

Jamieson B.D., Aldrovandi G.M. and Zack J.A. (1996) The SCID-hu mouse: an *in vivo* model for HIV-1 pathogenesis and stem cell therapy for AIDS. *Seminars in Immunology* **8**: 215-221.

Jamieson B.D., Uittenbogaart C.H., Schmid I. and Zack J.A. (1997) High viral burden and rapid $CD4^+$ cell depletion in human immunodeficiency virus type 1-infected SCID-hu mice suggest direct viral killing of thymocytes in vivo. *Journal of Virology* **71** (11): 8245-8253.

Jiang B., Herbert V.Y., Li Y., Mathis J.M., Alexander J.S. and Dugas T.R. (2007) HIV antiretroviral drug combination induces endothelial mitochondrial dysfunction and reactive oxygen species production, but not apoptosis. *Toxicology and Applied Pharmacology* **224**: 60-71.

Jiang H., Joy D.A., Furuya T. and Su X.Z. (2006) Current understanding of the molecular basis of chloroquine-resistance in *Plasmodium falciparum. Journal of Postgraduate Medicine* **52** (4): 271-276.

Jolicoeur P. (1991) Murine acquired immunodeficiency syndrome (MAIDS) an animal model to study the AIDS pathogenesis. *FASEB Journal* **5**: 2398-2405.

Joag S.V., Li Z., Foresman L., Pinson D.M., Raghavan R., Zhuge W., Adany I., Wang C., Jia F., Sheffer D., Ranchalis J., Watson A. and Narayan O. (1997) Characterization of the pathogenic KU-SHIV model of acquired immunodeficiency syndrome in macaques. *AIDS Research and Human Retroviruses* **13** (8): 635-645.

Joag S.V. (2000) Primate models of AIDS. *Microbes and Infection* **2**: 223-229.

Kaneshima H., Shih C.-C., Namikawa R., Rabin L., Outzen H., Machado S.G. and McCune J.M. (1991) Human immunodeficiency virus infection of human lymph nodes in SCID-hu mouse. *Proceedings of the National Academy of Sciences of the United States of America* **88**: 4523-4527.

Katewa S.D. and Katyare S.S. (2004) Treatment with antimalarials adversely affects the oxidative energy metabolism in rat liver mitochondria. *Drug and Chemical Toxicology* **27** (1): 41-53.

Katz R.A., Greger J.G. and Skalka A.M. (2005) Effects of cell cycle status on early events in retroviral replication. *Journal of Cellular Biochemistry* **94**: 880-889.

Kawai K., Tsuno N.H., Kitayama J., Okaji Y., Yazawa K., Asakage M., Hori N., Watanabe T., Takahashi K. and Nagawa K. (2003) Epigallocatechin gallate, the main component of tea polyphenol, binds to CD4 and interferes with gp120 binding. *Journal of Allergy and Clinical Immunology* **112**: 951-957.

Kelly L.M., Lisziewicz J. and Lori F. (2004) "Virostatics" as a potential new class of HIV drugs. *Current Pharmaceutical Design* **10**: 4103-4120.

Keyaerts E., Vijgen L., Maes P., Neyts J. and Van Ranst M. (2004) *In vitro* inhibition of severe respiratory syndrome coronavirus by chloroquine. *Biochemical and Biophysical Research Communications* **323** (1): 264-268.

Kim W.K., Tang Y., Kenny J.J., Longo D.L. and Morse III H.C. (1994) In murine AIDS, B cells are early targets of defective virus and are required for efficient infection and expression of defective virus in T cells and macrophages. *Journal of Virology* **68** (10): 6767-6769.

Kidd K.K. and Ruano G. (1995) Optimizing PCR. In: McPherson M.J., Hames B.D. and Taylor G.R. (editors). PCR 2 A Practical Approach. Oxford, IRL Press at Oxford University Press: 1-22.

Kindt T.J., Hirsch V.M., Johnson P.R. and Sawasdikosol S. (1992) Animal models for acquired immunodeficiency syndrome. *Advances in Immunology* **52**: 425-474.

Kish T.M., Budgeon L.R., Welsh P.A. and Howett M.K. (2001) Immunological characterization of human vaginal xenografts in immunocompromised mice. *American Journal of Pathology* **159** (6): 2331-2345.

Klinken S.P., Fredrickson T.N., Hartley J.W., Yetter R.A. and Morse III H.C. (1988) Evolution of B cell lineage lymphomas in mice with a retrovirus-induced immunodeficiency syndrome, MAIDS. *The Journal of Immunology* **140** (5): 1123-1131.

Koch J.A. and Ruprecht R.M. (1992) Animal models for anti-HIV therapy. *Antiviral Research* **19**: 81-109.

Kohmoto M., Uetsuka K., Ikeda Y., Inoshima Y., Shimojima M., Sato E., Inada G., Toyosaki T., Miyazawa T., Doi K. and Mikami T. (1998) Eight-year observation and comparative study of specific pathogen-free cats experimentally infected with feline immunodeficiency virus (FIV) subtypes A and B: terminal acquired immunodeficiency syndrome in a cat infected with FIV Petaluma strain. *Journal of Veterinary Medical Science* **60** (3): 315-321.

Kollmann T.R., Pettoello-Mantovani M., Zhuang X., Kim A., Hachamovitch M., Smarnworawong P., Rubinstein A. and Goldstein H. (1994) Disseminated human immunodeficiency virus 1 (HIV-1) infection in SCID-hu mice after peripheral inoculation with HIV-1. *Journal of Experimental Medicine* **179**: 513-522.

Koup R.A., Hesselton R.M., Safrit J.T., Somasundaran M. and Sullivan J.L. (1994) Quantitative assessment of human immunodeficiency virus type 1 replication in human xenografts of acutely infected Hu-PBL-SCID mice. *AIDS Research and Human Retroviruses* **10** (3): 279-284.

Krishna S., Uhlemann A.C. and Haynes R.K. (2004) Artemisinins: mechanism of action and potential for resistance. *Drug Resistance Updates* **7**: 233-244.

Kulaga H., Folks T., Rutledge R., Truckenmiller M.E., Gugel E. and Kindt T.J. (1989) Infection of rabbits with human immunodeficiency virus 1. *Journal of Experimental Medicine* **169**: 321-326.

Lagoja I.M., Pannecouque C., Van Aerschot A., Witvrouw M., Debyser Z., Balzarini J., Herdewijn P. and De Clercq E. (2003) N-aminoimidazole derivatives inhibiting retroviral replication via a yet unidentified mode of action. *Journal of Medicinal Chemistry* **46**: 1546-1553.

Lambert D.M., Bartus H., Fernandez A.V., Bratby-Anders C., Leary J.J., Dreyer G.B., Metcalf B.W. and Petteway Jr. S.R. (1993) Synergistic drug interactions of an HIV-1 protease inhibitor with AZT in different *in vitro* models of HIV-1 infection. *Antiviral Research* **21**: 327-342.

Lapenta C., Fais S., Rizza P., Spada M., Logozzi M.A., Parlato S., Santini S.M., Pirillo M., Belardelli F. and Proietto E. (1997) U937-SCID mouse xenografts: a new model for acute *in vivo* HIV-1 infection suitable to test antiviral strategies. *Antiviral Research* **36**: 81-90.

Lapenta C., Santini S.M., Proietti E., Rizza P., Logozzi M., Spada M., Parlato S., Fais S., Pitha P.M. and Belardelli F. (1999) Type I interferon is a powerful inhibitor of *in vivo* HIV-1 infection and preserves human $CD4^+$ T cells from virus-induced depletion in SCID mice transplanted with human cells. *Virology* **263**: 78-88.

Le Grand R., Clayette P., Noack O., Vaslin B., Theodoro F., Michel G., Roques P. and Dormont D. (1994) An animal model for antilentiviral therapy: effect of zidovudine on viral load during acute infection after exposure of macaques to simian immunodeficiency virus. *AIDS Research and Human Retroviruses* **10** (10): 1279-1287.

Levy J.A., Fraenkel-Conrat H. and Owens R.A. (1994) *Virology 3rd edition*. New Jersey, Prentice-Hall, Inc.: 125-140.

Lewis A.D. and Johnson P.R. (1995) Developing animal models for AIDS research-progress and problems. *Trends in Biotechnology* **13**: 142-150.

Li P.-F., Hao Y.-S., Zhang F.-X., Liu X.-H., Liu S.-L. and Li G. (2004) Signaling pathway involved in methionine enkephalin-promoted survival of lymphocytes infected by simian immunodeficiency virus in the early stage *in vitro*. *International Immunopharmacology* **4**: 79-90.

Liang B., Wang J.Y. and Watson R.R. (1996) Murine AIDS, a key to understanding retrovirus-induced immunodeficiency. *Viral Immunology* **9** (4): 225-239.

Lifson J.D., Rossio J.L., Arnaout R, Li L., Parks T.L., Schneider D.K., Kiser R.F., Coalter V.J., Walsh G., Imming R.J., Fisher B., Flynn B.M., Bischofberger N., Piatak Jr. M., Hirsch V.M., Nowak M.A. and Wodarz D. (2000) Containment of simian immunodeficiency virus infection: cellular immune responses and protection from rechallenge following transient postinoculation antiretroviral treatment. *Journal of Virology* **74** (6): 2584-2593.

Limoges J., Persidsky Y., Poluektova L., Rasmussen J., Ratanasuwan W., Zelivyanskaya M., McClernon D.R., Lanier E.R. and Gendelman H.E. (2000) Evaluation of antiretroviral drug efficacy for HIV-1 encephalitis in SCID mice. *Neurology* **54**: 379-389.

Lin J.H. (1997) Human immunodeficiency virus protease inhibitors. From drug design to clinical studies. *Advanced Drug Delivery Reviews* **27**: 215-233.

Lisziewicz J., Foli A., Wainburg M. and Lori F. (2003) Hydroxyurea in the treatment of HIV infection. *Drug Safety* **26** (9): 605-624.

Lodish H., Berk A., Zipursky S.L., Matsudaira P., Baltimore D. and Dornell J. (2002) *Molecular Cell Biology 4th edition*. New York, W.H. Freeman and Company: 361.

Long L.H., Clement M.V. and Halliwell B. (2000) Artifacts in cell culture: rapid generation of hydrogen peroxide on addition of (-)-epigallocatechin, (-)-epigallocatechin gallate, (+)-catechin and quercetin to commonly used cell culture media. *Biochemical and Biophysical Research Communications* **273**: 50-53.

Long L.H., Kirkland D., Whitwell J. and Halliwell B. (2007) Different cytotoxic and clastogenic effects of epigallocatechin gallate in various cell culture media due to variable rates of its oxidation in the culture medium. *Mutation Research* **634** (1-2): 177-183.

Lori F. (1999) Hydroxyurea and HIV: 5 years later from antiviral to immune-modulating effects. *AIDS* **13**: 1433-1442.

Lori F. and Lisziewicz J. (2000) Rationale for the use of hydroxyurea as an anti-human immunodeficiency virus drug. *Clinical Infectious Diseases* **30** (Suppl 2): S193-197.

Louwagie G.M., Bachmann M.O., Meyer K., Booysen F.L., Fairall L.R. and Heunis C. (2007) Highly active antiretroviral treatment and health related quality of life in South African adults with human immunodeficiency virus infection: a cross-sectional analytical study. *BMC Public Health* **7** (1):244.

Lova L., Groff A., Ravot E., Comolli G., Xu J., Whitman L., Lewis M., Foli A., Lisziewicz J. and Lori F. (2005) Hydroxyurea exerts a cytostatic but not immunosuppressive effect on T-
lymphocytes. *AIDS* **19**: 137-144.

Maggiolo F., Ripamanti D. and Suter F. Once-a-day HAART: dream or reality. *HIV Clinical Trials* **4** (3): 193-201.

Magnani M., Rossi L., Fraternale A., Silvotti L., Quintavalla F., Piedimonte G., Matteucci D., Baldinotti F. and Bendinelli M. (1995) FIV infection of macrophages: *in vitro* and *in vivo* inhibition by dideoxycytidine 5'-triphosphate. *Veterinary Immunology and Immunopathology* **46**: 151-158.

Manganelli R.E.U., Zaccaro L. and Tomei P.E. (2005) Antiviral activity *in vitro* of *Urtica dioica* L., *Parietaria diffusa* M. at K. and *Sambucus nigra* L. *Journal of Ethnopharmacology* **98**: 323-327.

Mankowski J.L., Clements J.E. and Zink M.C. (2002) Searching for clues: tracking the pathogenesis of human immunodeficiency virus central nervous system disease by use of an accelerated, consistent simian immunodeficiency virus macaque model. *The Journal of Infectious Diseases* **186** (Suppl 2): S199-208.

Mankowski J.L., Queen S.E., Clements J.E. and Zink M.C. (2004) Cerebrospinal fluid markers that predict SIV CNS disease. *Journal of Neuroimmunology* **157** (1-2): 66-70.

Martin L.N., Murphey-Corb M., Mack P., Baskin G.B., Pantaleo G., Vaccarezza M., Fox C.H. and Fauci A.S. (1997) Cyclosporin A modulation of early virologic and immunologic events during primary simian immunodeficiency virus infection in rhesus monkeys. *The Journal of Infectious Diseases* **176**: 374-383.

Mattapallil J.J., Letvin N.L. and Roederer M. (2004) T-cell dynamics during acute SIV infection. *AIDS* **18** (1): 13-23.

Mayhew C.N., Mampuru L.J., Chendil D., Ahmed M.M., Philips J.D., Greenberg R.N., Elford H.L. and Gallicchio V.S. (2002) Suppression of retrovirus-induced immunodeficiency disease (murine AIDS) by trimidox and didox, novel ribonucleotide reductase inhibitors with less bone marrow toxicity than hydroxyurea. *Antiviral Research* **56**: 167-181.

Mayhew C.N., Sumpter R., Inayat M., Cibull M., Philips J.D., Elford H.L. and Gallicchio V.S. (2005) Combination of inhibitors of lymphocyte activiation (hydroxyurea, trimidox, and didox) and reverse transcriptase (didanosine) suppresses development of murine retrovirus-induced lymphoproliferative disease. *Antiviral Research* **65**: 13-22.

Meers J., Del Fierro G.M., Cope R.B., Park H.S., Greene W.K. and Robinson W.F. (1993) Feline immunodeficiency virus infection: plasma, but not peripheral blood mononuclear cell virus titer is influenced by zidovudine and cyclosporine. *Archives of Virology* **132**: 67-81.

Mitsuya H., Weinhlod K.J., Furman P.A., St. Clair M.H., Lehrman S.N., Gallo R.C., Bolognesi D., Barry D.W. and Broder S. (1985) 3'-Azido-3'-deoxythymidine (BW A509U): an antiviral agent that inhibits the infectivity and cytopathic effect of human T-lymphotropic virus type III/lymphadenopathy-associated virus *in vitro. Proceedings of the National Academy of Sciences of the United States of America* **82**: 7096-7100.

Monceaux V., Fang H.T., Cumont M.C., Hurtel B. and Estaquier J. (2003) Distinct cycling $CD4^+$- and $CD8^+$-T-cell profiles during the asymptomatic phase of simian immunodeficiency virus SIVmac251 infection in rhesus macaques. *Journal of Virology* **77** (18): 10047-10059.

Monceaux V., Estaquier J., Février M., Cumont M.-C., Rivière Y., Aubertin A.-M., Ameison J.C. and Hurtel B. (2003) Extensive apoptosis in lymphoid organs during SIV infection predicts rapid progression towards AIDS. *AIDS* **17** (11): 1585-1596.

Montessori V., Press N., Harris M., Akagi L. and Montaner J.S.G. (2004) Adverse effects of antiretroviral therapy for HIV infection. *Canadian Medical Association Journal* **170** (2): 229-238.

Mosier D.E., Yetter R.A. and Morse III H.C. (1985) Retroviral induction of acute lymphoproliferative disease and profound immunosuppression in adult C57BL/6. *Journal of Experimental Medicine* **161**: 766-784.

Mosier D.E., Gulizia R.J., Baird S.M., Wilson D.B., Spector D.H. and Spector S.A. (1991) Human immunodeficiency virus infection of human-PBL-SCID mice. *Science* **251**: 791-794.

Mosier D.E. (1996) Viral pathogenesis in hu-PBL-SCID mice. *Seminars in Immunology* **8**: 255-262.

Mosmann T. (1983) Rapid colorimetric assay for cellular growth and survival: application to proliferation and cytotoxicity assays. *Journal of Immunological Methods* **65**: 55-63.

Mukhopadhyay A., Wei B., Zullo S.J., Wood L.V. and Weiner H. (2002) *In vitro* evidence of inhibition of mitochondrial protease processing by HIV-1 protease inhibitors in yeast: a possible contribution to lipodystrophy syndrome. *Mitochondrion* **1** (6): 511-518.

Mukoyama A., Ushijima H., Nishimura S., Koike H., Toda M., Hara Y. and Shimamura T. (1991) Inhibition of rotavirus and enterovirus infections by tea extracts. *Japanese Journal of Medical Science and Biology* **44** (4): 181-186.

Murata H., Hruz P.W. and Mueckler M. (2000) The mechanism of insulin resistance caused by HIV protease inhibitor therapy. *Journal of Biological Chemistry* **275** (27): 20251-20254.

Murphy F.A., Fauquet C.M., Bishop D.H.L., Ghabrial S.A., Jarvis A.W., Martelli G.P., Mayo M.A. and Summers M.D. (1995) *Virus Taxonomy*. New York, Springer-Verlag Wien: 193-204.

Nakane K. and Ono K. (1990) Differential inhibitory effects of some catechin derivatives on the activities of human immunodeficiency virus reverse transcriptase and cellular deoxyribonucleic and ribonucleic acid polymerase. *Biochemistry* **29**: 2841-2845.

Nakashima H., Ichiyama K., Hirayama F., Uchino K., Ito M., Saitoh T., Ueki M., Yamamoto N. and Ogawara H. (1996) Sulfated pentagalloyl glucose (Y-ART-3) inhibits HIV replication and cytopathic effects *in vitro*, and reduces HIV infection in hu-PBL-SCID mice. *Antiviral Research* **30**: 95-108.

Nakayama M., Suzuki K., Toda M., Okubo S., Hara Y. and Shimamura T. (1993) Inhibition of the infectivity of influenza virus by tea polyphenols. *Antiviral Research* **21**: 289-299.

Nam S., Smith D.M. and Dou S.P. (2001) Ester bond-containing tea polyphenols potently inhibit proteasome activity *in vitro* and *in vivo. The Journal of Biological Chemistry* **276** (16): 13322-13330.

Namikawa R., Weilbaecher K.N., Kaneshima H., Yee E.J. and McCune J.M. (1990) Long-term human hematopoiesis in the SCID-hu mouse. *Journal of Experimental Medicine* **172**: 1055-1063.

Nisole S. and Saïb A. (2004) Early steps of retrovirus replicative cycle. *Retrovirology* **1**: 9.

Norley S.G. (1996) SIV_{agm} infection of its natural African green monkey host. *Immunology Letters* **51**: 53-58.

North T.W., North G.L. and Pedersen N.C. (1989) Feline immunodeficiency virus, a model for reverse transcriptase-targeted chemotherapy for acquired immune deficiency syndrome. *Antimicrobial Agents and Chemotherapy* **33** (6): 915-919.

Nunnari G., Argyris E., Fang J., Melhman K.E., Pomerantz R.J. and Daniel R. (2005) Inhibition of HIV-1 replication by caffeine and caffeine-related methylxanthines. *Virology* **335**: 177-184.

Ohagen A., Luftig R.B., Reicin A.S., Yin L., Ikuta K., Kimura T., Goff S.P. and Höglund S. (1997) The morphology of the immature HIV-1 virion. *Virology* **228** (1): 112-114.

Ohnota H., Okada Y., Ushijima H., Kitamura T., Komuro K. and Mizuochi T. (1990) 3'-Azido-3'-deoxythymidine prevents induction of murine acquired immunodeficiency syndrome in C57BL/10 mice infected with LP-BM5 murine leukemia viruses, a possible animal model for antiretroviral drug screening. *Antimicrobial Agents and Chemotherapy* **34** (4): 605-609.

Ohrui H. (2006) 2'-deoxy-4'-*C*-ethynyl-2-fluoroadenosine, a nucleoside reverse transcriptase inhibitor, is highly potent against all human immunodeficiency viruses type 1 and has low toxicity. *The Chemical Record* **6**: 133-143.

Olyaei A.J., De Mattos A.M. and Bennet W.M. (2000) Renal toxicity of protease inhibitors. *Current Opinion in Nephrology and Hypertension* **9** (5): 473-476.

Okishima N., Hirata K., Moriguchi S. and Kishino Y. (1996) Vitamin E supplementation normalizes immune dysfunction murine AIDS induced by LP-BM5 retrovirus infection. *Nutrition Research* **16** (10): 1709-1718.

O'Neil S.P., Suwyn C., Anderson D.C., Niedziela G., Bradley J., Novembre F.J., Herndon J.G. and McClure H.M. (2004) Correlation of acute humoral response with brain virus burden and survival time in pig-tailed macaques infected with the neurovirulent simian immunodeficiency virus SIVsmmFGb. *American Journal of Pathology* **164** (4): 1157-1172.

O'Neill P.M., Bray P.G., Hawley S.R., Ward S.A. and Park B.K. (1998) 4-Aminoquinolines-past, present, and future: a chemical perspective. *Pharmacology and Therapeutics* **77** (1): 29-58.

Otani I., Fujii Y., Akari H., Mukai R., Mori K., Ono F., Kojima E., Machida M., Murakami K., Doi K. and Yosikawa Y. (1997) Effects of 6-chloro-2', 3'-dideoxyguanosine (6-Cl-ddG) in surface lymph nodes of rhesus monkeys (*Macaca Mulatta)* chronically infected with simian immunodeficiency virus (SIVmac239). *Journal of Veterinary Medical Science* **59** (10): 891-896.

Otani I., Akari H., Nam K.-H., Mori K., Suzuki E., Shibata H., Doi K., Terao K. and Yosikawa Y. (1998) Phenotypic changes in peripheral blood monocytes of cynomolgus monkeys acutely infected with simian immunodeficiency virus. *AIDS Research and Human Retroviruses* **14** (13): 1181-1186.

Palella Jr. F.J., Delany K.M., Moorman A.C., Loveless M.O., Fuhrer J., Satten G.A., Aschman D.J. and Holmberg S.D. (1998) Declining morbidity and mortality among patients with advanced human immunodeficiency virus infection. HIV Outpatient Study Investigators. *New England Journal of Medicine* **338** (13): 853-860.

Palmeira V.F., Kneipp L.F., Alviano C.S. and Dos Santos A.L. (2006) Secretory aspartyl peptidase activity from mycelia of the human fungal pathogen *Fonsecaea pedrosoi*: Effect of HIV aspartyl proteolytic inhibitors. *Research in Microbiology* **157** (9): 819-826.

Paton N.I., Aboulhab J. and Karim F. (2002) Hydroxychloroquine, hydroxycarbamide, and didanosine as economic treatment for HIV-1. *The Lancet* **359**: 1667-1668.

Pattengale P.K., Taylor C.R., Twomey P., Hill S., Jonasson J., Beardsley T. and Haas M. (1982) Immunopathology of B-cell lymphomas induced in C57BL/6 mice by dualtropic murine leukemia virus (MuLV). *American Journal of Pathology* **107**: 362-377.

Pattishall K.H. (1993) Discovery and development of zidovudine as the cornerstone of therapy to control human immunodeficiency virus infection. In: Adams J. and Merluzzi V.J. (editors). *The Search for Antiviral Drugs*. Boston, Birkhäuser: 23-43.

Pedersen N.C., Ho E.W., Brown M.L. and Yamamoto J.K. (1987) Isolation of a T-lymphotropic virus from domestic cats with an immunodeficiency-like syndrome. *Science* **235** (4790): 790-793.

Perno C.-F., Yarchoan R., Balzarini J., Bergamini A., Milanese G., Pauwels R., De Clerq E., Rocchi G. and Calio R. (1992) Different pattern of activity of inhibitors of the human immunodeficiency virus in lymphocytes and monocytes/macrophages. *Antiviral Research* **17**: 289-304.

Persidsky Y., Limoges J., McComb R., Bock P., Baldwin T., Tyor W., Patil A., Nottet H.S.L.M., Epstein L., Gelbard H., Flanagan E., Reinhard J., Pirruccello S.J. and Gendelman H.E. (1996) Human immunodeficiency virus encephalitis in SCID mice. *American Journal of Pathology* **149** (3): 1027-1053.

Peterson J., Dwyer J., Bhagwat S., Haytowitz D., Holden J., Eldridge A.L., Beecher G. and Aladesanmi J. (2005) Major flavonoids in dry tea. *Journal of Food Composition and Analysis* **18**: 487-501.

Pettoello-Mantovani M., Kollman T.R., Raker C., Kim A., Yurasov S., Tudor R., Wiltshire H. and Goldstein H. (1997) Saquinavir-mediated inhibition of human immunodeficiency virus (HIV) infection in SCID mice implanted with human fetal thymus and liver tissue: an *in vivo* model for evaluating the effect of drug therapy on HIV infection in lymphoid tissues. *Antimicrobial Agents and Chemotherapy* **41** (9): 1880-1887.

Pètursson G., Pálsson P.A. and Georgsson G. (1989) Maedi-visna in sheep: host-virus interactions and utilization as a model. *Intervirology* **30** (Suppl 1): 36-44.

Philips T.R., Prospero-Garcia O., Puaoi D.L., Lerner D.L., Fox H.S., Olmsted R.A., Bloom F.E., Hendriksen S.J. and Elder J.H. (1994) Neurological abnormalities associated with feline immunodeficiency virus infection. *Journal of General Virology* **75**: 979-987.

Pincus S.H. (2004) Models of HIV infection utilizing transgenic and reconstituted immunodeficient mice. *Drug Discovery Today: Disease Models* **1** (1): 49-56.

Power C., Moench T., Peeling J., Kong P.-A. and Langelier T. (1997) Feline immunodeficiency virus causes increased glutamate levels and neuronal loss in brain. *Neuroscience* **77** (4): 1175-1185.

Pozio E. and Morales M.A.G. (2005) The impact of HIV-protease inhibitors on opportunistic parasites. *TRENDS in Parasitology* **21** (2): 58-63.

Premanathan M., Arakaki R., Izumi H., Kathiresan K., Nakano M., Yamamoto N. and Nakashima H. (1999) Antiviral properties of a mangrove plant, *Rhizophora apiculata* Blume, against human immunodeficiency virus. *Antiviral Research* **44**: 113-122.

Przybyszewski W.M. and Kasperczyk J. (2006) Radical mechanism of hydroxyurea side toxicity. *Post□py Higieny i Medycyny Doswiadczalnej (online)* **60**: 516-526.

Pudney J. and Song M.J. (1994) Electron microscopic analysis of HIV-host interactions. *Tissue and Cell* **26** (4): 539-550.

Rauscher F.J. (1962) A virus-induced disease of mice characterized by erythrocytopoiesis and lymphoid leukemia. *Journal of the National Cancer Institute* **29**: 515-543.

Rayne F., Vendeville A., Bonhoure A. and Beaumelle B. (2004) The ability of chloroquine to prevent Tat-induced cytokine secretion by monocytes is implicated in its *in vivo* anti-human immunodeficiency virus type 1 activity. *Journal of Virology* **78** (21): 12054-12057.

Reid P., MacInnes H., Cong M.-E., Heneine W. and Garcia-Lerma G. (2005) Natural resistance of human immunodeficiency virus type 2 to zidovudine. *Virology* **336**: 251-264.

Reimann K.A., Tenner-Racz K., Racz P., Montefiori D.C., Yasutomi Y., Lin W., Ransil B.J. and Letvin N.L. (1994) Immunopathogenic events in acute infection of rhesus monkeys with simian immunodeficiency virus of macaques. *Journal of Virology* **68** (4): 2362-2370.

Romero D.L., Busso M., Tan C.-K., Reusser F., Palmer J.R., Poppe S.M., Aristoff P.A., Downey K.M., So A.G., Resnick L. and Tarpley W.G. (1991) Nonnucleoside reverse

transcriptase inhibitors that potently and specifically block human immunodeficiency virus type 1 replication. *Proceeding of the National Academy of Sciences of the United States of America* **88**: 8806-8810.

Rossi L., Serafini S., Franchetti P., Casabianca A., Orlandi C., Schiavano G.F., Carnevali A. and Magnani M. (2002) Inhibition of murine AIDS by a heterodinucleotide of azidothymidine and 9-(R)-2-(phosphonomethoxypropyl)adenine. *Journal of Antimicrobial Chemotherapy* **50**: 639-647.

Rowe W.P., Pugh W.E. and Hartley J.W. (1970) Plaque assay techniques for murine leukemia viruses. *Virology* **42**: 1136-1139.

Ruprecht R.M., O'Brien L.G., Rossoni L.D. and Nusinoff-Lehrman S. (1986) Suppression of mouse viraemia and retroviral disease by 3'-azido-3'deoxythimidine. *Nature* **323** (6087): 467-469.

Rychlik W., Spencer W.J. and Rhoads R.E. (1990) Optimization of the annealing temperature for DNA amplification *in vitro*. *Nucleic Acid Research* **18** (21): 6409-6412.

Rytik P.G., Kutcherov I.I., Muller W.E.G., Poleschuk N.N., Duboiskaya G.P., Kruzo M. and Podolskaya I.A. (2004) Small animal model of HIV-1 infection. *Journal of Clinical Virology* **31S**: S83-87.

Saldaini E., Matteucci D., Lopez-Cepero M., Specter S., Friedman H. and Bendirelli M. (1989) Friend leukemia complex infection of mice as an experimental model for AIDS studies. *Veterinary Immunology and Immunopathology* **21**: 97-110.

Sannella A.R., Messori L., Casini A., Vincieri F.F., Bilia A.R., Majori G. and Severini C. (2007) Antimalarial properties of green tea. *Biochemical and Biophysical Research Communications* **353**: 177-181.

Sato H., Orenstein J., Dimitrov D. and Martin M. (1992) Cell-to-cell spread of HIV-1 occurs within minutes and may not involve the participation of virus particles. *Virology* **186**: 712-724.

Savarino A., Gennero L., Chen H.C., Serrano D., Malavasi F., Boelaert J.R. and Sperber K. (2001) Anti-HIV effects of chloroquine: mechanisms of inhibition and spectrum of activity. *AIDS* **15**: 2221-2229.

Savarino A., Lucia M.B., Rastrelli E., Rutella S., Golotta C., Morra E., Tamburrini E., Perno C.F., Boelaert J.R., Sperber K. and Cauda R. (2004) Anti-HIV effects of Chloroquine. Inhibition of viral particle glycosylation and synergism with protease inhibitors. *Journal of Acquired Immune Deficiency Syndromes* **35** (3): 223-232.

Savoia D., Allice T. and Tovo P.A. (2005) Antileishmanial activity of HIV protease inhibitors. *International Journal of Antimicrobial Agents* **26** (1): 92-94.

Schmitt A.C., Ravazzolo A.P. and Van Poser G.L. (2001) Investigation of some *Hypericum* species native to Southern Brazil for antiviral activity. *Journal of Ethnopharmacology* **77**: 239-245.

Schmitz J.E., Kuroda M.J., Santra S., Sasseville V.G., Simon M.A., Lifton M.A., Racz P., Tenner-Racz K., Dalesandro M., Scallon B.J., Ghrayeb J., Forman M.A., Montefiori D.C., Rieber E.P., Letvin N.L. and Reimann K.A. (1999) Control of viremia in simian immunodeficiency virus infection by $CD8^+$ lymphocytes. *Science* **283**: 857-860.

Schmitz J.E., Kuroda M.J., Santra S., Simon M.A., Lifton M.A., Lin W., Khunkhun R., Piatak M., Lifson J.D., Grosschupff G., Gelman R.S., Racz P., Tenner-Racz K., Mansfield K.A., Letvin N.L., Monetfiori D.C. and Reimann K.A. (2003) Effect of humoral immune responses on controlling viremia during primary infection of rhesus monkeys with simian immunodeficiency virus. *Journal of Virology* **77** (3): 2165-2173.

Schubert U., Ott D.E., Chertova E.N., Welker R., Tessmer U., Princiotta M.F., Bennink J.R., Kräusslich H.-G. and Yewdell J.W. (2000) Proteasome inhibition interferes with Gag polyprotein processing, release and maturation of HIV-1 and HIV-2. *Proceedings of the National Academy of Sciences of the United States of America* **97** (24): 13057-13062.

Schwartz O., Moréchal V., Friguet B., Arenzona-Seisdedos F. and Heard J.M. (1998) Antiviral activity of the proteasome on incoming human immunodeficiency virus type 1. *Journal of Virology* **72** (5): 3845-3850.

Selematsela M. (2001) *Combination of an anti HIV drug (AZT) and an extract from Camellia sinensis/green tea (EGCg) in the treatment of murine AIDS*. MSc thesis, University of Pretoria, South Africa.

Sension M. (2004) Initial therapy for human immunodeficiency virus: broadening the options. *HIV Clinical Trials* **5** (2): 99-111.

Sequar G., Britt W.J., Lakeman F.D., Lockridge K.M., Tarara R.P., Canfield D.R., Zhou S.-S., Gardner M.B. and Barry P.A. (2002) Experimental coinfection of rhesus macaques with rhesus cytomegalovirus and simian immunodeficiency virus: pathogenesis. *Journal of Virology* **76** (15): 7661-7671.

Sharma S.K., Billaud J.-N., Tandon M., Billet O., Choi S., Kopka M.L., Philips T.R. and Lown J.W. (2002) Inhibition of feline immunodeficiency virus (FIV) replication by DNA binding polyamides. *Bioorganic and Medicinal Chemistry Letters* **12** (15): 2007-2010.

Shen Y., Shen L., Sehgal P., Zhou D., Simon M., Miler M., Enimi E.A., Henckler B., Chalifoux L., Sehgal N., Gastron M., Letvin N.L. and Chen Z.W. (2001) Antiretroviral agents restore mycobacterium-specific T-cell immune responses and facilitate controlling a fatal tuberculosis-like disease in macaques coinfected with simian immunodeficiency virus and *Mycobacterium bovis* BCG. *Journal of Virology* **75** (18): 8690-8696.

Shimamura T., Zhao W.-H. and Hu Z.-Q. (2007) Mechanism of action and potential for use of tea catechin as an anti-infective agent. *Anti-Infective Agents in Medicinal Chemistry* **6**: 57-62.

Siebelink K.H.J., Chu I.-H., Rimmelzwaan G.F., Weijer K., Van Herwijnen R., Knell P., Egberink H.F., Bosch M.L. and Osterhaus A.D.M.E. (1990) Feline immunodeficiency virus (FIV) infection in the cat as a model for HIV infection in man: FIV-induced impairment of immune function. *AIDS Research and Human Retroviruses* **6** (12): 1373-1378.

Simard C., Huang M. and Jolicoeur P. (1994) Murine AIDS is initiated in the lymph nodes draining the site of inoculation, and the infected B cells influence T cells located at distance, in noninfected organs. *Journal of Virology* **68** (3): 1903-1912.

Sklan E.H., Gazit A. and Priel E. (2000) Inhibition of murine AIDS (MAIDS) development in C57BL/6J mice by tyrphostin AG-1387. *Virology* **278**: 95-102.

Sonoda J., Koriyama C., Yamamoto S., Kozako T., Li H.C., Lema C., Yashiki S., Fujiyoshi T., Toshinaga M., Nagata Y., Akiba S., Takezaki T., Yamada K. and Sonoda S. (2004) HTLV-1 provirus load in peripheral blood lymphocytes of HTLV-1 carriers is diminished by green tea drinking. *Cancer Science* **95** (7): 596-601.

Sotir M., Switzer W., Schable C., Schmitt J., Vitek C. and Khabbaz R.F. (1997) Risk of occupational exposure to potentially infectious nonhuman primate materials and to simian immunodeficiency virus. *Journal of Medical Primatology* **26** (5): 233-240.

Spring M., Stahl-Hennig C., Stolte N., Bischofberger N., Heeney J., Ten Haaft P., Tenner-Racz K., Racz P., Lorenzen D., Hunsmann G. and Dittmer U. (2001) Enhanced cellular immune response and reduced $CD8^+$ lymphocyte apoptosis in acutely SIV-infected rhesus macaques after short-term antiretroviral treatment. *Virology* **279**: 221-232.

Staprans S.I., Dailey P.J., Rosenthal A., Horton C., Grant R.M., Lerche N. and Feinberg M.B. (1999) Simian immunodeficiency virus disease course is predicted by the extent of virus replication during primary infection. *Journal of Virology* **73** (6): 4829-4839.

St. Clair M.H., Richards C.A., Spector T., Weinhold K.J., Miller W.H., Langlois A.J. and Furman P.A. (1987) 3'-Azido-3'-deoxythymidine triphosphate as an inhibitor and substrate of purified human immunodeficiency virus reverse transcriptase. *Antimicrobial Agents and Chemotherapy* **31** (12): 1972-1977.

Stoddart C.A., Moreno M.E., Linquist-Stepps V., Bare C., Bogan M.R., Gobbi A., Buckheit R.W., Bedard J., Rando R.F. and McCune J.M. (2000) Antiviral activity of 2'-deoxy-3'oxa-4'-thiocyidine (BCH-10652) against lamivudine-resistant human immunodeficiency virus type 1 in SCID-hu thy/liv mice. *Antimicrobial Agents and Chemotherapy* **44** (3): 783-786.

Straub O.C. (1989) Caprine arthritis encephalitis - a model for AIDS? *Intervirology* **30** (Suppl 1): 45-50.

Strizki J.M., Xu S., Wagner N.E., Wojcik L., Liu J., Endres M., Palani A., Shapiro S, Clader J.W., Greenlee W.J., Tagat J.R., McCombie S., Cox K., Fawzi A.B., Chou C-C., Pugliese-Sivo C., Davies L., Moreno M.E., Ho D.D., Trkola A., Stoddart C.A., Moore J.P., Reyes G.R. and Baroudy B.M. (2001) SCH-C (SCH 351125), an orally bioavailable, small molecule antagonist of the chemokine receptor CCR5, is a potent inhibitor of HIV-1 infection *in vitro* and *in vivo. Proceedings of the National Academy of Sciences of the United States of America* **98** (22): 12718-12723.

Sumpter L.R., Inayat M.S., Yost E.E., Duvall W., Hagan E., Mayhew C.N., Elford H.L. and Gallicchio V.S. (2005) *In vivo* examination of hydroxyurea and the novel ribonucleotide reductase inhibitors trimidox and didox in combination with the reverse transcriptase inhibitor abacavir: suppression of retro-virus induced immunodeficiency disease. *Antiviral Research* **62**: 111-120.

Suruga Y., Makino M., Okada Y., Tanaka H., De Clerq E. and Baba M. (1998) Prevention of murine AIDS development by (R)-9-(2-phosphonylmethoxypropyl)adenine. *Journal of Acquired Immune Deficiency Syndromes* **18** (4): 316-322.

Swanstrom R. and Erona J. (2000) Human immunodeficiency virus type-1 protease inhibitors: therapeutic successes and failures, suppression and resistance. *Pharmacology and Therapeutics* **86**: 145-170.

Talbott R.L., Sparger E.E., Lovelace K.M., Fitch W.M., Pedersen N.C., Luciw P.A. and Elder J.H. (1989) Nucleotide sequence and genomic organization of feline immunodeficiency virus. *Proceedings of the National Academy of Sciences of the United States of America* **86**: 5743-5747.

Tao P. (1992) The inhibitory effects of catechin derivatives on the activities of human immunodeficiency virus reverse transcriptase and DNA polymerases. *Zhongguo Yi Xue Ke Xue Yuan Xue Bao* **14** (5): 334-338.

Taylor M.D., Korth M.J. and Katze M.G. (1998) Interferon treatment inhibits the replication of simian immunodeficiency virus at an early stage: evidence for a block between attachment and reverse transcription. *Virology* **241**: 156-162.

Ter Hofstede H.J.M., Burger D.M. and Koopman P.P. (2003) Antiretroviral therapy in HIV patients: aspects of metabolic complications and mitochondrial toxicity. *The Netherlands Journal of Medicine* **61** (12): 393-403.

Törnevik Y., Ullman B., Balzarini J., Wahren B. and Eriksson S. (1995) Cytotoxicity of 3'-azido-3'deoxythymidine correlates with 3'-azidothymidine-5'-monophosphate (AZTMP) levels, whereas anti-human immunodeficiency virus (HIV) activity correlates with 3'-azidothymidine-5'-triphosphate (AZTTP) levels in cultured CEM T-lymphoblastoid cells. *Biochemical Pharmacology* **49** (6): 829-837.

Torten M., Franchini M., Barlough J.E., George J.W., Mozes E., Lutz H. and Pedersen N.C. (1991) Progressive immune dysfunction in cats experimentally infected with feline immunodeficiency virus. *Journal of Virology* **65** (5): 2225-2230.

Tsai W.-P., Nara P.L., Kung H.-F. and Oroszlan S. (1990) Inhibition of human immunodeficiency virus infectivity by chloroquine. *AIDS Research and Human Retroviruses* **6** (4): 481-489.

Uckun F.M., Qazi S., Pendergrass S., Lisowski E., Waurzyniak B., Chen C.-L. and Venkatachalam T.K. (2002) *In vivo* toxicity, pharmacokinetics, and anti-human immunodeficiency virus activity of stavudine-5'-(ρ-bromophenyl methoxyalaninyl phosphate) (Stampidine) in mice. *Antimicrobial Agents and Chemotherapy* **46** (11): 3428-3436.

Vacca J.P., Dorsey B.D., Schleif W.A., Levin R.B., McDaniel S.L., Darke P.L., Zugay J., Quintero J.C., Blahy O.M., Roth E., Sardana V.V., Schlabach A.J., Graham P.I., Condra J.H., Gotlib L., Holloway M.K., Lin J., Chen I.-W., Vastag K., Ostovic D., Anderson P.S., Emini E.A. and Huff J.R. (1994) L-735,524: on orally bioavailable human immunodeficiency virus type 1 protease inhibitor. *Proceedings of the National Academy of Sciences of the United States of America* **91**: 4096-4100.

Van den Bout-Van den Beukel C.J.P., Koopmans P.P. and Van der Ven A.J.A.M. (2006) Possible drug-metabolism interactions of medicinal herbs with antiretroviral drugs. *Drug Metabolism Reviews* **38**: 477-514.

Van Rompay K.K., Otsyula M.G., Marthas M.L., Miller C.J., McChesney M.B. and Pedersen N.C. (1995) Immediate zidovudine treatment protects simian

immunodeficiency virus-infected newborn macaques against rapid onset of AIDS. *Antimicrobial Agents and Chemotherapy* **39** (1): 125-131.

Vincent M.J., Bergeran E., Benjannet S., Erickson B.R., Rollin P.E., Ksiazek T.G., Seidah N.G. and Nichol S.T. (2005) Chloroquine is a potent inhibitor of SARS coronavirus infection and spread. *Virology Journal* **2**: 69-79.

Walder R., Kalvatchev Z. and Apitz-Castro R. (1998) Selective *in vitro* protection of SIVagm-induced cytolysis by ajoene, [(E)-(Z)-4,5,9-trithiadodeca-1,6,11-triene-9 oxide]. *Biomedicine and Pharmacotherapy* **52**: 229-235.

Watanbe H., Miyaji C., Makino M. and Abo T. (1996) Therapeutic effects of glycyrrhizin in mice infected with LP-BM5 murine retrovirus and mechanisms involved in the prevention of disease progression. *Biotherapy* **9** (4): 209-220.

Watzinger F., Ebner K. and Lion T. (2006) Detection and monitoring of virus infection by real-time PCR. *Molecular Aspects of Medicine* **27**: 254-298.

Weber J.M. and Ruzindana-Umunyana A., Imbeault L. and Sircar S. (2003) Inhibition of adenovirus infection and adenain by green tea catechins. *Antiviral Research* **58**: 167-173.

Weisburger J.H. (1997) Tea and health: a historical perspective. *Cancer Letters* **114**: 315-317.

White D.O. and Fenner F.J. (1994) *Medical Virology 4th edition*. San Diego, Academic Press: 74-86.

Willet B.J., Flynn J.N. and Hosie M.J. (1997) FIV infection of the domestic cat: an animal model for AIDS. *Immunology Today* **13** (4): 182-189.

Witvrouw M., Pannecouque C., Van Laethem K., Desmyter J., De Clerq E. and Vandamme A.M. (1999) Activity of non-nucleoside reverse transcriptase inhibitors against HIV-2 and SIV. *AIDS* **13** (12): 1477-1483.

Wlodawer A. and Vondrasek J. (1998) Inhibitors of HIV-1 protease: a major success of structure-assisted drug design. *Annual Reviews of Biophysical and Biomolecular Structures* **27**: 249-284.

Xu Z.-Q., Buckweit Jr. R.W., Stup T.L., Flavin M.T., Khilevich A., Rizzo J.D., Lin L. and Zembower D.E. (1998) *In vitro* anti-human immunodeficiency virus (HIV) activity of the chromanone derivative, 12-oxocalanolide A, a novel NNRTI. *Bioorganic and Medicinal Chemistry Letters* **8**: 2179-2184.

Yamaguchi K., Honda M., Ikigai H., Hara Y. and Shimamura T. (2002) Inhibitory effects of (-)-epigallocatechin gallate on the life cycle of human immunodeficiency virus type 1 (HIV-1). *Antiviral Activity* **53**: 19-34.

Yarasheski K.E., Tebas P., Sigmund C., Dagogo-Jack S., Bohrer A., Turk J., Halban P.A., Cryer P.E. and Powderly W.G. (1999) Insulin resistance in HIV protease inhibitor associated diabetes. *Journal of Acquired Immune Deficiency Syndromes* **21** (3): 209-216.

Yazdanpanah Y. (2004) Costs associated with combination antiretroviral therapy in HIV-infected patients. *Journal of Antimicrobial Agents and Chemotherapy* **53**: 558-561.

Yetter R.A., Buller M.L., Lee J.S., Elkins K.L., Mosier D.E., Fredrickson T.N. and Morse III H.C. (1988) $CD4^+$ cells are required for development of a murine retrovirus-induced immunodeficiency syndrome (MAIDS). *Journal of Experimental Medicine* **168**: 623-635.

Zala C., Rouleau D. and Montaner J.S.G. (2000) Role of hydroxyurea in treatment of disease due to human immunodeficiency virus infection. *Clinical Infectious Diseases* **30** (Suppl 2): S143-150.

Zaveri N.T. (2006) Green tea and its polyphenolic catechins: medicinal uses in cancer and noncancer applications. *Life Sciences* **78**: 2073-2080.

Zucker S.D., Qin X., Rouster S.D., Yu F., Green R.M., Keshavan P., Feinberg J. and Sherman K.E. (2001) Mechanism of indinavir-induced hyperbilirubinaemia. *Proceeding of the National Academy of Sciences of the United States of America* **98** (22): 12671-12676.

Appendix A: Publication from this work

Animal Models Used for the Evaluation of Antiretroviral Therapies

Andreia S.P. Dias [a], Megan J. Bester [a], Rozane F. Britz [a] and Zeno Apostolides [*,b]

[a]*Department of Anatomy, Faculty of Health Sciences, University of Pretoria, Pretoria, South Africa,* [b]*Department of Biochemistry, Faculty of Natural and Agricultural Sciences, University of Pretoria, Pretoria, South Africa*

Abstract: Several animal models for the study of HIV/AIDS have been established and characterized and have been widely used to study the pathogenesis of HIV/AIDS as well as vaccine development. The purpose of this study was to review the literature and identify the animal models most frequently used for the evaluation of drugs, drug combinations, plant extracts and drug-plant combinations. Four of these animal models were evaluated namely the SIV model due to its similarities in pathogenesis of disease to humans, the FIV and the LP-BM5 model due to wide availability and the SCID murine model that combines components of both systems. The pathogenesis of disease in each model, application in the evaluation of drugs, drug combinations and plant extracts as well as the inherent advantages and disadvantages of each model are discussed. The LP-BM5 murine AIDS (MAIDS) model with its *in vitro* equivalent was identified as the animal model, although not identical to HIV/AIDS, most suitable for the rapid and cost effective initial screening of drugs, drug combinations, plant extracts and drug-plant combinations.

Keywords: HIV/AIDS, SIV, FIV, SCID/HIV mouse LP-BM5/MAIDS, antiviral, antiretroviral.

INTRODUCTION

Several animal models for HIV/AIDS both *in vitro* and *in vivo* have been established and include chimpanzees infected with HIV, simian immunodeficiency virus (SIV) model, feline immunodeficiency virus (FIV) model, ungulate lentivirus models, HIV infection of rabbits, transgenic mice, severe combined immunodeficient (SCID) mice as well as several murine oncornavirus models [65]. These models have been extensively studied and are used for vaccine development and have provided valuable information on the pathogenesis of HIV/AIDS.

The discovery of new drugs to combat HIV/AIDS involves either molecular modeling to identify new chemical entities that target specific viral proteins or screening extracts of plants often used by indigenous populations to treat disease in order to identify new molecules with antiretroviral activity. An example of the latter is found in sub-Saharan Africa where the incidence of HIV/AIDS is the highest in the world and the use of traditional medicinal plants has been met with some skepticism and concern due to the lack of scientific data.

To rapidly screen many new drugs, drug combinations, plant extracts and drug-plant combinations a model is required where firstly *in vitro* screening in cell culture can occur and if promising be followed by testing in an equivalent *in vivo* animal model. Furthermore effects such as pharmacological action, metabolism, toxicity, resistance and gene expression as well as several aspects of viral infectivity including cell-to-cell transmission, viral integration, replication and resistance can be investigated.

*Address correspondence to this author at the Department of Biochemistry, University of Pretoria, Hillcrest 0083, Pretoria, South Africa; Tel: +27-12-420-2486; Fax: +27-12-362 5302,
E-mail: zeno.apostolides@bioagric.up.ac.za

In this review, the animal models that are more frequently used for drug and plant extract testing will be discussed. These are the SIV model due to its similarities in pathogenesis of disease to humans, the FIV and the LP-BM5 model due to wide availability and the SCID murine model that combines components of both systems. The pathogenesis of disease in each model, application in the evaluation of drugs, drug combinations and plant extracts as well as the inherent advantages and disadvantages of each model are discussed.

ANIMALS MODELS FOR HIV/AIDS

Fourteen different animal models have been used to study HIV/AIDS [62, 65, 73] and are listed in Table **1**.

Four different classes of animal models shown in Table **1**, namely primate, ungulate, feline and murine models are available for the study of HIV/AIDS. The rabbit and the rat model were excluded from Table **1**. Rabbits can be experimentally infected with HIV however these animals fail to develop any AIDS-like symptoms despite p24 detection and isolation of HIV from peripheral blood mononuclear cells (PBMC) [69]. Recently it was discovered that cotton rats could be infected with HIV [113] and proviral HIV DNA could be isolated from the spleen and brain. The rats developed fever, weight loss, pulmonary disorders and inflammatory reactions in the brain and spleen. This rat model appears to hold great promise but it has not been widely used.

The purpose of this study was to identify a model from each class of animal that is most frequently used for the evaluation of drugs and plant extracts. In the primate and feline class, macaques infected with African SIV strains and specific pathogen-free cats infected with FIV respectively were identified as models most frequently used for drug and plant extract evaluation. From the ungulate class, no animal model was selected as these are very large experimental animals and these animals are rarely used for the evaluation of drug or plant extracts. The murine class could be further subdivided into murine models infected with HIV, the SCID

1570-162X/06 $50.00+.00

Table 1. Animal models for the study of HIV/AIDS

Animal	Virus	Disease	Ref.
Primate			
African Green Monkey	SIV_{agm}	Virus actively replicates but animals do not develop immunodeficiency	Norley,1996 [93]
Sooty Mangabeys	SIV_{sm}	Chronically viremic but do not develop any disease	Ansari, 2004 [3]
Mandrill monkey	SIV_{mnd}	High levels of viremia but its non-pathogenic to the host	Onanga *et al.*, 2002 [96]
Sykes' monkey	SIV_{syk}	Persistently infected but remain clinically healthy	Hirsch *et al.*, 1993 [50]
Rhesus monkeys	$SIV_{mac/sm}$	AIDS-like disease with immunodeficiency and opportunistic infections	Hirsch *et al.*, 1994 [51]
Cynomolgus monkeys	SIV_{mac}	AIDS-like disease with immunodeficiency	Giavedoni *et al.*, 2000 [35]
Pigtail monkeys	$SIV_{sm/agm}$	AIDS-like disease with immunodeficiency	Hirsch *et al.*, 1994 [51]
Chimpanzees[#]	HIV	Long-term persistent infection but no signs of clinical disease	Fultz *et al.*, 1989 [30]
Rhesus, pig-tailed, cynomolgus and bonnet monkeys	SHIV chimeric virus of SIV and HIV	AIDS-like disease with organ-specific diseases	Joag *et al.*, 1997 [58]
Ungulates			
Cows	BIV	Persistent lymphocytosis and lymphadenopathy	Carpenter *et al.*, 1992 [15]
Goats	CAEV	Arthtitis, encephalomyelitis, wasting, pneumonia	Straub *et al.*, 1989 [128]
Sheep	MVV	Progressive pneumonia, encephalomyelitis	Petursson *et al.*, 1989 [104]
Horses	EIAV	Fever, weight loss, anemia, edema	Coggins *et al.*, 1986 [18]
Feline			
Cats	FIV	AIDS-like disease in naturally infected cats. Experimental cats do not develop fatal immunodeficiency	Willet *et al.*, 1997 [138]
Murine			
SCID Mice	HIV	Severe $CD4^+$ T-cell depletion can remain persistently infected for 16 weeks	Pincus *et al.*, 2004 [106]
Transgenic Mice	Complete HIV-1 proviral sequences, subgenomic fragments or reporter genes linked to HIV-1 LTR	Skin and renal lesions, cardiomyopathy, nephropathy, CNS damage, immunoabnormalities	Pincus *et al.*, 2004 [106]
Mice	LP-BM5 MuLV	Lymphadenopathy, splenomegaly and hypergammaglobulemia. Mice die of respiratory failure	Jolicoeur *et al.*, 1991 [59]
Mice	Moloney MuLV	Chronic T-cell lymphopoiesis and leukemia	Fan *et al.*, 1991 [26]
Mice	Friend MuLV	Hepatosplenomegaly, anemia and leukemia	Koch *et al.*, 1992 [65]
Mice	Rauscher MuLV	Lymphoid leukemia, erythrocytopoiesis, splenomegaly	Rauscher *et al.*, 1962 [109]

[#]Research with chimpanzees infected with HIV/SIV is now banned in several countries.

murine model and murine models infected with murine leukemia virus, the LP-BM5 model.

The pathogenesis of disease in each model, application in the evaluation of drugs, drug combinations and plant extracts as well as the inherent advantages and disadvantages of each model are discussed. A comparison of the genetic organization of the virus in HIV, SIV, FIV and MuLV is shown in Fig. **1**.

THE SIMIAN IMMUNODEFICIENCY VIRUS MODEL

The Simian immunodeficiency viruses (SIVs) are perhaps the closest known relatives of HIV-1 and HIV-2 with very similar genomic organization. Several SIV isolates have been identified: SIV_{mac}/SIV_{sm} isolated from sooty mangabeys, SIV_{agm} from healthy African Green Monkey, SIV_{mnd} from mandrills, SIV_{syk} from Sykes' monkey and SIV_{cpz} isolated from healthy chimpanzees [52]. It is speculated that

HIV-1 originally arose from SIV_{cpz} and HIV-2 from SIV_{sm}. African Green monkeys and sooty mangabeys naturally infected with SIV_{agm} and SIV_{sm} respectively remain asymptomatic throughout their life and do not develop any disease despite being persistently infected [3, 93]. In contrast macaque monkeys such as *Macaca mulatta* (rhesus monkeys), *M. nemenstria* (pigtail monkeys) and *M. fascicularis* (cynomolgus monkeys) infected with SIV_{mac} or SIV_{sm} develop fatal disease characterized by severe immunodeficiency, susceptibility to opportunistic infections and finally death and have been reviewed by Hirsch and Johnson 1994 [51]. Due to the pathogenesis of disease being similar to HIV in humans, these experimentally infected monkeys have been used extensively to study the pathogenesis of HIV/AIDS, test antiviral efficacy of several compounds as well as develop and test vaccines.

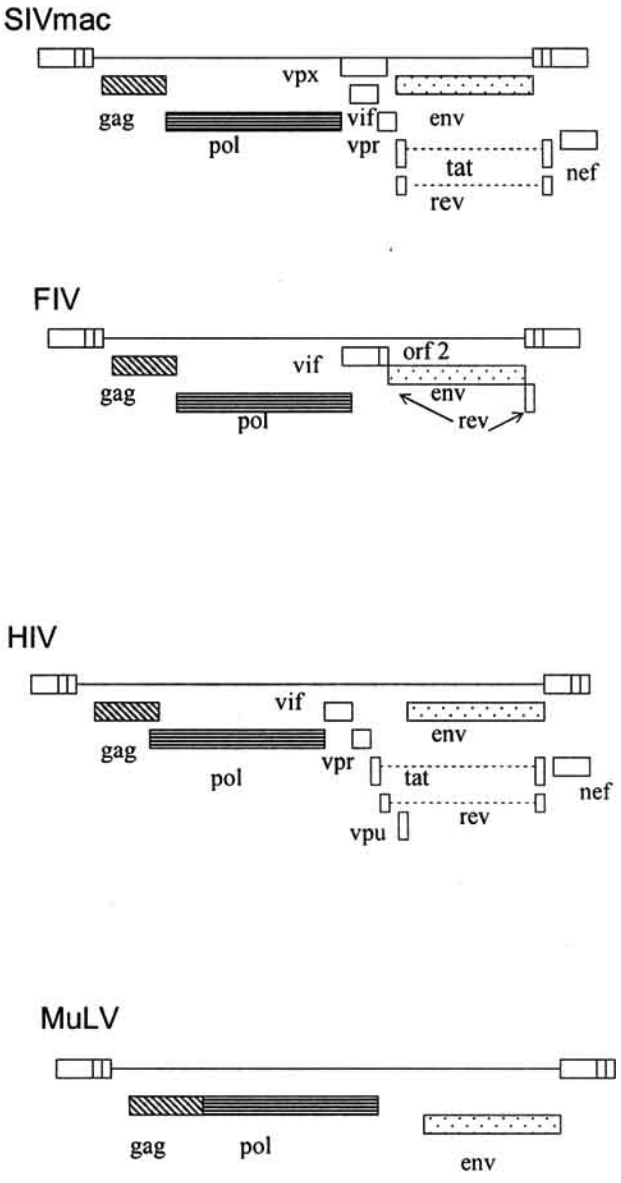

Fig. (1). Comparison of the genetic organization of SIV, FIV, HIV and LP-BM5 MuLV.

Following inoculation of monkeys like *M. mulatta* or *M. fascicularis* with SIV_{mac} 251, the virus spreads rapidly and can be detected 4 days post-infection [97]. Plasma viremia normally peaks at 8-14 days post-infection and then gradually decreases to a steady-state level by 2 months [83, 87, 115, 126]. Clearance of plasma viremia is associated with the appearance of SIV-specific CD8+ cytotoxic T-lymphocytes (CTL) and neutralizing antibodies. These two immune responses are responsible for controlling primary SIV infection [115, 116]. If these two immune responses are unable to reduce plasma viremia the animals rapidly progress to AIDS.

Lymphopenia with a loss of B-cells occurs in the peripheral blood during the first week of infection while T-cell counts stay steady for several weeks before decreasing to below control levels [85]. This initial steady state is due to a decrease in CD4 T-cells that is compensated by an initial increase in CD8 T-cells. As the viral load decreases, the CD8 T-cells also decrease resulting in a decrease in total T-cell counts. There is also a loss in naïve CD4 and naïve CD8 cells early in infection and this may represent changes in homeostatic control mechanisms i.e. homing of CD4 memory T-cell subsets from the periphery to secondary lymphoid organs. There are also changes in the CD8 memory T-cell subset. Early after infection there is an expansion of fully differentiated CD8 memory T-cells followed by a decrease and replacement of differentiated CD8 memory T-cells by undifferentiated cells.

In the lymph nodes, productively infected cells can be detected 5-8 days post infection and the viral RNA levels in the T-cells parallels p27 antigenemia in the blood [111]. The proportion of B cells in the lymph nodes is initially increased but then returns to normal levels [35]. There is also a decrease in CD4+ T-cells nodes and increase in CD8+ T-cells that correlates with clearance of plasma antigenemia [110].

SIV infection also induces cytokine dysregulation. High viral loads are associated with high levels of IFN-α/β and if the plasma IFN-α/β persists, the animals will progress rapidly to disease [35]. Other cytokines that are also found to increase during infection are IL-12, IL-18, IL-1β, IL-6, TNF-α and IL-10 [8, 35].

If the animals are able to control primary infection, an asymptomatic phase occurs that is characterized by low or undetectable levels of plasma viremia and the animals appear to be healthy. A strong SIV-specific antibody response controls viral replication and maintains low levels of viremia. During this phase that can vary from a few months to years there is a continued depletion of CD4 lymphocytes and a progression in lymph node pathology [87].

The terminal phase of disease is characterized by immunodeficiency, disseminated opportunistic infections and SIV invasion of most tissues. A decline in CD4+ lymphocytes occurs, disruption of macrophage functions, increased viral burden in the lymph nodes, spleen and plasma and a widespread dissemination of SIV in almost all the tissues and organ systems especially the gastrointestinal tract (GIT) with many animals dying from gastrointestinal dysfunction [49]. Infected monkeys are also more susceptible to opportunistic infections such as cytomegalovirus [117] microsproridia infections [41] and *Mycobacterium bovis* [119] infections.

SIV Induced Central Nervous System (CNS) Disease

Infection of *M. nemenstria* with a macrophage tropic and neurovirulent recombinant virus SIV/17E-Fr and an immunosuppressive virus SIV/DeltaB670 serves as a good model for the study of SIV invasion of the CNS. SIV enters and replicates in the CNS during the acute phase of infection, then becomes undetectable and re-appears 2 months post-infection [80]. Viral RNA is down-regulated after acute infection while viral DNA persists in all parts of the brain at steady-state levels throughout infection [17]. CD4+ cells are the predominant cell type in the brain parenchyma of uninfected and acutely infected monkeys. There is an increase in the CD8+ lymphocyte population in animals with moderate to severe encephalitis [80]. Severity of encephalitis can also be correlated with increased viral load, elevated levels of IL-6 and macrophage chemotactic protein-1 (MCP-1) in the cerebrospinal fluid (CSF) [81].

In *M. nemenstria* inoculated with SIVsmmFGb, infection results in lesions of the brain parenchyma and includes perivascular accumulation of macrophages, multinucleated giant cells and lymphocytes, parenchymal giant cells, microglial nodules, parenchymal granulomas and vacuolation of white matter tracts of the cerebrum and cerebellum often associated with choriomeningitis [97]. Physiological abnormalities can be detected within the first month in *M. mulatta* infected with SIVmac251 and include increase in temperature, decrease in motor activity and changes in auditory-evoked potentials [54].

Evaluation of Antiviral Therapy

The SIV model *in vivo* and *in vitro* cell culture models have extensively been used to assess the efficacy of several antiretroviral drugs and plant extracts. The animals that have been used are Rhesus monkeys infected with SIVmac239, SIV/deltaB670, SIVsmE66 and SIVmac251 and Cynomolgus monkeys infected with SIVmac251, SIVmac251/32H. *In vitro* cell culture models include human PBMC infected with SIV/deltaB670, co-cultures of human CD4+ Molt-4 cells and persistently infected Jurkat/SIVagm cell, MT4 and 174 x CEM cells with SIVmac251, CEM-SS T-cells with SIV (Delta), MT4 cells with SIVmac Molt-4 cells with SIVagm3 or SIVmndGB1. Several drugs including N-aminoimidazoles, methionine enkephalin and NNRTIs: tivirapine, loviride, delavirdine, nevirapine, pyridinone, MCK-442, drug combinations such as AZT, indinavir and lamivudine as well as hydroxyurea and *Rhizophora apiculata* (mangrove plant) extracts have been evaluated and the findings are summarized in Table **2**.

Advantages and Disadvantages

The advantages in using the SIV model are that the viral genome has great homology with HIV, and the disease and disease progression are very similar to HIV/AIDS. The use of an equivalent *in vitro* cell culture model allows rapid evaluation of drug toxicity and efficiency in reducing proviral DNA incorporation and viral replication in the host cell. Drugs with beneficial effects are subsequently used in *in vivo* animal studies to confirm antiretroviral activity and to determine the absorption, metabolism, distribution, excretion and toxicity (AMDET) of the drug or drug combination. This model has several disadvantages these include the high cost of animals (macaques cost between $5 000-$12 000 per animal) and housing. Availability of animals is limited and there is a risk to investigators of SIV infection [124] and therefore specialized laboratory facilities are required.

FELINE IMMUNODEFICIENCY VIRUS

The feline immunodeficiency virus (FIV) is a T-lymphotropic lentivirus that shares some homology with HIV and other lentiviruses [132]. FIV was first isolated from a group of immunodeficient cats in Petaluma, California [101] and has subsequently been found to infect cats in all parts of the world [14]. This immunodeficiency is not limited to feral and domesticated cats but can also be induced experimentally in specific pathogen free (SPF) cats [66]. These cats, however, can take several years (more than eight years) to develop the fatal immunodeficiency as they are kept in a pathogen-free environment and thus their exposure to other pathogens is limited. The FIV model for HIV has been reviewed by Willet *et al*. 1997 [138].

Following infection, plasma virus and PBMC-associated virus can be detected 2 weeks post-infection [5]. FIV proviral DNA can be detected as early as 1 week post-infection in the peripheral and mesenteric lymph nodes and peaks at 8 weeks in all lymph nodes [27]. Serum antibodies become detectable from 2 weeks post infection [5]. Cats develop a flu-like illness characterized by fever, diarrhea, dehydration and depression by 4-5 weeks following infection. Leucopenia with lymphopenia and neutroprenia are also present and a decrease in the percentage and absolute number of $CD4^+$ cells after inoculation occurs that remains low throughout infection [1, 21, 25, 53, 134]. $CD8^+$ cells, however, are found to increase following infection with a subsequent decrease in the $CD4^+/CD8^+$ cell ratio followed by an inversion of the ratio [1, 134, 53, 25, 5]. B-cell percentage and absolute number in the peripheral blood are not significantly altered nor are there significant changes in serum IgM and IgA. There is however, a significant elevation in IgG levels 2 years after infection [1].

Unlike HIV and SIV, FIV has a broader cell tropism by infecting Ig+/B cells in addition to $CD4^+$, $CD8^+$, monocytes/macrophages [5, 21, 25, 78]. During acute and chronic infection, FIV provirus can be detected in $CD4^+$, $CD8^+$ and B-cells with the highest viral burden occurring in $CD4^+$ cells during the acute infection and in B cells during chronic infection. A decrease in the $CD4^+$ cell population is caused by the elimination of cells, immune responses targeting infected cells or changes in $CD4^+$ cell turnover kinetics [21].

The non-cytolytic T-cells (non-CTL) elicit the first antiviral immune response to FIV and activity can be detected in the peripheral and mesenteric lymph nodes, spleen and blood one week after inoculation [27]. Virus-specific CTL responses are only detected in the blood 4 weeks post-infection and much later in the spleen and lymph nodes. The cell-mediated suppression of FIV-replication can be detected at 4 weeks post-infection and corresponds with the appearance of virus-specific CTL. Suppressor activity declines at week 8 post-infection, peaks again at 47 weeks and is absent in blood at 113 weeks. Long-term infection with FIV results in a progressive immune dysfunction characterized by an absence of primary and secondary antibody responses to T-dependent immunogens but these animals retain the ability to

Table 2. Drugs, Drug Combinations and Plants Extracts Evaluated in the SIV Animal Model

Compound	*In vitro/ in vivo*	Results	Ref.
6-Chloro2',3'dideoxy guanosine,	*In vivo* Rhesus monkeys with SIVmac239	↓ viral burden and suppressed hyperactivation of B-cell proliferation	Otani *et al.*, 1997 [99]
Cyclosporin A	*In vitro* human PBMC with SIV/deltaB670	Did not suppress SIV replication by measurement of p27 levels.	Martin *et al.*, 1997 [83]
	In vivo Rhesus monkeys with SIV/deltaB670	↓ duration of antigenemia, transient ↓ in virus burden, slower loss of $CD4^+$ cells	
Synthetic ajoene (active principle of garlic)	*In vitro* Co-cultures of human CD4+ Molt-4 cells with persistently infected Jurkat/SIVagm cells	Inhibited SIV-mediated cell fusion	Walder *et al.*, 1998 [136]
Interferon	*In vitro* MT4 and 174 x CEM cells with SIVmac251	Blocked early stage of SIV replication, step between attachment and reverse transcription	Taylor *et al.*, 1998 [133]
Didanosine/ddI	*In vivo* Cynomolgus monkeys with SIVmac251	↓ in viral load during acute infection, transient ↑ in IL6, IL1β, TNFα, IL10	Gigout *et al.*, 1998 [37]
12-oxocalonolide A (non-nucleoside reverse transcriptase inhibitor NNRTi)	*In vitro* CEM-SS T-cells with SIV (Delta)	Inhibited SIV replication	Xu *et al.*, 1999 [140]
Extract from *Rhizophora apiculata* (mangrove plant)	*In vitro* MT4 cells with SIVmac	Inhibited virus-induced cytopathogenicity	Premanathan *et al.*, 1999 [108]
NNRTIs: tivirapine, loviride, delavirdine, nevirapine, pyridinone, MCK-442	*In vitro* MT4 cells with SIVmac and Molt-4 cells with SIVagm3 or SIVmndGB1	All NNRTIs inhibited SIVagm3, nevirapine, delavirdine and pyridinone not effective against SIVmac251 and SIVmndGB1. The concentrations required to inhibit the SIV strains were 50-fold the concentrations required to inhibit HIV-1.	Witvrouw *et al.*, 1999 [139]
Tenofovir/PMPA	*In vivo* Rhesus monkeys with SIVsmE660	Did not block infection but prevented establishment of persistent productive infection	Lifson *et al.*, 2000 [75]
Thalidomide	*In vivo* Cynomolgus monkeys with SIVmac251/32H	Inhibited TNFα production, restored proliferative responses to SIV peptides, no reduction in viral burden	Di Fabio *et al.*, 2000 [23]
Tenofovir/PMPA	*In vivo* Rhesus monkeys with SIVmac239	Reduction of viral load and established long-term nonprogressor status in two animals	Spring *et al.*, 2001 [125]
Protease inhibitors: indinavir, saquinavir, ritonavir	*In vitro* HeLa H1-JC.37 cell line, 174 x CEM cells and PBMC with SIVmac239, SIVmac251 and 3' half clone of SIVmac239	Susceptibility to the protease inhibitors was similar to HIV	Giuffre *et al.*, 2003 [38]
AZT, indinavir and lamivudine combination	*In vivo* Cynomolgus monkeys with SIVmac251	Did not prevent infection but one treatment regimen allowed better control of viral replication	Benlhassan-Chahour *et al.*, 2003 [7]
N-aminoimidazoles	*In vitro* MT4 cells with SIVmac251	18 derivative were capable of inhibiting SIV replication, 7 were equally potent inhibitors of HIV-1, HIV-2 and SIV	Lagoja *et al.*, 2003 [70]
Methionine enkephalin	*In vitro* 174 x CEM cells with SIVmac239	Enhanced viability of SIV-infected cells and ↓ number of apoptotic cells	Li *et al.*, 2004 [74]
Hydroxyurea, PMPA and didanosine combination	*In vivo* Rhesus monkeys with SIVmac251	↑ peripheral CD4 T cells without affecting expression of activation markers	Lova *et al.*, 2005 [77]
Tenofovir/PMPA	*In vivo* Rhesus monkeys with SIVmac251	↓ mucosal viral loads, restoration of $CD4^+$ T cells in GALT and peripheral blood	George *et al.*, 2005 [34]

↑: increase.
↓: decrease.

elicit primary antibody responses to T-independent antigens [120, 134].

Lymphadenopathy is associated with FIV infection and the virus can be detected in the lymph nodes, spleen, gut-associated lymphoid tissue (GALT), bone marrow, thymus and tonsils [5]. Lesions are observed in the peripheral and central lymphoid organs as well as non-lymphoid organs and are characterized by a progressive hyperplasia and infiltra-

tion of lymphocytes, lymphoblasts, macrophages and apoptotic cells [5, 13].

FIV CNS Disease

FIV infection of the CNS is associated with several neurological abnormalities. These include development of a persistent anisocoria (inability of iris to constrict completely in response to light) by 3 months post-infection, intermittent delayed righting reflex and papillary responses, delays in auditory and visual evoked responses and dramatic changes in sleep patterns. Virus can be isolated from cerebral cortex, midbrain and cerebellum while FIV-specific antibodies can be detected in the CSF [107]. Neuronal loss and glial activation is accompanied with increased levels of glutamate. Widespread gliosis, perivascular cuffing and activation of astrocytes and microglia is observed while neuronal dropout is confined to the frontal cortices and basal ganglia [107].

Antiviral Drug Testing in FIV Model

The FIV *in vivo* model used for antiviral testing includes SPF cats infected with FIV-Petaluma or FIVUK8 and female cats infected with FIV-CABCpady00C. The *in vitro* cell culture model makes use of different cell types or cell lines and includes MYA-1 cells infected with the FIV strain T91 or

Table 3. Drugs, Drug Combinations and Plant Extracts Evaluated in the FIV Animal Model

Compound	*In vitro/ in vivo*	Results	Ref.
AZT and cyclosporin separately	*In vitro* MYA-1 cells with FIV strain T91 or N91	Only AZT tested *in vitro*. Dose-dependent protection against FIV-induced cell death as well as dose-dependent decrease in RT activity.	Meers *et al.*, 1993 [86]
	In vivo Conventional adult cats with FIV	Drugs did not prevent infection but lowered plasma virus titers at two weeks p.i. but levels then increased. No effect on PBMC virus titers.	
Dehydroepiandrosterone (DHEA)	*In vitro* Feline T cell FL4 with FIV-Petaluma	Inhibited RT activity as measured in culture supernatants	Bradley *et al.*, 1995 [11]
Dideoxycytidine 5'-triphosphate	*In vitro* Monocyte-derived macrophage and peritoneal macrophage cell cultures with FIV	Reduced FIV production by macrophages	Magnani *et al.*, 1995 [78]
	In vivo SPF cats with FIV isolate Pisa-M2	Protected most peritoneal macrophages	
9-[2R,5R-2,5-dihydro-5-phosphonomethoxy)-2-furanyl]adenine (D4API)	*In vitro* PBMC with FIV-Petaluma	Higher efficacy than AZT and PMEA but with more toxicity.	Hartmann *et al.*, 1997 [45]
	In vivo SPF cats with FIV-Petaluma	Abolished viremia and antibody responses but was severely toxic causing death of animals.	
Hypericum caprifoliatum, H. polyanthemum and *H. cannatum*	*In vitro* Crandell feline kidney cells with FIV-34TF10	Methanol extracts of *H. polyanthemum* and *H. cannatum* ↓ FIV in culture supernatant	Schmitt *et al.*, 2001 [114]
AZT/3TC combination	*In vitro* Feline T-cell lines chronically infected with FIVPet(FL-4 cells), FIVBang (FIVBang/FeT-J cells), FIVShi (FIVShi/FeT-J cells) or T-cell enriched PBMC with FIVUK8.	Inhibition of FIV replication in T-cell enriched cultures. Combination had an additive to synergistic effect on this culture. No significant effects on RT activity as measured in cell culture supernatant of the chronically infected T-cell lines	Arai *et al.*, 2002 [4]
	In vivo SPF cats with FIVUK8	Majority of cats were completely protected from FIV infection. Others showed delay in infection and antibody seroconversion. Toxicity seen at high doses	
1,8-Diaminooctane	*In vitro* Crandell feline kidney cells with FIV-34TF10	↓ viral replication in dose-dependent manner, ↓ Rev-dependent CAT system expression, ↓ unspliced and singly spliced viral mRNAs	Hart *et al.*, 2002 [43]
DNA binding polyamides	*In vitro* Fetal glial cell line G355-5 with FIV-34TF10 or PPR-34TF10env chimeric virus	↓ replication of FIV	Sharma *et al.*, 2002 [118]
Protease inhibitor TL-3	*In vivo* Female cats with FIV-CABCpady00C	Did not prevent viremia but ↓ viral loads and ↑ survival rate of symptomatic cats	De Rozieres *et al.*, 2004 [22]
Extracts from plants *Urtica dioica L., Parietaria diffusa M. et K.* and Sambucus nigra L.	*In vitro* Crandell feline kidney cells with FIV-Petulama	All extracts showed antiviral activity against FIV by inhibiting syncytia formation	Manganelli *et al.*, 2005 [79]

↑, ↓ as in Table **2**.

N91, the fetal glial cell line G355-5 infected with FIV-34TF10 or PPR-34TF10env chimeric virus, Crandell feline kidney cells infected with FIV-Petulama *or* FIV-34TF10 or PBMC infected with FIV-Petaluma. Drugs like AZT, cyclosporin, dehydroepiandrosterone (DHEA) and dideoxycytidine 5'-triphosphate, drug combinations like AZT/3TC and plant extracts of *Hypericum caprifoliatum, H. polyanthemum* and *H. cannatum* and *Urtica dioica L., Parietaria diffusa M. et K.* and *Sambucus nigra L*. been evaluated in the FIV model and the findings of these studies are presented in Table **3**.

Advantages and Disadvantages

The advantages of this model are that FIV is a lentivirus like HIV and has some homology to the HIV virus. The disease and disease progression also shares several similarities with HIV/AIDS. The virus is non-pathogenic to humans and is available in the *in vitro* cell culture and *in vivo* animal format. Another advantage is that cats are widely available and one can use SPF or domestic cats. The disadvantages are that SPF cats are fairly expensive ($500-$800) and the fatal immunodeficiency takes a long time to develop. All cats including control animals are at risk of becoming infected, as FIV is a natural host-virus system.

SEVERE COMBINED IMMUNODEFICIENT (SCID) MURINE MODEL

Severe combined immunodeficient (SCID) mice carry an autosomal, recessive mutation that prevents them from producing functional B and T lymphocytes [9]. The mice are unable to repair double-stranded DNA breaks or recombine their VDJ regions [47]. However, these mice continue to have a normal innate immunity with functional macrophages and natural killer activity [20]. Due to this SCID mutation, mice can be reconstituted with human tissues such as human thymus, liver, lung, lymph nodes, PBMC, U937 cells, HIV-infected monocytes, intestinal tissue and vaginal tissue [36, 40, 48, 60, 63, 71, 92, 102]. The SCID mouse model for studying HIV has been reviewed by Goldstein *et al.* 1996 [39].

The thy/liv Model

Human fetal thymus and liver of about 14-23 gestational weeks are implanted in SCID mice under the left or right or both kidney capsules [56, 67, 92]. The two tissues fuse and form a co-joint organ called the thy/liv implant [56]. This co-joint organ can sustain continued human T lymphopoiesis for a year and T cells can be detected in the peripheral circulation at 6 months [92]. The grafts have the appearance of normal human thymus with normal architecture and active T cell lymphopoiesis can be seen in the cortical and medullary areas [56, 92]. Thymocytes, hematopoietic blast cells, immature and mature forms of myelomonocytic cells and megakaryocytes are present and these implants have human progenitor cell activity for CFU-c, colonies of CFU-GM and BFU-E [92].

Mice can be infected with HIV either by directly injecting implant with HIV or by intraperitoneal injection [67]. HIV can be isolated from thymocytes, splenocytes and PMBC one month after infection. HIV *gag* DNA and RNA as well as *tat/rev* mRNA can be detected in the implant, PMBC, spleen and lymph nodes. This indicates that productive infection has been established and active viral replication is occurring. After HIV infection there is an increased expression of TNF-α, TNF-β and IL-2 mRNA in the peripheral lymphoid compartment. HIV can also be detected in CD4+ cells and this is associated with a rapid depletion of these cells at about 3 weeks post-infection with the majority of cells being depleted within a 6-day period [57]. The viral burden peaks when the CD4+ cell depletion occurs and then begins to decrease, as the CD4+ cells are almost all lost. It is suggested that this depletion is caused by direct viral killing of the cells rather than by apoptosis.

This model has also been engrafted with syngeneic human fetal large intestine tissue to create a model that may serve useful to study the mucosal transmission of HIV [37]. Closure of the ends of the implant occurs four months after implantation and a lumen is formed that contains histologically normal GIT mucosa. CD4+ cells are scattered throughout the lamina propria and appear to have migrated from the thy/liv implant since these cells are not seen in mice that only receive an intestinal implant. The mice are infected with HIV by injecting HIV into the intestinal implant or into the thy/liv implant. Scattered HIV-infected cells are seen in the intestinal crypts and the lamina propria when either infection route is used. This shows that HIV can spread from the intestine and infect the thy/liv implant or it could spread from the thy/liv implant and infect the intestinal implant.

The hu-PBL-SCID Model

This model was developed in attempt to overcome the difficulties of obtaining human fetal thymus and liver tissue for the thy/liv model. SCID mice are injected intraperitoneally with human PBMC [90]. There is survival and expansion of human CD3+ T cells as well as small number of B cells, monocytes and NK cells. CD3+ T cells show signs of activation and the memory T cells in CD4+ and CD8+ subsets are selectively expanded. A low number of T-cells are found in the peripheral blood and other lymphoid organs. Human B cells survive as differentiated plasma cells and are found in the lymph nodes and as cell adhesions to the peritoneal cavity. Immunoglobulin production can occur for up to a year. A small number of monocytes/macrophages can also be observed in lymphoid tissue. No human cells are detected in the thymus but are found in the perithymic lymph nodes adjacent to the thymic capsule.

HIV can be introduced by either intraperitoneal injection of the virus or by injecting the mice with HIV-infected PBMC [10, 68, 89]. Mice that are infected intraperitoneally become infected after 3-4 weeks but then the percentage of infected mice decrease between 6-8 weeks. Some animals can remain persistently infected for 16 weeks [89]. HIV can be detected in plasma, spleen, peritoneal lavage, peripheral blood lymphocytes, thymus, bone marrow and lymph nodes but can be more frequently isolated from the peritoneal lavage [68, 89]. HIV p24 antigen can be detected in plasma, spleen and peritoneal lavage, but no antibodies to HIV can be detected. In mice that are infected by reconstitution with HIV-infected PBMC virion, RNA can first detected after 7 days, peaks on day 11 and persists through day 17 [10]. Severe CD4+ lymphocyte depletion is observed 18-25 days after engraftment in the infected mice and the human immunoglobulin produced has a broad reactivity against HIV. HIV can be detected in the spleen, blood and peritoneal wash

cells. This latter method of infection may be more valuable as the viral strains are obtained from the donor and directly transferred to the mice without manipulations in cell culture. Also, key elements of the host immune response may be transferred.

HIV Encephalitis SCID Model

HIV-infected monocyte-derived macrophages (MDM) can be injected into the caudate, putamen, internal capsule and cortex of SCID mice [76, 102]. These mice develop a disease pathologically similar to HIV encephalitis characterized by astrogliosis, neuronal injury and inflammatory response. MDM are immune activated and express HLA-DR, IL-1β, IL-6 and TNF-α [102]. HIV p24 positive cells can be detected [76]. MDM can migrate and their migration results in the initiation of pathological changes in brain tissue distant from the site of initial injury [102]. The spread of infection is accompanied by cytopathic effects and includes multinucleated giant cell formation [76] Neural-inflammatory cell responses start soon after inoculation and neural damage is observed 3 days after inoculation and is prominent around the HIV-infected cells [102]. Pronounced astrogliosis, formation of migroglial nodules and signs of widespread migroglial activation is seen around the MDM [76]. There is a direct correlation between the number of virus-infected cells, astrogliosis and neuronal damage. A disadvantage of this model is that it does not allow for the study of regional differences and since there is no intact CNS, the anatomical and neuropathological events cannot be correlated [102].

Antiviral Therapy Testing

The SCID models, with SCID mice reconstituted with human fetal lymph node, lymphocytes, peripheral blood leukocytes, fetal thymus and liver, U937 cells, HIV-infected monocyte-derived macrophages have been used during the last decade to assess the short-term efficacy of several antiviral compounds. These drugs include bis(heteroaryl)piperazines (BHAPs), AZT, 2'-β-fluoro-2',3'-dideoxyadenosine (fddA), MDL 74,968 (acyclonucleotide derivative of guanine), nucleoside reverse transcriptase inhibitors (NRTIs): Abacavir, AZT, lamivudine, didanosine, stavudine and the findings of these studies are summarized in Table **4**.

Advantages and Disadvantages

The advantages identified with this model are that it is a small animal model; the mice are widely available and are excellent models for rapid drug evaluation. Another advantage is that this model makes use of HIV and many aspects of disease and disease progression is similar to that described for SIV and HIV/AIDS. Imbred mice are used in this model and this may be seen as both an advantage and disadvantage.

Table 4. Drugs and Drug Combinations Evaluated in the SCID Murine Model

Drug	Model	Results	Ref.
Bis(heteroaryl)piperazines (BHAPs)	SCID mice reconstituted with human fetal lymph node	Could block HIV replication but not as effective as AZT	Romero *et al.*, 1991 [111]
AZT	SCID mice reconstituted with human lymphocytes	Dose-response reduction in p24 antigen levels	Alder *et al.*, 1995 [2]
2'-β-fluoro-2',3'-dideoxyadenosine (fddA)	SCID mice reconstituted with human peripheral blood leukocytes	↓ frequency of viral recovery from peritoneal and splenic tissues, ↓ CD4+ T cell depletion	Boyle *et al.*, 1995 [10]
Sulfated pentagalloyl glucose (Y-ART-3)	SCID mice reconstituted with human peripheral blood leukocytes	↓ frequency of mice infected with HIV but not statistically significant. But semi-quantitative measure of HIV detection showed significant effect of drug.	Nakashima *et al.*, 1996 [91]
MDL 74,968 (acyclonucleotide derivative of guanine)	SCID.beige mice reconstituted with human peripheral blood leukocytes	↓ in virus burden and severity of infection	Bridges *et al.*, 1996 [12]
SID 791 (a bicyclam)	SCID mice reconstituted with human fetal thymus and liver	Inhibition of p24 antigen formation, dose-dependent ↓ in viremia	Datema *et al.*, 1996 [19]
Saquinavir	SCID mice reconstituted with human fetal thymus and liver	HIV infection was not prevented but viral loads were significantly ↓	Pettoello-Mantovani *et al.*, 1997 [103]
Type 1 consensus interferon (CINF)	SCID mice reconstituted with human U937 cells	Suppression of HIV infection and ↓ CD4 T cell depletion	Lapenta *et al.*, 1999 [72]
Nucleoside reverse transcriptase inhibitors (NRTIs): Abacavir, AZT, lamivudine, didanosine, stavudine	SCID mice inoculated with HIV-infected human monocyte-derived macrophages	Abacavir and lamivudine were the most successful in reducing both HIV-1 p24 antigen and viral load	Limoges *et al.*, 2000 [76]
2'-deoxy-3'-oxa-4'-thiocytidine (BCH-10652)	SCID mice reconstituted with human fetal thymus and liver	Dose-dependent inhibition of HIV replication	Stoddart *et al.*, 2000 [127]
SCH-C (SCH 351125)	SCID mice reconstituted with human fetal thymus and liver	Dose-dependent inhibition of HIV replication	Strizki *et al.*, 2001 [129]
Stampidine	SCID mice reconstituted with human peripheral blood lymphocytes	Dose-dependent inhibition of a NRTI-resistant HIV-strain	Uckin *et al.*, 2002 [135]

↑, ↓ as in Table **2**.

The advantage is that because the mice are genetically identical there should be less experimental variation which is better for statistical purposes. The disadvantage to using imbred mice is that one cannot assess whether the drug would work differently amongst different individuals. The other disadvantages are that this model is fairly difficult to establish and reconstitution success is not one hundred percent. The availability and the ethical issues surrounding the acquisition of fetal tissue are further factors that need to be considered.

LP-BM5/MURINE ACQUIRED IMMUNODEFICIENCY SYNDROME (MAIDS) MODEL

The LP-BM5 murine leukemia virus (MuLV) was originally described by Laterjet and Duplan and was derived from C57BL/6 mice that had received fractionated, low-dose irradiation [88]. This model has been reviewed in detail by Jolicoeur 1991 [59]. The LP-BM5 MuLV is a complex of retroviruses and consists of a replication-defective virus and two helper viruses [16]. The replication-defective virus has been identified as the disease-causing agent while the two-helper viruses are a B-tropic replication-competent virus and a mink cell focus-inducing virus. The helper viruses assist in the cell-to-cell spreading of the defective virus thereby accelerating the progression of disease. Not all mouse strains are susceptible to LP-BM5 and susceptible strains include C57BL/6, C57BL/10, B10.F, B10.F(13R), B10.P(10R) and I/St while resistant strains include CBA/J, LG/J, C57L/J and A/J mice [44, 55].

Following intraperitoneal inoculation of C57BL/6 mice with LP-BM5, the virus spreads rapidly and can be detected in the mediastinal lymph nodes 2 days post inoculation. The virus then spreads to the spleen and other lymph nodes (lumbar, cervical and inguinal) and can be detected in these organs after one week [121]. Virus can also be detected in thymus, liver, lungs, kidneys, bone marrow and brain at later stages [44, 121]. Like FIV infection, the defective virus is expressed in B-cells, macrophages and T-cells with the highest levels being expressed in the B-cells [61]. Splenic and peritoneal Mac-1^+ cells are also targets. $CD4^+$ T-cells and $CD8^+$ T cells start decreasing after 4 weeks, while B-cells, macrophages and MAC-1^+ cells are increased [141]. There is a rapid loss of T lymphocyte blastogenic responses to mitogens and alloantigens, loss of helper T-cell function and B-cell function. There is an increase in the extracellular Ig levels particularly in IgM which increases by five-fold [100, 141].

MAIDS also causes cytokine dysregulation and during the first week of infection, there is a transient expression of IFN-γ, IL-2, IL-5 and at lower levels IL-4 and IL-10 in the absence of restimulation or mitogens [33]. At 3-12 weeks, high levels of cytokines of Th2 clones including IL-4 and IL-10 are detected as well as the expression of IL-6, IL-1 and TNF. Th-1 related cytokines like Il-2 and IFN-γ production are, however, reduced. Th-2 cytokines are expressed variably but usually at high levels during the later stages of disease.

Splenomegaly and lymphadenopathy develop at 4 weeks post infection [141]. Splenomegaly is characterized by an increase in follicle size and progressive replacement of normal population of small lymphocytes with immunoblasts, plasmacytoid cells and plasma cells [44]. The spleen increases in size and weight and the normal architecture is destroyed. During the advanced stages of diseases, the spleen is filled with nodular masses of lymphoid cells. In the lymph nodes there is infiltration of deep cortex, medulla and thymic medullae by immunoblasts, plasmacytoid cells and plasma cells. Normal architecture is destroyed and almost all the nodes are enlarged and congested. During the advanced stages of disease the lungs, kidneys and liver are also infiltrated and there is extensive replacement of normal parenchyma [100]. The mice eventually die at approximately 24 weeks due to respiratory failure caused by enlargement of the mediastinal lymph nodes [88].

LP-BM5-Induced CNS Disease

Neurological signs can be seen at 12 weeks and include hind limb weakness progressing to paralysis, hind limb clasping, ataxia and a generalized tremor [64]. The brain undergoes extensive infiltration by lymphoid cells. There is infiltration of small areas of the choroid plexus and meninges with extensions into perivascular space by immunoblasts and plasmacytoid cells. This causes extensive destruction of choroid plexus and meninges. No lesions, however, can be seen in the spinal cord or brain.

Antiviral Drug Testing

Besides the *in vivo* animal model, an *in vitro* cell culture model has been established and this consists of LP-BM5-infected bone-marrow cell cultures and SC-1 mouse fibroblast cells with LP-BM5 virus. Both models have been used to evaluate a wide range of drugs such as AZT and lithium, IL-3 in combination with AZT and ddI and plant extracts of *Glycyrrhizin* and *Chlorella vulgaris*. The results of these studies are summarized in Table **5**.

Advantages and Disadvantages

The advantages of this model are that it is small, inexpensive ($10-$20), widely available and an *in vitro* cell culture equivalent that is suitable for rapid drug evaluation is available. Further advantages are that the risk for infection is low, as the virus is non-pathogenic to humans and the immunodeficiency induced in these mice has several similarities with HIV/AIDS. The disadvantages identified with this model are that the virus is not a lentivirus and lacks the accessory genes of HIV and the major cellular targets are the B cells and the CD4+ T-cell populations.

SUMMARY

The advantages and disadvantages of each model are summarized and compared in Table **6**.

CONCLUSION

Several *in vivo* animal and *in vitro* cell culture models are available for evaluation of the antiretroviral activity of drugs, drug combinations and plant extracts. The animal models reviewed in this article have extended present knowledge regarding the biochemical mechanisms, toxicity and the efficacy of many antiretroviral drugs. The SIV model appears to be the most similar to HIV/AIDS in humans particularly in disease progression. However, the disease progression is slow, cost of housing is high and availability of these animals is limited. A small animal model may therefore be

Table 5. Drugs, Drug Combinations and Plant Extracts Evaluated in the LP-BM5/MAIDS Model

Compound	*In vitro/in vivo*	Results	Ref.
AZT	*In vivo*	↓ splenomegaly, restored APC activity and mitogenic responses, prevented immunosuppression when given immediately after inoculation, ↓ RT activity in serum.	Ohnota *et al.*, 1990 [94]
AZT	*In vivo*	Protected mice when given orally or by subcutaneous infusion. Delayed but did not prevent infection.	Eiseman *et al.*, 1991 [24]
IL-3 in combination with AZT and ddI	*In vitro* LP-BM5-infected bone-marrow cell cultures	IL-3 ↓ bone-marrow toxicity of AZT and ddI when used in combination with either drug. It was less effective when used in triple combination.	Gallicchio *et al.*, 1994 [31]
Lithium	*In vivo*	↑ hematocrit, white blood cell count and platelets. ↑ bone marrow and spleen CFU-CM, BFU-E and CFU-Meg.	Gallicchio *et al.*, 1995 [32]
Vitamin E	*In vivo*	Improved immune dysfunction caused by virus. Suppressed ↑ lipid peroxides, splenomegaly and lymphadenopathy. ↑ NK activity, proliferation of T-cells and improved cytokine dysregulation.	Okishima *et al.*, 1996 [95]
Glycyrrhizin (plant extract)	*In vivo*	Extended survival, suppressed splenomegaly and lymphadenopathy	Watanbe *et al.*, 1996 [137]
Chlorella vulgaris (hot water extract)	*In vivo*	↑ IL-12 expression in macrophages and spleen, ↑ IFN-γ in spleen, enhance resistance to *Listeria monocytogenes*, ↓ IL-10.	Hasegawa *et al.*, 1997 [46]
PMPA and PMEA	*In vitro* SC-1 mouse fibroblast cells with LP-BM5	Less effective than AZT in inhibiting BM5eco. PMPA was the least toxic.	Suruga *et al.*, 1998 [131]
	In vivo	Prevented splenomegaly and lymphadenopathy, conserved mitogenic responses and ↓ activated B cells and viral replication.	
AZT and fludarabine monophosphate combination	*In vivo*	Fludarabine given alone ↓ disease progression and viral load. In combination with AZT: ↓ proviral DNA in spleen, bone marrow and lymph nodes and restored mitogenic responses	Fraternale *et al.*, 2000 [28]
Vitamin E and AZT	*In vivo*	Both inhibited splenomegaly but AZT was more effective. Both drugs normalized changes in INF-γ and TNF-α. Only Vitamin E suppressed NF-κβ	Hamada *et al.*, 2000 [42]
Tyrphostin AG-1387	*In vitro* SC-1 mouse fibroblast cells with LP-BM5	Dose-dependent inhibition of RT activity in culture supernatant. ↓ in viral protein amount.	Sklan *et al.*, 2000 [122]
	In vivo	↓ splenomegaly and lymphadenopathy. Restored responses to ConA. No viral RNA could be detected in treated mice.	
AZT, ddI and glutathione (GSH)-loaded erythrocyte triple combination	*In vivo*	Greater ↓ in bone marrow and brain proviral DNA content of macrophages than in mice treated with AZT and ddI combination. Restored proliferative responses to mitogens.	Fraternale *et al.*, 2002 [29]
Heteronucleotide of AZT and PMPA (AZTpPMPA)	*In vivo*	↓ in IgG level and proviral DNA in lymph nodes but greater ↓ was observed with AZT and PMPA combination or PMPA alone. ↓ in splenomegaly and lymphadenopathy.	Rossi *et al.*, 2002 [112]
Ribonucleotide reductase inhibitors: trimidox (TX), didox (DX) and hydroxyurea (HU)	*In vivo*	All drugs inhibited splemomegaly, ↓ IgG and proviral DNA content of spleen. HU was however more toxic and ↓ WBC, hematocrit femur cellularity, CFU-GM and BFU-E.	Mayhew *et al.*, 2002 [84]
Combinations of abacavir with either HU, TX or DX	*In vivo*	All combinations ↓ splenomegaly, IgG level, proviral DNA content of spleen. HU combination caused gross toxicity, ↓RBC count and CFU-GM	Sumpter *et al.*, 2004 [130]
Combinations of ddI with either HU, TX or DX	*In vivo*	↓ in splenomegaly, IgG level, B-cell activation and proviral DNA content of spleens by all combinations with DX and ddI combination being the most effective. Toxicity: combinations ↓ WBC count, HU combination ↓ hematocrit, HU and TX combinations ↓ femur cellularity, HU combination ↓ CFU-GM and BFU-E.	Mayhew *et al.*, 2005 [85]

↑, ↓ as in Table **2**.

more convenient for rapid drug and plant extract screening. A murine model like the SCID mice and the LP-BM5/MAIDS model may be more suitable for this purpose particularly the LP-BM5/MAIDS model. This model despite having some differences to HIV/AIDS in humans, which will have to be taken into consideration when evaluating data, has several advantages. The disease progression is fast for rapid drug screening, the mice are relatively inexpensive, there is an *in vitro* equivalent and the investigator does not run the risk of being infected with the virus unlike the SCID

Table 6. Advantages and Disadvantages of the SIV, FIV, SCID and LP-BM5/MAIDS Models in the Evaluation of the Antiretroviral Activity of Drugs and Plants

Model	SIV model	FIV model	SCID mouse	LP-BM5/MAIDS
Virus type	Lentivirus	Lentivirus	Lentivirus	Type C oncornavirus
Natural Virus-host system	No	Yes	No	No
Risk of investigator infection	Yes	No	Yes	No
Availability	Rhesus monkeys becoming scarce	Widely	Widely	Widely
Cost per animal ($)	5 000 – 12 000	500 – 800	40 – 60	10 – 20
Per diem costs ($)	10 – 20	4 – 6	Less than 1	Less than 1
Experimental duration	Variable depending on SIV strain. Very rapid strains like $SIV_{smm}PBj$ cause death in 7-14 days, $SIV_{mac}239$ causes death in 3-6 months, SIV_{mne} 1 year, $SIV_{mac}BK28$ 2-5 years	Experimentally infected cats take several years (more than eight) to develop AIDS	HIV infection usually stable for a month but some can stay persistently infected for up to 16 weeks	Mice die after approximately 4 – 6 months
Similarities with HIV/AIDS:				
Major cell targets	CD4 T cells, macrophages	CD4 T cells, macrophages	CD4 T cells, monocyte-derived macrophages	B-cells are major targets but CD4 T cells are needed to spread disease
Receptor	CD4, CCR5, few use CXCR4	CXCR4, may use feline homologue of CD9, maybe CCR5	Same as HIV	Unknown
Disease progression of acute phase, asymptomatic phase, terminal phase	Yes	Terminal phase only in naturally infected cats	Acute phase	No latency period
CD4 depletion	Yes	Yes	Yes	Yes
Virus-specific responses	CTL and antibodies	CTL and antibodies	Can engraft T lymphocytes that then develop CTL responses	No
Variable disease progression	Months-years	Months-years	Infection can be stable up to 16 weeks	No
Opportunistic infections	Yes	Yes	Yes	Yes
CNS disease	Yes	Yes	Yes	Yes
Destruction of lymph node architecture	Yes	Yes	No	Yes
Lymphomas	Yes	Yes	Yes	Yes
Used for drug evaluation	Yes	Yes	Yes	Yes
Used for medicinal plant evaluation	Yes	Yes	No	Yes
In vivo and *in vitro* models	Yes	Yes	Yes *In vitro* model of humans cells infected with HIV	Yes
Used for vaccine evaluation	Yes	Yes	Yes	No

model that uses HIV and human tissue. We conclude that the MAIDS model with its *in vitro* equivalent is the most suitable for screening medicinal plants for antiviral properties as well as evaluating drug-plant combinations. Such studies may provide the necessary scientific data required for endorsing the use of medicinal plants for AIDS sufferers.

ABBREVIATIONS

3TC = Lamivudine

AIDS = Acquired immunodeficiency syndrome

APC = Antigen presenting cell

AZT = Azidothymidine

BFU-E = Erythroid burst-forming units

BIV = Bovine immunodeficiency virus

CAEV = Caprine arthritis-encephalitis virus

CFU-c = Colony forming units in culture

CFU-GM = Granulocyte/macrophage colony forming units

ddI = Didanosine

EIAV = Equine infectious anemia virus

HIV = Human immunodeficiency virus

IFN = Interferon

IL = Interleukin

Ig = Immunoglobulin

MVV = Maedi-visna virus

MuLV = Murine leukemia virus

NK = Natural killer

PMPA = 9-phosphonylmethoxypropyl adenine

PMEA = 9-phosphonylmethoxyethyl adenine

TNF = Tumor necrosis factor

REFERENCES

[1] Ackley CD, Yamamoto JK, Levy N, Pedersen NC, Cooper MD. (1990). Immunologic abnormalities in pathogen-free cats experimentally infected with feline immunodeficiency virus. Journal of Virology. 64: 5652-5655.

[2] Alder J, Hui YH, Clement J. (1995). Efficacy of AZT therapy in reducing p24 antigen burden in a modeified SCID mouse model of HIV infection. Antiviral Research. 27: 85-97.

[3] Ansari AA. (2004). Autoimmunity, anergy, lentiviral immunity and disease. Autoimmunity Reviews. 3: 530-540.

[4] Arai M, Earl DD, Yamamoto JK. (2002). Is AZT/eTC therapy effective against FIV infection or immunopathogenesis? Veterinary Immunology and Immunopharmacology. 85: 189-204.

[5] Beebe AM, Dua N, Faith TG, Moore PF, Pedersen NC, Dandekar S. (1994). Primary stage of feline immunodeficiency virus infection: viral dissemination and cellular targets. Journal of Virology. 68: 3080-3091.

[6] Bendinelli M, Pistello M, Lombardi S, Poli A, Garzelli C, Matteucci D, Ceccherini-Nelli L, Malvaldi G, Tozzini F. (1995). Feline immunodeficiency virus: an interesting model for AIDS studies and an important cat pathogen. Clinical Microbiology Reviews. 8: 87-112.

[7] Benlhassan-Chahour K, Penit C, Dioszeghy V, Vasseur F, Janvier G, Rivieri Y, Dereuddre-Bosquet N, Dormont D, Le Grand R, Vaslin B. (2003). Kinetics of ymphocyte proliferation during primary immune response in macaques infected with pathogenic simian immunodeficiency virus SIVmac251: preliminary report of the effect of early antiviral therapy. Journal of Virology. 77: 12479-12493.

[8] Benveniste O, Vaslin B, Le Grand R, Fouchet P, Omessa V, Theodoro F, Fretier P, Clayette P, Boussin F, Dormont D. (19960. Interleukin 1β, interleukin 6, tumor necrosis factor α, and interleukin 10 responses in peripheral blood mononuclear cells of cynomolgus macaques during acute infection with SIVmac251. AIDS Research and Human Retroviruses. 12: 241-250.

[9] Bosma GC, Custer RP, Bosma MJ. (1983). A severe combined immunodeficiency mutation in the mouse. Nature. 301: 527-530.

[10] Boyle MJ, Connors M, Flanigan M.E, Geiger SP, Ford Jr H, Baseler M, Adelsberger J, Davey Jr RT, Lane HC. (1995). The human HIV/peripheral blood lymphocyte (PBL)-SCID mouse. The Journal of Immunology. 154: 6612-6623.

[11] Bradley WG, Kraus LA, Good RA, Day N.K. (1995). Dehydroepiandrosterone inhibits replication of feline immunodeficiency virus in chronically infected cells. Veterinary Immunology and Immunopathology. 46: 159-168.

[12] Bridges CG, Taylor DI, Ahmed PS, Brennan TM, Hornsperger J.-M, Nave J.-F, Casara P, Tyms AS. (1996). MDL 74,968, a new acyclonucleotide analog: activity against human immunodeficiency virus *in vitro* and in hu-PBL-SCID.Beige mouse model of infection. Antimicrobial Agents and Chemotherapy. 40: 1072-1077.

[13] Callanan JJ, Racz P, Thompson H, Jarrett O. (1993). Morphologic characterization of the lymph node changes in feline immunodeficiency virus infection as an animal model of AIDS. In: Racz P, Letvin NL and Gluckman JC Eds, Animal models of HIV and other retroviral infections. Karger, Basel. pp. 115-136.

[14] Carpenter MA, Brown EW, MacDonald DW, O'Brien SJ. (1998). Phylogeographic patterns of feline immunodeficiency virus genetic diversity in the domestic cat. Virology. 251: 234-243.

[15] Carpenter S, Miller LD, Alexandersen S, Whetstone CA, Van Der Maaten MJ, Viuff B, Wannemuehler Y, Miller JM, Roth JA. (1992). Characterization of early pathogenic effects after experimental infection of calves with bovine immunodeficiency-like virus. Journal of Virology. 66(2): 1074-1083.

[16] Chattopadhyay SK, Sengupta DN, Fredrickson TN, Morse III HC, Hartley JW. (1991). Characteristics and contributions of defective, ecotropic, and mink cell focus-inducing viruses involved in a retrovirus-induced immunodeficiency syndrome of mice. Journal of Virology. 65: 4232-4241.

[17] Clements JE, Babas T, Mankowski JL, Suryanarayana K, Piatak Jr M, Tarwater PM, Lifson JD, Zink MC. (2002). The central nervous system as a reservoir for simian immunodeficiency virus (SIV): steady-state levels of SIV DNA in brain from acute through asymptomatic infection. The Journal of Infectious Diseases. 186: 905-913.

[18] Coggins L. (1986). Equine retrovirus infection. In: Salzman LA Ed. Animal models of retrovirus infection and their relationship to AIDS. Academic Press, Inc., Florida. pp. 203-211.

[19] Datema R, Rabin L, Hinchenbergs M, Moreno MB, Warren S, Linquist V, Rosenwirth B, Seifert J, McCune JM. (1996). Antiviral efficacy *in vivo* of the anti-human immunodeficiency virus bicyclam SDZ SID 791 (JM 3100), an inhibitor of infectious cell entry. Antimicrobial Agents and Chemotherapy. 40: 750-754.

[20] Davis PH, Stanley Jr SL. (2003). Breaking the species barrier: use of SCID mouse-human chimeras for the study of human infectious diseases. Cellular Microbiology. 5: 849-860.

[21] Dean GA, Reubel GH, Moore PF, Pedersen NC. (1996). Proviral burden and infection kinetics of feline immunodeficiency virus in lymphocyte subsets of blood and lymph node. Journal of Virology. 70: 5165-5169.

[22] De Rozieres S, Swan CH, Sheeter DA, Clingerman KJ, Lin Y, Huitron-Resendiz S, Hendrikson S, Torbett BE, Elder JH. (2004). Assessment of FIV-C infection of cats as a function of treatment with the protease inhibitor, TL-3. Retrovirology. 1: 38-49.

[23] Di Fabio S, Trabattoni D, Geraci A, Ruzzante S, Panzini G, Fusi ML, Chiarotti F, Corrias F, Belli R, Verani P, Dalgleish A, Clerici M, Titti F. (2000). Study of immunological and virological parameters during thalidomide treatment of SIV-infected cynomolgus monkeys. Journal of Medical Primatology. 29: 1-10.

[24] Eiseman JL, Yetter RA, Fredrickson TN, Shapiro SG, MacAuley C, Bilello JA. (1991). Effect of 3'azidothymidine administered in drinking water or by continuous infusion on the development of MAIDS. Antiviral Research. 16: 307-326.

[25] English RV, Johnson CM, Gebhard DH, Tompkins MB. (1993). *In vivo* lymphocyte tropism of feline immunodeficiency virus. Journal of Virology. 67: 5175-5186.

[26] Fan H, Brightman K, Davis BR, Li Q. (1991). Leukomogenesis by Moloney murine leukemia virus. In: Fan HY, Chen ISY, Rosenberg N, Sugden W Eds. Viruses that affect the immune system. American Society for Microbiology, Washington, D.C. pp. 155-174.

[27] Flynn JN, Dunham S, Mueller A, Cannon C, Jarrett O. (2002). Involvement of cytolytic and non-cytolytic T cells in control of feline immunodeficiency virus infection. Veterinary Immunology and Immunopathology. 85 (3-4): 159-170.

[28] Fraternale A, Casabianca A, Tonelli A, Vallanti G, Chiarantini L, Brandi G, Celeste AG, Magnani M. (2000). Inhibition of murine AIDS by alternate administration of azidothymidine and fludarabine monophosphate. Journal of Acquired Immune Deficiency Syndromes. 23: 209-220.

[29] Fraternale A, Casabianca A, Orlandi C, Cerasi A, Chiarantini L, Brandi G, Magnani M. (2002). Macrophage protection by addition of glutathione (GSH)-loaded erythrocytes to AZT and DDI in a murine AIDS model. Antiviral Research. 56: 263-272.

[30] Fultz PN, McClure HM, Swenson RB, Anderson DC. (1989). HIV infection of chimpanzees as a model for testing chemotherapies. Intervirology. 30 (Suppl. 1): 51-58.

[31] Gallicchio VS, Hughes NK. (1994). Influence of interleukin-3 (IL-3) on the hematopoietic toxicity associated with combination antiviral drugs (zidovudine and DDI) *in vitro* using retrovirus-infected bone marrow cells. International Journal of Immunopharmacology. 16: 359-366.

[32] Gallicchio VS, Hughes NK, Tse K.-F, Ling J, Birch NJ. (1995). Effect of lithium in immunodeficiency: improved blood cell formation in mice with decreased hematopoiesis as the result of LP-BM5 MuLV infection. Antiviral Research. 26: 189-202.

[33] Gazzinelli RT, Makino M, Chattopadhyay SK, Snapper CM, Sher A, Hugin AW, Morse III H.C. (1992). $CD4^+$ subset regulation in viral infection. The Journal of Immunology. 148: 182-188.

[34] George MD, Reay E, Sankaran S, Dandekar S. (2005). Early antiretroviral therapy for simian immunodeficiency virus infection leads to mucosal $CD4^+$ T-cell restoration and enhanced gene expression regulating mucosal repair and regeneration. Journal of Virology. 79: 2709-2719.

[35] Giavedoni LD, Velasquillo MC, Parodi LM, Hubbard GB, Hodara VL. (2000). Cytokine expression, natural killer cell activation, and phenotypic changes in lymphoid cells from rhesus macaques during acute infection with pathogenic simian immunodeficiency virus. Journal of Virology. 74: 1648-1657.

[36] Gibbons C, Kollmann TR, Pettoello-Mantovani M, Kim A, Goldstein H. (1997). Thy/Liv-SCID-hu mice implanted with human intestine: an *in vivo* model for investigation of mucosal transmission of HIV. AIDS Research and Human Retroviruses. 13: 1453-1460.

[37] Gigout L, Vaslin B, Matheux F, Caufour P, Neildez O, Cheret A, Lebel-Binay S, Theodoro F, Dilda P, Benveniste O, Clayette P, Le Grand R, Dormont D. (1998). Consequences of ddI-induced reduction of acute SIVmac251 virus load on cytokine profiles in cynomolgus macaques. Research Virology. 149: 341-354.

[38] Giuffre AC, Higgins J, Buckheit Jr RW, North TW. (2003). Susceptibilities of simian immunodeficiency virus to protease inhibitors. Antimicrobial Agents and Chemotherapy. 47: 1756-1759.

[39] Goldstein H, Pettoello-Mantovani M, Kaptopodis NF, Kim A, Yurasov S, Kollmann TR. (1996). SCID-hu mice: a model for studying disseminated HIV infection. Seminars in Immunology. 8: 223-231.

[40] Grandadam M, Cesbron J.-Y, Candotti D, Vinatier D, Pauchard M, Capron A, Debre P, Huraux J.-M, Autran B, Agut H. (1995). Dose-dependent systemic human immunodeficiency virus infection of SCID-hu mice after intraperitoneal virus infection. Research Virology. 146: 101-112.

[41] Green LC, Didier PJ, Bowers LC, Didier ES. (2004). Natural and experimental infection of immunocompromised rhesus macaques (*Macaca mulatto*) with the microsporidian *Enterocytozoon bieneusi* genotype D. Microbes and Infection. 6: 996-1002.

[42] Hamada M, Yamamoto S, Kishino Y, Moriguchi S. (2000). Vitamin E suppresses the development of murine AIDS through the inhibition of nuclear factor-kappa B expression. Nutrition Research. 20: 1163-1171.

[43] Hart RA, Billaud J, Choi SJ, Philips TR. (2002). Effects of 1,8-diaminooctane on the FIV rev regulatory system. Virology. 304: 97-104.

[44] Hartley JW, Fredrickson TN, Yetter RA, Makino M, Morse III HC. (1989). Retrovirus-induced murine acquired immunodeficiency syndrome: natural history of infection and differing susceptibility of inbred mouse strains. Journal of Virology. 63: 1223-1231.

[45] Hartmann K, Ferk G, North TW, Pedersen NC. (1997). Toxicity associated with high dosage 9-[(2R,5R-2,5-dihydro-5-phosphonomethoxy)-2-furanyl]adenine therapy and attempts to abort early FIV infection. Antiviral Research. 36: 11-25.

[46] Hasegawa T, Kimura Y, Hiromatsu K, Kobayashi N, Yamada A, Makino M, Okuda M, Sano T, Nomoto K, Yoshikai Y. (1997). Effect o hot water extract of *Chlorella vulgaris* on cytokine expression patterns in mice with murine acquired immunodeficiency syndrome after infection with *Listeria monocytogenes*. Immunopharmacology. 35: 273-282.

[47] Hendrikson EA, Qin X, Bump EA, Schatz DG, Oettinger M, Weaver DT. (1991). A link between double-strand break related repair and V(D)J recombination: the *scid* mutation. Proceedings from the National Academy of Sciences of United States of America. 88: 4061-4065.

[48] Hesselton RM, Koup RA, Cromwell MA, Graham BS, Johns M, Sullivan JL. (1993). Human peripheral blood xenografts in the SCID mouse: characterization of immunologic reconstitution. The Journal of Infectious Diseases. 168: 630-640.

[49] Hirsch VM, Zack PM, Vogel AP, Johnson PR. (1991). Simian immunodeficiency virus infection of macaques: end-stage disease is characterized by widespread distribution of proviral DNA in tissues. The Journal of Infectious Diseases. 163: 976-988.

[50] Hirsch VM, Dapolito GA, Goldstein S, McClure H, Emau P, Fultz PN, Isahakia M, Lenroot R, Myers G, Johnson PR. (1993). A distinct African lentivirus from Sykes' monkeys. Journal of Virology. 67: 1517-1528.

[51] Hirsch VM. (1994). Pathogenic diversity of simian immunodeficiency viruses. Virus Research. 32: 183-203.

[52] Hirsch VM, Dapolito G, Goeken R, Campbell BJ. (1995). Phylogeny and natural history of the primate lentiviruses, SIV and HIV. Current Opinion in Genetics and Development. 5: 798-806.

[53] Hoffmann-Fezer G, Thum J, Ackley C, Herbold M, Mysliwietz J, Thefeld S, Hartmann K, Kraft W. (1992). Decline in $CD4^+$ cell numbers I cats with naturally acquired feline immunodeficiency virus infection. Journal of Virology. 66: 1484-1488.

[54] Horn TFW, Huttron-Resendiz S, Weed MR, Hendriksen SJ, Fox HS. (1998). Early physiological abnormalities after simian immunodeficiency virus infection. Proceedings from the National Academy of Sciences of the United States of America. 95: 15072-15077.

[55] Huang M, Simard C, Jolicoeur P. (1992). Susceptibility of inbred strains of mice to murine AIDS (MAIDS) correlates with target cell expansion and high expression of defective MAIDS virus. Journal of Virology. 66: 2398-2406.

[56] Jamieson BD, Aldrovandi GM, Zack JA. (1996). The SCID-hu mouse: an *in vivo* model for HIV-1 pathogenesis and stem cell therapy for AIDS. Seminars in Immunology. 8: 215-221.

[57] Jamieson BD, Uittenbogaart CH, Schmid I, Zack JA. (1997). High viral burden and rapid $CD4^+$ cell depletion in human immunodeficiency virus type 1-infected SCID-hu mice suggest direct viral killing of thymocytes *in vivo*. Journal of Virology. 71: 8245-8253.

[58] Joag SV, Li Z, Foresman L, Pinson DM, Raghavan R, Zhuge W, Adany I, Wang C, Jia F, Sheffer D, Ranchalis J, Watson A, Narayan O. (1997). Characterization of the pathogenic KU-SHIV model of acquired immunodeficiency syndrome in macaques. AIDS Research and Human Retroviruses. 13: 635-645.

[59] Jolicoeur PJ. (1991). Murine acquired immunodeficiency syndrome (MAIDS): an animal model to study the AIDS pathogenesis. FASEB Journal. 5: 2398-2405.

[60] Kaneshima H, Shih C, Namikawa R, Rabin L, Outzen H, Machado SG, McCune JM. (1991). Human immunodeficiency virus infection of human lymph nodes in the SCID-hu mouse. Proceedings from the National Academy of Sciences of United States of America. 88: 4523-4527.

[61] Kim WK, Tang Y, Kenny JJ, Longo DL, Morse III HC. (1994). In murine AIDS, B cells are early targets of defective virus and are required for efficienct infection and expression of defective virus in T cells and macrophages. Journal of Virology. 68: 6767-6769.

[62] Kindt TJ, Hirsch VM, Johnson PP, Sawasdikosol S. (1992). Animal models for acquired immunodeficiency syndrome. Advances in Immunology. 52: 425-473.

[63] Kish TM, Budgeon LR, Welsh PA, Howett MK. (2001). Immunological characterization of human vaginal xenografts in immunocompromised mice. American Journal of Pathology. 159: 2331-2345.

[64] Klinken SP, Fredrickson TN, Hartley JW, Yetter RA, Morse III HC. (1988). Evolution of B cell lineage lymphomas in mice with a retrovirus-induced immunodeficiency syndrome, MAIDS. The Journal of Immunology. 140: 1123-1131.

[65] Koch JA, Ruprecht RM. (1992). Animal models for anti-AIDS therapy. Antiviral Research. 19: 81-109.

[66] Kohmoto M, Uetsuka K, Ikeda Y, Inoshima Y, Shimojima M, Sato E, Inada G, Toyosaki T, Miyazawa T, Doi K, Mikami T. (1998). Eight-year observation and comparative study of specific pathogen-free cats experimentally infected with feline immunodeficiency virus (FIV) subtypes A and B: terinal acquired immunodeficiency

syndrome in a cat infected with FIV Petaluma strain. Journal of Veterinary Medical Sciences. 60: 315-321.

[67] Kollmann TR, Pettoello-Mantovani M, Zhuang X, Kim A, Hachamovitch M, Smarnworawong P, Rubinstein A, Goldstein H. (1994). Disseminated human immunodeficiency virus 1 (HIV-1) infection in SCID-hu mice after peripheral inoculation with HIV-1. Journal of Experimental Medicine. 179: 513-522.

[68] Koup RA, Hesselton RM, Safrit JT, Somasundaran M, Sullivan JL. (1994). Quantitative assessment of human immunodeficiency virus type 1 replication in human xenografts of acutely infected Hu-PBL-SCID mice. AIDS Research and Human Retroviruses. 10: 279-284.

[69] Kulaga H, Folks T, Rutledge R, Truckenmiller ME, Gugel E, Kindt TJ. (1989). Infection of rabbits with human immunodeficiency virus 1. The Journal of Experimental Medicine. 169: 321-326.

[70] Lagoja IM, Pannecouque C, Van Aerschot A, Witvrouw M, Debyser Z, Balzarini J, Herdewijn P, De Clercq E. (2003). *N*-aminoimidazole derivatives inhibiting retroviral replication *via* a yet unidentified mode of action. Journal of Medicinal Chemistry. 46: 1546-1553.

[71] Lapenta C, Fais S, Rizza P, Spada M, Logozzi MA, Parlato S, Santini SM, Pirillo M, Belardelli F, Proietti E. (1997). U937-SCID mouse xenografts: a new model for acute *in vivo* HIV-1 infection suitable to test antiviral strategies. Antiviral Research. 36: 81-90.

[72] Lapenta C, Santini S, Proietti E, Rizza P, Logozzi MA, Spada M, Parlato S, Fais S, Pitha PM, Belardelli F. (1999). Type 1 interferon is a powerful inhibitor of *in vivo* HIV-1 infection and preserves human $CD4^+$ T cells from virus-induced depletion in SCID mice transplanted with human cells. Virology. 263: 78-88.

[73] Lewis AD, Johnson PR. (1995). Developing animal models for AIDS research – progress and problems. TIBTECH. 13: 142-150.

[74] Li P, Hao Y, Zhang F, Liu X, Liu S, Li G. (2004). Signaling pathway involved in methionine enkephalin-promoted survival of lymphocytes infected by simian immunodeficiency virus in the early stage *in vitro*. International Immunopharmacology. 4: 79-90.

[75] Lifson JD, Rossio JL, Arnaout R, Li L, Parks TL, Schneider DK, Kiser RF, Coalter VJ, Walsh G, Imming RJ, Fisher B, Flynn BM, Bischofberger N, Piatak Jr M, Hirsch VM, Nowak MA, Wodarz D. (2000). Containment of simian immunodeficiency virus infection: cellular immune responses and protection from rechallenge following transient postinoculation antiretroviral treatment. Journal of Virology. 74: 2584-2593.

[76] Limoges J, Persidsky Y, Poluektova L, Rasmussen J, Ratanasuwan W, Zelivyanskaya M, McClernon DR, Lanier ER, Gendelman HE. (2000). Evaluation of antiretroviral drug efficacy for HIV-1 encephalitis in SCID mice. Neurology. 54; 379-389.

[77] Lova L, Groff A, Ravot E, Comolli G, Xu J, Whitman L, Lewis M, Foli A, Lisziewicz J, Lori F. (2005). Hydroxyurea exerts a cytostatic but not immunosuppressive effect on T lymphocytes. Acquired Immunodeficiency Syndromes. 19: 137-144.

[78] Magnani M, Rossi L, Fraternale A, Silvotti L, Quintavalla F, Piedimonte G, Matteucci D, Baldinotti F, Bendinelli M. (1995). FIV infection of macrophages: *in vitro* and *in vivo* inhibition by dideoxycytidine 5'-triphosphate. Veterinary Immunology and Immunopathology. 46: 151-158.

[79] Manganelli REU, Zaccaro L, Tomei PE. (2005). Antiviral activity *in vitro* of *Urtica dioica* L., *Parietaria diffusa* M. et K. and *Sambucus nigra* L. Journal of Ethnopharmacology. 98; 323-327.

[80] Mankowski JL, Clements JE, Zink MC. (2002). Searching for clues: tracking the pathogenesis f human immunodeficiency virus central nervous system disease by use of an accelerated, consistent simian immunodeficiency virus macaque model. The Journal of Infectious Diseases. 186 (Suppl. 2): S199-S208.

[81] Mankowski JL, Queen SE, Clements JE, Zink MC. (2004). Cerebrospinal fluid markers that predict SIV CNS disease. Journal of Neuroimmunology. 157 (1-2): 66-70.

[82] Martin LN, Murphy-Corb M, Mack P, Baskin GB, Pantaleo G, Vaccarezza M, Fox CH, Fauci AS. (1997). Cylosporin A modulation of early virologic and immunologic events during primary simian immunodeficiency virus infection in rhesus monkeys. The Journal of Infectious Diseases. 176: 374-383.

[83] Mattapallil JJ, Letvin NL, Roederer M. (2004). T-cell dynamics during acute SIV infection. Acquired Immunodeficiency Syndromes. 18: 13-23.

[84] Mayhew CN, Mampuru LJ, Chendil D, Ahmed MM, Phillips JD, Greenberg RN, Elford HL, Gallicchio VS. (2002). Suppression of retrovirus-induced immunodeficiency disease (murine AIDS) by trimidox and didox. Novel ribonucleotide reductase inhibitors with less bone marrow toxicity than hydroxyurea. Antiviral Research. 56: 167-181.

[85] Mayhew CN, Sumpter R, Inayat MS, Cibull M, Philips JD, Elford HL, Gallicchio VS. (2005). Combination of inhibitors of lymphocyte activation (hydroxyurea, trimidox, and didox) and reverse transcriptase (didanosine) suppresses development of murine retrovirus-induced lymphoproliferative disease. Antiviral Research. 65: 13-22.

[86] Meers J, Del Fierro GM, Cope RB, Park HS, Greene WK, Robinson WF. (1993). Feline immunodeficiency virus infection: plasma, but not peripheral blood mononuclear cell virus titer is influenced by zidovudine and cyclosporine. Archives of Virology. 132: 67-81.

[87] Monceaux V, Estaquier J, Fevrier M, Cumont M, Riviere Y, Aubertin A, Ameisen JC, Hurtrel B. (2003). Extensive apoptosis in the lymphoid organs during primary SIV infection predicts rapid progression towards AIDS. Acquired Immunodeficiency Syndromes. 17: 1585-1596.

[88] Mosier DE, Yetter AR, Morse III HC. (1985). Reetroviral induction of acute lymphoproliferative disease and profound immunosuppression in adult C57BL/6 mice. Journal of Experimental Medicine. 161: 766-784.

[89] Mosier DE, Gulizia RJ, Baird SM, Wilson DB, Spector DH, Spector SA. (1991). Human immunodeficiency virus infection of human-PBL-SCID mice. Science. 251: 791-794.

[90] Mosier DE. (1996). Viral pathogenesis in hu-PBL-SCID mice. Seminars in Immunology. 8: 255-262.

[91] Nakashima H, Ichiyama K, Hirayama F, Uchino K, Ito M, Saitoh T, Ueki M, Yamamoto N, Ogawara H. (1996). Sulfated pentagalloyl glucose (Y-ART-3) inhibits HIV replication and cytopathic effects *in vitro*, and reduces HIV infection in hu-PBL-SCID mice. Antiviral Research. 30: 95-108.

[92] Namikawa R, Weilbaecher KN, Kaneshima H, Yee EJ, McCune JM. (1990). Long-term hematopoiesis in the SCID-hu mouse. Journal of Experimental Medicine. 172: 1055-1063.

[93] Norley SG. (1996). SIV_{agm} infection of its natural African green monkey host. Immunology Letters. 51: 53-58.

[94] Ohnota H, Okada Y, Ushijima H, Kitamura T, Komuro K, Mizuochi T. (1990). 3'-Azido-3'-deoxythymidine prevents induction of murine acquired immunodeficiency syndrome in C57BL/10 mice infected with LP-BM5 murine leukemia viruses, a possible animal model for antiretroviral drug screening. Antimicrobial Agents and Chemotherapy. 34: 605-609.

[95] Okishima N, Hirata K, Moriguchi S, Kishino Y. (1996). Vitamin E supplementation normalizes immune dysfunction murine AIDS induced by LP-BM5 retrovirus infection. Nutrition Research. 16: 1709-1719.

[96] Onanga R, Kornfeld C, Pandrea I, Estaquier J, Souquiere S, Rouquet P, Mavoungnon VP, Bourry O, M'Boup S, Barre-Sinoussi F, Simon F, Apetrei C, Roques P, Muller-Trutwin MC. (2002). High levels of viral replication contrast with only transient changes in CD4(+) and CD8(+) cell numbers during the early phase of experimental infection with simian immunodeficiency virus SIV mnd-1 in Mandrillus sphinx. Journal of Virology. 76: 10256-63.

[97] O' Neil SP, Suwyn C, Anderson DC, Niedziela G, Bradley J, Novembre FJ, Herndon JG, McClure HM. (2004). Correlation of acute humoral response with brain virus burden and survival time in pigtailed macaques infected with neurovirulent simian immunodeficiency virus SIVsmmFGb. American Journal of Pathology. 164: 1157-1172.

[98] Otani I, Fujii Y, Akari H, Mukai R, Mori K, Ono F, Kojima E, Machida M, Murakami K, Doi K, Yoshikawa Y. (1997). Effects of 6-chloro-2', 3'-dideoxyguanosine (6-Cl-ddG) in surface lymph nodes of rhesus monkeys (*Macaca mulatto*) chronically infected with simian immunodeficiency virus (SIVmac239). Journal of Veterinary Medical Sciences. 59: 891-896.

[99] Otani I, Akari H, Nam K, Mori K, Suzuki E, Shibata H, Doi K, Terao K, Yosikawa Y. (1998). Phenotypic changes in peripheral blood monocytes of cynomolgus monkeys acutely infected with simian immunodeficiency virus. AIDS Research and Human Retroviruses. 14: 1181-1186.

[100] Pattengale PK, Taylor CR, Twomey P, Hill S, Jonasson J, Beardsley T, Haas M. (1982). Immunopathology of B-cell lymphomas induced in C57BL/6 mice by dualtropic murine leukemia virus (MuLV). American Journal of Pathology. 107: 362-377.

[101] Pedersen NC, Ho EW, Brown ML, Yamamoto JK. (1987). Isolation of a T-lymphotropic virus from domestic cats with immunodeficiency-like syndrome. Science. 235: 790-793.

[102] Persidsky Y, Limoges J, McComb R, Bock P, Baldwin T, Tyor W, Patil A, Nottet HSLM, Epstein L, Gelbard H, Flanagan E, Reinhard J, Pirruccello SJ, Gendelman HE. (1996.) Human immunodeficiency virus encephalitis in SCID mice. American Journal of Pathology. 149: 1027-1053.

[103] Pettoello-Mantovani M, Kollmann TR, Raker C, Kim A, Yurasov S, Tudor R, Wiltshire H, Goldstein H. (1997). Saquinavir-mediated inhibition of human immunodeficiency virus (HIV) infection in SCID mice implanted with human fetal thymus and liver tissue: an *in vivo* model for evaluating the effect of drug therapy on HIV infection in lymphoid tissues. Antimicrobial Agents and Chemotherapy. 41: 1880-1887.

[104] Petursson G, Palsson PA, Georgsson G. (1989). Maedi-visna in sheep: host-virus interactions and utilization as a model. Intervirology. 30 (Suppl. 1): 36-44.

[105] Philips TR, Prospero-Garcia O, Puaoi DL, Lerner DL, Fox HS, Olmsted RA, Bloom FE, Hendrikson SJ, Elder JH. (1994). Neurological abnormalities associated with feline immunodeficiency virus infection. Journal of General Virology. 75: 979-987.

[106] Pincus SH. (2004). Models of HIV infection utilizing transgenic and reconstituted immunodeficienct mice. Drug Discovery Today: Disease Models. 1(1): 49-56.

[107] Power C, Moench T, Peeling J, Kong P-A, Langelier T. (1997). Feline immunodeficiency virus causes increased glutmate levels and neuronal loss in brain. Neuroscience. 77: 1175-1185.

[108] Premanathan M, Arakaki R, Izumi H, Kathiresan K, Kakano M, Yamamoto N, Nakashima H. (1999). Antiviral properties of a mangrove plant, *Rhizophora apiculata* Blume, against human immunodeficiency virus. Antiviral Research. 44: 113-122.

[109] Rauscher FJ. (1962). A virus-induced disease of mice characterized by eryrhrocytosis and lymphoid leukemia. Journal of the National Cancer Institute. 29: 515-543.

[110] Reimann KA, Tenner-Racz K, Racz P, Montefiori DC, Yasutomi Y, Lin W, Ransil BJ, Letvin NL. (1994). Immunopathogenic events in acute infection of rhesus monkeys with simian immunodeficiency virus of macaques. Journal of Virology. 68: 2362-2370.

[111] Romero DL, Busso M, Tan C-K, Reusser F, Palmer JR, Poppe SM, Aristoff PA, Downey KM, So AG, Resnick L, Tarpley WG. (1991). Nonnucleoside reverse transcriptase inhibitors that potently and specifically block human immunodeficiency virus type 1 replication. Proceedings from the National Academy of Sciences of United States of America. 88: 8806-8810.

[112] Rossi L, Serafini S, Franchetti P, Casabianca A, Orlandi C, Schiavano GF, Carnevali A, Magnani M. (2002). Inhibition of murine AIDS by a heterodinucleotide of azidothymidine and 9-(R)-2-(phosphonomethoxypropyl)adenine. Journal of Antimicrobial Chemotherapy. 50: 639-647.

[113] Rytik PG, Kutcherov II, Muller WEG, Poleschuk NN, Duboiskaya GP, Kruzo M, Podolskaya IA. (2004). Small animal model of HIV-1 infection. Journal of Clinical Virology. 31S: S83-87.

[114] Schmitt AC, Ravazzolo AP, Von Poser GL. (2001). Investigation of some *Hypericum* species native to Southern of Brazil for antiviral activity. Journal of Ethnopharmacology. 77: 239-245.

[115] Schmitz JE, Kuroda MJ, Santra S, Sasseville VG, Simon MA, Lifton MA, Racz P, Tenner-Racz K, Dalesandro M, Scallon BJ, Ghrayeb J, Forman MA, Montefiori DC, Rieber EP, Letvin NL, Reimann KA. (1999). Control of viremia in simian immunodeficiency virus infection by $CD8^+$ lymphocytes. Science. 28: 857-860.

[116] Schmitz JE, Kuroda MJ, Santra S, Simon MA, Lifton MA, Lin W, Khunkhun R, Piatak M, Lifson JD, Grosschupff G, Gelman RS, Racz P, Tenner-Racz K, Mansfield KA, Letvin NL, Montefiori DC, Reimann KA. (2003). Effect of humoral immune responses on controlling viremia during primary infection of rhesus monkeys with simian immunodeficiency virus. Journal of Virology. 77: 2165-2173.

[117] Sequar G, Britt WJ, Lakeman FD, Lockridge KM, Tarara RP, Canfield DR, Zhou S, Gardner MB, Barry PA. (2002). Experimental coinfection of rhesus macaques with rhesus cytomegalovirus and simian immunodeficiency virus: pathogenesis. Journal of Virology. 76: 7661-7671.

[118] Sharma SK, Billaud J, Tandon M, Billet O, Choi S, Kopka ML, Philips TR, Lown JW. (2002). Inhibition of feline immunodeficiency virus (FIV) replication by DNA binding polyamides. Bioorganic and Medicinal Chemistry Letters. 12: 2007-2010.

[119] Shen Y, Shen L, Sehgal P, Zhou D, Simon M, Miller M, Enimi EA, Henckler B, Chalifoux L, Sehgal N, Gastron M, Letvin NL, Chen ZW. (2001). Antiretroviral agents restore mycobacterium-specific T-cell immune responses and facilitate controlling a fatal tuberculosis-like disease in macaques coinfected with simian immunodeficiency virus and *Mycobacterium bovis* BCG. Journal of Virology. 75: 8690-8696.

[120] Siebelink KHJ, Chu I, Rimmelzwaan GF, Weijer K, Van Herwijnen R, Knell P, Egberink HF, Bosch ML, Osterhaus ADME. (1990). feline immunodeficiency virus (FIV) infection of cats as a model for HIV infection in man: FIV-induced impairment of immune function. AIDS Research and Human Retroviruses. 6: 1373-1378.

[121] Simard C, Huang M, Jolicoeur P. (1994). Murine AIDS is initiated in the lymph nodes draining the site of inoculation, and the infecet B cells influence T cells located at a distance, in noninfected organs. Journal of Virology. 68: 1903-1912.

[122] Sklan EH, Gazit A, Priel E. (2000). inhibition of murine AIDS (MAIDS) development in C57BL/6J mice by tryphostin AG-1387. Virology. 278: 95-102.

[123] Soldaini E, Matteucci D, Lopez-Cepero M, Specter S, Friedman H, Bendinelli M. (1989). Friend leukemia complex infection of mice as an experimental model for AIDS studies. Veterinary Immunology and Immunopathology. 21: 97-110.

[124] Sotir M, Switzer W, Schable C, Schmitt J, Vitek C, Khabbaz RF. (1997). Risk of occupational exposure to potentially infectious nonhuman primate materials and to simian immunodeficiency virus. Journal of Medical Primatology. 26: 233-240.

[125] Spring M, Stahl-Hennig C, Stolte N, Bischofberger N, Heeney J, Ten Haaft P, Tenner-Racz K, Racz P, Lorenzen D, Hunsmann G, Dittmer U. (2001). Enhanced cellular immune response and reduced $CD8^+$ lymphocyte apoptosis in acutely SIV-infected macaques after short-term antiretroviral treatment. Virology. 279: 221-232.

[126] Staprans SI, Dailey PJ, Rosenthal A, Horton C, Grant RM, Lerche N, Feinberg MB. (1999). Simian immunodeficiency virus disease course is predicted by the extent of virus replication during primary infection. Journal of Virology. 73:, 4829-4839.

[127] Stoddart CA, Moreno ME, Linquist-Stepps VD, Bare C, Bogan MR, Gobbi A, Buckheit Jr RW, Bedard J, Rando RF, McCune JM. (2000). Antiviral activity of 2'-deoxy-3'-oxa-4'-thiocytidine (BCH-10652) against lamivudine-resistant human immunodeficiency virus type 1 in SCID-hu thy/liv mice. Antimicrobial Agents and Chemotherapy. 44: 783-786.

[128] Straub OC. (1989). Carpine arthritis encephalitis – a model for AIDS? Intervirology. 30 (Suppl. 1): 45-50.

[129] Strizki JM, Xu S, Wagner NE, Wojcik L, Liu J, Hou Y, Endres M, Palani A, Shapiro S, Clader JW, Greenlee WJ, Tagat JR, McCombie S, Cox K, Fawzi AB, Chou C-C, Pugliese-Sivo C, Davies L, Moreno ME, Ho DD, Trkola A. Stoddart CA, Moore JP, Reyes GR, Baroudy BM. (2001). SCH-C (SCH 351125), an orally bioavailable, small molecule antagonist of the chemokines receptor CCR5, is a potent inhibitor of HIV-1 infection *in vitro* and *in vivo*. Procceedings of the National Academy of Science USA. 98: 12718-12723.

[130] Sumpter LR, Inayat MS, Yost EE, Duvall W, Hagan E, Mayhew CN, Elford HL, Gallicchio VS. (2004). *In vivo* examination of hydroxyurea and the novel ribonucleotide reductase inhibitors trimidox and didox in combination with the reverse transcriptase inhibitor abacavir: suppression of retrovirus-induced immunodeficiency disease. Antiviral Research. 62: 111-120.

[131] Suruga Y, Makino M, Okada Y, Tanaka H, De Clercq E, Baba M. (1998). Prevention of murine AIDS development by (R)-9-(2-phosphonylmethoxypropyl)adenine. Journal of Acquired Immune Deficiency Syndrome and Human Retrovirology. 18: 316-322.

[132] Talbott RL, Sparger EE, Lovelace KM, Fitch WM, Pedersen NC, Luciw PA, Elder JH. (1989). Nucleotide sequence and genomic organization of feline immunodeficiency virus. Proceedings from the National Academy of Sciences of United States of America. 86: 5743-5747.

[133] Taylor MD, Korth MJ, Katze MG. (1998). Interferon treatment inhibits the replication of simian immunodeficiency virus at an early stage: evidence for a block between attachment and reverse transcription. Virology. 241: 156-162.

[134] Torten M, Franchini M, Barlough JE, George JW, Mozes E, Lutz H, Pedersen NC. (1991). Progressive immune dysfunction in cats experimentally infected with feline immunodeficiency virus. Journal of Virology. 65: 2225-2230.

[135] Uchin FM, Qazi S, Pendergrass S, Lisowski E, Waurzyniak B, Chen C-L, Venkatachalam TK. (2002). *In vivo* toxicity, pharmacokinetics, and anti-human immunodeficiency virus activity of stavudine-5'-(ρ-bromophenyl methoxyalaninyl phosphate) (stampidine) in mice. Antimicrobial Agents and Chemotherapy. 46: 3428-3436.

[136] Walder R, Kalvatchev Z, Apitz-Castro R. (1998). Selective *in vitro* protection of SIVagm-induced cytolysis by ajoene, [(E)-(Z)-4,5,9-trithiadodeca-1,6-11-triene-9 oxide]. Biomedicine and Pharmacotherapy. 52: 229-235.

[137] Watanbe H, Miyaji C, Makino M, Abo T. (1996). Therapeutic effects of glycyrrhizin in mice infected with LP-BM5 murine retrovirus and mechanisms involved in the prevention of disease progression. Biotherapy. 9: 209-220.

[138] Willet BJ, Flynn JN, Hosie MJ. (1997). FIV infection of the domestic cat: an animal model for AIDS. Immunology Today. 13: 182-189.

[139] Witvrouw M, Pannecouque C, Van Laehem K, Desmyter J, De Clercq E, Vandamme A. (1999). Activity of non-nucleoside reverse transcriptase inhibitors against HIV-2 and SIV. Acquired Immunodeficiency Syndromes. 13: 1477-1483.

[140] Xu Z, Buckheit Jr RW, Stup TL, Flavin MT, Khilevich A, Rizzo JD, Lin L, Zembower DE. (1998). *In vitro* anti-human immunodeficiency virus (HIV) activity of the chromanone derivative, 12-oxocalanolide A, a novel NNRTI. Bioorganic and Medicinal Chemistry Letters. 8: 2179-2184.

[141] Yetter RA, Buller RML, Lee JS, Elkins KL, Mosier DE, Fredrickson TN, Morse III H.C. (1988). $CD4^+$ T cells are required for development of a murine retrovirus-induced immunodeficiency syndrome (MAIDS). Journal of Experimental Medicine. 168: 623-635.

Received: March 10, 2006 **Revised: June 5, 2006** **Accepted: June 12, 2006**